

PLASTIN3 AS A THERAPEUTIC TARGET IN SPINAL MUSCULAR ATROPHY

by

Aziza. R. Al-Rafiah
(BSc, MSc)

Submitted for the degree of Doctor of Philosophy (PhD)

Sheffield Institute for Translational Neuroscience

University of Sheffield



May 2015

ABSTRACT

Spinal muscular atrophy (SMA) is a devastating childhood motor neuron disease caused by mutations in the survival motor neuron 1 gene (*SMN1*). *SMN1* and *SMN2* are nearly identical genes producing the survival of motor neuron (SMN) protein. SMN protein plays a crucial role in mRNA splicing and β -actin mRNA transport along the axons. In SMA the mutation leads to the loss of *SMN1*, which cannot be fully compensated by the *SMN2* gene, which predominantly produces a truncated protein. The loss or reduction of SMN protein leads to motor axonal defects and motor neuron cell death. There are currently no treatments available but therapies have focused on increasing SMN through replacing *SMN1* or increasing full length SMN from *SMN2*. The actin-binding protein Plastin 3 (PLS3) has been reported as a modifier for SMA, making it a potential therapeutic target. Recently, it was shown that the overexpression of the *PLS3* gene improved axonal outgrowth in SMN-deficient motor neurons of SMA Zebrafish and cultured motor neurons from mouse embryos.

Gene therapy using viral vectors was carried out *in vitro* and *in vivo* to assess whether the overexpression of PLS3 could rescue neuronal loss in SMA and be developed as a therapy. The *SMN Δ 7* mouse model produces low levels of SMN, modelling severe SMA disease with an average lifespan of 12 days and loss of motor neurons. This study has established that the *SMN Δ 7* mice have little or no detectable PLS3 from birth, making it a good model for developing PLS3 gene therapy. Lentiviral vectors were able to upregulate PLS3 expression in different cell lines. Transduction of NSC34 cells with LV-PLS3 vector led to a five-fold increase in expression of PLS3 compared to controls. In *smn*-deficient MNs, expression of PLS3 restored axonal length and showed a strong neuroprotective effect.

Pre-clinical *in vivo* proof-of-concept studies using adeno-associated virus serotype 9 (AAV9) encoding PLS3 in *SMN Δ 7* mice showed high transduction efficiency and overexpression of PLS3 specifically targeted to neurons in the central nervous system (CNS). This led to a small but significant increase of lifespan by 54%. However, PLS3 was not able to prevent disease onset. Although there was no improvement of phenotype, this study has demonstrated the potential use of PLS3 as a target for gene therapy, possibly in conjunction with other modulators of disease.

ACKNOWLEDGMENTS

First and foremost, I would like to thank the Almighty Allah, the most gracious, the most merciful, for blessing, protecting me and giving me this chance to convert a dream into reality.

My deepest gratitude goes to my parents for making me believe in myself and soaking me with their endless support, encouragement and precious prayers which made me fulfill my dream. I would like to express my sincere gratitude to my sisters, who provided me with the strength and advice especially when I needed them most.

Secondly, my endless appreciation goes to my supervisor, Prof. Mimoun Azzouz for his invaluable support, inspiring guidance and scientific input. Thank you for your constructive guidance, encouragement, and support. The knowledge I gained from you throughout the study contributed immensely to my scientific, academic and personal development.

Also, I would like to thank my co-supervisor Dr Ke Ning for his academic support and guidance. In particular, I owe my deepest gratitude to Dr Kayleigh Iremonger for her great academic support and help. Your comforting words and big smile always cheered me up! I am also very grateful to Dr. Katherine Lewis for her valuable and immeasurable support. My special thanks goes to Evangelia Karyka for her tremendous technical support. Many thanks Dr. Christopher J Binny, Dr. Vera Lukashchuk, Dr. Jayanth Chandran and Dr. Saul Herranz Martin for their great support. I must thank Ian Coldicott for his patience and help with *in vivo* work. I am indebted to all of my colleagues in the Sheffield Institute for Translational Neuroscience (SITraN) and in particular everyone in Professor Mimoun Azzouz's lab for their great support and willingness to help.

I would also thank all my friends throughout the UK for providing emotional support and making this journey easier and full of joyful memories.

Last but not least, special thanks and appreciation are due to my husband, Abdul-Rahman who provided endless encouragement, support, and patience throughout my studies. My kids thank you for being at my side during the most stressful, as well as the most exciting periods during my PhD. You were my comfort zone in the toughest moments and in your lovely eyes I felt the warmth even in the coldest nights.

Finally I would like to thank King Abdul Aziz University, Jeddah, who has supported the work described in this thesis, through the Royal Embassy of Saudi Arabia Cultural Bureau in London.

*This thesis is dedicated to my loving parents,
Badriyah and Rashed*

PUBLICATIONS

Paper

Joseph Scarrott, Saul Martin Herranz, Aziza Al-Rafiah, Pamela Shaw, Mimoun Azzouz. Current Developments in Gene Therapy for ALS/MND. Expert Opinion on Biological Therapy (2015) 15(7).

Published Abstracts/Conferences

Aziza AL-Rafiah*, Evangelia Karyka, Ke Ning, Mimoun Azzouz. Plastin 3 as therapeutic target in spinal muscular atrophy. British Neurosci. Assoc. Abstr., Vol. 22: PXX, 2013. ISSN 1345-8301 2013.

Aziza AL-Rafiah*, Evangelia Karyka, Ke Ning, Mimoun Azzouz. Plastin 3 as therapeutic target in spinal muscular atrophy. Human Gene Therapy. May 2014, 25(5): A1-A22.

AWARDS

- 1- The best poster titled, RNA processing and therapeutic strategies for spinal muscular atrophy at the 6th Saudi scientific international conference held on 11th Oct 2012 at the Brunel university London.
- 2- The best poster titled, Plastin 3 as therapeutic target in spinal muscular atrophy at the 7th Saudi scientific international conference held on 12th Feb 2013 at the Edinburgh University.
- 3- Prize for the 2nd best poster titled, Plastin 3 as therapeutic target in spinal muscular atrophy at the Department of Neuroscience Research Day, the University of Sheffield, 10th Oct 2014 (2nd place).

LIST OF CONTENTS

1	ABSTRACT	i
2	ACKNOWLEDGMENTS.....	ii
3	PUBLICATIONS.....	iv
4	AWARDS	iv
5	LIST OF CONTENTS	v
6	LIST OF FIGURES.....	ix
7	LIST OF TABLES	x
8	LIST OF ABBREVIATIONS.....	xi
1	CHAPTER 1: INTRODUCTION	1
1.1	Spinal Muscular Atrophy	1
1.1.1	Disease classification and clinical features.....	1
1.2	Survival of motor neuron (SMN)	4
1.2.1	<i>SMN</i> gene	4
1.2.2	SMN protein.....	6
1.2.3	Motor Neuron Dysfunction in SMA	11
1.2.4	Other SMA disease modifiers	13
1.3	Plastin3	15
1.3.1	Human Plastin Gene.....	15
1.3.2	Plastin3 protein.....	16
1.3.3	The role of PLS3 in SMA	18
1.4	Models of SMA	21
1.4.1	<i>In vitro</i> Models of SMA.....	21
1.4.2	Animal models of SMA	21
1.5	Therapeutic strategies in SMA	26
1.5.1	Drug Treatment Approaches	29
1.5.2	Gene therapy	33

1.5.3	Gene therapy approaches in SMA disease	36
1.6	Clinical trials	39
1.7	Project Aims	41
2	CHAPTER 2: MATERIALS AND METHODS.....	42
2.1	Materials	43
2.1.1	Equipment	43
2.1.2	Reagents and chemicals	43
2.1.3	Buffers and solutions.....	43
2.1.4	Cells and media	43
2.1.5	43	
2.1.6	Ethics statement	44
2.1.7	Maps of the LV and AAV Plasmids	45
2.1.8	DNA Preparation.....	45
2.1.9	Protein extraction and quantification:	45
2.1.10	Spectrophotometry	46
2.2	<i>In Vitro</i> Experimental Work	47
2.2.1	Cell Lines and Cell Culture.....	47
2.2.2	Primary Motor Neuron Culture.....	47
2.2.3	Generation of Viral Plasmids	49
2.3	<i>In Vivo</i> Experimental Methods.....	66
2.3.1	Breeding and Genotyping of Transgenic Mice	66
2.3.2	Housing	67
2.3.3	Recruiting Experimental Mice	68
2.3.4	Viral Vector Delivery.....	68
2.3.5	Behavioural and Clinical Assessment.....	69
2.3.6	Tissue Collection.....	69
2.3.7	Histological Analysis	70

3	CHAPTER 3: PLASTIN3 EXPRESSION IN SMN Δ 7 MOUSE MODEL OF SPINAL MUSCULAR ATROPHY	73
3.1	Aims	74
3.2	Introduction	74
3.3	Results	77
3.3.1	Pls3 protein expression is downregulated in SMN Δ 7 mice.....	77
3.3.2	<i>Pls3</i> mRNA expression over time.....	82
3.3.3	Localisation of Pls3 in SMN Δ 7 mice.....	83
3.4	Discussion.....	91
3.4.1	Pls3 expression variations in the CNS of SMN Δ 7 mice.....	91
3.4.2	Pls3 levels in the muscle	93
3.4.3	Pls3 levels in SMN heterozygote mice	94
3.4.4	Localisation of Pls3 in P10 SMN Δ 7 mice	95
3.4.5	Summary	97
4	CHAPTER 4: PLS3-MEDIATED NEUROPROTECTION IN AN <i>IN VITRO</i> MODEL OF SPINAL MUSCULAR ATROPHY	98
4.1	Aims	99
4.2	Introduction	99
4.3	Results	102
4.3.1	Construction of LV-PLS3	102
4.3.2	Lentiviruses mediate efficient overexpression of PLS3 in cell lines .	105
4.4	Discussion.....	117
4.4.1	PLS3 staining pattern of different cell types.....	117
4.4.2	PLS3 is involved in axonogenesis and rescues the axon length in SMN Δ 7 MNs.	118
4.4.3	Summary	120
5	Chapter 5 : Adeno-associated vector serotype 9 (AAV9) encoding PLS3 gene therapy study in SMN Δ 7 mouse model of SMA	121
5.1	Aims	122
5.2	Introduction	122

5.3	Results	125
5.3.1	Construction of AAV-PLS3 vectors	125
5.3.2	Virus production and purification	132
5.3.3	scAAV-PLS3 gene transfer <i>in vivo</i>	136
5.3.4	Gene transfer efficiency of ssAAV9-delivered via cisterna magna... 137	
5.3.5	Efficacy study.....	139
5.3.6	Body Weight	139
5.3.7	Effect of ssAAV9-PLS3 on mouse life span.....	143
5.3.8	The power calculation	145
5.4	Discussion.....	151
5.4.1	ssAAV9-mediated gene transfer to the CNS	151
5.4.2	ssAAV9-PLS3 mediate marginal increased in the life span of SMN Δ 7 152	
5.4.3	PLS3 does not rescue disease phenotype	153
5.4.4	Expression of PLS3 in different vectors	154
5.4.5	Summary	155
6	Chapter 6: General Discussion.....	156
6.1	PLS3 levels in the SMN Δ 7 SMA mouse model	157
6.2	Overexpression of PLS3 by viral vectors.....	159
6.3	Considerations for clinical studies.....	161
6.4	Future work	163
6.5	Final conclusions	165
7	BIBLIOGRAPHY	166
8	APPENDIX	181

LIST OF FIGURES

FIGURE 1.1. <i>SMN1</i> AND <i>SMN2</i> SPLICING	5
FIGURE 1.2. ROLE OF SMN PROTEIN IN SNRNP ASSEMBLY.....	7
FIGURE 1.3. ROLE OF SMN PROTEIN IN AXONS	10
FIGURE 1.4. PLASTIN PROTEIN ISOFORMS STRUCTURE	17
FIGURE 1.5. THERAPEUTIC STRATEGIES FOR SMA	28
FIGURE 1.6. SMA THERAPEUTICS PIPELINE AS OF FEBRUARY 2015.....	39
FIGURE 2.1. THE IODIXANOL SOLUTIONS LAYERS.....	58
FIGURE 3.1. PLS3 PROTEIN LEVELS IN POSTNATAL DAY 1 <i>SMNΔ7</i> MICE.....	79
FIGURE 3.2. PLS3 PROTEIN LEVELS IN POSTNATAL DAY 5 <i>SMNΔ7</i> MICE.....	80
FIGURE 3.3. PLS3 PROTEIN LEVELS IN P10 <i>SMNΔ7</i> MICE	81
FIGURE 3.4. <i>PLS3</i> MRNA LEVELS OVER TIME IN THE BRAIN, SPINAL CORD AND MUSCLE OF <i>SMNΔ7</i> MICE	82
FIGURE 3.5. PLS3 IMMUNOSTAINING IN THE BRAIN CORTICAL SECTIONS OF WT AND KO P10 PUPS 84	84
FIGURE 3.3.6. PLS3 IMMUNOREACTIVITY IN CERVICAL (A) AND LUMBAR (B) SPINAL CORD OF P10 WT AND KO <i>SMNΔ7</i> MICE.....	87
FIGURE 3.7. DOUBLE LABELING PLS3 AND SMI32 IN THE SPINAL CORD SECTIONS FROM <i>SMNΔ7</i> MICE (KO) AT P10 OF AGE.....	89
FIGURE 3.8. CO-LOCALIZATION OF PLS3 PROTEIN LEVELS IN THE SPINAL CORD OF WT / KO AT P10 OF AGE WITH CGRP.....	90
FIGURE. 4.1. INSERTION OF PLS3 INTO THE LENTIVIRAL VECTOR.....	103
FIGURE 4.2. VALIDATION OF LV-PLS3 PLASMID 72 HOURS FOLLOWING TRANSFECTION OF HEK293T CELLS.....	104
FIGURE 4.3. VALIDATION OF LV-PLS3 VIRUS TRANSDUCTION EFFICIENCY IN HEK293T BY WESTERN BLOT	106
FIGURE 4.4. VALIDATION OF LV-PLS3 VIRUS IN HEK293T CELLS BY IMMUNOFLUORESCENCE.....	108
FIGURE 4.5. VALIDATION OF LV-PLS3 VIRUS IN NSC34 CELLS	110
FIGURE 4.6. LV-MEDIATED PLS3 EXPRESSION IN NSC34 ASSESSED BY IMMUNOFLUORESCENCE.....	111
FIGURE 4.7. LV-MEDIATED PLS3 NEUROPROTECTION IN <i>SMNΔ7</i> PURIFIED MOTOR NEURONS	114
FIGURE 4.8. IMPACT OF LV-PLS3 TREATMENT ON AXON LENGTH IN SMN DEFICIENT MOTOR NEURONS.....	116
FIGURE 5.1. INSERTION OF PLS3 INTO THE SCAAV BACKBONE.....	127
FIGURE 5.2. VALIDATION OF THE SCAAV-BASED PLASMIDS EXPRESSING PLS3	128
FIGURE 5.3. PLS3 CLONING INTO SSAAV BACKBONE	130
FIGURE 5.4. VALIDATION OF THE SSAAV-BASED PLASMID EXPRESSING PLS3.	131
FIGURE 5.5. PRODUCTION OF HIGH QUALITY AAV9 VIRUSES.....	133
FIGURE 5.6. VALIDATION OF SCAAV9-PLS3 AND SSAAV9-PLS3 VIRUSES	135
FIGURE 5.7. POSTNATAL DAY 21 PLS3 PROTEIN LEVELS FOLLOWING SCAAV9-PLS3 IV DELIVERY IN P1 MICE	136
FIGURE 5.8. WB ANALYSIS OF THE SPINAL CORD FOLLOWING CISTERNA MAGNA DELIVERY OF SSAAV9-PLS3.....	138
FIGURE 5.9 BODY WEIGHT ASSESSMENT OF <i>SMNΔ7</i> MICE	142
FIGURE 5.10 SURVIVAL CURVE AND DISEASE DURATION OF <i>SMNΔ7</i> MICE	144
FIGURE 5.11 TRANSDUCTION OF SPINAL MOTOR NEURONS IN <i>SMNΔ7</i> MICE.....	147
FIGURE 5.12 TRANSDUCTION EFFICIENCY OF SPINAL MOTOR NEURONS IN <i>SMNΔ7</i> MICE IN SSAAV9- PLS3 TREATED MICE.....	149

LIST OF TABLES

TABLE 1.1 CLASSIFICATION OF SPINAL MUSCULAR ATROPHY	2
TABLE 1.2 SMA SEVERITY CORRELATED TO <i>SMN2</i> COPY NUMBER	3
TABLE 1.3 MOUSE MODELS OF SMA.....	24
TABLE 1.4 SUCCESSFUL PRECLINICAL STUDIES USING THE VECTOR-BASED GENE THERAPY APPROACH FOR SMA TREATMENT	38
TABLE 2.1 LIST OF CELL LINES USED IN THIS STUDY	43
TABLE 2.2 LIST OF PRIMARY ANTIBODIES USED.....	44
TABLE 2.3 LIST OF SECONDARY ANTIBODIES USED	44
TABLE 2.4 SEQUENCING PRIMERS FOR PLS3 CONSTRUCTS	52
TABLE 2.5 ABSORBANCE, P24 AND SERIAL DILUTION VALUES FOR LV-PLS3 TITRATION	55
TABLE 2.6 TITRES OF LV-PLS3 STOCK	55
TABLE 2.7 PREPARATION OF IODIXANOL SOLUTIONS.....	57
TABLE 2.8 PRIMERS USED FOR QPCR	60
TABLE 2.9 PRIMERS USED FOR REAL TIME PCR (RT-PCR).....	66
TABLE 2.10 PRIMERS USED FOR GENOTYPING.....	67
TABLE 2.11 VIRAL VECTOR DOSE ADMINISTERED.....	69
TABLE 5.1 VIRAL TITRES OF HIGH QUALITY FRACTIONS (VIRAL GENOMES PER ML).....	134
TABLE 5.2 VIRAL CONCENTRATIONS USED FOR TRANSDUCTION OF HEK293T CELLS	134
TABLE 5.3 TRANSDUCTION EFFICIENCY OF LUMBAR SPINAL MOTOR NEURONS (GFP)	148
TABLE 5.4 TRANSDUCTION EFFICIENCY OF LUMBAR SPINAL MOTOR NEURONS (PLS3)	150

LIST OF ABBREVIATIONS

AAV	Adeno-associated virus
ABDs	Actin-binding domains
ASO	Antisense Oligonucleotide
BBB	Blood Brain Barrier
BCA	Bicinchoninic Acid Protein
BSA	Bovine Serum Albumin
C	Cytosine
Carb	Carbenicillin
cDNA	Copy deoxyribonucleic acid
CGRP	Calcitonin-gene related peptide
CH	Calponin homology
CMV	Cytomegalovirus
CNS	Central nervous system
DAPI	Diamidino-2-phenylindole
DMEM	Dulbecco's minimum essential medium
DNA	Deoxyribonucleic acid
DPBS	Dulbecco's Phosphate Buffered Saline
Dpf	Days post fertilization
DPX	Di-N-Butyle Phthalate in Xylene
DRG	Dorsal root ganglia
E. Coli	<i>Escherichia. coli</i>
E13	Embryonic day 13
EB	Elution buffer
EIAV	Equine Infectious Anaemia Virus
ELISA	Enzyme Linked Immunosorbent Assay
ESE	Exonic splice enhancer
ESS	Exonic splice silencer
FCS	Fetal calf serum
FITC	Fluorescein isothiocyanate
FL-SMN	Full length SMN protein

GAPDH	Glyceraldehyde 3-phosphate dehydrogenase
GFP	Green fluorescent protein
HBSS	Hank's Balanced Salt Solution
HD	Huntington's disease
HDAC	Histone deacetylase inhibitors
HEK	Human embryonic kidney
HIV	Human Immunodeficiency Virus
hnRNP	Heterogeneous nuclear ribonucleoproteins
HRP	Horseradish peroxidase
IV	Intravenous
Lsm	Sm like protein
LV	Lentiviral Vector
LVs	Lentiviruses
MND	Motor neuron disease
MNs	Motor neurons
MO	Morpholino technique
MOI	Multiplicity of Infection
mRNA	Messenger ribonucleic acid
mRNPs	Silent messenger ribonucleoprotein
MT	Melting temperature
NB	Neurobasal- medium
NeuN	Neuronal antigen fox-3
NF-H ₂ O	Nuclease-free water
NGS	Normal goat serum
NMJ	Neuromuscular junction
NSC	Neuroblastoma spinal cord cells
NSE	Neuron Specific Enolase
OCT	Optimum cutting temperature
P	Postnatal day
PAGE	Polyacrylamide gel electrophoresis
PBS	Phosphate buffered saline
PCR	Polymerase chain reaction

PD	Parkinson's disease
PEI	Polyethylenimine
PFA	Paraformaldehyde
PLS1	I-plastin
PLS2	L-plastin
PLS3	T-plastin
PTEN	Phosphatase and tensin homolog
PVDF	Polyvinylidene difluoride
QPCR	Quantitative polymerase chain reaction
RNA	Ribonucleic acid
RT-PCR	Real time polymerase chain reaction
SAHA	suberoylanilide hydroxamic acid
scAAV	Self-complementary adeno-associated virus
SDS	Sodium dodecyl sulphate
SEM	Standard error of the mean
siRNA	Small interfering RNA
SMA	Spinal muscular atrophy
SMI-32	The nonphosphorylated neurofilament marker
SMN	Survival motor neuron
SMN Δ 7	SMN deleted exon7
snRNPs	Small nuclear ribonucleo proteins
SPF	Specified pathogen free
ssAAV	Single stranded adeno-associated virus
ssDNA/RNA	Single stranded DNA/RNA
T	Thymidine
TSA	Trichostatin A
TU	Transducing Unit
VGCCs	voltage-gated Ca ²⁺ channels
VP	Viral proteins
VSV G	vesicular stomatitis virus G
β -ME	Beta-Mercaptoethanol buffer

CHAPTER 1: INTRODUCTION

1.1 Spinal Muscular Atrophy

Spinal Muscular Atrophy (SMA) is a childhood form of motor neuron disease characterized by the loss of alpha motor neurons (MNs) of the anterior horns in the spinal cord, resulting in symmetrical muscular weakness and hypotonia (Simic et al., 2008). It is a relatively common lethal autosomal recessive disease (the second after cystic fibrosis), with an early onset, usually in childhood (Prior et al., 2009, Cherry and Androphy, 2012). The prevalence of the disease is 1/6,000 - 1/10,000 of children, where about 50% of those affected die before the age of two (Aschauer et al., 2013).

1.1.1 Disease classification and clinical features

Werdnig first described SMA in 1891, and in 1995 the survival of motor neuron (SMN) gene was identified as the causative gene for SMA (Lefebvre et al., 1995). 95% of SMA cases result from the deletion of SMN1 (Prior et al., 2009), while 5% of the cases are caused by small mutations (splice mutants, small deletions and missense mutations) in the SMN1 gene (Alías et al., 2009) leading to the reduction of the SMN protein (Prior et al., 2009, Cherry and Androphy, 2012).

The clinical severity of SMA can vary widely, ranging from death in infancy to disability in adulthood. The disease has been classified into: Type I, Type II, Type III and type IV, depending on the clinical manifestations and age at onset of disease (Table 1-1) (Hua et al., 2011, Wertz and Sahin, 2015). Type I is the most severe through to type IV which is the least severe.

Table 1-1 Classification of spinal muscular atrophy

Type	Age of disease onset	Clinical symptoms
Werdnig-Hoffmann disease (SMA Type I)	New born - 6 months	Never sit without help
Chronic SMA (SMA Type II)	6 - 18 months	Sit but cannot stand or walk
Kugelberg-Welander disease (SMA Type III)	After 18 months without aid	Stand and walk
Adult type (SMA Type IV)	>18 years	Stand and walk without aid

(Hua et al., 2011, Wertz and Sahin, 2015)

SMA Type I (Werdnig-Hoffmann disease) is lethal in children; the onset of the disease occurs by 6 months leading to death before the age of 2 years, usually due to respiratory failure (Schreml et al., 2013, Wertz and Sahin, 2015). Those affected never develop the ability to sit without aid (Dubowitz, 1999).

SMA Type II (chronic SMA) is the intermediate form of the disease in terms of its severity, with age of onset from 6 - 18 months. Children are able to sit unsupported, however they never acquire the ability to stand or walk independently (Wadman et al., 2012a, Wertz and Sahin, 2015). They survive beyond the age of 2 and can live into adolescence or even longer (Russman et al., 1996).

SMA Type III (Kugelberg-Welander disease) is the mild form of the disease. The onset of the disease starts after 18 months (Kinali et al., 2002, Wertz and Sahin, 2015) and patients are usually able to walk, although most of them lose the ability to walk around puberty (Kinali et al., 2004). The life expectancy of these patients can be normal (Russman et al., 1996).

SMA Type IV was added to the disease classification in order to account for patients with adult onset (>18 years) and mild symptoms. Patients with SMA type IV are able to walk and do not suffer from respiratory and nutritional problems (Aschauer et al., 2013, Wertz and Sahin, 2015).

In cases where *SMN1* is deleted copy number of *SMN2* modulates the severity of SMA (Lefebvre et al., 1995) (Table 1-2), with the majority of patients retaining between 2 and 4 copies of *SMN2* (Chang et al., 2001, Locatelli et al., 2015). Nevertheless, the expressed SMN protein amount from *SMN2* gene does not provide sufficient protection from SMA (McAndrew et al., 1997). However, there are families with identical *SMN2* copy numbers that may have radically different disease severity (Oprea et al., 2008), implying that additional factors must also contribute to disease. [

Table 1-2 SMA severity correlated to *SMN2* copy number

SMA Type	Severity	SMN2 copies
Type I	Severe	One or two
Type II	Intermediate	Three
Type III	Mild	Three or four

(Chang et al., 2001)

1.2 Survival of motor neuron (SMN)

1.2.1 *SMN* gene

The human *SMN* gene is located on chromosome 5 region 5q11.2 - 5q13.3 and encodes SMN, a 294 amino acid protein implicated in Ribonucleic acid (RNA) splicing as part of the small nuclear ribonucleoprotein (snRNP) complex (Sahashi and Sobue, 2014), stabilisation of the axonal growth cone in neurons, and the formation of neuromuscular junctions (Melki et al., 1990).

In humans the *SMN* gene exists in two copies, the telomeric copy (*SMN1*) and the centromeric copy (*SMN2*) (Zheleznyakova et al., 2011). The two *SMN* isoforms have 99.9% sequence homology, have equivalent promoters (Echaniz-Laguna et al., 1999), and express RNA (Lefebvre et al., 1995) and protein ubiquitously (Coovert et al., 1997). Of the functional full length SMN (FL-SMN) protein, 90% is derived from *SMN1*, while the rest (10%) is produced by *SMN2* (Helmken et al., 2003, Locatelli et al., 2015). *SMN2* is an inverted repeat of *SMN1* with a single mutation (cytosine -thymine (C-T) at position 6 of exon 7) that results in 90% of its translated product being truncated and non-functional (Lorson et al., 1999). The mutation in *SMN2* disrupts the exonic splice enhancer site (ESE) (Cartegni and Krainer, 2002) and forms an exonic splicing silencer site (ESS) (Kashima and Manley, 2003, Sahashi and Sobue, 2014), which results in the splicing out of exon 7 (Sahashi and Sobue, 2014). The *SMN2* gene, therefore, generates mostly a transcript lacking exon 7 (*SMN Δ 7*) (Figure 1.1) (Lefebvre et al., 1995, Sahashi and Sobue, 2014). This gives rise to a truncated and highly unstable protein with a severely decreased oligomerisation efficiency and reduced functional activity (Locatelli et al., 2015).

Approximately 10% of SMN2 transcripts are able to undergo correct splicing to include exon 7 and producing FL-SMN (Cho and Dreyfuss, 2010, Locatelli et al., 2015).

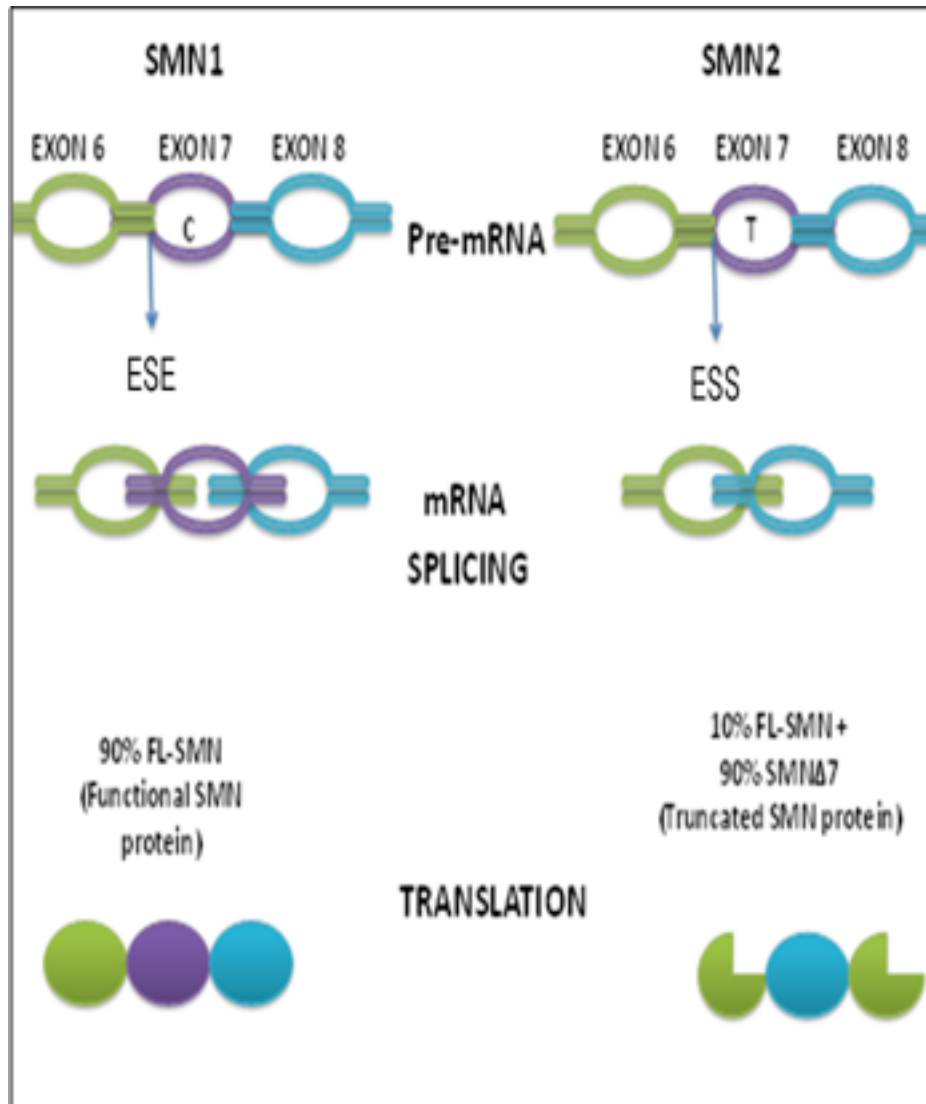


Figure 1.1. SMN1 and SMN2 Splicing

The two *SMN* human gene copies are located on chromosome 5 in the 5q13 region and differ by a single nucleotide exchange (C-to-T) on exon 7. This mutation affects *SMN2* splicing resulting in SMN Δ 7 mRNA, lacking exon 7. When translated a truncated, unstable, and easily degraded protein is produced. Despite this around 10% of SMN2 transcripts undergo correct alternative splicing to form fully functional full length protein. SMN, survival motor neuron, full-length SMN protein (FL-SMN), exonic splice enhancer site (ESE) and exonic splicing silencer site (ESS)

1.2.2 SMN protein

SMN is a ubiquitously expressed protein crucial for cell survival, independently of cell type. In humans, high levels of the protein are found in the spinal cord, kidney, liver and brain tissues (Coover et al., 1997). The SMN protein is 38 kDa in size and is localized in the cytoplasm and in structures in the nucleolus known as "gemini of coiled bodies" (gems), that associate with nuclear coiled bodies (Young et al., 2000, Borg and Cauchi, 2014).

SMN is involved in pre-mRNA splicing (Pellizzoni et al., 1999) and it also binds to heterogeneous nuclear ribonucleoprotein (hnRNP-R) (Rossoll et al., 2002).

1.2.2.1 The role of SMN protein in snRNPs assembly

95% of mammalian genes produce more than one mRNA from a single transcript through the process of alternate splicing, whereby different exons are removed to generate different proteins or isoforms (Chen and Manley, 2009, Borg and Cauchi, 2014). Splicing is carried out by the spliceosome, a large RNA-protein complex composed of five small nuclear ribonucleoprotein particles (snRNPs) and many proteins, which recognise splice sites, bind and catalyse the removal of introns (Figure 1.2). SMN protein is essential in snRNP assembly in every cell type, including neurons (Avila et al., 2007, Burghes and Beattie, 2009, Li et al., 2014).

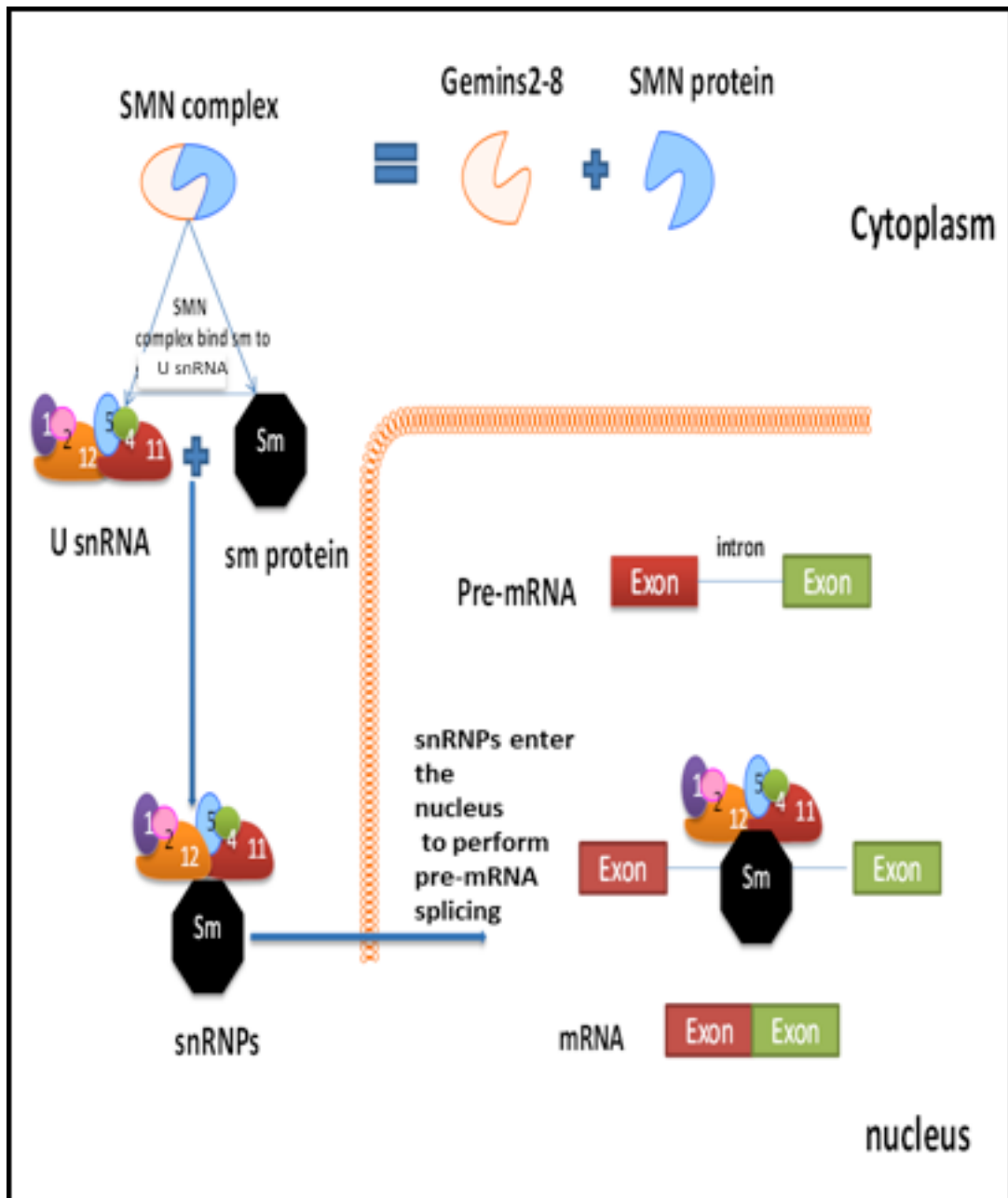


Figure 1.2. Role of SMN protein in snRNP assembly

The SMN complex (SMN protein and Gemins 2-8) mediates the assembly of Sm core proteins onto U-snRNAs, forming active snRNPs that enter the nucleus to perform pre-mRNA splicing. Survival motor neuron (SMN), small nuclear ribonucleoprotein particles (snRNPs) and heptameric ring of Sm proteins (sm protein). This diagram was adapted and modified from (Workman et al., 2009)

SMN along with other proteins known as Gemins 2–8 form the SMN complex, which allows a heptameric ring of Sm proteins (proteins to associate onto snRNA) (Pellizzoni, 2007, Tisdale et al., 2013), allowing for the cytoplasmic assembly of snRNPs (Fischer et al., 1997). snRNPs are RNA-protein complexes that, along with other proteins and unmodified pre-mRNAs, form the spliceosome, a large protein complex involved in splicing pre-mRNAs (Figure 1.2) (Tarn and Steitz, 1997, Li et al., 2014). Once the snRNPs are formed they get transferred into the nucleus where they carry out pre-mRNA splicing (Pellizzoni, 2007, Li et al., 2014). Therefore, SMN has been shown to be essential in the formation of snRNPs.

1.2.2.2 The function of SMN protein in motor axon growth

SMN protein granules are located in growth cones and axons of MNs (Sharma et al., 2005, Fallini et al., 2012, Dombert et al., 2014) where it forms a ribonucleoprotein complex (Zhang et al., 2006). SMN was shown to be involved in the transport of RNA complexes containing hnRNP-R, Sm-like proteins (lsm), and β -actin mRNA within MNs to the axon tips (Todd et al., 2010, Ting et al., 2012). Defects in the mRNA transport process cause alterations of synapses and the formation of truncated axons (Figure 1.3) (Rossoll et al., 2002, Fallini et al., 2012).

This finding was supported by the work done in zebrafish where knockdown of the *smn* gene lead to axonal defects (McWhorter et al., 2003). The reduced axonal growth resulting from *smn* protein deficiency in MNs was correlated with reduced β -actin protein and mRNA levels in growth cones (Rossoll et al., 2003). Furthermore, lsms were found in a RNP complex in axons (Young et al., 2001). It has been postulated that the reduced level of *Smn* protein affects the assembly of lsm proteins resulting in a reduced transportation of mRNA and β -actin to the axon tip, which in

turn reduces specific gene expression at the synapse causing its alteration (Workman et al., 2009). On the other hand, several SMA mouse studies showed no axon outgrowth defect *in vivo* (Murray et al., 2009). Murray et al, have shown in *Smn*^{-/-};SMN2 mice, a model of severe SMA that reduced *Smn* levels have no detectable effect on morphology of pre-symptomatic development in either vulnerable or stable motor units, indicating that abnormal pre-symptomatic developmental processes are unlikely to be a prerequisite for subsequent pathological changes to occur *in vivo* (Murray et al., 2009). The potential implications for developmental versus a degenerative mechanism of SMA disease pathogenesis is still unclear.

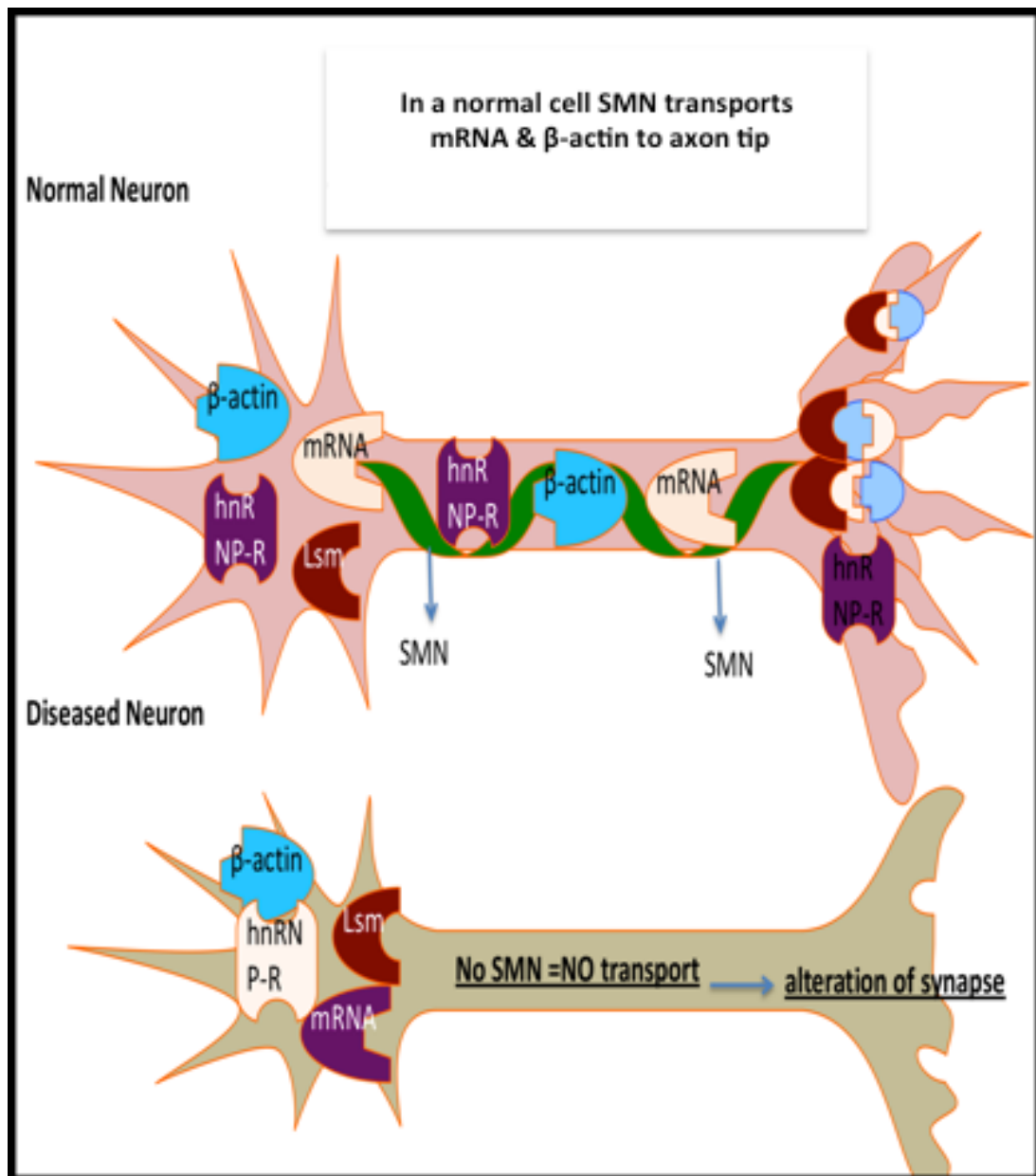


Figure 1.3. Role of SMN protein in axons

SMN was shown to be involved in the transport of RNA complexes such as hnRNP-R, Lsm, mRNA and β -actin within MNs to the axon tips. Disruption of this transport can cause alterations of the synapse. Survival motor neuron (SMN), Sm like protein (Lsm), heterogeneous nuclear ribonucleoprotein (hnRNP-R) and messenger ribonucleoprotein (mRNA). This diagram was adapted and modified from (Coady and Lorson, 2010)

Additionally, a role of Smn in neuromuscular junction (NMJ) development was also suggested (Kariya et al., 2008, McGovern et al., 2008, Kong et al., 2009).

Furthermore, pre-synaptic defects such as impaired synaptic vesicle release, intermediate filament aggregates, and poor terminal arborisation have been identified in motor neurons when SMN is absent or depleted (Kariya et al., 2008, McGovern et al., 2008, Kong et al., 2009, Ting et al., 2012). Moreover, β -actin mRNA and protein staining was reduced in growth cones and distal axons (Rossoll et al., 2003). These findings suggest a crucial role for Smn in neurodevelopment.

1.2.3 Motor Neuron Dysfunction in SMA

The key clinical feature of SMA is the selective and progressive loss of motor neurons. Loss of innervation of muscles has been described throughout the body in various affected muscle fiber types, which was thought to be due to defects in synaptic maturation or maintenance (Swoboda et al., 2005, Ling et al., 2011). Due to poor synapse formation and lack of differentiation, SMA patients usually show abnormal migration of MNs towards the ventral roots of spinal cords before later succumbing to necrosis (Simic et al., 2008, Shababi et al., 2014). Several SMA animal models, such as *Drosophila*, zebrafish and mouse are characterized by axon degeneration and neuromuscular junction (NMJ) defects (Chan et al., 2003, McWhorter et al., 2003, Rossoll et al., 2003, Jablonka et al., 2004, Winkler et al., 2005, Boon et al., 2009, Martinez et al., 2012). In the SMA Δ 7 mouse model, defects in axonal transport of synapse proteins have been reported, suggesting the presence of defects in NMJs and synapses of MNs (Dale et al., 2011). A mild SMA mouse model showed altered NMJ morphology and reduced neurotransmitter release (Wadman et al., 2012b, Ruiz and Tabares, 2014). Defects have also been seen in the structure of the pre- and post-synaptic apparatus with accumulation of vesicles and changes in receptor clustering reported (Martínez-Hernández et al., 2013). To date,

two main hypotheses have been proposed to simplify the molecular mechanism behind the death of motor neurons: (a) Loss of splicing activity and (b) dysfunction in transportation of mRNA to the axon tips.

SMN has been shown to be crucial in catalyzing the formation of snRNPs. In SMA there is enough SMN produced by *SMN2* to allow cell survival, but a lack of snRNPs caused by low SMN levels may restrict or modulate the splice sites selected. This could produce a lack of certain proteins due to other splice variations being favored. Gabanella et al. showed that the activity of snRNP assembly is reduced dramatically in the spinal cords from SMA mice and this assembly correlates with the disease severity (Avila et al., 2007). Some snRNPs are down-regulated by the disease; however, this change is not motor-neuron-specific and is only seen at late stage of the disease (Zhang et al., 2008, Bäumer et al., 2009) suggesting this is not solely responsible for disease.

Axonal growth defects and synaptic alteration are due to impaired trafficking and reduced transportation of molecules such as β -actin mRNA, which results in reduced specific gene expression at the synapse (Rossoll et al., 2003, Workman et al., 2009, Fallini et al., 2012, Shababi et al., 2014). SMN may be involved in RNA metabolism and transportation. In the cell body of motor neurons, mRNAs are packaged into translationally silent messenger ribonucleoproteins (mRNPs) and transported along the axon to distant parts of the cell to be produced on demand. In SMA there is a disruption of β -actin localisation in the neuronal growth cones suggesting transport impairment. The role of SMN in mRNA localisation and axonal transport is not clear (Fallini et al., 2012), but SMN may form part of the mRNP complex, similar to the snRNP complex; therefore, a lack of SMN prevents efficient formation of

mRNPs and disruption of transport to the distal parts of the neurons (Di Penta et al., 2009).

Depleted SMN protein levels in the growth cone of MNs also causes reduced axonal length (Oprea et al., 2008). Zebrafish expressing low levels of SMN display significant motor defects and shorter axons with fewer branches (Hao et al., 2012). This leads to abnormalities at both the NMJ and the synapse. SMN protein over-expression can restore MN synapses and NMJ defects (Wadman et al., 2012b, Shababi et al., 2014). Surprisingly, SMN deficiency appears to affect only some muscles; for example, NMJ defects have been reported in the diaphragm but not in the soleus muscle (Voigt et al., 2010, Mikesh et al., 2011). The loss of innervation of affected muscles is thought to be due to the defects in synaptic maturation or maintenance (Ling et al., 2011).

1.2.4 Other SMA disease modifiers

Many proteins in the nucleus, growth cones and MN axons interact with SMN. Some of these have been reported to act as SMA disease modifiers (Oprea et al., 2008). Actin protein levels in growth cones of SMN-deficient MNs are reduced, suggesting that it may be important in the pathology of MNs in SMA. (Rossoll et al., 2003, Ning et al., 2010). Rossoll and colleagues suggested a role for SMN in the transport of these complexes, such as hnRNP-R, Lsm and β -actin mRNA within MNs (Rossoll et al., 2002).

In MNs, SMN has been shown to associate with various molecules involved in RNA binding such as hnRNP-R, Plastin3 (PLS3) and Profilin II (Giesemann et al., 1999, Oprea et al., 2008, Chen et al., 2010, Akten et al., 2011, Fallini et al., 2011). The

RNA-binding proteins PLS3 and hnRNP-R were reported to co-localize with SMN in MNs and also associate with β -actin mRNA (Rossoll et al., 2003, Oprea et al., 2008). In addition, hnRNP-R protein was previously identified as one of the proteins involved in RNA processing, where hnRNP-R binds RNA (Rossoll et al., 2002). Interestingly, PLS3 or hnRNP-R knockdown causes axon defects similar to SMN deficiency while PLS3 or hnRNP-R overexpression led to an increase in axonal length (Rossoll et al., 2003, Oprea et al., 2008).

Profilin II is expressed predominantly in MNs; profilins are known to control β -actin dynamics and bind strongly to SMN (Bowerman et al., 2009). Furthermore, it has been shown that profilin II and hnRNP-R interact with both SMN and β -actin. Profilin II and PLS3 have been implicated in SMA actin dysregulation, where knockout of profilin II upregulates PLS3 expression in SMA mice. However, restoration of PLS3 protein and depletion of profilin II does not rescue SMA phenotype (Bowerman et al., 2009). This suggests that other actin dynamics regulators must contribute to rescue the SMA phenotype.

Silencing of the Phosphatase and tensin homolog (PTEN), known to act as a regulator of cell growth, rescued axon length defects in cultured *Smn*-deficient MNs (Ning et al., 2010). Subsequently, a study reported that PTEN depletion led to an increase in survival of *Smn*-deficient MNs (Ning et al., 2010). Recently, another study by the same group showed that systemic suppression of PTEN was able to decrease SMA severity and prolong survival in a SMA mouse model (Little et al., 2014). A single injection of self-complementary adeno-associated virus serotype 9 expressing small interfering RNA (siRNA) against PTEN (scAAV9-siPTEN) at post-natal day 1 resulted in a 3-fold extension of the life span of *SMN Δ 7* mice,

revealing that PTEN can act as a disease-modifier in SMN Δ 7 mice (Little et al., 2014).

1.3 Plastin3

Fimbrins/plastins are a family of extremely conserved actin-bundling proteins (Arpin et al., 1994). The discovery of PLS3 as a potential disease modifier has opened up new prospects of understanding the exact mechanism of SMA pathology (Ackermann et al., 2012) and has shed light on the role of PLS3 in protecting against the disease. Eukaryotic cells express a large amount of actin-binding proteins (Delanote et al., 2005). According to Bretscher & Weber many biological processes involve a dynamic network of proteins in eukaryotic cells within the actin cytoskeleton, including cell motility, cell substrate adhesion, intracellular transport, endocytosis and exocytosis, cytokinesis, and cell morphology (Bretscher and Weber, 1980). Furthermore, increasing evidence has shown that actin cross-linking or actin-bundling proteins may control actin dynamics in addition to structuring the cortical actin cytoskeleton (Giganti et al., 2005).

1.3.1 Human Plastin Gene

Two ubiquitous plastin isoforms have been identified in humans, (L and T). The T isoform has been found in cells of all solid tissues, which have replicative potential such as fibroblasts, epithelial cells, melanocytes, and endothelial cells. In contrast, the L isoform is expressed in the hematopoietic cell line only (Lin et al., 1993).

The T-plastin and L-plastin isoforms were mapped to chromosomes X and 13, respectively. Each gene was composed of 16 exons and was approximately 90 kbp in size. The T-plastin and L-plastin proteins have 83% identical C-terminal amino acids

(Otto, 1994). A potential calcium-binding site was localised to the N terminal part of the protein (De Arruda et al., 1990, Castresana and Saraste, 1995). The *PLS3* gene is a protein-coding gene encoding a T-plastin, PLS3. Alternate splicing results in multiple transcript variants of PLS3 (Ackermann, 2011). Several diseases are associated with PLS3, including cutaneous T-cell lymphoma and osteoporosis (Yokobori et al., 2013).

1.3.2 Plastin3 protein

In 1979 a family of 70 kDa cytoplasmic polypeptides named plastins were discovered (Matsudaira and Burgess, 1979). There are three types of plastins, PLS1 (I-plastin), PLS2 (L-plastin) and PLS3 (T-plastin), all of which are differentially expressed and have similar modular structural domains (Lyon et al., 2013). They are evolutionarily conserved, versatile modulators of the actin cytoskeleton and thus play an important part in cell migration, adhesion and endocytosis (Lyon et al., 2013).

As a general rule it can be concluded that members of the plastin family have been identified in cellular regions containing polarized actin filaments and in areas with high actin filament turnovers (Arpin et al., 1994). In addition to solid tissues with replicative potential PLS3 is also found in muscle, brain, spinal cord, uterus, and the oesophagus (Delanote et al., 2005).

1.3.2.1 Plastin protein structure

PLS3 can be subdivided into three modules a pair of actin-binding domains (ABDs), variable spacer domains, and a regulatory domain (Castresana and Saraste, 1995). Furthermore, there are two N-terminal EF hand motifs which are variably implicated

in Ca^{2+} binding, and two C-terminal actin binding domains (ABDs) each made up of two calponin homology (CH) domains (Delanote et al., 2005) (Figure 1.4).

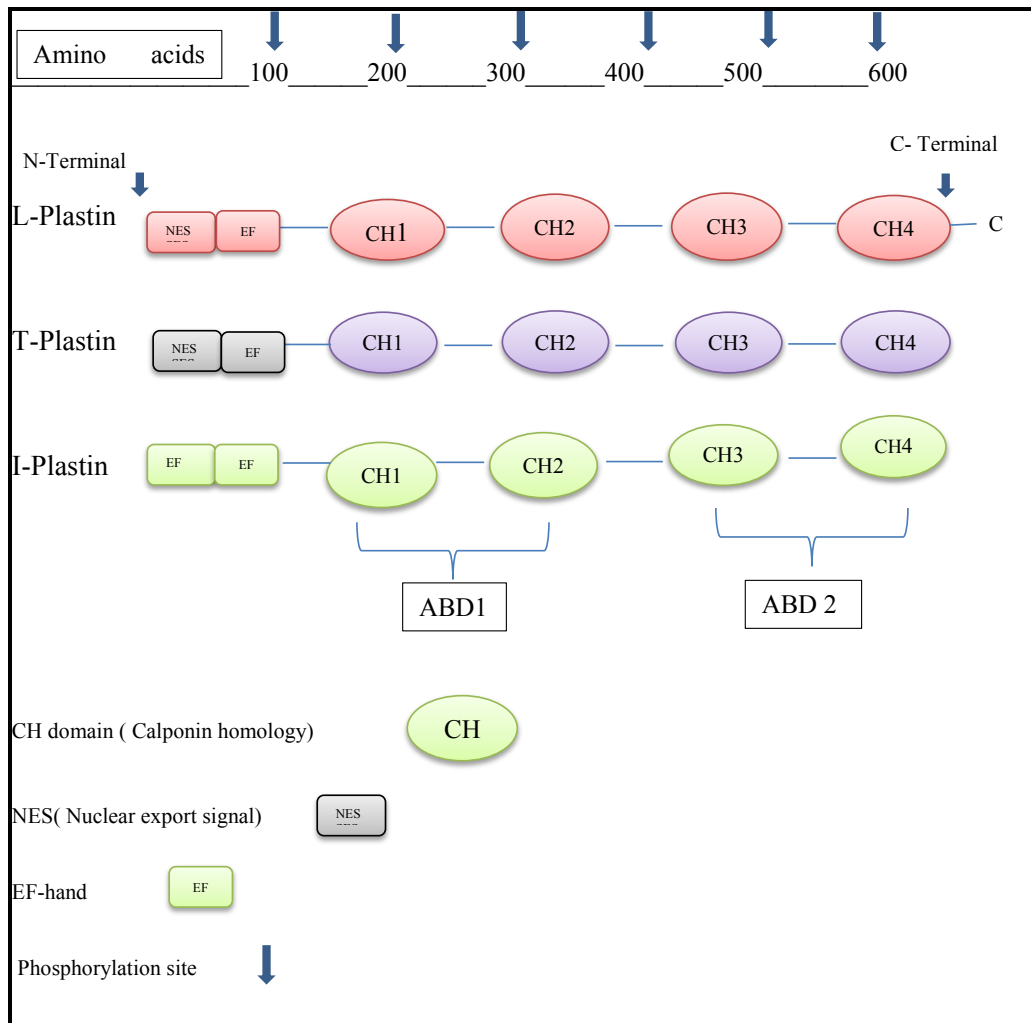


Figure 1.4. Plastin protein isoforms structure

Domain organization in plastin isoforms of different types. A scale (in amino acids) is drawn on top of the figure. The protein has an N-terminal headpiece of ~100 amino acids containing two EF-hand Ca^{2+} -binding motifs and two actin-binding domains (ABDs) consisting of ABD1 (residues ~100–300) and ABD2 (residues ~400–600), and each ABD contains two calponin-homology (CH) domains. Note that human T- and L-plastin contain a nuclear export signal (NES). Modified from (Delanote et al., 2005)

The process of bundling actin filaments requires that each ABD bind to an individual actin filament (Volkman et al., 2001). As a consequence, plastin without the

C-terminal ABD (ABD2) cannot bundle actin (Giganti et al., 2005). The CH domains are shared by signalling and cytoskeletal proteins such as dystrophin, α -actinin, and spectrin. The tandem CH domain is generally involved in actin binding (Delanote et al., 2005).

Giganti and colleagues recently investigated the calcium sensitivity of T-plastin (Giganti et al., 2005). The two calmodulin-like calcium-binding domains in plastins, known as EF hands, suggest that actin-binding or other functions of plastins could be regulated by calcium. The somewhat weak homology in the calcium binding domains of T- and L-plastin isoforms could suggest that their actin binding activities are differentially regulated by calcium (Namba et al., 1992). This activity could contribute to the maintenance and assembly of the actin cytoskeleton of plasma membrane protrusions *in vivo*.

1.3.3 The role of PLS3 in SMA

PLS3 is a key regulator that restores processes depending on actin dynamics in SMA MNs. Three studies in humans have shown a correlation between PLS3 expression and SMA severity in pre- and post-pubertal females, with higher levels of PLS3 being associated with a reduction in SMA disease severity, even after correcting for SMN copy number (Oprea et al., 2008, Hao et al., 2012, Yanyan et al., 2013).

A transcriptome-wide differential expression analysis performed on total RNA from lymphoblastoid cells taken from SMN1-deleted patients with discordant disease outcomes revealed a significant association between disease severity and PLS3 expression. Further analysis of blood samples from a diverse population of SMA patients and from healthy controls confirmed this association (Oprea et al., 2008).

Stratified analysis of blood samples from SMA type I, II and III patients demonstrated that only post-pubertal females show an inverse correlation between circulating PLS3 and SMA severity, suggesting a role for PLS3 as an age- and sex-specific modifier of SMA. The researchers suggest that this sex-specific effect may be due to PLS3 mapping to Xq23 (Stratigopoulos et al., 2010, Bernal et al., 2011).

Since PLS3 expression has been shown to be modulated by SMN in SMA patients with *SMN1* deletions and in zebrafish and down regulation of *Pls3* over time when *Smn* is depleted early *Pls3* depletion may affect the development of motor neuron axons in these models and may affect motor neuron survival, contributing to the SMA phenotype.

In a *smn*^{-/-} zebrafish model, *Pls3* mRNA splicing and protein stability are unaffected, but *Pls3* protein levels overall are reduced, therefore, SMN is involved in translation of *Pls3*, although the mechanism is unknown. Partially restoring *Pls3* in these animals rescued presynaptic defects and motor behaviour, suggesting that *Pls3* is not merely a correlate of SMN expression, but instead plays a significant role in SMA pathology (Hao et al., 2012). Unfortunately, a full restoration of *Pls3* was not possible and therefore researchers were unable to test the effect on survival (Hao et al., 2012). *Pls3* orthologs act as SMN modifier genes in *C. elegans* and *Drosophila*, possibly involving endocytosis and RNA processing pathways (Dimitriadi et al., 2010).

PLS3 overexpression stabilised axons, reduced axon pruning and counteracted the poor connectivity seen in SMA NMJs (Ackermann et al., 2012). PLS3 overexpression also increased the number of vesicles available in the presynaptic pool. Ubiquitous overexpression modestly improved survival and motor function in

SMA mice. Hence, this may be a potential therapeutic target for SMA (Ackermann et al., 2012).

Investigations into the function of PLS3 have begun to shed light on its role in protecting against SMA. Removal of the ability of PLS3 to bind to or cross-link actin filaments, by deleting one or both of its actin binding domains (ABD1/2) (Fig. 1.4), did not fully prevent the molecule from rescuing *smn*^{-/-} mutant zebrafish. This suggested that PLS3 function might involve an additional role unrelated to its interaction with actin. Further deletion studies determined that the EF hand motifs, and specifically their interaction with Ca²⁺ ions, are essential for PLS3 function in MNs development (Lyon et al., 2013). This is supported by the observation in SMA of calcium dysregulation in the growth cone during motor axon outgrowth (McGivern et al., 2013).

A crucial role of Pls3 down regulation in the pathology of SMA was proposed. It is important to demonstrate whether the restoration of Pls3 expression can rescue the axonal phenotype in spinal motor neurons cultured from a clinically relevant mouse model of SMA. In addition to furthering understanding of the function of Pls3, a potential use for Pls3 in gene therapy for SMA can be proposed. Since PLS3 expression has been shown to be modulated by SMN in SMA patients with *SMN1* deletions and in zebrafish. However, there are some limitations that need to be taken in to consideration to achieve successful therapy for SMA, such as a clinical time-window. This will need to combine therapies that both target pathways that rescue MN function and increase SMN levels or any other modifier such as PLS3.

The use of PLS3 overexpression to extend lifespan demonstrates that PLS3 is a disease modifier of SMA and a good potential therapeutic target for SMA. PLS3 can

be used in a gene therapy approach but may be required to be delivered in combination with other disease modulators to give meaningful rescue to motor neurons and alleviate the disease phenotype sufficiently. Meeting these challenges will likely be essential to cure SMA, particularly in its most severe cases.

1.4 Models of SMA

To clarify the complex functions of the SMN protein and the pathology of SMA, the availability of SMA experimental models has been important. Several different models have been used, each with advantages and disadvantages to study different aspects of the disease.

1.4.1 *In vitro* Models of SMA

In vitro models are mainly useful for early testing of potential therapies and understanding molecular pathways involved in SMA. SMA has been modelled *in vitro* using various techniques, including siRNA transfection or transduction with the aim of decreasing SMN protein levels in neuroblastoma spinal cord NSC-34 cells and primary neurons to disease levels (Acsadi et al., 2009). Purified motor neurons from the SMN mouse model have also been used as an *in vitro* model of SMA (Ning et al., 2010). SMA type I fibroblasts have been widely used as experimental tool in the field of SMA research (Coovert et al., 1997).

1.4.2 Animal models of SMA

In addition to cell models, animal models have also been used to understand the role of SMN protein in SMA (Rossoll et al., 2003, McGovern et al., 2008)}. The disruption of *SMN* has been investigated in various species including, *Drosophila*, *C. elegans*, zebrafish and mouse, with the aim of modelling the disease and gaining

fundamental knowledge about the molecular role of SMN protein (Schmid and DiDonato, 2007). All SMA models have a single *Smn* gene which corresponds to human *SMN1* (*hSMN1*), the absence of which is lethal in all model organisms (Schmid and DiDonato, 2007); therefore, all models are heterozygous or have an insertion of human *SMN2* to compensate for the loss of *Smn*.

1.4.2.1 Mouse Models

Mouse models are used extensively in studying SMA and the role of SMN protein. Mice have a single copy of the *Smn* gene, which is homologous to the human *SMN1*, and the knockout of this gene was shown to result in embryonic lethality (Schrang et al., 1997). Frugier et al. (2000) used the Cre-LoxP system to generate a transgenic mouse with a deletion of exon 7 in the *Smn* gene (Frugier et al., 2000). Mice expressing Cre-recombinase specifically under the Neuron-Specific Enolase (NSE) promoter were crossed to exon 7 knockout mice. This approach resulted in offspring with an average survival age of 25 days, suggesting that the pathological phenotype seen in the disease is a result of the SMN protein deficiency in MNs (Jao et al., 2012).

Another approach to study SMA was through introducing the human *SMN2* gene along with its own promoter into *Smn*^{-/-} mice by microinjecting a plasmid construct into mouse oocytes (Schrang et al., 1997). The expression of SMN2 in these mice rescued the embryonic lethality; however, the mice developed SMA phenotype (Foust et al., 2010). The severity of this phenotype depended on the gene copy number introduced into the mice; i.e. the most severe phenotype was observed in those with a low SMN2 gene copy number (Monani et al., 2000).

In a different study, *Smn*^{-/-}, *SMN2*^{+/+} model was used to indicate whether the lack of

smn protein is responsible for the maintenance or development of MNs (Schmid and DiDonato, 2007). In particular, it was seen that low levels of smn led to excessive cell death in the telencephalon region and to some morphological defects in the spinal nerves of the mutant embryos (Schmid and DiDonato, 2007).

Previously, it was shown that the level of SMN Δ 7 was higher in Type I and Type II compared to Type III SMA patients (Sreedharan et al., 2008); therefore, it was important to check if the presence of SMN Δ 7 had a positive or a negative effect in SMA patients. To do so, a *Smn*^{-/-}, *SMN2*^{+/+}, *SMN Δ 7*^{+/+} triple transgenic model was generated (Le et al., 2005) by introducing a *SMN* complementary deoxyribonucleic acid (cDNA) lacking exon 7 in a severe SMA mouse model described previously (Frugier et al., 2000). The lifespan of these mice increased up to 13 days compared to the 5 day lifespan of the *Smn*^{-/-}, *SMN2*^{+/+} mice, suggesting that the expression of the SMN Δ 7 protein is not detrimental (Le et al., 2005). This triple transgenic mouse model is widely used for therapy development for SMA (see details in section 1.5).

Table 1-3 Mouse models of SMA

Genotype	Lifespan	Phenotype	Reference
Smn ^{-/-} ; SMN2 ^{+/+}	(4-5) Days	Severe defects in skeletal muscle and spinal cord MNs	(Hsieh-Li et al., 2000)
Smn ^{-/-} ; SMN2 ^{+/+} ; SMN Δ 7 ^{+/+}	(13) Days	Less severe than the Smn ^{-/-} ;SMN2 model	(Le et al., 2005)
Neuron specific SMN mutation	(25) Days	Denervation of muscle and tremors	(Frugier et al., 2000)
Muscle specific SMN mutation	(33) Days	Paralysis due to severe muscle defects	(Cifuentes-Diaz et al., 2001)
Smn ^{-/-} ; SMN2 ^{+/+} ; SMN (A111G) ^{+/+}	> 1 year	Moderate model	(Madabusi, 2012)

Although with these mouse models the key feature is neuronal defects there are also other changes caused in other organs by reduced SMN protein which indicates that SMN is important for different cell types in addition to MNs. Table 1.4 shows other organs affected by lack of SMN.

Table 1-4 Summary of multi-system phenotypes observed in SMA mouse models

Organ	Mouse model	Observation	Reference
Muscle	SMN2 and severe Taiwanese	Molecular changes occur in muscle prior to, and independent of, motor degeneration	(Monani et al., 2000) (Mutsaers et al., 2011)
	SMN2	Premature differentiation of skeletal muscle satellite cells and failure to efficiently form multinucleated myotubes	(Hayhurst et al., 2012)
	SMN Δ 7	Decreased muscle fiber size	(Hayhurst et al., 2012)
	Conditional mouse model, restoration of SMN in muscle	SMN has a role in muscle growth	(Martinez et al., 2012)
	Muscle-specific SMN knockout mouse	Muscle-specific loss of SMN caused muscle necrosis with a dystrophic phenotype, led to muscle paralysis and death	(Cifuentes-Diaz et al., 2001)
Heart	SMN Δ 7	Cardiac defects apparent at P7; bradycardia developed by P14	(Bevan et al., 2010)
	SMN2, SMN Δ 7	Cardiac remodeling initiates embryonically and mice have physiological defects such as a drastically reduced heart rate; interventricular septum remodeling initiated at P3–P5	(Shababi et al., 2010b)
	Severe Taiwanese	Interventricular septum thinning	(Gogliotti et al., 2012)
	Severe inducible mouse model	Significant bradycardia from P3	(Gogliotti et al., 2012)

Lung	Severe Taiwanese	Discoloration of the lungs suggestive of atelectasis or pulmonary infarction	(Schreml et al., 2013)
Intestine		Intestinal edema	(Schreml et al., 2013)
Liver	Severe Taiwanese	Reduced expression of hepatic Igfals mRNA in neonatal liver	(Hua et al., 2011)
	Liver-specific SMN knockout mouse	Liver-specific loss of SMN was embryonically lethal, and resulted in iron overload and liver atrophy	(Vitte et al., 2004)
Bone	Mild Taiwanese	Osteoporotic bone phenotype with decreased levels of osteoblast differentiation markers	(Hsieh-Li et al., 2000) (Shanmugarajan et al., 2009)
Pancreas	2B1	Abnormalities in pancreatic islet cells with more α cells than β cells; fasting hyperglycemia, hyperglucagonemia, and glucose resistance	(Bowerman et al., 2012)

1.5 Therapeutic strategies in SMA

Currently there is no cure for SMA, and therefore treatment is centered on increasing the quality of life of patients through relieving secondary symptoms. To date the pathogenesis of SMA is not completely understood (James and Sumner, 2011) however a lot of effort has been made in trying to understand the molecular mechanism of the disease in order to target different therapeutic approaches (Coady and Lorson, 2010, James and Sumner, 2011, Castro and Iannaccone, 2014). Based on the evidence that SMN expression levels correlate with the disease severity in

humans (Farag, 2010), therapeutic development for SMA is mainly focused on increasing SMN protein levels by: (a) enhancing *SMN2* gene transcription (Rossoll et al., 2003); (b) modulating *SMN2* splicing (James and Sumner, 2011) ; (Figure 1.5)(c) gene therapy based SMN replacement using viral vectors. Other therapeutic procedures focus on neuroprotection and cell replacement (Farag, 2010).

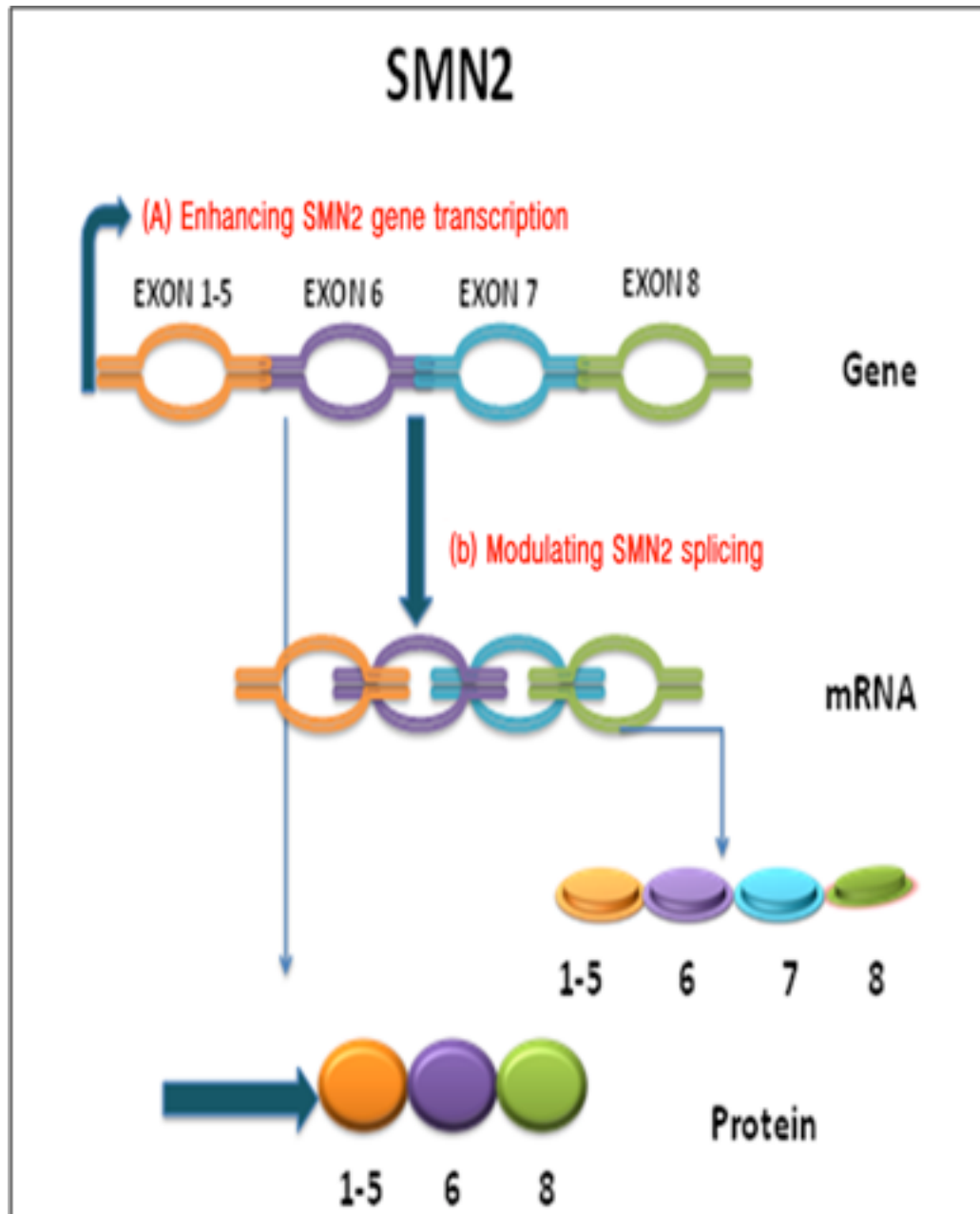


Figure 1.5. Therapeutic strategies for SMA

The diagram represents the action of ASOs or small nucleotide drugs to: (A) Increase the expression levels of SMN transcripts and SMN protein (both full length and truncated). (B) Activate inclusion of exon 7 upon splicing of SMN2 pre-mRNA therefore increasing SMN

In clinical trials, various compounds have been tested for their ability to increase *SMN2* expression (Chang et al., 2001, Coady and Lorson, 2010, James and Sumner, 2011). Some successes have been achieved in finding molecules that have the ability to increase the amount of full length SMN protein produced from the remaining *SMN2* gene (Castro and Iannaccone, 2014). However, to date, therapies have been tested in type II and III patients but not the most severe type I patients. Therapies have showed marginal or no success in milder phenotypes, and therefore are unlikely to have any effect on the more severe cases (Coady and Lorson, 2010).

The biggest limitation to SMN therapy is the optimal window for therapy and the delay in diagnosis. Previous SMN replacement studies have shown that delaying treatment significantly reduces the phenotype rescue and the survival improvement. However early diagnosis is difficult in human patients, leading to a delay in treatment. This shows that there is a need to identify other therapeutic strategies which could be used in conjunction with SMN replacement which could potentially reverse some of the damage done in early stages of disease. This will be addressed further in section 1.3.3.

1.5.1 Drug Treatment Approaches

1.5.1.1 Enhancing *SMN2* gene transcription

Increasing the expression of the SMN protein from *SMN2* gene is one of the main potential therapeutic strategies that could be used in targeting the disease (Chang et al., 2001). Familial studies performed on individuals suffering from SMA (type II and III) showed that both gene copies of *SMN1* were absent in these patients as well as in asymptomatic patients (Rossoll et al., 2003). In each of the studied families, there was an individual who was lacking the *SMN1* gene but showed no SMA

symptoms. It was shown that these individuals had 4-5 copies of *SMN2* gene and showed normal levels of SMN protein in their fibroblasts (Rossoll et al., 2003). In other studies involving mice, it was found that *Smn*^{-/-} mice with two cDNA copies of the *SMN2* gene inserted, showed a longer survival time (about 3 weeks after birth) (Pagliardini et al., 2000).

A screening assay of more than 555,000 compounds was performed in order to identify small drugs that would interact with the FL-SMN2 mRNA, and the results yielded two compounds - Trichostatin A (TSA) and Sodium Butyrate, which were found to increase the levels of SMN protein in patient-derived cells (Jarecki et al., 2005). These two compounds belong to a class of histone deacetylase (HDAC) inhibitors resulting in the up regulation of about 2% of the total genes (Bowerman et al., 2009). Further experiments showed that TSA treatment in *Smn*^{-/-}; *SMN2*^{+/+} transgenic mice resulted in a 1.5 to 2 fold increase in SMN protein levels and *SMN2* transcript levels; however, the effect on life span was not reported (Sendtner, 2010). On the other hand, sodium butyrate was shown to increase the lifespan of *Smn*^{-/-}; *SMN2*^{+/+} transgenic mice by 4-5 days compared to untreated littermates (Chang et al., 2001).

Another HDAC inhibitor, suberoylanilide hydroxamic acid (SAHA) was found to reduce motor neuron degeneration and increase SMN protein levels, which resulted in about a 30% increase in the lifespan of the *Smn*^{-/-}; *SMN2*^{+/+} transgenic mice (Riessland et al., 2010).

Valproic acid, an HDAC inhibitor used as an anti-epileptic drug (Brichta et al., 2003, Sumner et al., 2003), was shown to elevate the SMN protein levels in SMA fibroblast cells by either activating the SMN promoter or preventing the exon 7

skipping of SMN2 during transcription (Vance et al., 2009). In a study where the $smn^{-/-}$; SMN2^{+/+} transgenic mice were used, valproic acid was reported to normalize motor function, reduce motor neuron death and increase spinal SMN protein levels (Strong et al., 2007).

Another study using the drug D156844, which belongs to the 2,4-diaminoquinazoline family, revealed an increase in the survival of the SMN Δ 7 mice by 21-30% by enhancing overall SMN expression in these mice (Butchbach et al., 2010).

In summary, these drugs rely on increasing the SMN protein expression through increase of the endogenous SMN2 gene in the CNS which can ameliorate the phenotype and survival of SMN Δ 7 SMA mice if expression is induced prior to motor neuron loss.

1.5.1.2 Modulating SMN2 splicing

The quite unique genetic situation of SMA patients, who lack functional SMN1 but carry the misspliced SMN2 copy gene, creates the possibility of correcting SMN2 splicing by antisense oligonucleotides or drugs (Wirth et al., 2015).

The antisense oligonucleotides (ASO) approach has been used to silence specific splicing sites in SMN pre-mRNA, specifically targeting SMN2 exon 7, to increase the amount of FL-SMN produced. When administered systemically, ASO was shown to increase the inclusion of exon 7 in SMN2 in liver, kidney and muscles. However, ASOs do not cross the blood brain barrier (BBB) so no change in the SMN protein level was observed in the spinal cord (Saunders et al., 2009). Therefore, in order to prove the potential therapeutic benefits of this approach in SMA, a new method of delivering ASO across the BBB was required (Long et al.,

2008). In order to overcome the BBB problem the ASO is injected directly into the CNS so that it does not have to cross the BBB.

The discovery of intronic splicing silencer N1 (ISS-N1) is a promising target for ASO therapy. One study assessed a morpholino (MO) oligomer against ISS-N1 and delivered this MO to SMN Δ 7 SMA pups at postnatal day 0 (P0) by intracerebroventricular (ICV) injection. Significant survival from 15 days to more than 100 days was observed when administered early on. Delayed CNS MO injection showed moderate efficacy and mild survival advantage, suggesting that early CNS ASO administration is essential for SMA therapy. Following ICV treatment an increase of F-L SMN2 transcript as well as SMN protein in neural tissue was observed, but only minimally in peripheral tissue. This suggests that SMN CNS increases will have a major impact on SMA, and an early increase of the SMN level will result in correction of motor phenotypes (Porensky et al., 2012).

In another recent study [Singh NN et al](#), reported that an antisense oligonucleotide, ISTL1 was able to fully correct SMN2 exon 7 splicing and restore high levels of SMN in SMA patient cells through sequestration of ISS-N2 (Singh et al., 2015).

Hydroxyurea is another compound that was used with an aim to modulate the SMN2 splicing pattern allowing the formation of the full length protein (Grzeschik et al., 2005). A study where lymphoblastoid cells from SMA patients were subjected to different concentrations of hydroxyurea showed that a high dose of the compound significantly increased the level of full length SMN mRNA and therefore the levels of SMN protein (Grzeschik et al., 2005). The exact mechanism of how hydroxyurea works in SMA is still unknown, however, it is thought that it changes the SMN2 splicing pattern giving rise to the full length SMN protein (Lorson and Androphy,

2000, Coady and Lorson, 2010).

1.5.2 Gene therapy

Gene therapy is the transfer of nucleic acid to repair or replace aberrant genes to stop or cure disease. An advantage of using gene therapy is the selective and long-term treatment of cells and tissues (Davidson and Breakefield, 2003). Various gene therapy approaches have been developed such as using viral vectors, which aim towards efficiently transferring the desired therapeutic gene to the target tissue (Davidson and Breakefield, 2003).

A trans-splicing system has been employed to introduce more full length SMN from *SMN2* by introducing therapeutic RNA with the SMN1 sequence and antisense RNA to block the splice site to discourage splicing of exon 7. In studies by Coady and Lorson (2010) and Lorson and Androphy (2000), *Smn*^{-/-}; *SMN2*^{+/+} neonate mice were injected with plasmids co-expressing these two RNAs, resulting in a 70% increase in the survival of these mice compared to untreated controls (Lorson and Androphy, 2000, Coady and Lorson, 2010).

Introduction of naked DNA for gene therapy is not as efficient or targeted as viral delivery. Several viral vectors have been developed, each having distinct advantages and disadvantages. The two most common viral vectors undergoing pre-clinical trials in treatment of SMA are derived from lentivirus and adeno-associated virus (AAV) (Passini et al., 2010).

1.5.2.1 Lentivirus Gene Therapy

Lentiviruses (LVs) belong to the Retroviridae family that possesses a positive single-strand RNA genome, which integrates into the host genome. There are several

serotypes of lentivirus that have the ability to infect different natural hosts, including humans and primates (Azzouz et al., 2004a, Nanou and Azzouz, 2009).

Lentiviral vectors (LV) can transduce both dividing and non-dividing cells, including neurons (Azzouz et al., 2002), which make them particularly appealing for neurodegenerative diseases where the target cell is the neuron. They are efficiently used for gene transfer into various types of neurons in the nervous system (Martin-Rendon et al., 2001). The integration into the host genome results in stable and long-term gene expression (Deglon et al., 2000). LV has a large cloning capacity, about 8-10 kb of gene sequence can be packaged, allowing larger genes to be targeted for gene therapy. Another key feature of LV is the low immunogenicity, decreasing potential for adverse reactions.

The major disadvantage of LV vectors is safety concerns due to random integration; integration into the host genome has the potential for oncogenesis (growth of tumorous cells). The safety and design of these vectors are being refined and could be widely used for human clinical trials in the near future (Valori et al., 2010). An ongoing phase I/II trial for a Parkinson's disease treatment (ProSavin Oxford BioMedica) has shown a long-term safety profile using an LV vector (Palfi et al., 2014). Another disadvantage is that the large-scale production of LV is not possible with the current technology.

1.5.2.2 Adeno-Associated Viruses (AAV)

Adeno-associated viruses (AAV) belong to the Parvoviridae family of viruses. They are small, single-stranded, nonpathogenic DNA viruses that require a helper virus (such as adenovirus) for their replication and life cycle completion (Davidson and Breakefield, 2003).

Similar to LVs, AAV vectors can transduce both dividing and non-dividing cells with good efficiency, making them attractive for neurodegenerative diseases. In addition, AAV show no or little immunogenicity, making them very safe. There are several serotypes of AAV which target different tissues with varying efficiency and stability of expression (McCarty et al., 2001). In adults, a luciferase reporter gene delivered via different AAV serotypes produced low expression with AAV2, 3, 4 and 5; moderate expression with AAV1, 6 and 8; and high expression with AAV7 and 9 (Zincarelli et al., 2008). Interestingly, AAV9 can strongly transduce MNs in the Central nervous system (CNS) following intravenous administration, along with other tissues such as cardiac tissue and skeletal muscle (Benkhelifa-Ziyyat et al., 2013). AAV vectors have stable gene expression levels even though they do not integrate into the host genome.

A drawback to the use of AAV vectors is their small cloning size capacity (about 4.5 kb) and their inability to efficiently transduce all cell types (Davidson and Breakefield, 2003).

In addition to conventional AAV, self-complimentary viruses are also being used commonly in gene therapy. AAV can be altered to package two copies or dimeric inverted repeats of small genomes, resulting in self-complementary adeno-associated virus (scAAV) (McCarty et al., 2001). The scAAV vector is more efficient in cell transduction due to faster initiation of gene expression, as the need for complementary strand synthesis is bypassed.

1.5.3 Gene therapy approaches in SMA disease

1.5.3.1 Lentivirus–Mediated Gene Therapy in SMA

Sustained SMN protein expression is important for cell survival, therefore, a lentivirus-based gene therapy approach to replace the SMN1 gene in SMA patients is an attractive therapeutic strategy (Nanou and Azzouz, 2009).

Equine Infectious Anaemia Virus (EIAV)-based LVs were found to transduce MNs upon intramuscular injection. Azzouz and colleagues expressed SMN cDNA in lentiviral vectors in order to restore SMN protein levels in cell culture (Azzouz et al., 2004b). The virus was injected in various muscles (the gastrocnemius and facial muscle) of SMA mice and showed transduction of ~70% MN leading to reduction of motor neuron death and extended life span by an average of 20–38% (Azzouz et al., 2004b).

Earlier reports of gene therapy using LV in an SMA mouse model showed promising results, with successful retrograde delivery of SMN-expressing lentivirus (pseudotyped with rabies G protein) to motor neurons in the lumbar spinal cord after delivery into multiple muscles (Azzouz et al., 2004b). Although the LV showed promising results, the use of the lentiviral vectors in the clinic is limited due to their risk of insertional mutagenesis. However, they are very useful for *in vitro* studies due to their long-term expression and high efficiency of transduction. Another major obstacle is the production of the large amount of virus required for muscle delivery in human therapeutics (Arnold and Burghes, 2013).

1.5.3.2 Adeno-Associated Viruses (AAV) - Gene Therapy in SMA

Several studies have proven the efficacy of AAV vectors in animal models of neurodegeneration (Table 1-5). Valori et al. (2010) used scAAV9 to introduce SMN into an SMA model: scAAV9 vectors were injected into mice at postnatal day 1, which resulted in a 100% rescue of treated animals, increasing life expectancy from 27 to over 340 days (median survival of 199 days) (Valori et al., 2010). The scAAV9 therapy allowed for a complete correction of motor function, prevented MN death and rescued the weight loss phenotype close to normal (Valori et al., 2010).

Another study by Foust et al. (2010) showed that scAAV9 was able to infect approximately 60% of MNs when it was inserted intravenously to newborn mice (Foust et al., 2010). In this study, scAAV9 was delivered to postnatal day 1 SMA mouse pups resulting in the rescue of motor function and increased the life span (Foust et al., 2010). Moreover, following intramuscular injection of AAV9 it has been shown to cause a widespread transduction in the spinal cord and peripheral tissues (Cearley and Wolfe, 2006, Benkhelifa-Ziyyat et al., 2013). A unique transduction characteristic for AAV9 is the variation in capsid surface regions (DiMatteo et al., 2008), which may increase cell entry allowing more vector genomes to enter the cell and therefore more protein to be produced (Cearley and Wolfe, 2006).

Interestingly, it was shown that AAV9 might be used in human patients after successful transduction of MNs in neonatal macaques (Foust et al., 2010). Recently, transgene expression in neurons in both the CNS and PNS was generated after fetal administration of AAV9 to macaques (Mattar et al., 2012). It was also reported that the AAV9 vector genome was able to undergo axonal transport (Cearley and Wolfe,

2006). This may be useful in severe SMA cases in order to provide prenatal treatment.

Table 1-5 Successful preclinical studies using the vector-based gene therapy approach for SMA treatment

Vector	Mouse model	Routes/sites of administration	Dose	Timing Post-natal day	Impact on survival (increase)	Ref.
EIAV-SMN	SMN Δ 7	IM: Hindlimb, gastrocnemius, diaphragm, muscles (facial, intercostal, tongue)	4.0 -7.0 \times 10 ⁸ TU	2	20%	(Azzouz et al., 2004b)
scAAV9-SMN		IV: Temporal facial vein IV or ICV	5.0 \times 10 ¹¹ vg	1	Complete rescue	(Foust et al., 2010)
scAAV9-SMNopti		IV: Temporal facial vein	1.0 \times 10 ¹¹ vg	1	400%	(Valori et al., 2010)
		IV: Temporal facial vein	4.5 \times 10 ¹⁰ vg	1	1350%	(Dominguez et al., 2011)
		IM: triceps muscles gastrocnemius and Limbs	7 \times 10 ¹⁰ vg	1	1260%	(Benkhelifa-Ziyyat et al., 2013)
SMN2 Trans-Splicing Vector	(<i>smn</i> ^{-/-} , <i>hSMN2</i> ^{+/+})	ICV	1.14 \times 10 ¹² (plasmid copies)	1	75%	(Coady and Lorson, 2010)
SMN Trans-Splicing/IGF-1 Dual Vector	SMN Δ 7	ICV	10 μ g (plasmid DNA)	2	Trans-splicing: 50% IGF: 75% Dual: 100%	(Shababi et al., 2010a)
scAAV8-SMN		ICV: Lumbar intraparenchymal	1.7 \times 10 ¹⁰ vg	0	880%	(Passini et al., 2010)
AAV8-SMN		ICV: Lumbar intraparenchymal	5.0 \times 10 ¹⁰ vg	0	230%	(Passini et al., 2010)
scAAV9-SMN		ICV	1 \times 10 ¹¹ vg	2	475%	(Shababi et al., 2015)

Adapted from (Tam et al., 2014)

1.6 Clinical trials

Many of the successful preclinical therapeutic studies have been translated into clinical trials. However, to date none of the treatments have proven to be effective for all SMA types (Passini et al., 2010, Wadman et al., 2012a). A number of drug compounds that have been tested in early clinical trials based on neuroprotective effects seen in preclinical studies, such as gabapentin, showing mixed results. One clinical trial in Italy showed that gabapentin was a potent treatment for SMA when tested on 120 type II or III SMA patients for 12 months (Merlini et al., 2003). On the other hand, a placebo-controlled clinical trial with type II or III SMA in the United States showed no improvement in 84 patients (Miller et al., 2001).

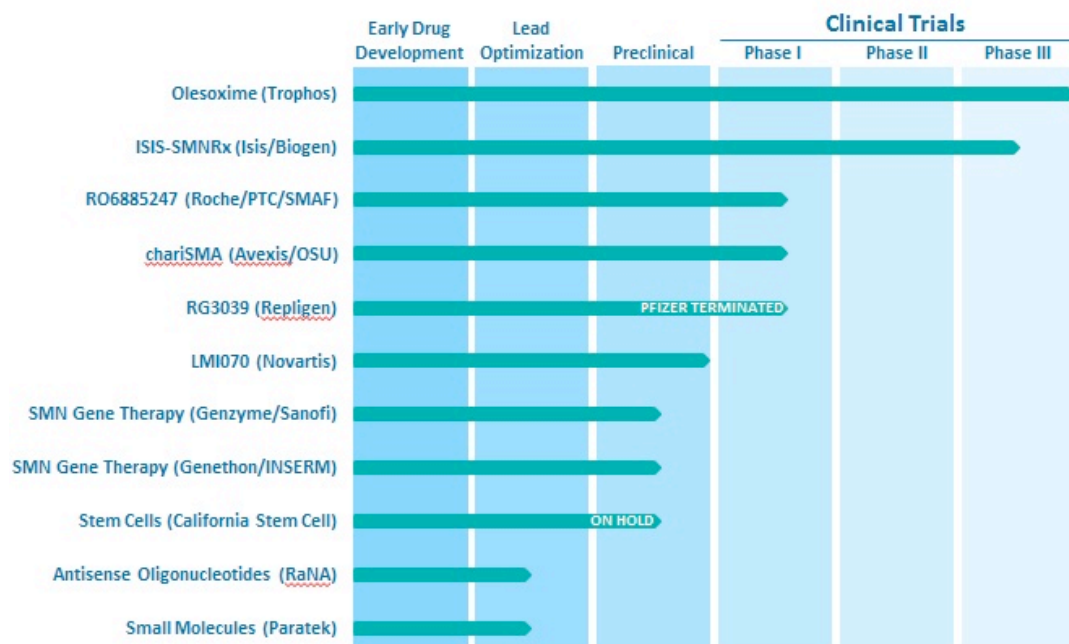


Figure 1.6. SMA therapeutics pipeline as of February 2015

Current pre-clinical and clinical trials in progress for SMA therapies. Drug name and company shown (Taken from SMAfoundation.org)

Several clinical trials are currently ongoing (

Figure 1.6), and showing promising results. Of particular interest is the drug Olesoxime, a mitochondrial pore modulator. Trophos Pharmaceuticals has shown promising results in large, multicentre clinical trials with Olesoxime. They are currently finishing phase 3 clinical trials and initiating the regulatory process of manufacture.

A gene therapy clinical trial based upon the pre-clinical work by Foust and colleagues (Foust et al., 2010) is beginning phase I trials using scAAV9 in SMA type I patients. The primary objective of this study is to evaluate the safety and efficacy of scAAV9.CB.SMN, which aims to replace the missing SMN1 (ClinicalTrials.gov Identifier: NCT02122952).

Recently, ISIS Pharmaceuticals has completed Phase I and proceeded to a Phase II clinical trial of ISIS-SMNRx, an ASO designed to increase SMN protein expression by restoring exon 7 inclusion in SMN2 transcripts (Clinicaltrials.gov ID: NCT01839656). A total of 28 patients have been recruited, 15 with type II SMA and 13 with type III SMA and will receive SMNRx as a single-dose treatment administered intrathecally (Mulcahy et al., 2014).

1.7 Project Aims

The aim of this thesis is to investigate the role of PLS3 as a therapeutic target for SMA. The *PLS3* gene will be modulated using viral vectors to mediate neuroprotection in experimental models of SMA.

The first stage will assess the expression pattern of Pls3 in the SMN Δ 7 mouse model, to explore the changes in Pls3 expression when SMN is depleted. Once this has been established, a lentiviral vector will be used to overexpress PLS3 and evaluate the neuroprotective effects of PLS3 in MNs isolated from SMN Δ 7 mice.

Secondly an AAV9 vector will be used to overexpress *PLS3* in the CNS *in vivo* in the SMN Δ 7 mouse model. The aim will be to determine whether PLS3 overexpression can improve SMA survival and rescue the disease phenotype within the CNS.

This study is part of a large programme of work with the ultimate goal of taking these viral vectors to the clinic to identify specific therapeutic targets for SMA.

The project specific aims can be summarised as follows:

- 1-Assess the expression pattern of Pls3 in SMN Δ 7 mouse model
- 2-Evaluate the neuroprotective effects of PLS3 in an *in vitro* model of SMA (purified MNs).
- 3-Generate a pre-clinical proof-of-concept using adeno-associated vector serotype 9 (AAV9) encoding PLS3 in SMN Δ 7 mouse model of SMA.

CHAPTER 2: MATERIALS AND METHODS

2.1 Materials Equipment

The list of the main equipment used in this project is given in (Appendix 1).

2.1.2 Reagents and chemicals

All the analytical grade chemicals, solvents, consumables and reagents were supplied by Thermo Fisher Scientific Inc. (Loughborough, UK) or Sigma (Cambridge, UK).

2.1.3 Buffers and solutions

All the solutions, dyes and in-house prepared buffers used for different experiments are listed with their ingredients in the text below.

2.1.4 Cells and media

All cell lines used in this study with their relevant information are listed in Table 2.1.

Table 2-1 List of Cell lines used in this study

Cell line	Full name	Culture medium
HEK293T cells	Human embryonic kidney cell line	Dulbecco's modified Eagle Medium (DMEM)
NSC34 cells	A hybrid mouse motor neuron-neuroblastoma cell line	

2.1.5 Ethics statement

All *in vivo* experiments were regulated under the UK Home Office Animals (Scientific Procedures) Act 1986. With the approval from the University of Sheffield Ethical Review Sub-Committee, and the UK Animal Procedures Committee (London, UK), the Studies in this project were conducted under Project License (40/3640).

Table 2-2 List of Primary Antibodies used

Target Protein	Host	Supplier	Cat No.	Use	Dilution
Primary Antibodies					
Human PLS3	Rabbit	Abcam	ab45769	WB + IF	1:500
Mouse PLS3	Rabbit	Aviva	ARP56623_P050	WB	1:500
α -Tubulin	Mouse	Calbiochem	Cp06	WB	1:1000
GFP	Chicken	Abcam	ab13970	IHC + IF	1:200
β -actin	Rabbit	Abcam	ab8227	WB	1:2000
GABDH	Mouse	Calbiochem	CB1001	WB	1:2000
AAV VP1,2,3	Rabbit	ARP	03-61084	WB	1:250
NeuN	Mouse	Millipore	MAB377	IF	1:500
CGRP	Mouse	Abcam	ab47027	IF	1:500

Table 2-3 List of Secondary Antibodies used

Target Protein	Host	Supplier	Cat No.	Use	Dilution
Secondary Antibodies					
Rabbit-A568	Goat	Invitrogen	A11036	IF+IHC	1:1000
Mouse-A594	Goat	Invitrogen	A1105	IF + IHC	1:2000
Mouse-A350	Goat	Invitrogen	A11045	IF	1:2000
Mouse-A488	Goat	Life tech	A11017	IF	1:2000
Chicken-A488	Goat	Life tech	A-11039	IF	1:2000
Mouse-HRP	Goat	Bio-Rad	170-6516	WB	1:3000

2.1.6 Maps of the LV and AAV Plasmids

The Maps of the LV-PLS3 Plasmid and AAV-PLS3 used in this project are given in Appendix 2.

2.1.7 DNA Preparation

All the plasmid DNAs were generated with QIAprep Spin Miniprep (QIAGEN, 27106) and QIAGEN Plasmid plus Mega (QIAGEN, 12981) kits, according to manufacturer's protocol and eluted in nuclease free water (NF-H₂O) or elution buffer (EB). During viral production all ultra-centrifugation steps were performed by using the Optima L-100K Ultracentrifuge (Beckman Coulter). The plasmid DNA concentrations were measured using the Nanodrop1000 (Labtech), (ND-1000 v3.2.1 software). The plasmid purity and exact band size were detected by electrophoresing the samples on 1% agarose gels. Then the gels were visualized using the GENi imaging machine (Syngene, 12834038).

2.1.8 Protein extraction and quantification:

Protein extraction was accomplished by cell lysis solution (RIPA buffer) which is composed of 50 mM Tris-HCl pH 8, 150 mM NaCl, 2 mM (ethylenediaminetetraacetic acid, Melford) EDTA, 1% Igepal CA630 (Sigma) and 0.1% sodium dodecyl sulphate (SDS) (Sigma), supplemented with 1% Protease Inhibitor Cocktail (Sigma). The cell pellet was resuspended in 50-150 μ L of the lysis solution and incubated for 30 minutes on ice to lyse the cell. The cell debris was separated from the protein content by centrifugation at 13,000 g for 10 minutes, and then the supernatant was transferred into a clean 1.5 ml tube.

The extracted protein was measured by Bicinchoninic Acid Protein Assay (BCA) kit (Fisher). As per the manufacturer's guidelines eight serially diluted protein standards in addition to 10 μ L of (one in ten) diluted samples were added separately and in duplicates to the aliquoted BCA working reagent. Reagent A was added to reagent B in a 50:1 ratio, then aliquoted into a 96-well plate in a quantity of 100 μ L per well. The plate was incubated for 30 minutes at 37 °C. During incubation copper II in the working reagent was reduced by the proteins of the samples and standards to copper I, which interacts with the bicinchoninic acid and forms a purple-blue complex. A spectrophotometer plate reader can detect the absorbed light by this complex at 570 nm. The protein quantity is directly proportional to the absorbance value. Using the Excel programme (Microsoft), the absorbance values of a set of standard dilutions were plotted against their known concentrations in order to construct a reference standard curve. The unknown protein concentration of each sample was determined against the diluted standard curve value of Bovine Serum Albumin (BSA), based on the equation of the standard curve. To calculate the actual protein concentration in each sample, the results were multiplied by ten, which was the dilution factor.

2.1.9 Spectrophotometry

Fluorescence measurements were performed using a FLUOstar Omega plate reader (BMG Labtech) for all the assays that require microplate reader for either UV/Vis absorbance measurements. Using a Varian Cary Eclipse spectrofluorimeter the Fluorescence measurements were recorded.

2.2 *In Vitro* Experimental Work

2.2.1 Cell Lines and Cell Culture

HEK293T cells, a human embryonic kidney cell line, were used for transfection, western blots and LV/AAV production. The cells are immortalized by the adenoviral E1A/E1B protein and express the SV40 large T antigen. A hybrid mouse motor neuron-neuroblastoma cell line, NSC34 cells (Cashman et al., 1992), was used for transfection and western blots. All cell lines, were cultured in tissue culture flasks (CELLSTAR, Greiner, Germany) in (DMEM with 4.5 g/L Glucose, L-glutamine, without Na Pyruvate, Lonza) supplemented with 10% fetal calf serum (FCS, Biosera), 100 U/ml of penicillin and 100 µg/ml streptomycin (penicillin G sodium and streptomycin sulphate in 0.85% saline, Invitrogen). The cells were incubated at 37 °C in a CO₂ incubator with 95% humidified and 5% CO₂ air environment. Twice a week the culture media were refreshed. Once the cells reached around eighty percent confluency they were ready to be either harvested or passaged. All experiments were performed on passage 15-25 cells. For AAV production HEK293T cells were used in order to produce higher viral titres. Primary motor neurons from SMNΔ7 mouse embryos were kindly provided by Dr. Ke Ning (University of Sheffield) as described below.

2.2.2 Primary Motor Neuron Culture

Primary motor neurons were purified from the spinal cords of embryonic day 13 (E13) mouse embryos and cultured at 37 °C with 5% CO₂ at 95% humidity. Briefly, 10 mm coverslips were coated overnight at 4 °C with 5% poly-DL-ornithine hydrobromide 1x 500 mg dissolved in 10 ml Borate buffer 0.15 M pH 8.35, filtered through 0.22 µm sterile filter (Sigma, p-8638) in 35 mm dishes with 4x10 mm rings

(Greiner bio-one, 627170). Hank's Balanced Salt Solution (HBSS) (Sigma, H8264) was used to wash out the poly-ornithine before coating the coverslips again with 2.5 µg/ml laminin (Invitrogen, 23017-015) that was prepared by diluting 0.75 mg/ml laminin stock in 50 mM Tris pH 7.4, in HBSS. A pregnant mouse was sacrificed using Schedule 1 method of cervical dislocation at E13 and the embryos were collected. Dissected spinal cords were placed into dissection buffer (Beta-Mercaptoethanol – 10nM concentration (β-ME) (Invitrogen, 313500) in HBSS). The cells were suspended for 15min at 37 °C with 0.1% trypsin for MNs – (Worthington, TLR3-3707). Trypsin inhibitor – Sigma, 500mg dissolved in 49ml HBSS and 1ml of 1M HEPES (Sigma, T-6522) and filtered through a 0.22 µm sterile filter then was used to deactivate trypsin. P75 panning antibody – p75 NGF receptor antibody (Abcam, ab8877) monoclonal antibody against extracellular domain of p75 was used at a concentration of 1:5000 in 10 mM Tris, pH 9.5 to pre coat the plate before placing the cell suspension in order to select motor neurons. The primary motor neurons were detached by depolarizing solution (30 mM KCl + 0.8% NaCl, while the unattached cells were washed off with Neurobasal- medium (NB medium) GIBCO (Invitrogen), 1x Glutamax-1, 2% horse serum, 1x B27 with 0.2 µM β-ME). The primary motor neurons were plated on the pre-coated coverslips at concentration of 2000-5000 cells/coverslip in Gibco NB supplemented with 2% of B27 (Gibco, 12587-010), 1% glutamax (GIBCO, 35050), 2% (v/v) horse serum donor (Linaris, SHD3250YK), 100 U/ml of penicillin and 100 µg/ml streptomycin, 0.2 µM β-ME and 0.5 mM L-glutamine (GIBCO, 35050), and incubated for 24 hours before transduction at 37°C in a humidified incubator with 5% CO₂.

2.2.3 Generation of Viral Plasmids

The human gene of interest (*PLS3*) containing a Kozak sequence (GCCACC) was sub-cloned, using appropriate sites in the destination expression viral plasmids; SIN-PGK-cPPT-WHV (Addgene, 12252) plasmid for the LV viral plasmids or pAAV CMV MCS (Addgene, 46954) for the AAV viral plasmids) with ampicillin resistance property (Figure 2.1). The LV /AAV viruses encoding for the reporter gene green fluorescent protein (GFP) were generated within our laboratory group prior to starting the project. The concentration of LV-GFP was 2.45 E8 vp/ml and 1.93 E11 vp/ml for AAV- GFP. The bacterial cell stocks which express these vectors were kept at -80°C in 30% glycerol. They were incubated in LB Broth (LBb) (Merck Millipore, 1102850500) with the suitable antibiotic (Carbenicillin (Carb) (substitute for Ampicillin) 50 µg/ml) (Sigma, C3416) or (Kanamycin, 50 µg/ml (Sigma, K4000). All constructs were sequenced by Core Genomic Facility, Medical School at the University of Sheffield (Appendix 3).

2.2.3.1 PLV-PLS3

A lentiviral Vector (LV) expressing PLS3 was generated by extracting the PLS3 gene from pcDNA3.1-PLS3-V5/His6 Vector, provided by Prof. Dr. Brunhilde Wirth, (Institute of Human Genetics, University Hospital of Cologne, Germany) and cloned into the lentiviral Vector SIN-PGK-cPPT-GDNF-WHV.

Briefly, the lentiviral Vector SIN-PGK-cPPT-GDNF-WHV was isolated out of the glycerol stock, and purified using miniprep kit (QIAGEN), GDNF was cut out using *Bam*HI and *Xho*I. To linearize the plasmid 1-3 µg of the extracted plasmid DNA was digested by mixing it with 0.5µl *Xho*I (NEB, R0146), 0.5µl *Bam*HI (NEB, R0136), 2

μl NEB buffer 3 (NEB, B7003), 2 μl of 10x BSA; (NEB, B9001), and topped with nuclease-free water (NF-H₂O) up to a total of 20 μl . The mixture was incubated for 2 hours at 37°C. Then at 1:4 ratio 4 μl DNA loading buffer blue (BioLine, bio37045) was mixed with 12 μl of the digestion mixture then the mixture was loaded on 1% agarose gel. The samples were electrophoresed at 120 V for 1hr. The band corresponding to the plasmid backbone was isolated and purified using (QIAquick) gel extraction kit according to the manufacturer's protocol (QIAGEN). The final DNA sample was eluted in 50 μl of elution buffer (EB). The PLS3 insert was digested out of the pcDNA3 vector. After a restriction digest with the same enzymes and gel electrophoresis, the isolated insert was purified from the gel. PLS3 fragment was ligated into the linearized LV-vector, using T4 DNA Ligase (NEB, M02025). The required concentration of the insert was calculated according to the equation below:

$$\text{Weight of insert (ng)} = \text{weight of vector (ng)} \times \frac{\text{Size of insert (kbp)}}{\text{Size of vector (kbp)}} \times \text{molar ratio} \frac{\text{Insert}}{\text{vector}}$$

Then 30ng of vector was used at vector to insert molar ratio of 1:3 and 1: 6. 0. Around 1-50ng of ligation mixture was used to transform NEB 5-alpha Competent *Escherichia. coli* (*E. coli*) (High Efficiency) (BioLabs, C2987I) by incubating 100 μl of cells on ice for 30 minutes. Heat-shock at 42 °C was applied for 30 seconds and the tubes were incubated on ice for 2 minutes. A volume of 0.9ml of preheated broth with Catabolite repression (S.O.C) medium (Sigma-Aldrich, S1797) was added to the tubes and incubated at 37 °C for 1 hour with shaking at 225-250 rpm. The cells were plated on selective media (Lysogeny broth agar plates supplemented with 50 $\mu\text{g/ml}$ carbenicillin), 200 μl of the transformation mixture was plated and incubated

at 37 °C overnight. The purified plasmid DNA from the colonies were analyzed by restriction analysis and sequenced. PGK promoters were used: PGK forward: 5-GGGAATTCCGATAATCAAC-3 and PGK reverse: 5-CCTTCGCTTTCTGGGCTCA-3. The reaction contained 100 ng of vector DNA and 10pmol of the primer (Table 2.4). Sequencing service was provided by Core Genomic Facility, Medical School the University of Sheffield (Appendix3). Megaprep of the ligated construct from the transformed NEB 5-alpha cells was prepared and stored at -20 °C.

2.2.3.2 PAAV-PLS3

A self-complementary adeno-associated virus (scAAV9) expressing PLS3 was generated by extracting the PLS3 gene from pcDNA3.1-PLS3-V5/His6 vector and cloning into scAAV CMV GFP (VPK-418-DJ: AAV-410, Cell Biolab ICN) between restriction sites *Bam*HI and *Xba*I. Firstly, PLS3 was amplified using forward and reverse primers as follow: the polymerase chain reaction (PCR) mix was prepared by mixing 1µl of DNA template, 400 nM of each primer; Forward primer PLS3-*Bam*HI-FOR: ACTAC GGATCC GCC ACC ATG GAT GAG ATG GCT ACC ACT and; Reverse primer PLS3-*Xba*I-REV: CGCGAC TCTAGA TTA CAC TCT CTT CAT TCC C; 10 µl of FIREPol 5x Master Mix and topped up to 50 µl with NF-H₂O. The PCR mixture was run on a GS2 thermal cycler (G-Storm). According to the following program: first the temperature was set for 3min at 95°C then each cycle was started with denaturation for 30sec at 95 °C, annealing at 60 °C for 30sec and elongation for 30 sec at 72 °C, and DNA was amplified in 35 cycles. An extra elongation period at 72 °C for 7 minutes was made and finally held at 4 °C. The PCR product was extracted and treated with the appropriate enzymes *Xba*I (NEB, R0146S) and *Bam*HI (1µl *Xba*I, 1 µl *Bam*HI, 4 µl buffer4, 4 µl H₂O and all the

DNA) and incubated for 2 hours at 37 °C. Then it was ligated into *Bam*HI- *Xba*I digested scAAV-CMV full vector and transformed into competent *E. coli* cells.

For the conventional AAV-PLS3 vector, the *PLS3* gene was extracted from pcDNA3.1-PLS3-V5/His6 plasmid and cloned into pAAV CMV MCS.

Firstly, PLS3 was PCR amplified as above, using primers: PLS3-*Eco*RI-FOR: GAT GCC GAATTC CAG CGT GCC ACC ATG GAT GAG ATG GCT ACC ACT and; PLS3-*Xba*I-REV: AGCAA TCTAGA TTA CAC TCT CTT CAT TCC C. The PCR product was treated with restriction enzymes *Eco*RI and *Xba*I and subcloned into *Eco*RI-*Xba*I digested pAAV CMV MCS vector. After ligation the mixture was transformed into NEB 5- alpha competent *E. coli* as described above. The picked clones were analysed by restriction analysis as explained in section (2.3.3.2) and the purified plasmid DNA was sequenced. The primers for sequencing anneal to the CMV promoter and are represented in Table 2.4:

Table 2-4 Sequencing primers for PLS3 constructs

Gene	Primer Sequence	Concentration
scAAV CMV FW:	TCATATGCCAAGTACGCCCC Binds within CMV promoter/enhancer region	100 nM
scAAV-FW:	TCGTGACCCCTAAAATGGGC Binds before the promoter region	100 nM
scAAV-PolyA REV:	GCATCGAGTCAGGTCAGCTT	100 nM
PLS3seq1 FW:	CCACCATGGATGAGATGGCT	100 nM
PLS3seq2 FW	TTTGAGGGCTGGGAAACCTC	100 nM
PLS3seq3 FW:	CCTGCAAGATGCCCTGGTAA	100 nM
PLS3seq4 :	TGATGGGCAGGGGAATGAAG	100 nM

The reaction contained 100ng of vector DNA and 10 pmol of each primer (Table 2.4). Core Genomic Facility, Medical School, at the University of Sheffield provided the sequencing service (Appendix 3). Megaprep of the ligated construct from the transformed NEB 5-alpha cells was prepared and stored at -20 °C. All the details were done as above (see section 2.3.3.2).

2.2.3.3 LV viral production LV-PLS3

For lentiviral production 3×10^6 HEK293T cells per 100mm² dish were plated and transfected after 24 hours of plating with a mix of four plasmids: pMD.2G: plasmid encoding the vesicular stomatitis virus G (VSV-G) envelope, pCMVDR8.92; packaging plasmid encoding all the viral genes needed in trans, SIN-W-PGK; transfer plasmid containing (PLS3) and pRSV-Rev; plasmid encoding the rev protein of Human Immunodeficiency Virus (HIV)-1. Viral production was performed as previously described (Deglon et al, 2000). Briefly, the DNA mixture was prepared by mixing 3 µg of pRSV-Rev, 13 µg of pCMVΔR8.92, 13 µg pMD. G and 13 µg of SIN-W-PGK-PLS3 or SIN-W-PGK-GLE1 in 0.25 M CaCl₂. The mixture was then added drop-wise to an equal volume of 2x HBS buffer pH 7.1 and allowed to stand for 20 minutes at room temperature. The mixture was added to the cells and incubated for 6 hours at 37 °C. Then the media was replaced with fresh media (10 ml) and the cells were incubated for three days. At 72 hours post transfection, the viral supernatant was harvested, filtered through 0.45 µm filter and concentrated by ultracentrifugation for 90 minutes at 19,000 rpm and at 4 °C.

The viral pellet was suspended in 1.8 ml Phosphate buffered saline (PBS) supplemented with 1% Bovine Serum Albumin (BSA) (Sigma), divided into 50 µl aliquots and stored at -80 °C. Finally, Lentiviral titration was performed by Enzyme

Linked Immunosorbent Assay (ELISA) which targets HIV-1 p24 antigen (ZMC No. 0801111, ZeptoMetrix Corporation) as described below.

2.2.3.4 Lentiviral titration by ELISA

Lentiviral titration was performed by ELISA, which targets HIV-1 p24 antigen (ZMC No. 0801111, ZeptoMetrix Corporation) according to the manufacturer's protocol. The Microplate wells were coated with a monoclonal antibody specific for the p24 gag gene product of HIV-1. Samples and standards were added to the plate and were incubated for two hours to allow the antigen capture and recognition by the antibody. Substrate solution was added and the reaction was stopped by acidification thereby obtaining a yellow colour. Within 15 minutes optical density was read for each well at 450nm using a microplate reader. The density of the colour is proportional to the amount of HIV-1 p24 antigen present. The absorbance values of a set of standard dilutions from 1/500 to 1/1562500 were plotted (Table 2.5). The viral particle number in each sample was determined against the diluted standard curve. The amount of viral protein determined by the assay was converted into the number of viral particles. According to the manufacturer 1ng/ml of p24 corresponded to 1.2×10^4 transducing Units (TU) per ml. This was used for final titre calculations. The titre was presented as Transducing Units per ml (TU/ml), which is equivalent to the functional viral particles per ml. The absorbance values of a set of standard dilutions were plotted (Table 2.5). The viral particles number per ml of each sample was determined against the diluted standard curve values, based on the following calculations.

Table 2-5 Absorbance, P24 and serial dilution values for LV-PLS3 titration

Dilution series	Mean Absorbance	p24 (pg/ml)
100	0.438	30.41
500	0.235	14.73
2500	0.143	5.01
12500	0.086	0.15
62500	0.0575	67.99
312500	0.4555	12.77

$$\text{P24 antigen concentration in the viral stock (ng/ml)} = \frac{\text{Optical density (OD)} \times \text{dilution factor}}{1000}$$

This was used for final titre calculations. Eg. The highest dilution, (1: 312500) was converted to undiluted reading of 12.77 pg/ml. Then the concentration of p24 antigen was multiplied by dilution factor to get its concentration in the stock sample (12.77x312500 =21,250,000 pg/ml of p24). According to the manufacturer's protocol, 1ng/ml of p24 corresponds to 1.2×10^4 TU per ml. Therefore to convert ng/ml to TU/ml= 21,250 ng/ml x 1.2×10^4 TU/ml = 2.55×10^8 TU/ml (Table 2.6).

Table 2-6 Titres of LV-PLS3 stock

Samples	Absorbance	P24 concentrations	Titre TU/ml
1	0.0575	67.99	2.55×10^8
2	0.4555	12.77	2.44×10^8

The unconcentrated vector has been produced at high titre, which is suitable for *in vitro* applications.

2.2.3.5 AAV9 Viral production of AAV-PLS3

The AAV-PLS3 virus was prepared in house by the aid of the technical support of our lab group. A small scale AAV production for each vector was performed in order to test whether the PLS3 cassette could be successfully packaged into the AAV virion, prior to large-scale production.

Large-scale viral vector stocks of AAV-PLS3 were generated by polyethylenimine (PEI), (PEI; iodixanol; 5xPBS-MK, pH 7.0) cell transfection method with a ratio 3:1 ($\mu\text{g PEI}/\mu\text{g DNA}$). 30 confluent dishes of HEK293T cells around 80-90% cultured in 15 cm dishes, in DMEM (10 % FBS, 1% pen/strep), 20 ml per plate were co-transfected with the following plasmids: 13 μg of vector plasmid (AAV9-PLS3)/AAV2/9 packaging plasmid and 26 μg of the helper plasmid (pDGM6). 33 μl of PEI (1 $\mu\text{g} / \mu\text{l}$) = 33 μg of DNA complex was added carefully to a single plate and distributed well by delicate agitation. Five days (120 hours) post transfection the supernatant was collected and treated with Benzonase (Sigma, E1014-5KU) at a concentration of 250 unit/ μl for 2 hours at 37°C, during incubation the medium was mixed every half hour. Cell debris was removed by a short centrifugation (3850 x g/ 3-5 minutes, Sigma 3-16PK, rotor 11180) in 8x 50 ml tubes, then the supernatant was transferred to the top part of the Nalgene filtering unit (0.22 μm vacuum filter – Thermo Scientific Nalgene Rapid-Flow filter unit), (Thermo scientific, 595-3320) and vacuum was applied. The resulting clarified supernatant containing virus was concentrated in Amicon Ultra-15 Centrifugal 100K Filters (Millipore, UFC910024). Supernatant containing virus was added onto the filter and centrifuged 3800 x g at 4 °C until the volume of 27-28 ml is achieved. In order to purify the viral particles iodixanol gradient ultracentrifugation using Quick-Seal 39 ml tubes (Beckman Coulter #344326) was used. Several different percent concentrations of iodixanol

solutions (Sigma Aldrich, D1556-250ML), (stock is 60% w/v) were prepared in PBS with 2.5 mM KCl (PBS-MK) and 1mM MgCl₂ (

Table 2-7). The PBS-MK stock was 5 x concentrations. All the solutions were prepared as follows in 50 ml tubes:

Table 2-7 Preparation of Iodixanol solutions

Percentage Iodixanol	Iodixanol 60% stock	5M NaCl	5 x PBS-MK (See below)	H₂O	Phenol Red
15%	12.5 ml	10ml	10 ml	17.5 ml	-
25%	20.8 ml	-	10 ml	19.2 ml	100 µl
40%	33.3 ml	-	10 ml	6.7 ml	-
54%	45 ml	-	-	5 ml	100 µl

The centrifuge was set to 18⁰C. A tube with sterile PBS (for topping up the virus layer) was prepared. The iodixanol solutions were layered very carefully using disposable syringes (Figure 2.1).

Then the tubes were transferred to the type 70 Ti rotor (Beckman Coulter) at 69,000 RPM for 1 hour 20 minutes at 18⁰C using maximum acceleration and no brake. After centrifugation, the clear fraction of the 40% layer would contain the virus. To isolate the fractions, the tubes were clamped in a retort stand and a 19-gauge needle was inserted into the top of the tube to introduce air.

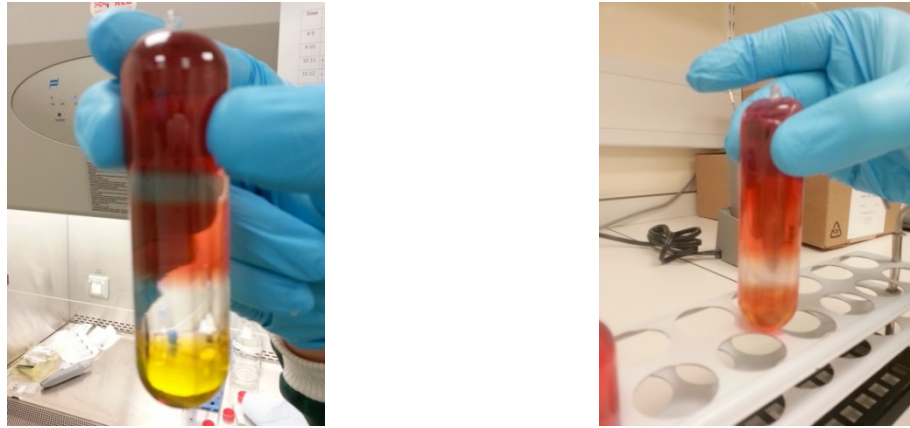


Figure 2.1. The iodixanol solutions layers.

Quick-Seal tubes prior to (left) and after (right) centrifugation. Solutions are layered very carefully using disposable syringes in the following order: 4 ml of 15% iodixanol / 1M NaCl in PBS-MK buffer (1x phosphate buffered saline (PBS), 1 mm MgCl₂, and 2.5 mM KCl). 9 ml of 25% iodixanol in PBS-MK buffer containing Phenol Red (slightly pink). 9 ml of 40% iodixanol in PBS-MK buffer. 5 ml of 54% iodixanol containing Phenol Red (slightly yellow). The space in the top of the tube is filled with PBS using syringe with a small gauge needle

Fractionation was the best method to extract the pure virus sample and separate it from debris and empty capsids. A standard 19 gauge syringe needle was inserted approximately 1 cm from the bottom of the tube with the bevel pointing upwards, and was pushed half way into the tube, towards the upper portion of the 60% iodixanol layer. Placing the needle in this manner caused slow leakage of the solution through the needle out of its other end in a drop-wise fashion. The drops were collected in samples of approximately 250-500 μ l in 1500 μ l plastic tubes. Samples were collected until the entire 40% layer and the first half of the 25% layer have been collected.

In order to assess the purity of the viral preparation, viral samples were run in SDS Polyacrylamide gel electrophoresis (PAGE) gel and the gel was stained with SYBRO RUBY (Lonza, 50562) as described below. 6 μ l of each fraction was diluted with water (1:1), combined with 4x Laemmli loading buffer (3 μ L) and was boiled

for 5 minutes at 95 °C. The viral samples were loaded onto a 10% SDS-polyacrylamide gel (Bio-Rad, Hemel Hempstead, UK) and was run at 180 V for 40 minutes. Then the gel was fixed for 20 minutes with 10% methanol / 7% acetic acid. The gel was placed into the staining container and wrapped in aluminium foil to protect from light during the staining process. The volume that was used to stain per gel was 50 ml / 8 cm x 10 cm x 0.75 mm. The gel was gently agitated at room temperature overnight. To minimize background fluorescence the gel was transferred to a clean staining dish and washed with a 10% methanol / 7% acetic acid solution for 30 minutes for three times. The stained gel was visualized using a 300 nm UV and fluorescent imaging was performed using Syngene, GENi. A western blot analysis was also performed to detect AAV viral proteins (VP) by using an antibody against the AAV capsid proteins VP1, VP2 and VP3. Fractions containing pure virus were pooled together and were considered as high quality virus prep, while the rest were considered as low quality virus prep. The Pooled AAV fractions were concentrated and desalted in the final buffer PBS/35 mM NaCl by centrifuging through Amicon Ultra centrifugal filter device.

The titre of all viral solutions was determined by quantitative polymerase chain reaction (Q-PCR) (See section 2.2.6.8) with serial dilutions of the vector plasmid DNA. HEK-293 cells at a density of approximately 10^5 / well (6-well plate) were transduced with two different volumes of the viral supernatant. Five days post transduction, protein was extracted and analysed by WB.

2.2.3.6 Quantification of AAV by real-time PCR

The standards (linearized plasmid, serially diluted tenfold; 10^{-1} , 10^{-2} , 10^{-3} , 10^{-4} , 10^{-5} and 10^{-6}) were prepared. The AAV samples were diluted in to three different

dilutions, 1 in 100, 1 in 1000 and 1 in 10,000 in water. Then master mix for each sample and standard in triplicate was Prepared (Primer Mix 1 μ L (Table 2.8), SYBR green master mix 12.5 μ L and water 1.5 μ L). 15 μ L of master mix was added to each well that will be used on plate. 10 μ L of sample or standard were added to each well in triplicate while 10 μ L of water to the negative control. The plate was sealed and centrifuged to remove air bubbles. QPCR was performed by MX3000-P Real-time PCR system (BIO-RAD), following the program below:

95 C	10 min	} 40 Cycles
95 C	30 seconds	
60 C	1 min	
95 C	1 min	
55 C	30 seconds	
95 C	30 seconds	

The titer was calculated by multiplying the dilution factor and 100 to obtain titer/ml.

Table 2-8 Primers used for qPCR

Gene	Primer Sequence	Concentration
FW:	ATT TTA TGT TTC AGG TTC AGG GGG AGG TG	100 nM
REV: Poly A R	GCG CAG AGA GGG AGT GGA CTA GT	100 nM

2.2.3.7 Designing qPCR primers

All the Primers were designed to match the following criteria: the GC content range was 40% to 60%, a primer melting temperature (MT) between 58 °C to 65 °C, amplicon product size of 50 bp to 150 bp and 20 bp to 32 bp lengths.

Then primers properties were assessed by Primer-Blast algorithm:

(<http://www.ncbi.nlm.nih.gov/tools/primer-blast/>).

2.2.3.8 Transduction of HEK293T / NSC-34 cells with LV-PLS3/AAV-PLS3

virus

HEK293T cells / NSC34 were plated at a density of 150,000-250,000 cells /well in 2 ml full medium on a 6-well plate and incubated overnight at 37°C in CO₂ incubator.

The virus volume required for transduction was calculated using the following equation:

$$\text{Volume from virus stock (ml)} = \frac{\text{Multiplicity of infection (MOI)} \times \text{no. of cells}}{\text{Viral titre}}$$

The calculated virus volume was added to each well, after the removal of 1ml of the medium from each well. After 6 hours incubation the cells were topped up with 1ml of full medium and incubated for another 3-5 days. Protein was extracted and quantified as described in section (2.2.2).

2.2.3.9 *In vitro* transduction and immunostaining of primary motor neurons

Primary motor neurons (MNs) were isolated from E13 spinal cord from controls (Smn^{+/+}; SMN2^{+/+} and Smn^{+/-}; SMN2^{+/+}), and SMA (Smn^{-/-}; SMN2^{+/+}) embryos. After 24h plating, MNs were transduced with LV-PLS3 / LV-GFP and no virus at an MOI of 20 and 40 for immunocytochemistry. The µl of the virus that must be added to transduce the cells at a specific MOI are estimated by the following formula: µls of virus= [(number of cells/well) x MOI] / titre. Transduction efficiency was assessed by counting the GFP positive cells under the fluorescence microscope after transduction with LV-GFP, and was found to be 70-80% at an MOI of 40. Plates were incubated at 37 °C and 5% CO₂ for 7days and immunostained with anti-

Tubulin and anti-PLS3. Double staining was performed with anti-tubulin (1:1000) and anti-PLS3 (1:500) for overnight at 4 °C. Then the secondary (1:200) was added for 2 hours at RT: goat anti rabbit A568 Alexa red (PLS3), goat anti mouse A350 blue (Tubulin). Images were taken by confocal microscope. The axon length was measured by ImageJ plugin NeuronJ.

2.2.3.10 Western Blot analysis

Before being denatured, the extracted protein samples were added to laemmli buffer (2% SDS, 10% glycerol, 5% 2-mercaptoethanol, 0.002% bromophenol blue & 62.5 mM Tris-HCl pH 6.8). The extracted protein samples were heated to 95 °C for five minutes in order to denature proteins. Then the samples were adjusted to 10µl with dH₂O so that the samples contained either 20 µg or 40 µg of protein, and diluted 1:1 with 2x loading buffer. The samples (20 µl) were loaded onto a 10% SDS-polyacrylamide gel, Gel casting cassette (Bio-Rad, Hemel Hempstead, UK). The gel was run at 180 V for 40 minutes. An electrical field of 120 V for 90 minutes on ice was applied to transfer the proteins onto a methanol-preactivated Polyvinylidene difluoride (PVDF) membrane (Milipore Immobilon). To check the transfer, the membrane was stained with Ponceau stain for 5 minutes. After several washes with water, the membrane was blocked with 5% non-fat milk in TBST (40.03 g of NaCl, 15.76 g of Tris base, 5 ml of Tween (Sigma) in 5 litres of dH₂O), to prevent non-specific binding of the antibodies to the membrane for 2 hours at room temperature. The primary antibody was diluted in 5% milk/TBST as described in table 2 and then the membrane was incubated with the primary antibody at 4 °C with overnight shaking (Table 2.2). After 24 hours incubation, the membrane was washed three times with TBST (15 minutes each time). After the washes, the membrane was incubated with the secondary antibody (horseradish peroxidase (HRP) conjugated)

for 2 hours at room temperature, as detailed in Table 2.3. Then the membrane was washed again three times with TBST (same conditions as before). To detect the protein of interest, the membrane was developed using ECL Plus chemiluminescence detection kit (Biological industries, 20-500-120) visualized using G-Box (Sygene). Quantification of the protein was carried out by Alpha Imager computer software using densitometry. Each western blot was also probed with an antibody (housekeeping gene GAPDH or cytoskeleton marker tubulin) to measure accuracy of protein loading per well. This provides a semi-quantitative method for normalising samples and allowing comparison but can have an error of up to 20% (Eaton et al., 2013). The density of each band was integrated and the ratio between densitometric values for each sample was obtained. The variation in protein expression was calculated by a comparison between the samples and the controls.

In addition to the above standard WB protocol applied in this study, some optimising of steps were done. For example, to test the Ab sensitivity different protein concentrations or Ab were used. Furthermore the incubation temperature was changed from 4 °C to room temperature.

In addition, PLS3 (plastin 3, T isoform) Blocking Peptide, the middle region of protein made by Aviva Systems Biology, (100 µg) (Catalog#: AAP00000) was used to enhance the antibody specificity.

2.2.3.11 Immunocytochemistry

Immunofluorescence staining was performed on HEK293T cells/ and primary motor neurons. In a 6-well plate, the cells were plated onto glass coverslips at a density of 5×10^4 cells per well. HEK293T cells were transduced for five days with LV-PLS3. Primary motor neurons were transduced for Seven days to investigate the effect of

PLS3 overexpression on axon length in WT, heterozygous, and SMA mouse embryos. After transduction, the cells were washed with Dulbecco's Phosphate Buffered Saline (DPBS), and fixed by incubating them for 15 minutes in 4% Paraformaldehyde (PFA) in PBS (pH 7.3) at room temperature. The cells were then washed once with DPBS and stored at 4 °C until the staining procedure was performed. Cell membranes were permeabilized by incubating the cells in cell staining blocking solution (0.3% Triton X-100 and 10% Goat serum in DPBS) for 2 hours at room temperature (also prevent non-specific binding of the secondary antibody). Blocking solution was removed and cells were incubated with anti-rabbit PLS3 antibody (ab45769) diluted at 1:500 in PBS overnight (Table 2.2). The next day, after three times 10 minutes washes with PBS, to remove any unbound antibody, the cells were incubated with anti-rabbit fluorescent secondary antibody with an Alexa red 568 conjugate (Invitrogen A1105) diluted at 1:200 in PBS for 1 hour in the dark at room temperature. Finally, the cells were washed again for three times for 10 minutes in PBS and were mounted on glass slides using Vectashield hard set mounting medium with diamidino-2-phenylindole (DAPI) (Vector laboratories). Confocal microscope images of chosen fields were obtained using a Leica SP5 microscope system at 63x magnification and were analysed using ImageJ software.

2.2.3.12 Real-time Quantitative-PCR for PLS3 expression

One ml of TRIzol reagent per 50-100 mg of tissue (Life Technologies, 15596-026) was added to harvest the tissues following the manufacturer's protocol. The Direct-zol™ RNA MiniPrep (Zymo research, R2052) was used to isolate of RNA. Simply, one volume ethanol (95-100%) was added to one volume sample homogenate (1:1)

in TRI Reagent. Then the samples were applied to the Zymo-Spin™ IIC Column and centrifuged for 1 minute. After transferring the column into a new Collection Tube, 400 µl Direct-zol™ RNA PreWash3 was added to the column and centrifuged for 1 minute. 700 µl RNA Wash Buffer was added to the column and centrifuged for 1 minute. To ensure complete removal of the wash buffer, the column was centrifuged for an additional 2 minutes in an empty collection tube. Then the column was transferred carefully into an RNase-free tube. 25 µl of RNase-Free Water4 was added to the column matrix directly and centrifuged at max speed for 1 minute. The eluted RNA was stored at -80°C or used immediately.

By using NANODROP1000, the concentration of extracted RNA was measured. The PCR reaction consisted of; 25 µl of PCR mix; 1 µl of DNA template, 1.34 µM of forward primer and 1.34 µM of reverse primer 0.5 µM, 10 µl of (5x FIREPol Master Mix, Solis BioDyne) and topped up with NF-H₂O to a final volume of 25 µl (Table 2.9). Real-time PCR was performed by, CFX96 Touch Real-time PCR detection system (Bio Rad, CFX96) following the program below:

50 C	10 min	} 40 Cycles
95 C	5 min	
95 C	10 seconds	
60 C	30 seconds	

The CFX Manager software was used to analyse the signal intensity and expression values were normalized to Glyceraldehyde 3-phosphate dehydrogenase (GAPDH).

Table 2-9 Primers used for Real time PCR (RT-PCR)

Gene	Primer Sequence	Conc.
FW-PLS3	PLS3- <i>EcoRI</i> -F – 5' GAT GCC GAATTC CAG CGT GCC ACC ATG GAT GAG ATG GCT ACC ACT 3'	100 µM
REV-PLS3	PLS3- <i>XbaI</i> -R – 5' AGCAA TCTAGA TTA CAC TCT CTT CAT TCC C 3'	100 µM
FW-Mouse-PLS3	PLS3mouseF 5' AATGAAGCACTGGCAGCTT	100 µM
REV-Mouse-PLS3	PLS3mouseR 5'GTGCGATTTGATTGAGCAGA	100 µM
FW-GAPDH	Forward 5'GGAAGCTCACTGGCATGGC3'	300 µM
REV-GAPDH	Reverse – 5' TAGACGGCAGGTCAGGTCCA 3'	300 µM

2.3 *In Vivo* Experimental Methods

2.3.1 Breeding and Genotyping of Transgenic Mice

All *in vivo* experimental work was performed according to the UK Home Office Animals (Scientific Procedures) Act 1986. FVB.Cg-Tg (SMN2*delta7) 4299Ahmb Tg (SMN2) 89Ahmb *Smn1*^{tm1Msd}/J SMNΔ7 mice (The Jackson Laboratory stock 005025) were used for all *in vivo* studies. These mice are triple mutant mice on a FVB background. They have two transgenes inserted, the human SMN gene lacking exon 7 and the full-length human SMN2 gene copy, while they are also lacking the murine *Smn* gene (Le et al., 2005). For breeding carrier animals were used and to detect the presence of the transgene PCR reaction was performed. At the day of birth tail clips were taken and incubated for 1 hour at 65 °C in 15 µl DNA extraction buffer (DNA extraction solution 1.0. Epicentre Biotechnologies) and then inactivated at 98 °C for 5 minutes. The PCR reaction was then performed using three primers to

recognize Smn with two different reverse primers specific for either the mutated or the wild-type gene (Table 2.10).

2.3.2 Housing

All Mice were obtained and bred under specified pathogen free (SPF) or conventional conditions. They were kept in a 12-hour dark-light photocycle with free access to water and food at a standardised room temperature of 21°C at the animal facilities of the University of Sheffield. Each cage was lined with sawdust (ecopure chips premium) and paper wool (Datesand, UK) was used as bedding material.

Table 2-10 Primers used for genotyping

Primer	Sequence	Concentration
Smn Wild-Type Reverse	5' TTTCTTCTGGCTGTGCCTTT 3'	1.34 μ M
Smn Targeted-Mutation Reverse	5' GGTAACGCCAGGGTTTCC 3'	0.5 μ M
Smn Forward	5' CTCCGGGATATTGGGATTG 3'	1.34 μ M

The PCR reaction composed of 1 μ l of template, 5 μ l PCR Mix (5x FIREPol Master Mix, Solis BioDyne) 1.34 μ M of forward primer and 1.34 μ M or 0.5 μ M of either Targeted-Mutation or wild type or reverse primer, and H₂O to a final volume of 25 μ l.

The PCR program was as follows:

- 95°C 3 minutes
 - 95°C 30 seconds
 - 52°C 30 seconds
 - 72°C 30 seconds
 - 72°C 7 minutes
 - 10 °C forever
- 

The PCR mixture was electrophoresed at 140 V for 30 minutes on a 1.5% agarose gel with 0.5 µg/uL ethidium bromide. The bands were expected to be as follows (Wild-type at 800 bp, homozygous transgenic at 500 bp and hemizygous carriers were expected to have two bands, one at 800 bp and one at 500 bp. Using GENi imaging system (Syngene) the bands were visualized.

2.3.3 Recruiting Experimental Mice

For the AAV9-PLS3 study (Chapter 5) *Mus musculus*, smn delta 7 strain (FVB background) smn^{+/+}, smn^{-/+} and smn^{-/-} litter mates were used. This is a triple transgenic model of SMA, which more closely resembles the human disease.

2.3.4 Viral Vector Delivery

At postnatal day one the animals were injected in the cisterna magna under gas anesthesia (IsoFlo, 100% w/w isoflurane inhalation vapor, Abbott, liquid) using anesthesia apparatus (Burtons). 10µl of viral vector solution was injected to each animal using a 10 µl 33-Guage Hamilton syringe (ESS Lab). A few minutes after recovery the animals were rolled in sawdust from their cage and returned to the cage with their mother. All the injections were performed by Ian Coldicott,

research technician in our group.

Table 2-11 Viral vector dose administered

Virus	Titre	Dose
AAV9-PLS3	3.89E13 vp / ml	1E10 virus particles
AAV9-GFP	1.2E13 vp / ml	2E10 virus particles

2.3.5 Behavioural and Clinical Assessment

Mice were weighed daily and observed for normal behaviours and disease onset. After day 8 mice were checked for activity levels, grooming, respiration, gait and motor skills as indicators of disease onset. When mice showed severe respiratory distress they were humanely culled by cervical dislocation.

2.3.6 Tissue Collection

When the mice were deemed ready for sacrifice they were euthanized by intraperitoneal injection of 500mg/kg of sodium pentobarbital (sodium pentobarbital, 20% w/v solution for injections, JML). Intracardiac perfusion of cold PBS containing 5 units/mL Heparin (2000 units/mL heparin, Sigma) was immediately performed for histological analysis followed by perfusion with 4% PFA using an in vivo perfusion system (AutoMate Scientific). Then the organs were collected and incubated overnight at 4 °C in 4% PFA. Only brain and spinal cord were further incubated in 30% sucrose in PBS for at least one day before being cryoembedded in optimum cutting temperature medium (OCT, Dako).

2.3.7 Histological Analysis

Using a Leica cryostat brains were sectioned at 20µm and Lumbar spinal cords were sectioned at 10µm and mounted onto slides.

2.3.7.1 Immunohistochemistry

To assess Pls3 expression (Chapter 3) in brain and spinal cord, anti-PLS3 and a DAB peroxidase substrate kit (Vector) were used. First the tissue was incubated for 20 minutes in 2% hydrogen peroxide in methanol to block endogenous peroxidase. Then the sections were washed in water for 1 minute followed by TBS for 5 minutes. Then the slides were incubated for 30 minutes with normal serum in TBS at room temperature to block any non-specific binding.

Slides were then incubated with the primary antibody, polyclonal rabbit antibody against PLS3 (Abcam) at a dilution of 1:50 in TBS for 2 hours at RT. The sections were washed twice with TBS for 5 minutes then incubated with the secondary antibody for 30 minutes at room temperature. This was followed by washes for 2x 5 minutes in TBS before incubation for 30 minutes with the ABC reagent at room temperature. Then the slides were washed for a further 2x 5 minutes in TBS and incubated for 5 minutes in diaminobenzidine (DAB) at room temperature. A final wash for 5 minutes was done before being dehydrated through 70%, 95% and absolute ethanol, haematoxylin was used for counter staining. Then the slides were placed in xylene before being mounted with coverslips using Di-N-Butyl Phthalate in Xylene (DPX) and the images were taken with Nikon microscope using NIS-Elements software (Improvision) at 40x magnification.

2.3.7.2 Immunofluorescence

Immunofluorescence was performed to stain for neuronal or motor neuronal markers (Neuronal nuclei (NeuN) and Calcitonin-gene related peptide (CGRP) respectively) as well as for PLS3 and GFP. First the slides were washed for 10 minutes 5 times with PBS before being incubated with 10% normal goat serum (NGS) and 0.3% Triton X-100 (Sigma) in PBS for 2 hours at room temperature.

For the PLS3 expression (Chapter 3) two primary antibodies were incubated together, for brain sections rabbit antibody against PLS3 (Abcam) alongside a mouse antibody against NeuN (Millipore) all diluted 1:200 in PBS and incubated overnight at 4 °C. Three washes were applied to all sections in PBS. Secondary antibodies were added, a goat Alexa fluor 594-conjugated anti-mouse antibody (Invitrogen) and a goat Fluorescein isothiocyanate (FITC)-conjugated anti-rabbit antibody (Jackson), 1:200 in PBS for 2 hours at room temperature. Then all slides were washed 3 times for 10 minutes in PBS. Spinal cord sections were stained with rabbit antibody against PLS3 (Abcam) alongside either a mouse primary antibody against the nonphosphorylated neurofilament (SMI32) or CGRP diluted at 1:200 and a goat Alexa-Fluor594- conjugated anti-mouse antibody as described above.

For AAV9- PLS3 study (chapter5), spinal cord Sections were stained with a rabbit antibody against PLS3 (Abcam) or with a chicken antibody against GFP (Abcam) alongside a mouse antibody against CGRP (Abcam), all of which were diluted 1:200 and incubated at 4 °C overnight. A goat Alexa fluor 488-conjugated anti-mouse antibody (Invitrogen), or goat Alexa fluor 488-conjugated anti chicken (Life tech) and a goat FITC- conjugated anti-rabbit antibody (Jackson) used were as secondary antibodies. They were diluted at 1:200 and incubated for 2 hours at room

temperature. The Washing and blocking steps were performed for all slides as detailed above. Vectashield hard-set mounting medium with DAPI (Vector laboratories) was used for mounting. CGRP-Positive MNs were counted to assess PLS3 transduction. Images were taken with both a fluorescence microscope (Nikon) using NIS-Elements software (Improvision) at 100x magnification which were analysed using ImageJ software and with a confocal microscope using a Leica SP5 microscope system.

**CHAPTER 3: PLASTIN3 EXPRESSION IN SMN Δ 7 MOUSE
MODEL OF SPINAL MUSCULAR ATROPHY**

3.1 Aims

This chapter aims to assess the expression of *pls3* mRNA and its corresponding protein distribution throughout the central nervous system in a SMA mouse model since PLS3 expression has been shown to be modulated by SMN in SMA patients with *SMN1* deletions and in zebrafish. In this chapter characterization of *Pls3* expression and Pls3 protein levels in a SMA mouse model (*SMN Δ 7*) at different time points of the disease were carried out to assess whether SMN dosage influences Pls3.

3.2 Introduction

PLS3 is detected in muscle, brain, spinal cord, uterus, oesophagus and preferentially expressed in mitotic cells such as fibroblasts, endothelial cells, epithelial cells, and melanocytes (Lin et al., 1993). PLS3 is highly expressed in fetal and adult human spinal cord, and is increased in rat cells during neuronal differentiation, suggesting a role in neuronal outgrowth (Giavazzi et al., 2006). Members of the plastin family have been identified in cellular regions containing polarised actin filaments, and in areas with high actin filament turnover (Delanote et al., 2005). Due to the fact that all plastin isoforms regulate the actin cytoskeleton, plastins have always been seen as cytoplasmic proteins (Lin et al., 1993). However, Delanote et al. have shown that endogenous PLS3, as well as overexpressed T- and L-plastin, had the ability to travel between the nucleus and cytoplasm in HeLa and Jurkat cells (Delanote et al., 2005).

Recently a number of studies have suggested a role for PLS3 in regulating actin turnover in SMA (Oprea et al., 2008, Hao et al., 2012). PLS3 has roles in decreasing the disassembly rate of actin, which affects actin turnover and the length of actin

filaments (Giganti et al., 2005). Given that actin is the most abundant cytoskeletal protein found within the synapses of mature neurons (Matus et al., 1983, Sato-Yoshitake et al., 1989) this activity makes PLS3 an interesting candidate for involvement in neurodegenerative diseases such as SMA. It has been reported that at the pre-synaptic terminal, actin has a crucial role in regulation and maintenance of synaptic vesicle pools, axonal vesicle trafficking, mobility of vesicles, and neurotransmitter release (Delanote et al., 2005, Giganti et al., 2005, Bowerman et al., 2009, Ackermann et al., 2012).

Therefore, actin-binding and actin-regulating proteins have an attractive regulation role of actin dynamics at the synapse, which is considered to be necessary for adequate NMJ function and maturation. Rossoll et al. (2003) reported dramatic reduction of β -actin mRNA and protein levels in cultured motor neurons isolated from a severe SMA mouse model (Rossoll et al., 2003). This disruption in the actin cytoskeleton may explain the degeneration of NMJs in the severe SMA mice which is a central event in SMA pathogenesis (Kariya et al., 2008, McGovern et al., 2008).

SMN has also been shown to undergo a shift from nuclear to cytoplasmic and predominantly axonal localisation during maturation of the human CNS (Giavazzi et al., 2006), suggesting a role for SMN in neurodevelopment (Bowerman et al., 2009). T-plastin seems to co-localize with SMN in granules throughout MN axons and growth cones (Sharma et al., 2005, Oprea et al., 2008). Both proteins have a similar cellular localisation and are believed to interact with each other, where they form a ribonucleoprotein complex (Zhang et al., 2006, Oprea et al., 2008). *In vivo*, in murine MNs, confocal microscope analysis showed co-localisation of Pls3 and Smn in granules throughout MN axons and growth cones, however *in vitro* assays showed

no direct interaction (Oprea et al., 2008). Suggesting that the interaction is indirect, possibly through complexes with other proteins, such as SMN and its binding partner hnRNP R. This complex interacts with β -actin mRNA causing translocation to the axons and growth cones of MNs (Rossoll et al., 2003).

A potential association between PLS3 and SMN has been observed in SMA families (Oprea et al., 2008, Bernal et al., 2011, Yanyan et al., 2013), and in SMA models such as *Smn* knockout zebrafish and mice (Oprea et al., 2008, Bowerman et al., 2009, Hao et al., 2012). In families with SMN mutations, siblings who were asymptomatic for SMA showed high levels of PLS3 whilst reduced PLS3 levels were reported in siblings affected by SMA, suggesting that overexpression of PLS3 can overcome the loss of SMN. Further studies in zebrafish models *in vivo* and SMA PC12 cells *in vitro* showed that high Pls3 levels increased the amount of F-actin in motor neurons, resulting in improved axon outgrowth (Oprea et al., 2008).

In this study Pls3 expression was assessed in SMN Δ 7 mice, an SMA mouse model where *Smn* is depleted (Le et al., 2005). This is a triple transgenic mouse generated by overexpression of both human *SMN2* gene (*SMN2*^{+/+}) and the *SMN1* gene lacking exon 7 (SMN Δ 7), and lacking murine *smn* gene (*smn*^{-/-}). The overexpression of human SMN genes provides a small amount of full length SMN protein but predominantly truncated, non-functional protein, as seen in human disease. The murine gene is removed to prevent murine SMN rescuing the lack of full length human SMN. Non-transgenic littermates used as control animals still have a copy of the human SMN genes, but also have both copies of the mouse gene (SMN2^{+/+}, SMN Δ 7^{+/+}, *smn*^{+/+}) therefore do not show disease.

SMN Δ 7 mice, are a well-established model of SMA (Le et al., 2005), commonly used in disease research. They display progressive muscle weakness and die on average 2 weeks after birth, mimicking severe SMA in humans.

It is not known whether levels of SMN directly influence PLS3 levels, however, it is known that PLS3 is a modifier of SMN (Oprea et al., 2008). This study will try to confirm this in the SMN Δ 7 SMA mouse model, and to determine whether this is developmentally regulated.

Both *Pls3* mRNA and Pls3 protein expression was measured at three different time points: early (P1), mid- (P5) and late stages (P10) of the disease progression, to determine whether a correlation exists between disease severity and Pls3 expression.

3.3 Results

Protein expression was examined in the brain and spinal cord, due to the location of the motor neurons. The muscle from the thigh was also collected and examined being as the motor neurons have the end plates in the muscles. The thigh muscles were chosen as this muscle is commonly affected in disease and paralysis of hind limbs is an indicator of disease progression.

3.3.1 Pls3 protein expression is downregulated in SMN Δ 7 mice

Firstly, *pls3* levels within the brain, spinal cord and muscle of SMN Δ 7 mice were compared to their wild type and heterozygous littermates (n = 6) at postnatal days 1, 5 and 10 (P1, P5, P10). Tissue homogenates were prepared from SMN2 $+/+$, SMN Δ 7 $+/+$,*smn* $+/+$ (defined as wild type) (WT), heterozygous

SMN2^{+/+},SMN Δ 7^{+/+},*smn*^{+/-} (defined as carrier or HET) and SMN2^{+/+}, SMN Δ 7^{+/+},*smn*^{-/-} (defined as SMN Δ 7 or KO). RNA and protein were extracted from tissue, and Pls3 expression was measured by western blot and qPCR.

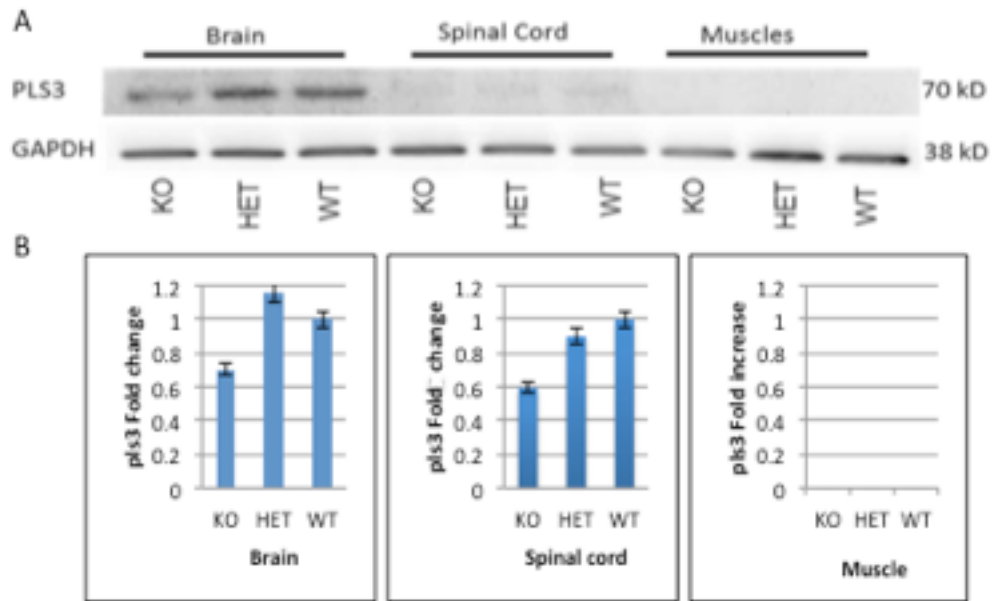


Figure 3.1. Pls3 protein levels in postnatal day 1 SMN Δ 7 mice

(A) Representative image of Western blot showing pls3 protein expression in brain, spinal cord and muscle tissues from wild type (WT), heterozygous (HET), and SMN Δ 7 (KO) P1 neonate mouse pups. The membrane was probed with mouse anti-PLS3 antibody; GAPDH was used as the house keeping control (n=3). (B) Densitometry for Pls3 fold change: brain, spinal cord and muscle (left to right panels). WT, HET and KO pups (n=3). Error bars represent (SEM)

At postnatal day 1 there was no statistically significant difference between genotypes for Pls3 protein levels in the brain, spinal cord or in thigh muscle (Figure.3.1B). None of the genotypes showed detectable Pls3 protein in muscle and only low detection in the spinal cord (Figure.3.1A). This suggests that Smn levels do not appear to affect Pls3 levels at P1. There was no discernible difference between protein levels in any of the genotypes at this age, which correlates with the lack of phenotype in P1 pups. The KO pups were phenotypically indistinguishable from their WT littermates in the first 48 hours after birth.

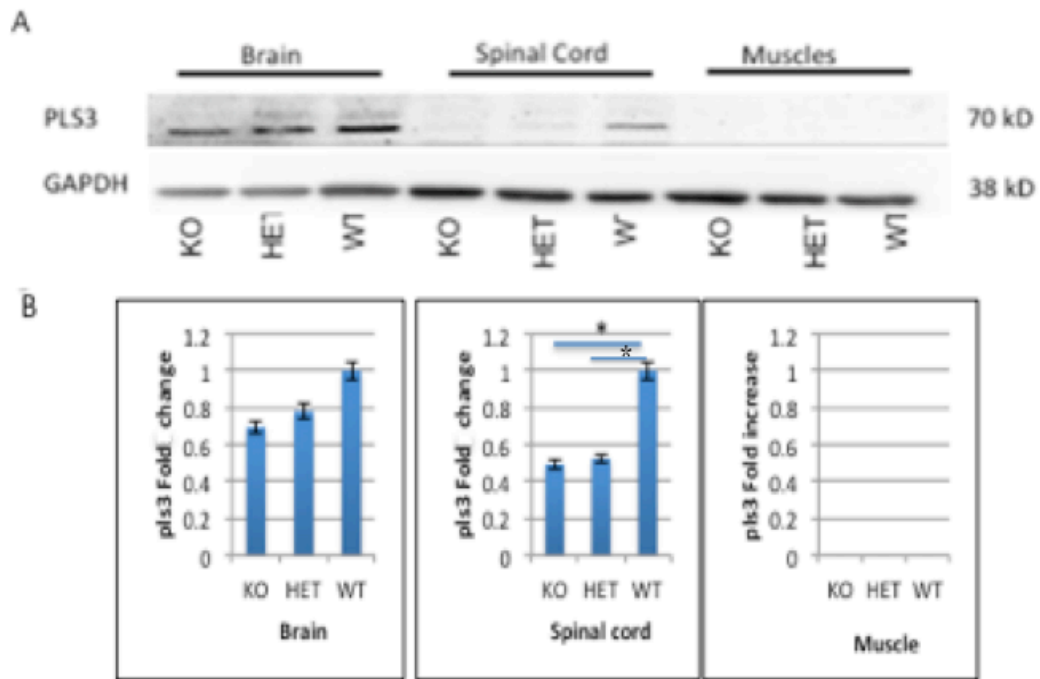


Figure 3.2. Pls3 protein levels in postnatal day 5 SMN Δ 7 mice

(A) Representative image of Western blot showing Pls3 expression in brain, spinal cord, and muscle tissues from postnatal day 5 wild type (WT), heterozygous (HET), and SMN Δ 7 (KO) neonate mouse pups. The membrane was probed with mouse anti- Pls3 antibody, GAPDH is the house keeping control. (B) Densitometry for Pls3 fold change: brain, spinal cord and muscle (left to right panels). WT, HET and KO pups (n=3). A value of one-way ANOVA (*p < 0.05) was considered to be statistically significant. Error bars represent (SEM)

Pls3 was detected and showed no significant difference in the P5 brains of all genotypes (Figure. 3.2A). However, the current analysis revealed that Pls3 protein levels were significantly lower in P5 spinal cord of KO and HET when compared to WT (p < 0.05, n=3) (Figure 3.2). Pls3 was undetectable in muscle of the 3 groups tested (Figure 3.2).

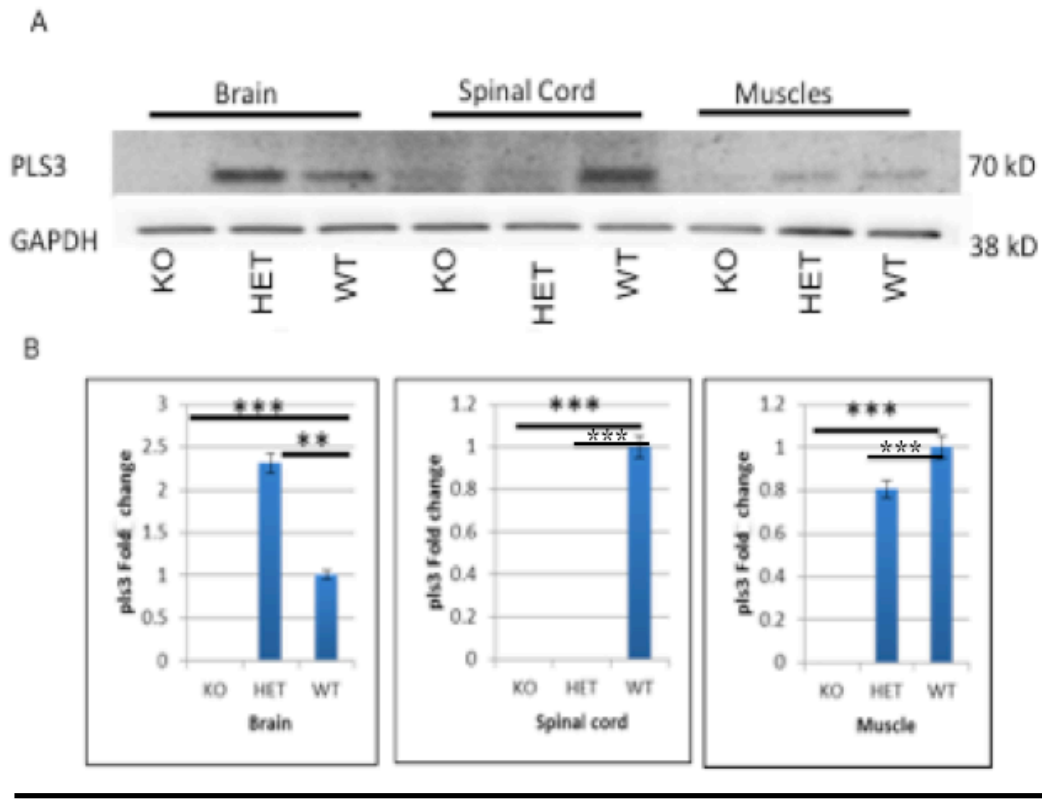


Figure 3.3. Pls3 protein levels in P10 SMN Δ 7 mice

(A) Western blot showing pls3 expression in brain, spinal cord and muscle tissues from P10 wild type (WT), heterozygous (HET), and SMN Δ 7 neonates (KO) (n=3). The membrane was probed with mouse anti-pls3 antibody, GAPDH is the house keeping control. (B) Densitometry for Pls3 fold change: brain, spinal cord and muscle (left to right panels). WT, HET and KO pups (n=3). A value of one-way ANOVA (*p < 0.05, **p < 0.01, ***p < 0.001) was considered to be statistically significant. Error bars represent (SEM)

Western blot analysis performed at postnatal day 10 revealed a significant decline of Pls3 protein levels in the KO brain and spinal cord compared to previous time points (P1 and P5) and the same tissues in HET and WT (Figure 3.3), suggesting that SMN levels did affect Pls3 expression at P10 in the CNS and muscles. It is also noteworthy to state the significant reduction of Pls3 protein in spinal cord of HET pups (Figure 3.3). Surprisingly Pls3 levels were higher in HET compared to WT brains (Figure 3.3).

3.3.2 *Pls3* mRNA expression over time

mRNA expression was examined to see how the pattern of expression changes for each of the genotypes as the disease progresses, and whether this correlated with the protein.

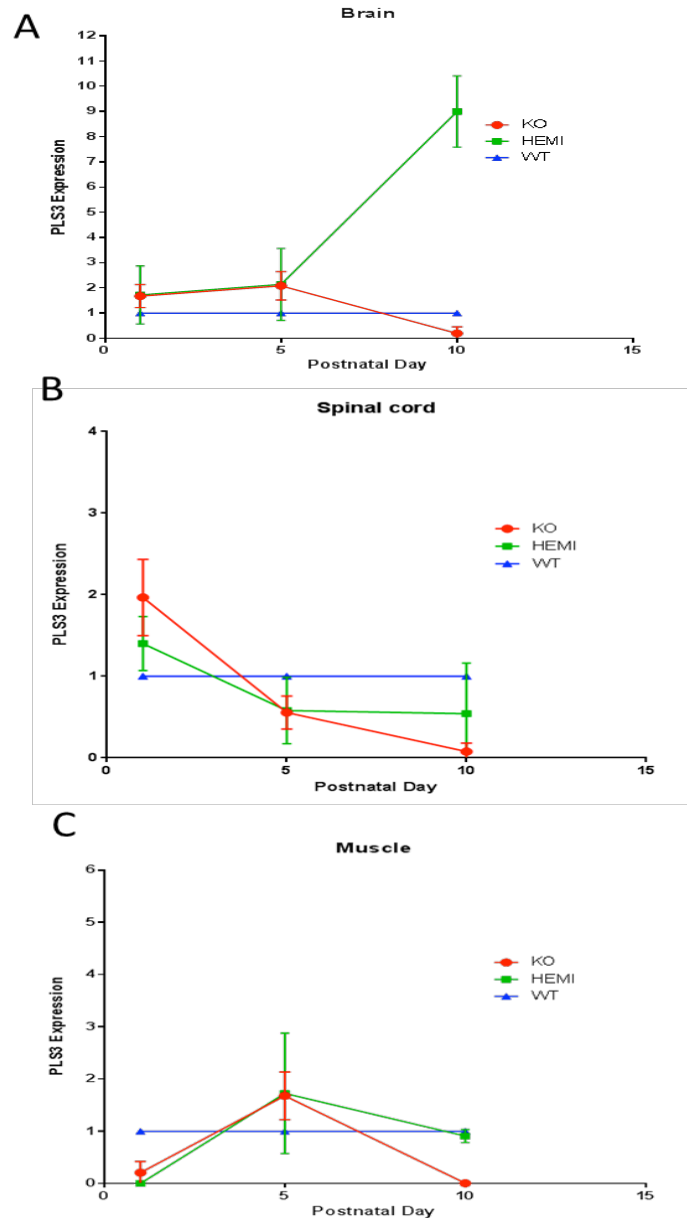


Figure 3.4 *Pls3* mRNA levels over time in the brain, spinal cord and muscle of SMN Δ 7 mice Time course experiment for *Pls3* mRNA expression quantification in brain at three different time points (P1, P5 and P10). Wild type (WT), heterozygous (HET), and SMN Δ 7 (KO) neonate mouse pups (n=3). Error bars represent \pm SEM. (A) Brain, (B) Spinal cord and (C) muscle

This data confirmed differential *Pls3* expression between SMN knockout mice from the SMN Δ 7 line and their wild-type littermates in the analysed tissue. At early time points (postnatal days 1 and 5) there were no differences in *Pls3* mRNA levels between any of the genotypes in brain (Figure 3.4A). However, by P10 *Pls3* is almost undetectable in KO mice (Figure 3.4A). Unexpectedly, there was an approximately three-fold upregulation of *Pls3* mRNA in HET mice compared to wild type mice (Figure 3.4A), the mRNA change that was reflected in the protein levels (see Figure 3.3).

In spinal cord there were no differences in *Pls3* mRNA levels at P1 between any of the genotypes (Figure 3.4B). By postnatal day 5 there was almost similar decrease in *Pls3* mRNA in HET and KO, however, a steady increase in WT. By P10 upregulation of *Pls3* in WT, while HET *Pls3* levelled off, and KO animals showed reduction in *Pls3* expression to almost undetectable levels.

In muscle, *Pls3* mRNA was almost absent for all at P1 and showed a significant increase in WT up to p10 (Figure 3.4C). By P5 *Pls3* expression peaks in HET and KO to around 3 times the level of WT *Pls3*. By postnatal day 10 *Pls3* mRNA levels in both HET and KO declined, however, HET *Pls3* was as WT level whilst KO was undetectable (Figure 3.4C).

3.3.3 Localisation of Pls3 in SMN Δ 7 mice

Following the quantification of plastin 3 expression in brain, spinal cord and muscle tissues in SMN Δ 7 mice at both mRNA and protein levels, qualitative histological analysis of the protein localisation was carried out in order to confirm the difference between the genotypes, with specific interest in whether Pls3 was enriched in specific cell types in brain and spinal cord. PLS3 staining was assessed qualitatively

by immunohistochemistry to address its cellular expression by probing tissue with anti-PLS3 antibody (n=3 per group).

Tissue sections were taken from the brain and spinal cord of P10 KO and WT mice. Motor neurons were identified morphologically by size and shape within the ventral horn of the cervical and lumbar spinal cord sections.

DAB staining was performed on spinal cord and brain sections (Figures 3.5 and 3.6), followed by co-immunostaining for PLS3 and NeuN, in brain (Figure. 3.7). In addition, SMI32 and CGRP served as motor neuron markers for the spinal cord sections (Fig. 3.8, 3.9 and 3.10). Due to technical challenges processing tissues from P1 and P5 animals this was only carried out in P10 pups.

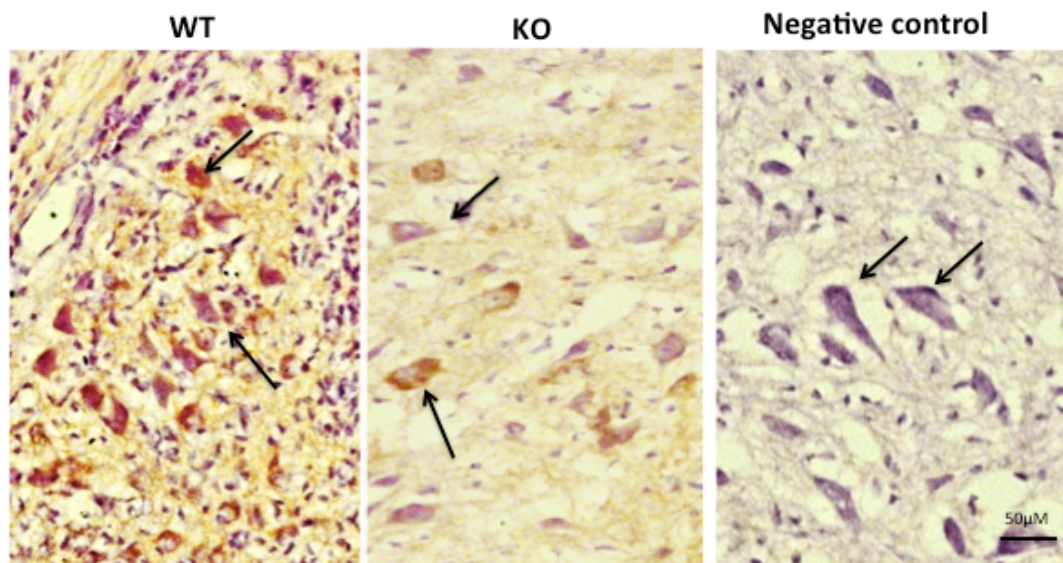


Figure 3.5. PLS3 immunostaining in the brain cortical sections of WT and KO P10 pups

Immunohistochemical staining showing PLS3 expression in brain from P10 wild type (WT) and SMN Δ 7 mice (KO) (n=3 per group). Brain sections from WT showing immune reactivity of PLS3 associated with a large number of neurons in the brain cortex (brown) (arrows). SMN Δ 7 mice (KO) brain sections showed minimal reactivity of PLS3 associated with neurons (arrows). Negative control (no primary antibody) showed purple neuronal staining (arrows) (reflecting haematoxylin counter stain) with no PLS3 positive cell staining. Scale bar (scale = 50 μ m)

Immunostaining for Pls3 on WT and KO brain sections at P10 indicated a reduction in Pls3 signal intensity in brain tissue in KO animals compared to WT group (Figure. 3.5), consistent with western blotting data (Figure. 3.3) and mRNA analyses (Figure.3.4) described earlier in this chapter. Pls3 reactivity was associated with the nucleus as well as cytoplasm of cells with long processes, resembling neuronal morphology (Figure 3.5).

To confirm that brain neurons express Pls3 WT brain sections were stained with Pls3 and neuronal marker NeuN to identify their co-localisation in neurons. Using WT brain sections NeuN-positive cells were seen to express Pls3 as reported in Figure. 3.6A. Pls3 was found in the cytoplasm of cell bodies and excluded from the nucleus. The NeuN neuronal marker co-localised with the nuclear stain, DAPI.

KO brain sections were stained with Pls3 and NeuN to identify their localisation (Figure. 3.6B). Examination of KO brain section confirmed low levels of Pls3 protein in NeuN-positive neurons. This observation is in agreement with Western blot findings described above. These data, alongside the WT data, show that Pls3 is detectable in WT neurons but is depleted in KO brain.

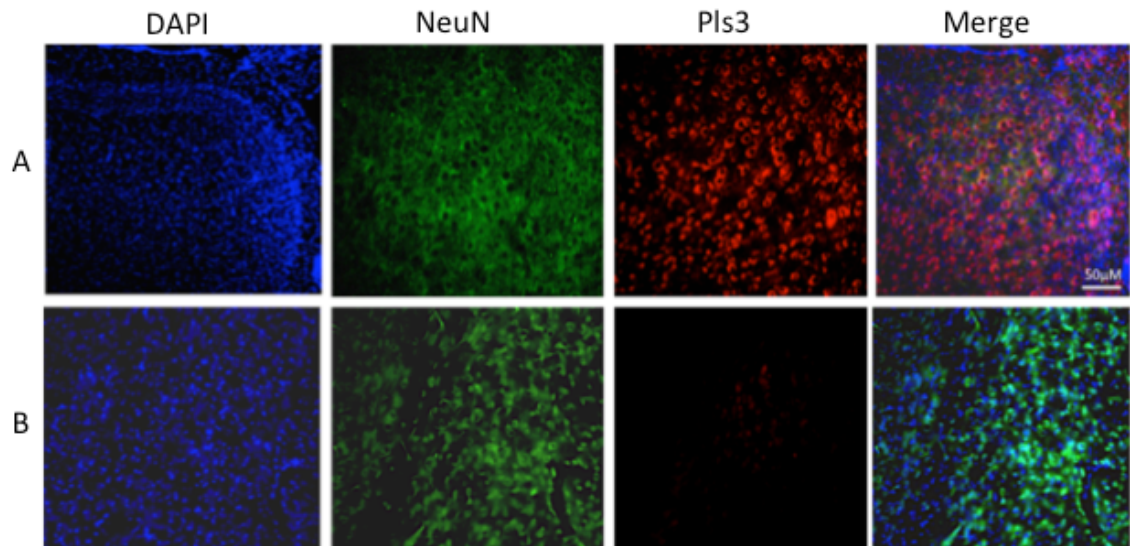


Figure 3.6. Co-localisation of Pls3 protein levels in the brain of WT / KO at P10 of age with NeuN

(A) WT brain section showing co-localisation of Pls3 with the neuronal marker NeuN of P10. (B) Brain section from SMN Δ 7 mice (KO) demonstrating very weak co-localisation between NeuN and the Pls3, (n=3). The nucleus stained with DAPI. The sections were stained for DAPI- Diamidino-2-phenylindole (blue), NeuN- Neuronal nuclei (green) and Pls3- Plastin3 (red). A: WT, B: KO, (scale = 50µm)

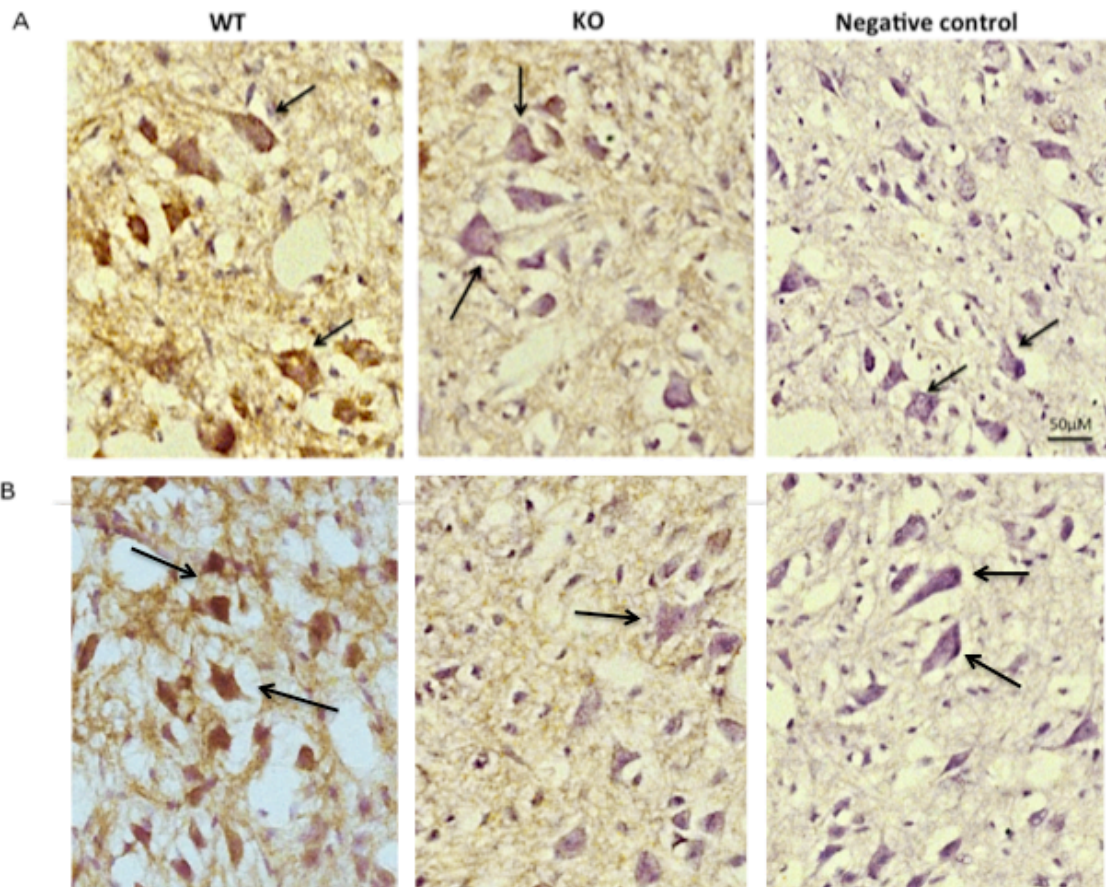


Figure 3.7. Pls3 Immunoreactivity in cervical (A) and lumbar (B) spinal cord of P10 WT and KO SMN Δ 7 mice

Immunohistochemical staining showing Pls3 expression in the spinal cord from P10 wild type (WT) and SMN Δ 7 mice (KO) (n=3). WT spinal cord sections showing Pls3 immunoreactivity in large number of MNs in the anterior horn of the spinal cord (brown) (arrows), when compared to sections from SMN Δ 7 mice KO section, which showed minimal reactivity of Pls3 associated with MNs (arrows). Negative control (no primary antibody) showed purple neuronal staining (arrows) (reflecting haematoxylin counter stain) with no Pls3 positivity. Scale bar (scale = 50 μ m), (A) Cervical spinal cord sections, (B) Lumbar spinal cord sections

Investigating Pls3 protein expression in spinal motor neurons is relevant to SMA, therefore markers such as SMI32 and CGRP were used to explore localisation of Pls3 in spinal motor neurons. Pls3 immuno-reactivity on spinal cord sections in P10 pups revealed a reduction in Pls3 signal intensity in both cervical and lumbar spinal cord of KO animals compared to WT group (Figure. 3.7).

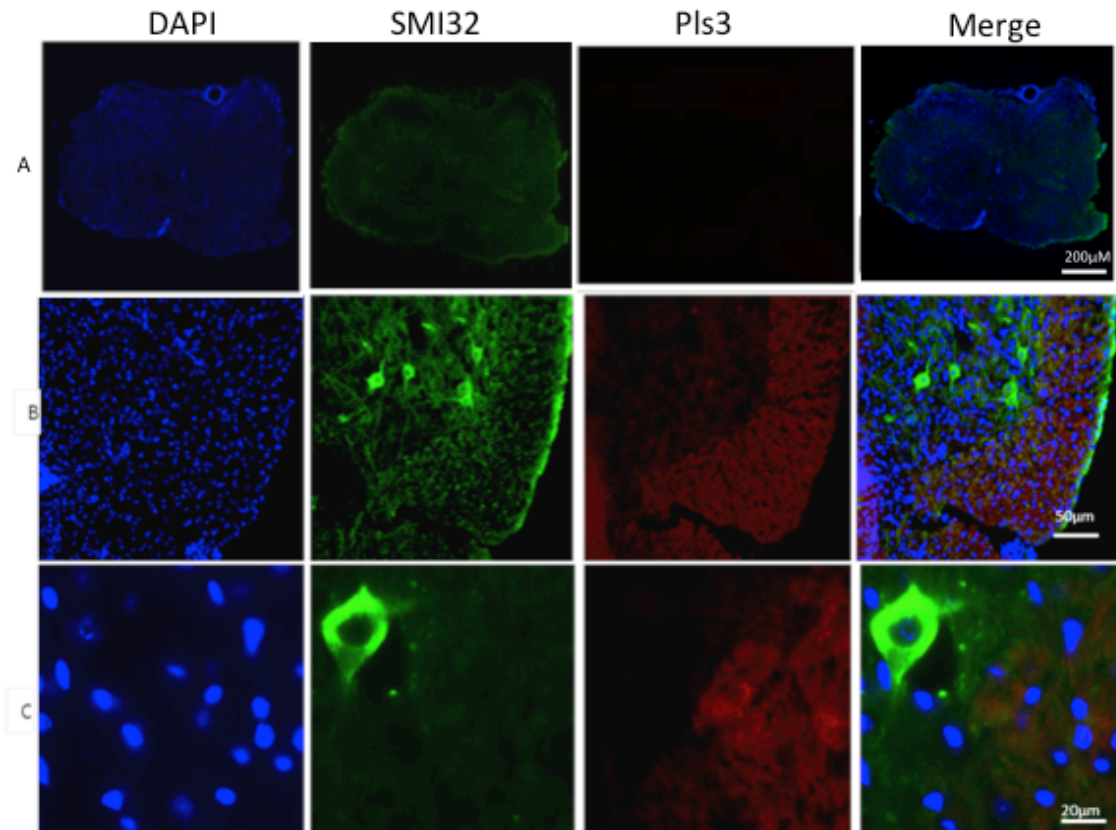


Figure 3.8. Double labeling with Pls3 and SMI32 antibodies in the spinal cord sections of P10 WT pups

Wild type spinal cord section showing double labelling with Pls3 and the neuronal marker SMI32 in P10 wild type (WT) (n=3). The sections were stained for DAPI- Diamidino-2-phenylindole (blue), SMI32 (green) and Pls3- Plastin3 (red). A: Scale bar = 200 μ m, B: Scale bar = 50 μ m, C: Scale bar = 20 μ m

WT spinal cord sections were stained with Pls3 and SMI32 to identify their co-localisation in neurons (Figure. 3.8). SMI32 detects cytoplasmic neurofilament protein, which is predominantly expected in motor neurons. Pls3 signal was detected in white matter regions, suggesting that Pls3 expression can be found either in the myelinated axons or other cells such as glial cells (astrocytes and microglia) or oligodendrocytes. Labelling with neuronal marker SMI32 showed no co-localisation with Pls3.

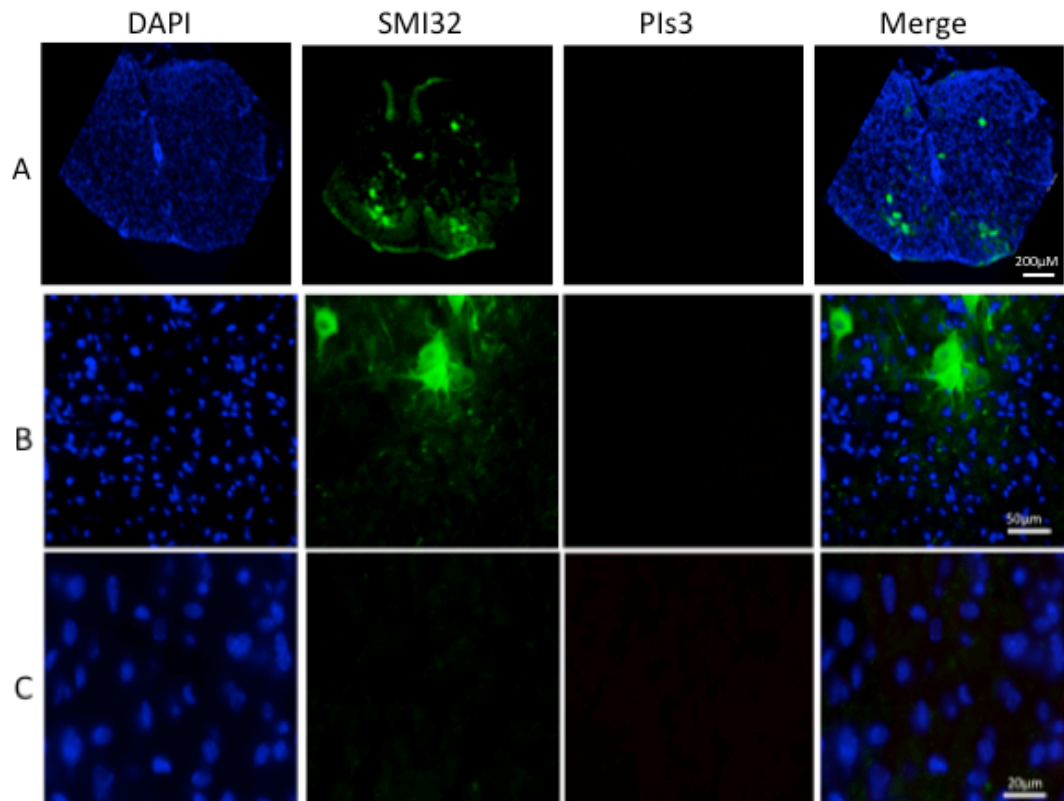


Figure 3.9. Double labeling Pls3 and SMI32 in the Spinal Cord sections from SMN Δ 7 mice (KO) at P10 of age

SMN Δ 7 mice (KO) spinal cord section showing absence of co-localisation of Pls3 with the neuronal marker SMI32 (n=3). The sections were stained for DAPI- Diamidino-2-phenylindole (blue), SMI32- nonphosphorylated neurofilament marker (green) and Pls3- Plastin3 (red). A: Scale bar = 200 μ m, B: Scale bar = 50 μ m, C: Scale bar = 20 μ m

Spinal cord sections collected from KO were stained with Pls3 and SMI32 antibodies to identify possible localisation of Pls3 in motor neurons. No cells were found to express Pls3, and therefore no co-localisation with SMI32 staining was observed (Figure. 3.9).

Another MN marker, CGRP, was used to perform co-immunostaining with Pls3 in spinal cord (Figure. 3.10). WT and KO spinal cord sections were co-stained with Pls3 and CGRP to identify their co-localisation in MNs.

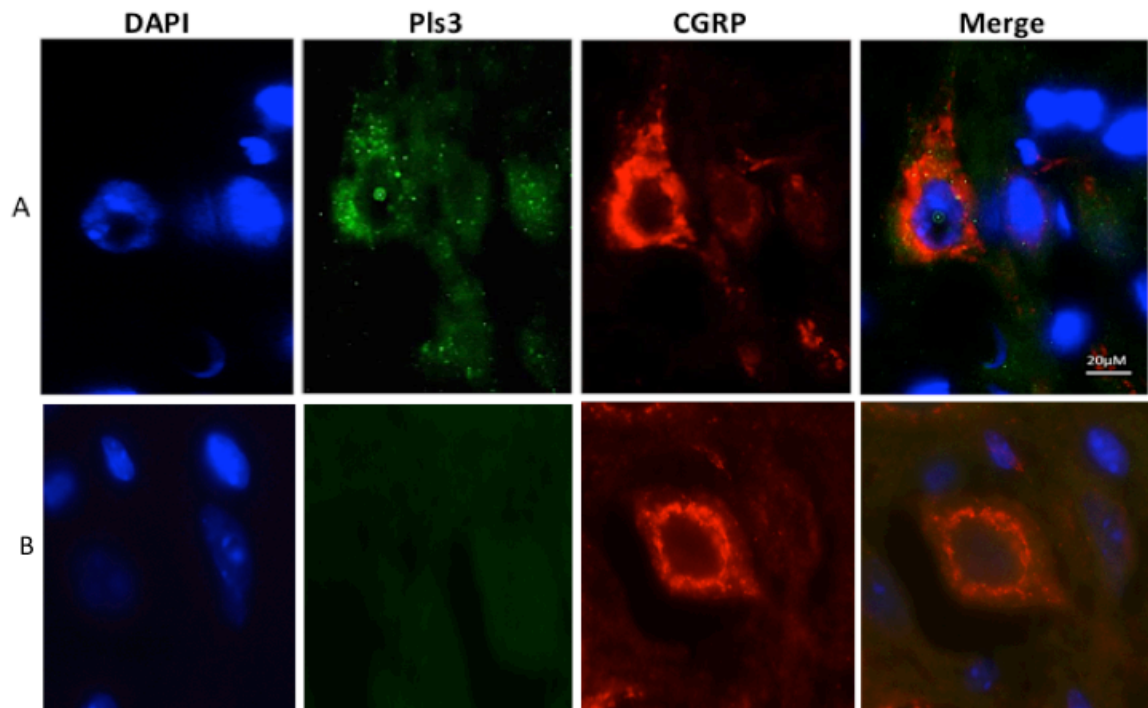


Figure 3.10. Co-localization of Pls3 protein levels in the spinal cord of WT / KO at P10 of age with CGRP

(A) Wild type (WT) spinal cord section showing co-localisation of Pls3 with the motor neuronal marker CGRP from P10, (n=3). (B) Spinal cord section from SMN Δ 7 mice (KO) showing no co-localisation between CGRP and the Pls3,(n=3). The sections were stained for DAPI- Diamidino-2-phenylindole (blue), Pls3- Plastin3 (green) and CGRP- Calcitonin Gene-Related Peptide (red). A: WT, B: KO, (scale = 20 μ m)

In the WT spinal cord, MNs were found to express Pls3, which co-localised with CGRP staining (Figure. 3.10A). Pls3 was found in the cytoplasm of large cell bodies and nucleus. KO spinal cord sections were also stained with Pls3 and CGRP to identify the co-localisation in MNs. No cells however were found to express Pls3; and subsequently no co-localisation with CGRP staining was seen (Figure. 3.10B), suggesting depletion of Pls3 protein levels in KO MNs.

3.4 Discussion

In this chapter, it was shown that *Pls3* is expressed in the brain, spinal cord and muscle of the SMN Δ 7 mice and their non-transgenic littermates, consistent with human and other studies on SMA animal models such as zebrafish (De Arruda et al., 1990, Oprea et al., 2008, Bowerman et al., 2009, Hao et al., 2011). When *Smn* is depleted, however, *Pls3* levels are decreased over time as the disease progresses in a tissue specific pattern. This study revealed that *Smn* depletion in KO pups was associated with near complete ablation of *Pls3* levels in spinal cord and brain by the end stage of disease progression (P10) in all tissue types analysed. Given that it is believed that *Smn* and *Pls3* interact and function to promote axon growth and motor neuron survival (Hao et al., 2012), the decrease in *Pls3* may contribute to neuronal death in SMA.

3.4.1 *Pls3* expression variations in the CNS of SMN Δ 7 mice

A downregulation of *Pls3* mRNA or *Pls3* protein expression in brain, spinal cord and muscle of the SMN Δ 7 mouse model at early stages of development was observed. There were no significant differences in *Pls3* levels between any of the genotypes at postnatal day 1 in any tissues (Figure. 3.1, Figure. 3.4); however, by postnatal day 10 there was little or no detectable mRNA or protein in the CNS of *Smn* knockout mice (Figure. 3.3, Figure. 3.4). Similar findings have been reported by two independent studies in different SMA mouse and zebrafish models, where *Pls3* was reduced in brain and spinal cord of animals lacking *Smn* (Oprea et al., 2008, Hao et al., 2011). The similarities in *Pls3* expression between human SMA patients in previous studies and SMN Δ 7 mice in the current study indicate that SMN Δ 7 mice are a good model for testing potential *PLS3*-based therapeutics for human SMA. The discrepancy

between the WB results (Figure. 3.3) and the immunostaining (Figure 3.5 and 3.7) in *Pls3* reduction in KO mice may simply be by-product of having fewer cells present.

Another study in an intermediate mouse model supports the same findings where the levels of *Pls3* were reduced in the brain and spinal cord of *Smn2B^{-/-}* mice at P21 compared to their wild type littermates (Bowerman et al., 2009). Previous studies in human SMA patients showed that *PLS3* was expressed at a very low level in blood cells (Oprea et al., 2008, Stratigopoulos et al., 2010, Yanyan et al., 2013).

The role of *PLS3* in motor neuron development is unknown, and its association with SMN in developing MNs has not been investigated. *PLS3* overexpression stabilised axons, reduced axon pruning, and ameliorated poor connectivity seen in SMA model NMJs (Oprea et al., 2008, Boon et al., 2009, Ackermann et al., 2012). Therefore, *PLS3* deficient MNs are more likely to have shorter axons, poor connectivity at NMJs and axon instability. SMN loss is also known to cause the same defects in MNs (Rossoll et al., 2003, Simic et al., 2008, Bowerman et al., 2009). This suggests that both SMN and *PLS3* interact and function to promote axon growth and motor neuron survival (Oprea et al., 2008, Bowerman et al., 2009). Therefore, the loss of one of these proteins may contribute to the cause of neuronal death and may accelerate the disease progression.

Overexpressing both SMN and *PLS3* might provide a better therapeutic effect for SMA and other neuromuscular diseases, since previous studies have shown that *PLS3* managed to rescue axonal defects associated with reduced SMN protein levels in MNs (Oprea et al., 2008).

In the current study, the down regulation of *Pls3* levels (Figure. 3.4) was consistent with *Smn* depletion, which may contribute to the modification of SMA phenotype.

Both mRNA and protein levels showed the same pattern of down regulation, indicating a transcriptional and not a translational effect. This suggests that the decrease in Pls3 protein is caused by a decrease in mRNA levels. On the other hand, a recent study of Pls3 in zebrafish *smn*^{-/-} mutants showed that *pls3* RNA levels were unaffected by *Smn* levels (Hao et al., 2012). This discrepancy may be due to different mechanisms of Pls3 regulation in the different species. There are 2 possibilities for a mechanism by which SMN reduces PLS3. Firstly, SMN is responsible for shuttling molecules along the axon to the synapse. PLS3 mRNA may rely on SMN to deliver it to the nerve terminals and a loss of SMN leads to a build-up of *PLS3* in the cell body and eventual degradation without translation. Secondly, SMN is also involved in a splicing complex. Loss of SMN may affect *PLS3* mRNA levels due to the loss of splicing complexes in these models. However, zebrafish *smn*^{-/-} mutants (Hao et al., 2012) do not show any alterations in the splicing of endogenous *pls3*, which indicates that *Smn* does not affect *pls3* transcription, *pls3* RNA or Pls3 protein stability. Moreover, another study in mice (Ackermann et al., 2012) showed that *Pls3* overexpression had no effect on *smn* expression. In addition, one study in PC12 (human cells) (Oprea et al., 2008) reported that the overexpression of PLS3 has no influence on SMN levels. Therefore, we could conclude that in mammals plastin3 seems to exert its modifying effects independently of SMN (Ackermann et al., 2012). These findings suggest that PLS3 has mechanisms of neuronal protection that are independent of SMN.

3.4.2 Pls3 levels in the muscle

Unexpectedly, in muscle at postnatal days 5 up regulation of *Pls3* mRNA was observed in both carrier (HET) and knockout (KO) mice. By day 10, *Pls3* mRNA

was almost undetectable in KO mice and decreased to WT levels in HET mice (Figure. 3.4). One explanation for the elevated level of *Pls3* in early stages of the KO mice is that *Pls3* could be derived from the maternal RNA. In a published study (Boon et al., 2009) to understand the relationship between SMN and PLS3, both *Smn* and *Pls3* protein levels in zebrafish *smn* mutant (*smnY262stop*^{-/-} zebrafish) larvae were analysed. Interestingly, it was reported that *Smn* protein was present at high levels until approximately 4 days post fertilization (dpf) due to maternal contribution of RNA and protein in the yolk (Boon et al., 2009). Then, these levels decreased gradually – reaching low levels by ≈ 7 dpf until the mutants died at ≈ 12 dpf. It should be also noted that these zebrafish mutants do not mimic the human situation for SMA patients. However, similar findings have been reported in blood of SMA children, where their PLS3 expression was higher at early stages of development (3 years), and gradually the levels decreased with age (Yanyan et al., 2013). In our study the peak observed in *Pls3* mRNA was not seen in the corresponding protein analysis (Fig. 3.2), which may be due to the detection limit of western blots; protein levels may be very low, and therefore undetectable. This difference may also be due to a delay in translation from RNA to protein. The protein peak may fall after day 5 but proteins have reduced again by day 10 (Figure. 3.2).

3.4.3 *Pls3* levels in SMN heterozygote mice

In heterozygotes, where SMN is reduced but not ablated, *Pls3* decreased to similar levels as KOs in spinal cord at day 5 but stayed at a steady level up to day 10 (Figure. 3.4). Since HET mice have the same life span as WT mice, it was expected that half the amount of SMN would be sufficient for neuronal survival. A 50%

reduction in SMN does not appear to have an effect on PLS3 in muscle but shows changes in PLS3 levels in the CNS, suggesting that the interaction between SMN and PLS3 is different and/or less important in muscle than CNS. Muscle tissue is rich in actin filaments, therefore PLS3 may be regulated preferentially by proteins other than SMN in this tissue, and so PLS3 levels may be unaffected by the loss of SMN in muscle.

In brain tissue, at P5 *pls3* mRNA in HET mice increased above WT levels (Figure. 3.4). One possible reason could be a compensation of PLS3 after day 5 to help with axonal outgrowth in a bid to overcome the reduction of SMN.

3.4.4 Localisation of Pls3 in P10 SMN Δ 7 mice

Pls3 is decreased at a tissue level, but it is not known whether it is enriched in specific cell types or whether the lack of SMN is targeted to specific cells. Pls3 expression was assessed qualitatively by immunohistochemistry (IHC) to address its cellular expression. Due to the technical challenges and size of spinal cord at P1 and P5 only P10 mice could be reliably analysed by IHC. Examination of tissues from SMN Δ 7 mice at P10 by IHC confirmed reduced Pls3 signal in both the spinal cord and brain of KO mice (Figure. 3.5, 3.6, 3.7, 3.8, 3.9 and 3.10).

Cellular localisation was firstly observed with DAB staining and Pls3 appeared to localise in cells with neuronal morphology in WT mice (Figure. 3.5 and 3.6). Fluorescent immunohistochemistry was then carried out to allow neuronal markers to be used to confirm cell types. NeuN is a pan-neuronal marker commonly staining the nucleus and to a lesser extent the cytoplasm. A large number of neuronal cells were found to express Pls3, which was co-expressed with NeuN staining in the WT brain (Figure. 3.7A). Co-expression of Pls3 in brain with NeuN also revealed a

decrease of Pls3 levels in KO SMN Δ 7 SMA mice compared to WT littermates, in agreement with Bowerman et al. (2009), who reported decreased level of Pls3 in the brain of an intermediate SMA mouse model (Bowerman et al., 2009).

Pls3 did not appear to co-localise with the neuronal marker, SMI32 in spinal cord. SMI32 detects cytoplasmic neurofilament protein, which predominantly expressed by MNs. Co-localisation of Pls3 with the MN marker CGRP was detected in spinal cord lumbar sections. CGRP is specific for calcitonin gene related peptide, a neuropeptide that is expressed in the MNs mainly in the peri-nuclear location and sensory neurons in dorsal root ganglia (DRG).

In spinal cord Pls3 distribution was as expected, being expressed in the white matter where mostly glial cells and myelinated axons are located. A strong Pls3 signal was detected in the white matter regions in the spinal cord indicating that Pls3 may be localised to either axons or oligodendrocytes (Figure. 3.8). Double labelling with CGRP confirmed localisation of Pls3 to motor neuron cell bodies (Figure. 3.10) but did not label axons.

3.4.5 Summary

To sum up, this chapter characterized Pls3 localisation and *Pls3* expression and protein levels in an intermediate SMA mouse model (SMN Δ 7 SMA mouse model) at different stages of the disease. Our study has shown down regulation of Pls3 over time when *Smn* is depleted. Early Pls3 depletion may affect the development of motor neuron axons in these models and may affect motor neuron survival, contributing to the SMA phenotype. This chapter raises many interesting questions that need addressing with regards to the expression of Pls3 such as: What is the mechanism by which *Smn* deficiency reduces Pls3 levels? Does Pls3 feedback and self-regulate transcription of its own mRNA? Moreover, further evidence is required to support the role of Pls3 down regulation in the pathology of spinal muscular atrophy, and to demonstrate whether the restoration of Pls3 expression can rescue the axonal phenotype in spinal motor neurons cultured from a clinically relevant mouse model of SMA. In addition to furthering understanding of the function of Pls3, a potential use for Pls3 in gene therapy for SMA can be proposed.

**CHAPTER 4: PLS3-MEDIATED NEUROPROTECTION IN
AN *IN VITRO* MODEL OF SPINAL MUSCULAR ATROPHY**

4.1 Aims

Chapter 3 showed that when *Smn* is depleted *Pls3* is also down regulated, suggesting an important role of *Pls3* in axonal outgrowth and neuronal survival in SMA. This chapter aims to test whether overexpression of PLS3 would slow or prevent MN loss. The present study aims to evaluate the neuroprotective effect of lentiviral – mediated gene transfer of PLS3 in an *in vitro* model of SMA.

4.2 Introduction

The identification of PLS3 as a modifier for SMA (Oprea et al., 2008) opened new opportunities towards understanding the mechanisms of SMA pathology in this childhood condition (Ackermann et al., 2012) and identifying potential therapies. Neuroprotection is considered to be an effective treatment option for many CNS disorders including neurodegenerative diseases (Azzouz et al., 2004b).

PLS3 is an actin-binding protein that can influence F-actin levels and rescue neuronal axon growth defects arising from SMN deficiency in cultured primary SMA MNs (Oprea et al., 2008, Hao et al., 2012). Triple-label experiments were performed with *Smn*, *Pls3*, and actin in primary murine MNs, and showed that endogenous *Smn* and *Pls3* co-localize in granules throughout the axons of MNs and accumulate at F-actin–rich growth cones (Oprea et al., 2008). It was reported that PLS3 would likely act via modification of the actin cytoskeleton in axons, which is essential for axonogenesis (Hao et al., 2012). Moreover, further evidence was provided for actin dynamics involvement in SMA pathogenesis in *Smn*-deficient cells and SMA mice (Ackermann et al., 2012). These data suggest that PLS3 may

modify SMA pathogenesis through stabilisation of the axon terminals by raising the F-actin level.

Several studies have shown that PLS3 overexpression can rescue MN deficits in SMA models. MNs lacking *Smn* showed no alteration in survival but showed reduced axonal length and reduced growth cone area, most likely due to disturbed distribution of actin in the distal axon and growth cone (Rossoll et al., 2003). A Taiwanese SMA mouse model conditionally overexpressing PLS3 showed that PLS3 overexpression stabilised axons, reduced axon pruning, and enhanced poor connectivity seen in SMA NMJs, albeit without ameliorating motor impairment or the survival phenotype (Ackermann et al., 2012). In SMN-depleted neuronal PC12 cells and primary mouse MN cultures derived from SMA null mice, PLS3 overexpression was able to rescue axon outgrowth defects (Oprea et al., 2008) without changing SMN expression levels (Oprea et al., 2008, Stratigopoulos et al., 2010). This rescue of axon length and outgrowth defects in MNs associated with *Smn* deficiency suggests that PLS3 is a therapeutic target for SMA. It would be expected that overexpression of PLS3 in the SMN Δ 7 mice would be able to rescue the SMA phenotype by increasing axonal length and dendrite branching; therefore, in this study axonal length will be used as a measurement of efficacy.

It can be hypothesised that overexpression of PLS3 in SMN Δ 7 mice would have a similar effect to SMN and subsequently ameliorate their SMA phenotype. In order to test this hypothesis, lentiviral vectors (LV) expressing PLS3 were generated as an *in vitro* gene transfer strategy.

In this study, LV was selected as a gene delivery vector because of its ability to efficiently transfer genes to the central nervous system cells both *in vitro* and *in vivo*,

which is essential for treatment of SMA. LVs are opening up new treatment approaches for many neurological disorders such as motor neuron diseases (MND), Huntington's disease (HD) and Parkinson's disease (PD). LVs can transduce both dividing and non-dividing cells, including neurons (Azzouz et al., 2002). It has been reported that lentiviruses were able to deliver the genes efficiently into different types of primary neurons from a broad range of different species including man, resulting in long-term gene expression (Azzouz et al., 2002, Bienemann et al., 2003). LV can produce stable expression of the target gene which allows a single-dose therapy rather than the need for repeated treatments, making it even more appealing (Azzouz et al., 2002). In addition, these vectors have been developed to a very high level in order to be produced safely for clinical trials (Sinn et al., 2005).

In this chapter, a LV mediating expression of PLS3 has been generated and produced at high titres. Three cell types were used for viral validation (HEK293T, NSC34 and spinal motor neurons) in order to assess the LV transduction efficiency in different cell types. HEK293T cells are widely used in cell biology research and are well characterised; they are easy to grow, transfect and transduce very readily. NSC34 are a neuronal cell line and are more relevant than HEK293T cells because they are motoneuron-like cells. However, both cell lines have endogenous PLS3 and SMN proteins. Spinal motor neurons derived from SMN Δ 7 embryos will also be used to validate the LV-PLS3 as they are derived from the same mouse model used for in vivo proof-of-concept (chapter 5 of this thesis), therefore they lack Smn but express murine Pls3. Using different cell lines gives power to the study and also allows us to see whether there is a cell-specific effect of the virus.

Prior to testing the efficacy of the virus *in vivo*, it is crucial to determine the gene transfer efficiency of our vector and whether the transgene is biologically active. The main purpose of this chapter is to investigate the neuroprotective effect of LV-PLS3 in MNs isolated from the SMN Δ 7 SMA mouse model. To successfully achieve this aim, LV expressing PLS3 has been generated, titred, and then validated in cell such as HEK293T, NSC34 and primary MNs. A second function for SMN in axonal mRNA transport has also been proposed that may likewise contribute to axonal defect in MNs with smn deficiency (See et al., 2014).

The impact of LV-PLS3 treatment on axonal length was assessed to see whether the axonal deficits caused by lack of Smn can be reversed by overexpression of PLS3.

4.3 Results

4.3.1 Construction of LV-PLS3

Gene transfer mediated by viral vectors can achieve a stable and efficient transduction of non-dividing cells such as neurons (Azzouz et al., 2002). Lentiviral vectors were the first choice for attempting delivery of SMN to motor neurons *in vitro* due to: i) high transduction efficiency *in vitro* and ii) easy and short production protocol compared to other vector systems like AAV. The current chapter summarises LV-PLS3 vector design, titration, validation in cell lines, and assessment of its ability to enhance axonal length in purified Smn-deficient motor neurons.

4.3.1.1 Subcloning of PLS3 into lentiviral vector.

The lentiviral vector expressing PLS3 was generated by extracting the PLS3 gene from pcDNA3.1-PLS3-V5/His6 plasmid, provided by Prof. Dr. Brunhilde Wirth, (Institute of Human Genetics, University Hospital of Cologne, Germany) and cloned

into the lentiviral backbone SIN-PGK-cPPT-GDNF-WHV. Figure 4.1a shows the plasmid-map of LV-PLS3 vector contains PGK promoter. PLS3 was cloned between *Bam*HI and *Xho*I restriction sites; several clones were generated and assessed by restriction digestion (Figure. 4.1b). The LV-PLS3 plasmid's ability to express PLS3 was validated in HEK239T and NSC34 cells.

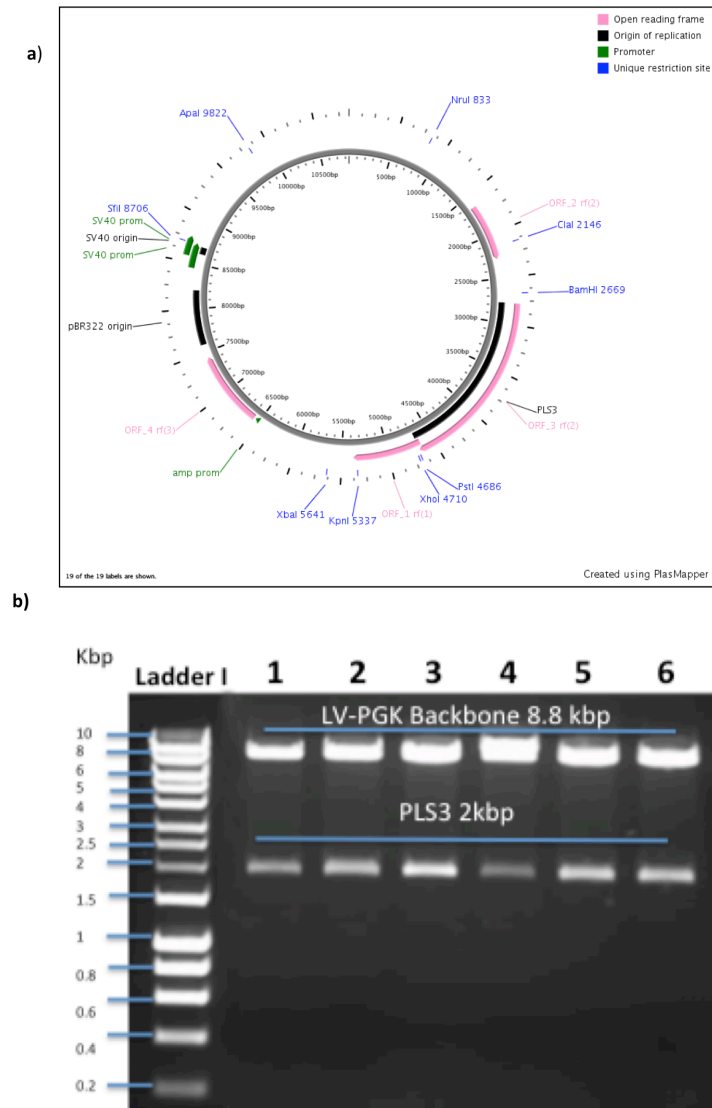


Figure. 4.1. Insertion of PLS3 into the Lentiviral vector

A) Plasmid map of LV-PLS3 containing PGK promoter showing unique restriction sites. B) The gel picture shows *Bam*HI - *Xho*I digests of six clones. The larger fragment ~ 8.8 kbp represents LV plasmid backbone while the smaller ~ 2 kbp represents the PLS3 insert. Lanes; 1-6: six clones, M Hyperladder 1 DNA marker.

Screening of the samples by digesting the plasmid DNA with the *Bam*HI and *Xho*I restriction enzymes confirmed the presence of the insert and control vector (plasmid only) (Figure. 4.1b). Two bands are present: the size of the upper band is about 8.8 kbp corresponding to the plasmid backbone, and the lower band about 2 kbp corresponding to the insert (PLS3). This digestion resulted in the correct band size confirming that the PLS3 DNA was successfully cloned into the LV vector. Sequencing of the plasmid has confirmed that the correct orientation of the PLS3 gene without any mutations had been obtained (see appendix3).

4.3.1.2 Validation of LV-PLS3 plasmid in HEK293T cells by Western blot

In order to confirm that the PLS3 gene was expressed by the newly generated LV-PLS3 plasmid, 1×10^5 HEK293T cells were transfected with 3 μ g of the LV-PLS3 plasmid using the PEI transfection method. Cells were harvested 72 hours post transfection and the PLS3 protein levels were assessed by western blot. PLS3 was detected using rabbit anti-PLS3 primary antibody. The un-transfected cells were considered to be a negative control.

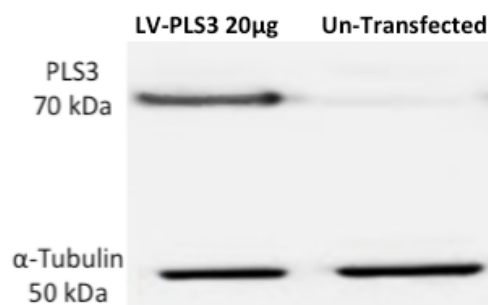


Figure 4.2. Validation of LV-PLS3 plasmid 72 hours following transfection of HEK293T cells

The western blot shows the presence of a 70 kDa band representing the PLS3 protein. 20 μ g of protein was loaded as indicated. Un-transfected cells show endogenous PLS3 protein

level. The membrane was probed with anti-PLS3 antibody. α -Tubulin was the loading control

Anti-PLS3 antibody detected a band at 70 kDa, which corresponds to the expected molecular weight of PLS3 protein. Western blot analysis revealed overexpression of PLS3 protein in cells transfected with LV-PLS3 plasmid when compared to un-transfected controls (Figure. 4.2), showing that the LV-PLS3 construct is functional. Low level of endogenous PLS3 could be seen in un-transfected cells (Figure. 4.2). Following successful validation of LV-PLS3 plasmid, it was decided to proceed with lentiviral production.

4.3.2 Lentiviruses mediate efficient overexpression of PLS3 in cell lines

LV-PLS3 virus was produced using the four-plasmid transfection method, in which the cells were transfected with the lentivirus vector plasmid expressing PLS3, one envelope plasmid and two packaging plasmids (see M & M Chapter 2). The virus was then collected from the media, filtered from cellular debris and concentrated using ultracentrifugation. A titre of 2.55×10^8 TU/ml was confirmed using a p24 ELISA kit as detailed in Materials and Methods (chapter 2). The p24 ELISA kit used to determine the titre cannot exclude empty viral particles, therefore it was necessary to validate the efficiency of the viral packaging prior to undertaking further studies using LV-PLS3.

4.3.2.1 Validation of LV-PLS3 by Western blot

To validate the efficiency of the virus, transduction of HEK293T cells was performed using the LV-PLS3 virus at different MOIs (1, 10, and 50) (see section 2.2.4.11 for MOI calculations). The cells were harvested 5 days post transduction for

protein analysis. A negative control of un-transduced cells was also included. An antibody specific for human PLS3 protein was used.

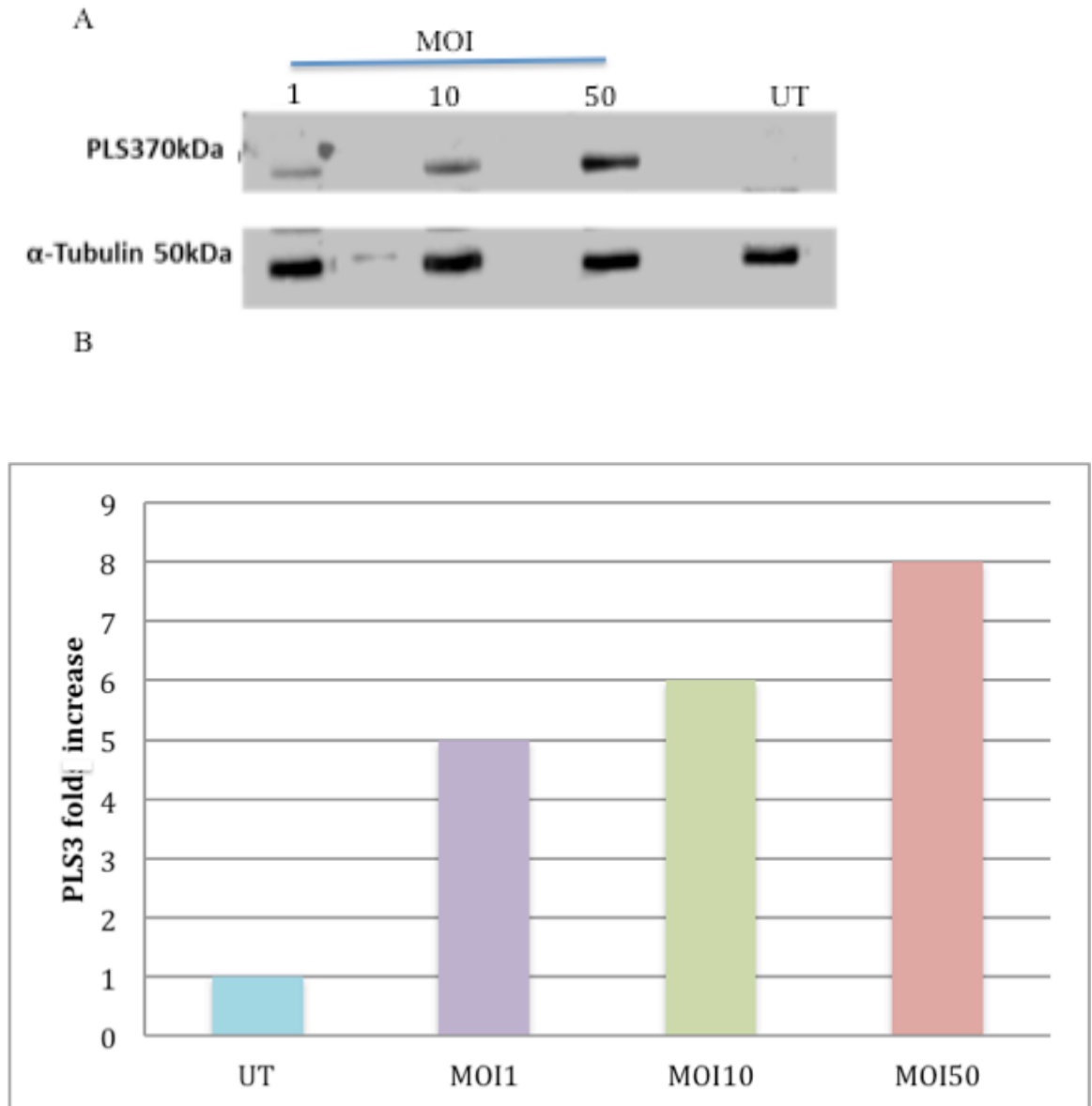


Figure 4.3. Validation of LV-PLS3 virus transduction efficiency in HEK293T by western blot

(A) Western blot showing PLS3 protein expression in HEK293T cells transduced with LV-PLS3 at MOIs 1, 10, and 50 un-transduced cells (UT) was considered as negative control for this experiment. The membrane was probed with anti-human PLS3 antibody. α -Tubulin was the loading control. (B). Densitometry analysis of PLS3 levels in transduced cells with different MOIs of LV-PLS3 (1, 10, and 50) normalized to untransduced control cells (UT).

The virus was able to overexpress PLS3 (Figure. 4.3). The western blot (Figure. 4.3A) revealed the presence of a 70 kDa band representing the PLS3 protein and 50 kDa band for α -tubulin as a house keeping control. In un-transduced cells the endogenous PLS3 showed low expression levels. The densitometry analysis indicated correlation between the increased expression levels of transgene PLS3 with the increase in MOI used. Densitometry analysis of PLS3 (Figure. 4.3B) shows 6 - fold increases in PLS3 expression with MOI10 at day 5 post-transduction as compared to un-transduced (UT) cells. There were no signs of toxicity or obvious difference in growth rate even at higher MOI.

4.3.2.2 Validation of LV-PLS3 plasmid by immunofluorescence

Immunofluorescence was used to assess the expression and localisation of PLS3 in HEK293T cells at 72 hours after transduction with LV-PLS3 at MOI 5 and 10, compared to the un-transduced HEK293T cells as a control (Figure. 4.4).

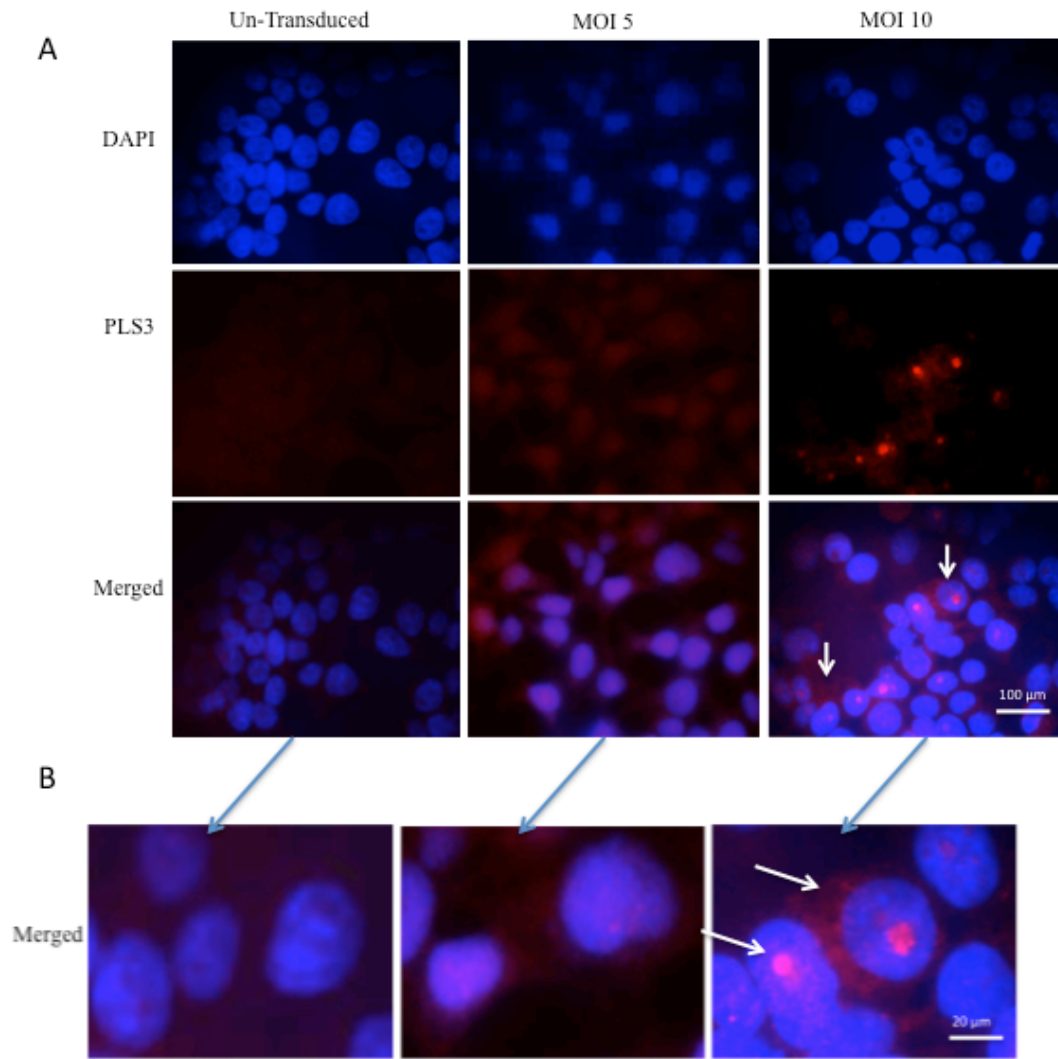


Figure 4.4. Validation of LV-PLS3 virus in HEK293T cells by immunofluorescence

HEK293T cells were transduced with LV-PLS3 at MOI 5 or 10. Un-transduced cells were considered as negative control. PLS3 (red) and the nucleus stained with DAPI- Diamidino-2-phenylindole (blue). The arrows white arrows in B indicate PLS3 expression in both nucleolus and cytoplasm. (A) Scale bar 100 μm and (B) scale bar 20 μm

The results summarised in Figure. 4.4. show overexpression of human PLS3 with around 80 % of cells transduced with an MOI of 10. An antibody specific for human PLS3 protein was used. The PLS3 localization was observed in a pattern of granular staining covering an area within the cytoplasm and nucleus. This experiment confirmed that the LV-PLS3 vector is capable of mediating PLS3 gene delivery and expression *in vitro*.

4.3.2.3 Validation of LV-PLS3 virus in NSC34 cells

To examine transduction in a neuronal-like cell line, NSC34 cells were transduced with LV-PLS3 vector at different MOIs 5, 10, 20, 40 and 80.

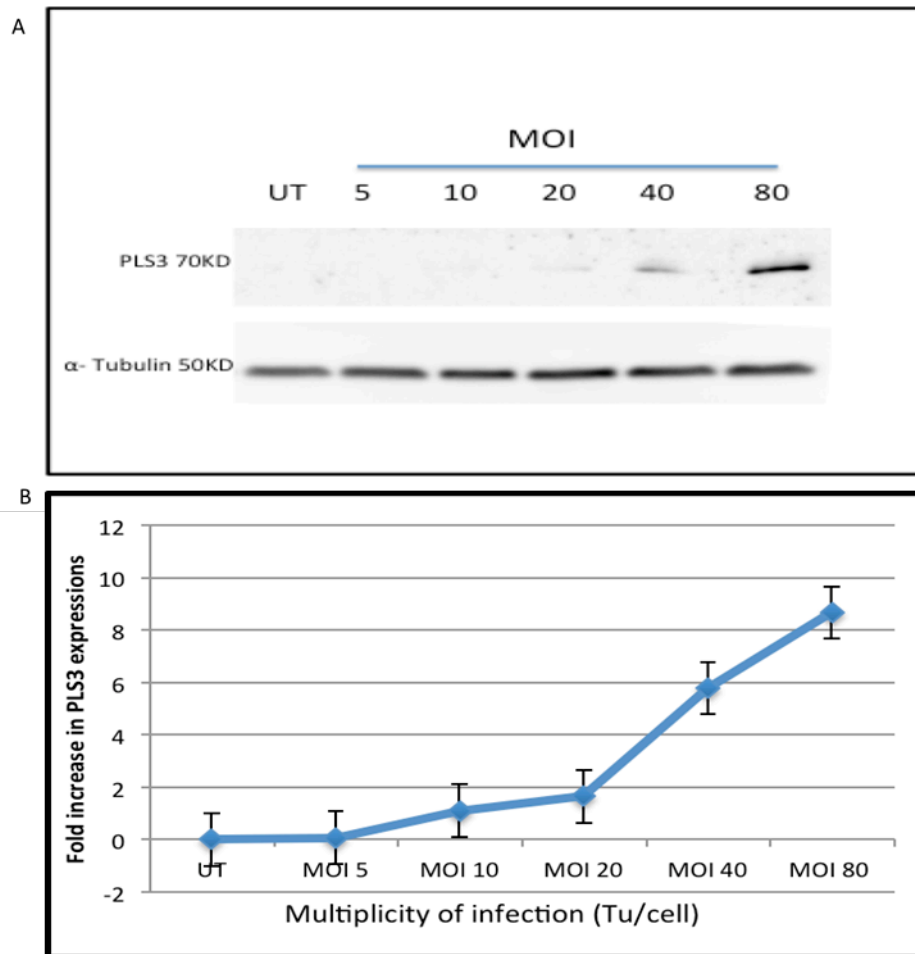


Figure 4.5. Validation of LV-PLS3 virus in NSC34 cells

(A) Western blot showing NSC34 cells transduced with LV-PLS3 at MOI 5,10,20,40 or 80 and probed with anti- human PLS3 antibody, α -Tubulin was the loading control (n=3). Un-transduced (UT) cells were considered as negative control. (B) A dose response curve of LV-PLS3 at 5 days after transduction, along with the western blot data at each multiplicity of infection (MOI) used

The western blot revealed the presence of a 70 kDa band representing the PLS3 protein and 50 kDa band for α -tubulin as a loading control (Figure. 4.5A). The densitometry analysis indicated a positive correlation between PLS3 expression and the MOI (Figure.4.5B). The transduced cells showed no overt signs of toxicity (indicated by a change in cell morphology, reduced adherence or presence of dead cells) or obvious difference in growth rate even when the viral vector was used at

higher MOI. The treated cells showed no difference in confluence at any of the daily checks from untransduced controls.

Immunofluorescence was used to assess the expression of PLS3, 5 days after transduction with different MOIs (20, 40 and 80) of LV-PLS3 compared to the untransduced NSC34 cells.

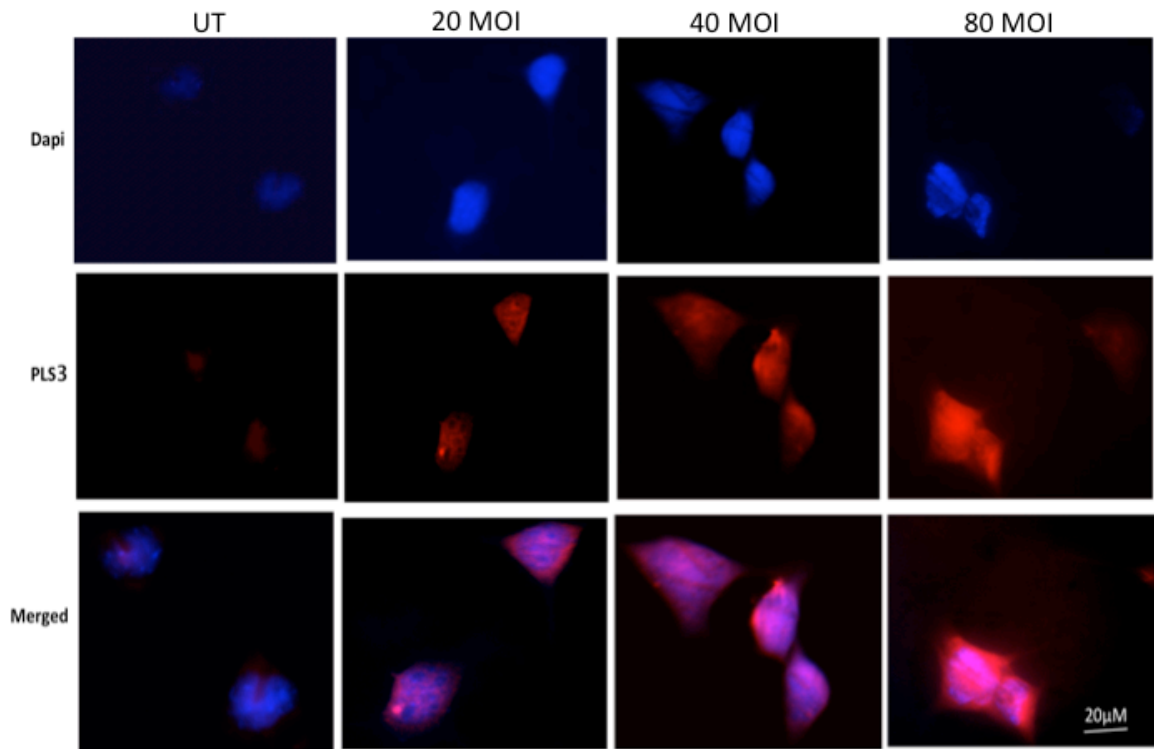


Figure 4.6. LV-mediated PLS3 expression in NSC34 assessed by immunofluorescence

NSC34 cells were transduced with LV-PLS3 at MOIs 20, 40 and 80. Un-transduced cells (UT) were used as a negative control. PLS3 (red) and the nucleus stained with DAPI-Diamidino-2-phenylindole (blue). Scale bar 20 μm.

The PLS3 localisation was observed throughout the NSC34 cells, which was associated with cytoplasm and nucleus. However, the staining pattern was different compared to HEK cells that showed a granular reactivity of PLS3 (see Figure 4.4). This observation may be due to cell type differences. This experiment confirmed that

the LV-PLS3 vector is functional and able to mediate PLS3 expression in motor neuron-like cells.

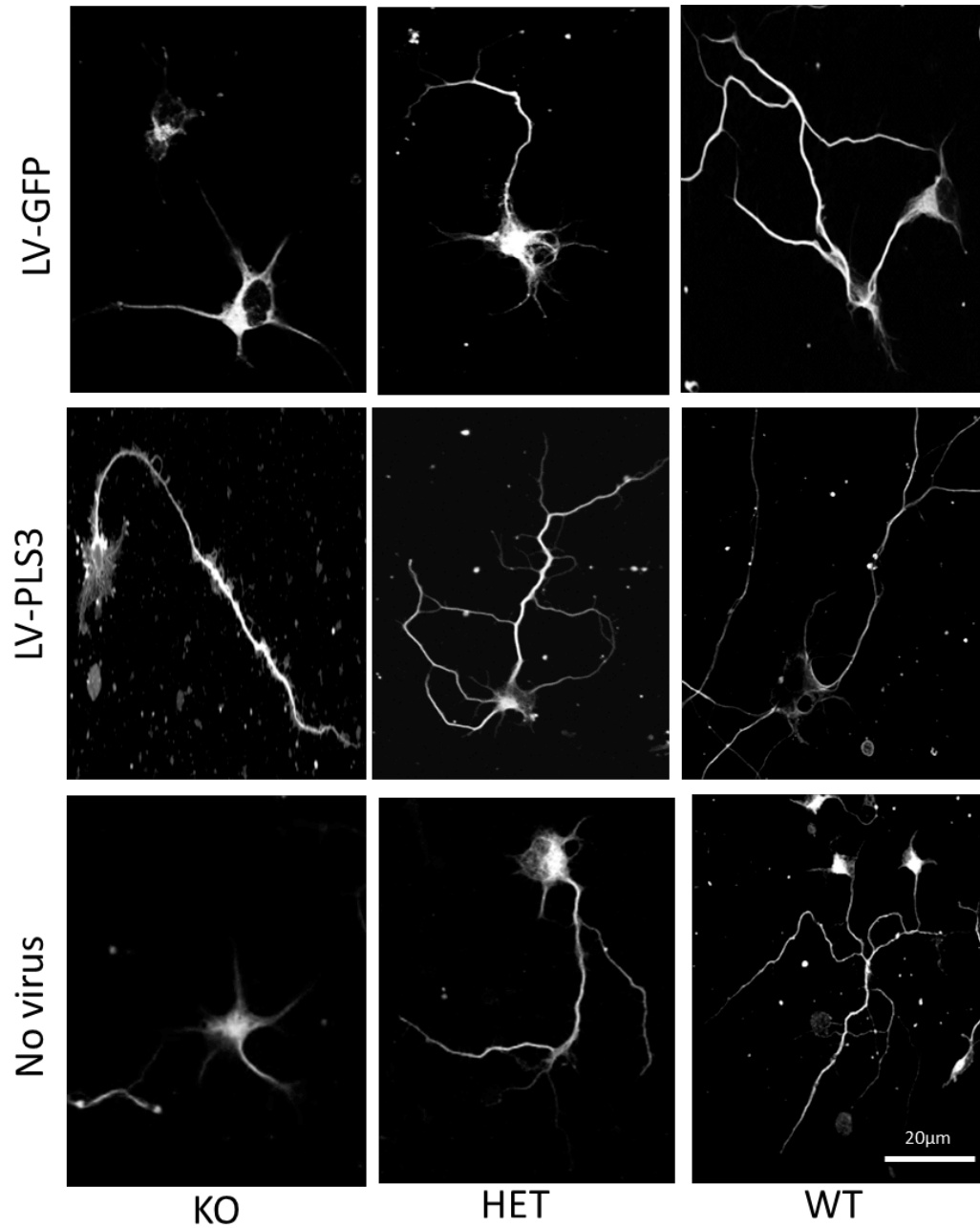
4.3.2.4 PLS3 overexpression promotes motor neuron axonal growth

The effect of PLS3 overexpression was examined within diseased cells, using purified motor neurons from the SMN Δ 7 mouse model. This mouse model resembles severe SMA carrying two human SMN2 copies on a null *Smn* background (Le et al., 2005). The rationale behind using this particular model in our studies is that previous report revealed that purified motor neurons from SMN Δ 7 embryos exhibit truncated axons with smaller growth cones (Monani et al., 2000, Rossoll et al., 2003, Jablonka et al., 2004). To test for potential neuroprotective ability of LV-PLS3, primary motor neurons were isolated at day E13 from WT (SMN2^{+/+}, SMN Δ 7^{+/+}, *Smn*^{+/+}), HET (SMN2^{+/+}, SMN Δ 7^{+/+}, *Smn*^{+/-}), and KO (SMN2^{+/+}, SMN Δ 7^{+/+}, *Smn*^{-/-}) embryos. After 24 hrs in culture, MNs were transduced with a lentivirus expressing either PLS3 or a green fluorescent protein (GFP) as control virus. A second control group of MNs were left un-transduced. MNs were 4%PFA fixed after 7 days in culture and immunostained with an anti-tubulin antibody to assess axonal length measurements (Figure. 4.7).

Neurons were visualised down the microscope and axons chosen if the entire axon length could be seen in a single field. Neurons with tangled axons or lots of branches were excluded as the main axon couldn't easily be identified and measured. 100 neurones were imaged for each genotype and ImageJ was used to draw a line from the start of the axon at the cell body to the tip of the axon. In the case of axons with branches (see figure 4.7, wt neuron with no virus) the main axon was chosen as the

thickest and longest branch and other branches were excluded from length calculations.

A



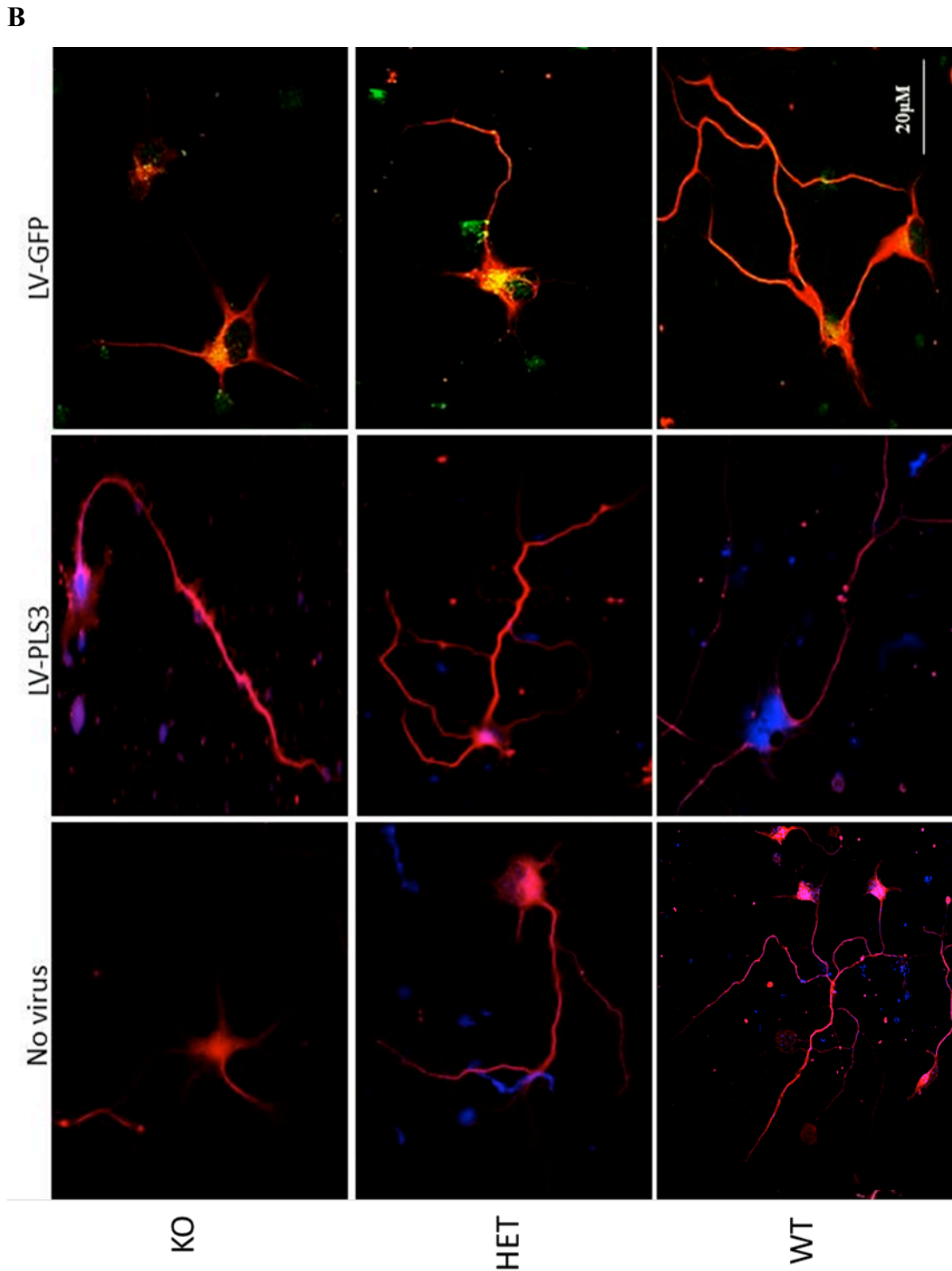


Figure 4.7. LV-mediated PLS3 neuroprotection in SMN Δ 7 purified motor neurons

Motor neurons isolated from E13 wild type (WT), heterozygous (HET), and SMN Δ 7 (KO) embryos were transduced with LV-PLS3 or LV-GFP at MOI 80. (A) axon length differences between all the genotypes, (B) axonal localisation of PLS3. PLS3-Plastin3 (blue), tubulin (red) and GFP (green). Scale bars: 20 μ m

A weak PLS3 signal was detected in untreated HET and WT MNs but not in untreated KO, suggesting that endogenous PLS3 can be detected. After transduction of MNs with LV-PLS3 virus, all genotypes showed PLS3 expression. Visually, the KO has very short axons except when treated with LV-PLS3 virus. The LV-PLS3-treated MN axon lengths appear comparable to un-transduced or PLS3-transduced MNs from heterozygous and WT embryos (Figure. 4.7). Cytoplasmic hair-like projections were seen in 30% of MNs. KO MNs treated by LV-GFP showed no changes in axon length, supporting that the changes in PLS3-treated KO cells were due to PLS3 and not the LV virus.

4.3.2.5 Axonal length statistical analysis

To explore whether lentiviral mediated expression of PLS3 controls axonal growth in purified MNs, the axon length was measured using the ImageJ plugin NeuronJ. Values from four independent experiments (n=4) were pooled together and the results were expressed as the standard error of mean (\pm SEM).

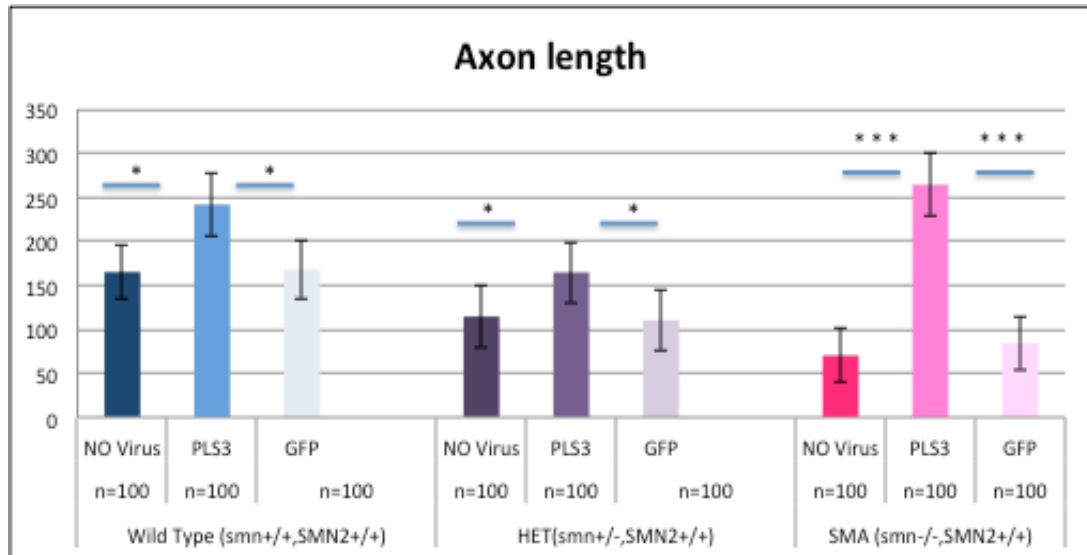


Figure 4.8. Impact of LV-PLS3 treatment on axon length in *Smn* deficient motor neurons

The bar chart shows the effect of LV-PLS3 treatment on axon length in wild type, heterozygous (HET), and SMA knockout (KO) embryos. Y-axis represents axon length in μm . A value of one-way ANOVA ($*=p < 0.05$, $***=p < 0.001$) was considered to be statistically significant, average neurite lengths (N = 100 neurites)

In agreement with previous reports (Rossoll et al., 2003, Oprea et al., 2008), our *in vitro* study showed a significant reduction in axon length of *Smn*-deficient MNs when compared to cells from either WT or heterozygous embryos (One way ANOVA, $p < 0.001$). Our studies revealed that overexpression of PLS3 through LV-PLS3 led to a highly significant rescue (ANOVA, $P < 0.001$) of average axon length and outgrowth defects associated with *Smn* down-regulation (N=100 axons) (Figure. 4.8). Expression of PLS3 in heterozygotes and wild type neurons also significantly increased axon length (ANOVA, $P < 0.05$). As expected, the GFP virus showed no effect on axon length in any genotype.

This data provides evidence that PLS3 is important for axonogenesis. The *in vitro* data revealed that PLS3 can rescue MN axon deficits existing in *SMN Δ 7* primary cultures.

4.4 Discussion

The data described in this part of the thesis revealed that modulation of PLS3 expression may play an important role in promoting axonal growth in healthy and diseased MNs. The detrimental effect of low *Smn* levels on axonal length was significantly rescued ($P < 0.001$) by PLS3 overexpression (Figure. 4.8). Previously generated data demonstrated reduced levels of *Pls3* expression in various tissues of the *SMN Δ 7* mouse model at early stages of development (Chapter 3). A similar finding was seen in purified *Smn*-deficient MNs from *SMN Δ 7* mouse model (Sleigh et al., 2011). Therefore, spinal MNs from *SMN Δ 7* mouse embryos were cultured for *in vitro* analysis to study the impact of lentiviral-mediated expression of PLS3 on axonal morphology. Spinal MNs cultured from *SMN Δ 7* mice at E13 showed significantly impaired axon growth when compared to WT and HET. To evaluate the neuroprotective effect of PLS3 in an *in vitro* SMA model, a lentiviral vector containing a PLS3 expression cassette was generated, and used to look at its ability to rescue axonal growth deficit in *Smn*-depleted MNs.

4.4.1 PLS3 staining pattern of different cell types

The LV-PLS3 virus showed a significant overexpression of PLS3 in 3 different cell types, with up to 7 fold increase, leading to the use of this vector for neuroprotection in MNs.

PLS3 expression was observed throughout the NSC34 cells, and was associated with the cytoplasm and nucleus. This was similar to PC12 cells, where endogenous PLS3 and *Smn* showed diffuse staining in the cytoplasm (Oprea et al., 2008). However, the staining pattern was different in HEK cells, which showed a granular reactivity of PLS3. It has also been shown in primary murine MNs that *Pls3* and *Smn* co-localise

in granules (Oprea et al., 2008). The reason behind this difference in Pls3 expression pattern in the cells mentioned above is unknown.

4.4.2 PLS3 is involved in axonogenesis and rescues the axon length in SMN Δ 7 MNs.

The LV-mediated overexpression of PLS3 in spinal MNs cultured from SMN Δ 7 mice rescued the observed axonal defects, with no apparent toxicity. There was a significant increase in axonal length ($P < 0.001$) in SMN Δ 7 MNs when treated with LV-PLS3. Notably, the axon length of the treated MNs was similar to that seen in wild type PLS3-treated neurons, and greater than in untreated wild type neurons, suggesting that LV encoding PLS3 compensate *Smn*-deficiency. This demonstrates that the LV-PLS3 virus was efficient at upregulating PLS3, and suggests a neuroprotective effect of PLS3 on MNs isolated from SMN Δ 7 mice. It has been shown in a previous study that overexpression of PLS3 rescued the outgrowth defects and axon length in MNs associated with *Smn* down-regulation in SMA models using zebrafish and mouse embryos (Oprea et al., 2008). However, this study has shown that a novel and more clinically relevant method of gene therapy can be used to successfully rescue MN defects.

Interestingly, further emerging evidence supports the role of PLS3 in axonogenesis. It has been demonstrated that knockdown of PLS3 in primary mouse MNs reduced axonal length, reproducing the effects of SMN deficiency (Bäumer et al., 2010, Hao et al., 2012). This was replicated in zebrafish, where injection of morpholinos targeting *Pls3* caused shortening of axons and increased axon branching, again mimicking the effect of silencing *Smn* (Hao et al., 2012). Further supporting a similar functional role between *Smn* and *Pls3*, SMN over-expression in

differentiated PC12 cells increases axon length in a similar way to over-expression of PLS3 (Oprea et al., 2008). This suggests that PLS3 could potentially modify SMA axon phenotypes through SMN and mRNA binding, since the reduced axon growth resulting from SMN protein deficiency in MNs was correlated with reduced β -actin protein and mRNA levels in growth cones (Rossoll et al., 2003).

These findings support the involvement of PLS3 down regulation in SMA pathology. An important role in promoting axonal outgrowth in both healthy and *Smn*-deficient motor neurons can be proposed. It is worth highlighting that the most significant increase in axonal length after LV-PLS3 transduction was reported in *Smn*^{-/-} MNs, in comparison to other genotypes (heterozygous and wild type). Thus, enhancing PLS3 expression represents an important therapeutic strategy to improve the health of the MN axons in SMA.

The molecular mechanisms for PLS3 involvement in SMA are unclear. Understanding the molecular mechanisms by which PLS3 act as a genetic modifier for SMA will be important in understanding the mechanisms of disease pathogenesis. PLS3 overexpression has been demonstrated to increase levels of F-actin, and it has been suggested that its role in stabilising actin filaments is crucial to axon development and therefore rescue of SMA pathology (Bowerman et al., 2009). However, the expression of a set of partial PLS3 molecules in zebrafish support a mechanism for PLS3 in SMA beyond that of actin binding (Lyon et al., 2013). PLS3 mutants lacking the actin binding domains were able to partially rescue SMA phenotype whereas mutants lacking the calcium binding were unable to rescue phenotype. This suggests that calcium binding, independent from actin binding, may also play a role in SMA disease.

This suggests that PLS3 might have an additional function unrelated to its interaction with actin (Bowerman et al., 2009).

4.4.3 Summary

The neuroprotective property of gene therapy mediated PLS3 expression has been shown to increase axonal length in both healthy and diseased *Smn*-deficient MNs, but it is not known whether it would improve mouse survival or disease phenotype *in vivo*. In this current study, only axonal length was assessed, but MN survival, NMJ and neuronal health could also be determined to see whether PLS3 also improves the quality of the MNs. It is important to test viral vector-mediated PLS3 gene therapy *in vivo* in a mouse model of SMA. The aim of the next chapter was to generate *in vivo* gene therapy proof-of-concept in *SMN Δ 7* mouse model.

**Chapter 5 : Adeno-associated vector serotype 9 (AAV9)
encoding PLS3 gene therapy study in SMN Δ 7 mouse model of
SMA**

5.1 Aims

In chapter 4, it was reported that lentiviral delivery of the PLS3 gene led to significant transgene expression and rescued axonal length in primary Smn-deficient motor neurons. The neuroprotective ability of a viral vector encoding PLS3 has never been tested in a mouse model of SMA, therefore the work described in the present chapter will evaluate a gene therapy approach using viral vectors encoding PLS3 in SMN Δ 7 mouse model. This *in vivo* proof-of-concept study will assess the survival of SMN Δ 7 mice following delivery of adeno-associated virus serotype 9 vectors encoding PLS3 (AAV9-PLS3) into the cisterna magna.

5.2 Introduction

Chapter 4 demonstrated that PLS3 overexpression in cultured Smn-deficient motor neurons ameliorates axon outgrowth defects and restores axon length; suggesting that restoration of PLS3 may rescue early lethality in a well-characterised mouse model of SMA. Early postnatal delivery of PLS3 may ameliorate SMA phenotype via delayed axon pruning and improvement of motor function. Since PLS3 is an actin-binding protein, its restoration may regulate actin dynamics, which may prevent muscular atrophy due to MN degeneration and therefore SMA pathogenesis. This chapter aims to establish the impact of PLS3 modulation in an SMA mouse model *in vivo*. With a clinical application in mind, an AAV-based vector will be used, due to its improved safety profile over lentivirus vectors. In this chapter, two different types of AAV backbones will be tested: single stranded AAV (ssAAV) and self-complimentary AAV (scAAV). ssAAV consist of a single-stranded DNA genome, which requires a cellular stress or a helper virus to promote the production of the complementary strand and replication, resulting in slow onset of transgene

expression (Davidson and Breakefield, 2003). In order to overcome this problem, scAAV was generated, in which the DNA contains two complementary sequences that produce an intra-molecular double strand upon release from the viral particles (McCarty et al., 2001, Davidson and Breakefield, 2003, McCarty et al., 2003). The advantage of using scAAV compared to the conventional ssAAV is that it allows a faster expression of the transgene *in vivo* (McCarty et al., 2001, McCarty et al., 2003, Wang et al., 2003, Duque et al., 2009, Valori et al., 2010, Gray et al., 2011, Aschauer et al., 2013) However, the need for two complementary sequences in the scAAV genome limits the packaging capacity with the maximum size of the target gene being 2.2kb. Conventional AAV is required for larger inserts up to 4.4kb. The size of the PLS3 insert is on the limit of virus packaging capability for scAAV (Hermonat et al., 1997); therefore, it wasn't clear whether a functional scAAV9 virus could be made.

One of the main obstacles of gene therapy in neurodegenerative diseases is the difficulty in crossing the blood brain barrier (BBB) to gain access to the cells of interest and allow wide dissemination throughout the CNS. AAV serotype 9 (AAV9) has been shown to infect a broad range of cells in the CNS and has been shown to be able to cross the BBB (Foust et al., 2010, Valori et al., 2010, Aschauer et al., 2013). A previous study post intracranial delivery of AAV virus showed high transduction efficiency as a result of axonal transport of viral particles to sites distal to the vector injection site (Cearley and Wolfe, 2006), revealing its ability to mediate wide spread transduction in the CNS.

AAV9 has been chosen for *in vivo* experiments based on previous studies showing high gene transfer to the CNS following intravenous (IV) delivery of this vector into

neonatal mice (Valori et al., 2010). Different serotypes of AAV have different capsid protein sequences and these variations greatly influence the ability of each serotype to transduce particular cell types and brain regions (Miyake et al., 2011). Following intravenous (IV) administration of various AAV serotypes AAV1, 5, 6, 8, 7 and 9 in adult mice, bioluminescence analysis revealed that three expression levels were achieved; low expression (AAV2, 3, 4, and 5), moderate expression (AAV1, 6, and 8) and high expression (AAV7 and 9) (Zincarelli et al., 2008). Numerous AAV serotypes appear to efficiently transduce basal and lateral amygdala (BLA) neurons; however, AAV8 and AAV9 appeared to be ideal serotypes to use when targeting BLA neurons, as both achieved high titres and transduced BLA neurons well (Holehonnur et al., 2014). Another study tested the ability of several single-stranded adeno-associated viral (ssAAV) serotypes to deliver transgenes to the brain and spinal cord in neonatal mice. Following jugular vein injection of ssAAV vectors (serotypes 1, 8 and 9) in neonate mice, all three serotypes were detected in both the brain and spinal cord; however, ssAAV9 was the most efficient (Miyake et al., 2011). AAV9 can strongly transduce MNs in the CNS following intravenous administration, as well as other tissues such as cardiac tissue and skeletal muscle (Benkhelifa-Ziyyat et al., 2013), making it an ideal candidate for SMA therapy.

In addition, several studies have shown that scAAV9 virus is able to cross the BBB and transduce cells of the CNS safely, with high efficiency and long-term transgene expression, demonstrated even in well-developed adult animal models (Kaspar et al., 2003, Foust et al., 2009, Foust et al., 2010, Valori et al., 2010, Gray et al., 2011, Aschauer et al., 2013, Benkhelifa-Ziyyat et al., 2013). Moreover, it was reported that after intravenous injection of scAAV9 vector expressing SMN, the virus was able to cross the BBB and transduce motor neurons, upregulate SMN protein expression,

and improve the survival of SMA mice, cats and non-human primates (Duque et al., 2009, Foust et al., 2010, Valori et al., 2010). This means it can be introduced to the CNS using relatively non-invasive techniques, which is essential for patients to improve their quality of life. Furthermore, Benkelifa-Ziyyat et al. (2013) reported that upon intramuscular injection of scAAV9-SMN virus, it was able to travel in a retrograde manner via axonal transport and transduce cells of the CNS, and significantly improve the survival rate of the SMN mouse model (Benkelifa-Ziyyat et al., 2013).

5.3 Results

5.3.1 Construction of AAV-PLS3 vectors

The viral vectors were generated and produced in-house. To produce a viral vector expressing the gene of interest, PLS3 was subcloned into the backbone of the AAV viral genome. The human PLS3 gene was transferred from pcDNA3.1-PLS3-V5/His6 into the self-complementary AAV vector (scAAV-CMV-GFP), and the conventional AAV vector (pAAV CMV MCS). The maps of the resulting vectors are described in Figure 5.3 and in appendix 2.

5.3.1.1 scAAV vectors encoding PLS3

A comparison was made between two scAAV viral vectors expressing PLS3 under the control of either the CMV full or minimal promoter. This was done in order to achieve a virus that successfully expressed PLS3, within the size limit of the vector packaging capacity.

The full CMV promoter is around 650bp, and the minimal promoter is the 3' 120bp-long fraction of it. Full CMV promoter gives the strongest level of expression, the

minimal is also fairly strong in transfection assays and is supposed to be the minimal sequence required to initiate gene expression (Doll et al., 1996, Hermonat et al., 1997).

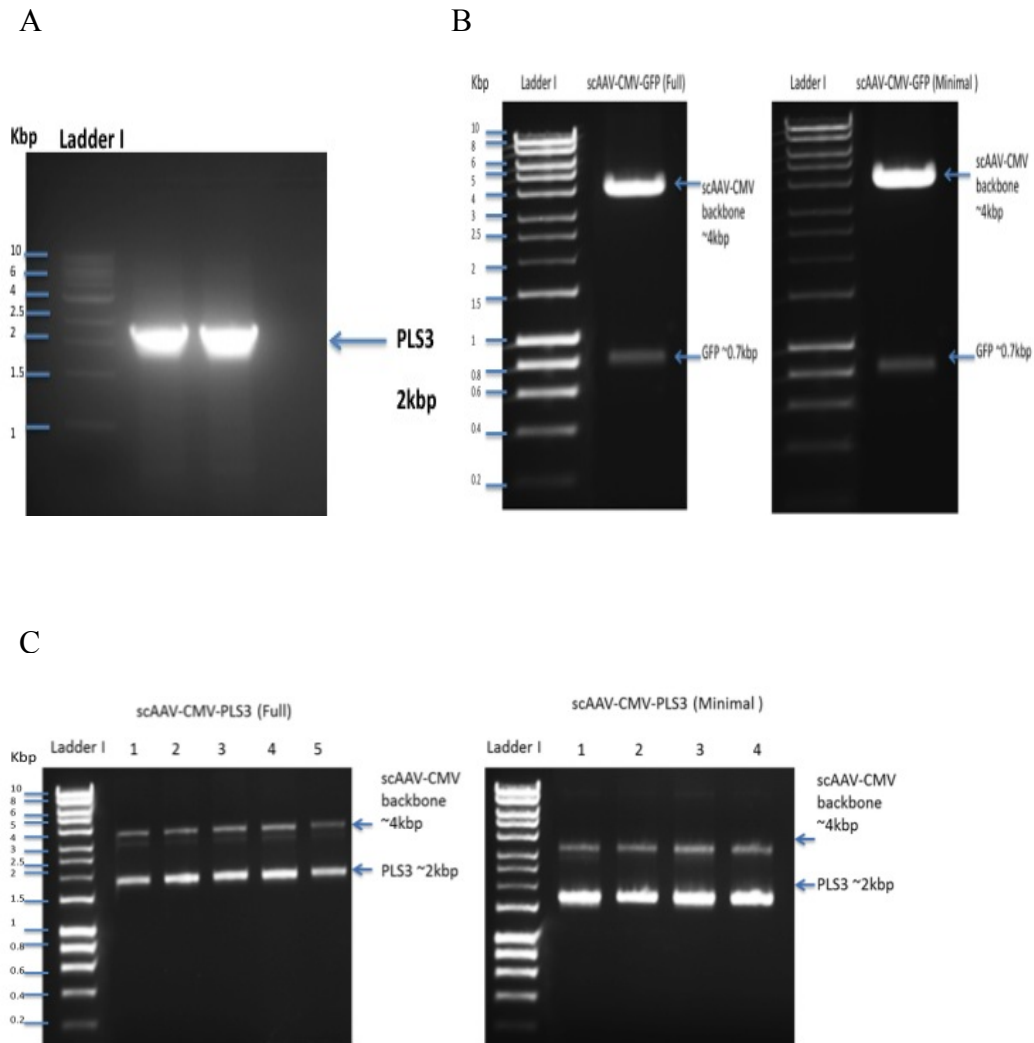


Figure 5.1. Insertion of PLS3 into the scAAV backbone

(A) PCR product amplified from digested pcDNA3.1-PLS3-V5/His6 shows human PLS3 fragment at 2 kb. (B) scAAV-CMV-GFP (Full and Minimal) plasmids were cut by *Bam*HI – *Xba*I. The larger fragment ~ 4 kbp represents the plasmid backbone scAAV-CMV while the smaller ~0.7kbp represents the excised GFP. (C) scAAV-CMV-PLS3 (Full/ Minimal) plasmids digested by *Bam*HI – *Xba*I. The larger fragment ~ 4 kbp represents the plasmid backbone scAAV-CMV while the smaller ~2kbp represents PLS3. Lanes; 1-5: five clones analysed.

The *PLS3* gene that was used in viral subcloning for all viruses was amplified by PCR (Figure. 5.1A). The scAAV-CMV-GFP Full/Minimal promoter plasmids were digested with the restriction enzymes *Bam*HI – *Xba*I to remove the GFP cassette (Figure. 5.1B) and replaced with the desired PLS3 insert; the correct band size after

digestion confirmed that the gene was successfully cloned into all vectors (Figure. 5.1C). In addition, sequencing of the plasmid confirmed the correct orientation of the insert and that no spontaneous mutations have occurred (see appendix 3).

HEK293T cells were transfected with the generated plasmids in order to confirm the efficiency of PLS3 expression prior to viral production. Western blot confirmed successful overexpression of PLS3 with both vector plasmids (Figure. 5.2A, Figure. 5.2B). The un-transfected cells have a low endogenous level of PLS3 and were used as control. Densitometry showed that the overexpression of the plasmid using the minimal promoter plasmid was almost double that of the full promoter plasmid (Figure. 5.2C).

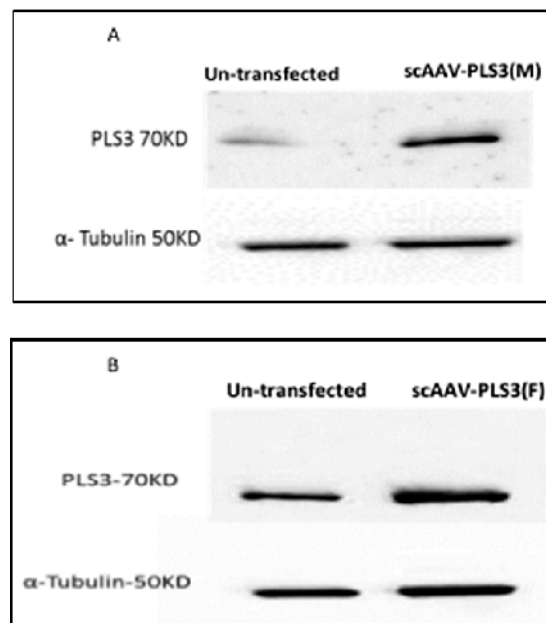


Figure 5.2. Validation of the scAAV-based plasmids expressing PLS3

Western blots showing scAAV-PLS3 mediated transgene expression in HEK293T cells. (A) scAAV-PLS3 with the minimal CMV promoter, (B) scAAV-PLS3 with the full CMV promoter. The membrane was probed with the primary anti-PLS3 antibody, and α -Tubulin was used as the loading control. PLS3 was detected at 70 kDa. Un-transduced cells were considered as negative control for this experiment and had a low levels of endogenous PLS3.

Following successful validation of both scAAV plasmids, scAAV-PLS3 with minimal CMV promoter was chosen to make a virus. The minimal promoter allowed a larger packaging capacity, which was important as the *PLS3* gene size is considered close to the maximum packaging capacity of scAAV vector.

5.3.1.2 ssAAV encoding PLS3

The pAAV CMV MCS (ssAAV) vector was digested with the restriction enzymes *EcoRI* and *XbaI* to remove the MCS cassette and replaced with the desired insert, PLS3 (Figure 5.3). The map of the AAV9-PLS3 vector is presented in Figure 5.3A

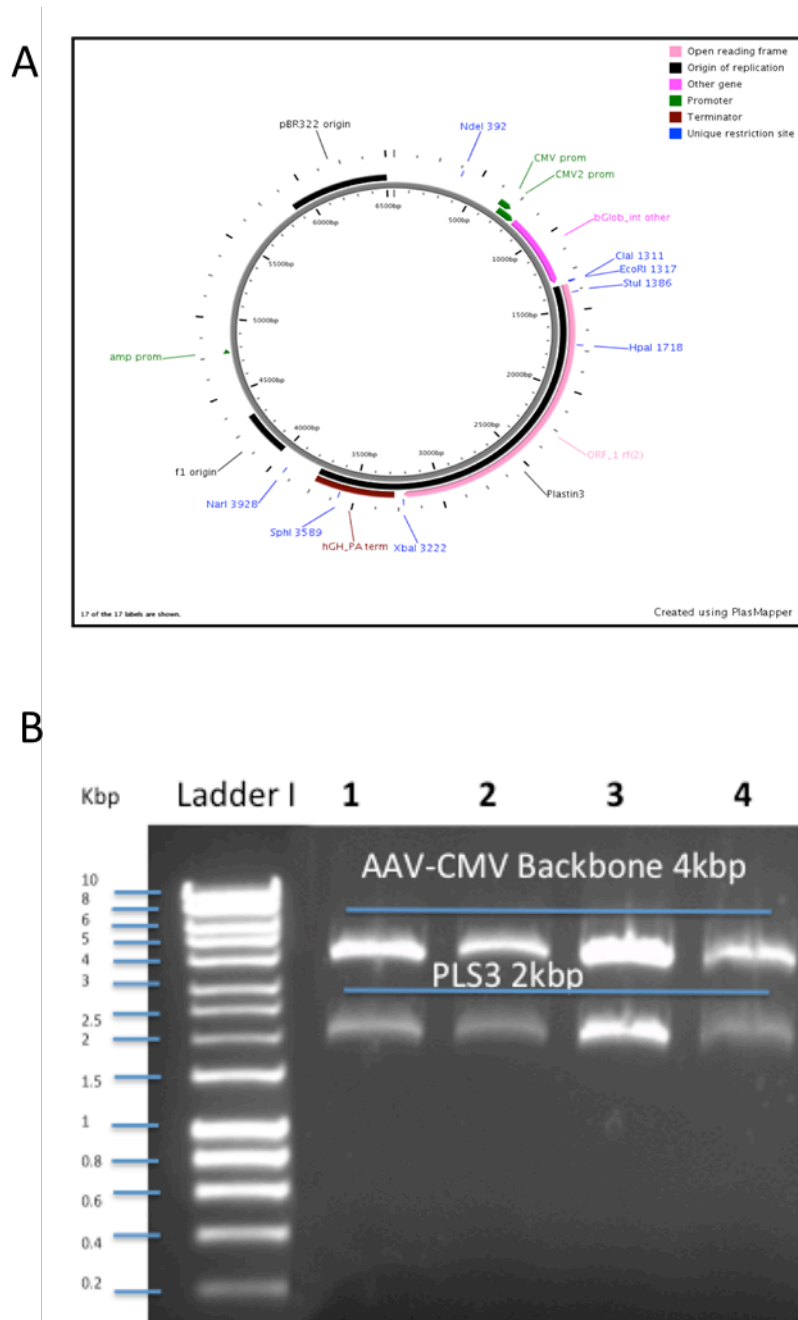


Figure 5.3. PLS3 cloning into ssAAV backbone

(A) Plasmid map represents the AAV9-PLS3 sequence with unique restriction sites. (B) *EcoRI* – *XbaI* digest of four clones. The 4 kbp fragment represents the plasmid backbone AAV-CMV while the 2 kbp one represents the PLS3 insert

The plasmid showed successful double digestion of AAV9-PLS3, giving the expected size for the insert PLS3 (2 kbp) and the AAV-CMV backbone (4 kbp) (Figure. 5.3B). The orientation of the insert and the sequence of AAV9-PLS3 plasmid were validated by sequencing (see appendix 2). HEK293T cells were transfected with AAV9-PLS3 plasmid in order to confirm the efficiency of the plasmid prior to viral production.

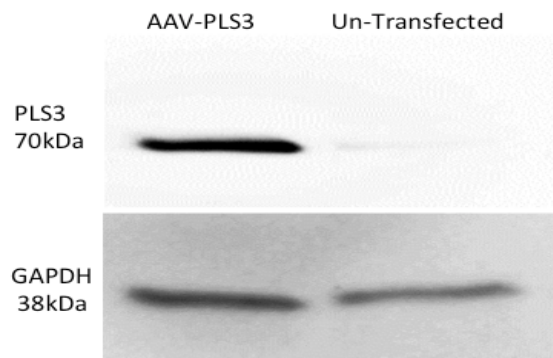


Figure 5.4. Validation of the ssAAV-based plasmid expressing PLS3.

Western blot using protein extracts from HEK293T cells transfected with the AAV-PLS3 using the PEI transfection method. The membrane was probed with the primary anti-PLS3 antibody, GAPDH was the loading control. Un-transfected cells were considered a negative control for this experiment. PLS3 was detected at ~70 kDa

Overexpression of PLS3 was confirmed by western blot (Figure 5.4). A low level of endogenous PLS3 was seen in un-transfected cells and a much stronger band was seen in transfected cells (Figure 5.4) suggesting the generated plasmid is functional and produces the desired transgene.

5.3.2 Virus production and purification

Following the validation of the plasmids, scAAV-PLS3 (with minimal CMV promoter) virus and ssAAV-PLS3 were produced (see Chapter 2 for details). In order to assess the purity of the viral preparation, samples of the viral fractions were collected and run on an SDS-PAGE gel and stained with SYBRO RUBY. Fractions were pooled and western blot analysis was performed on the high quality fraction to detect viral proteins by using an antibody against the AAV capsid proteins VP1, VP2 and VP3.

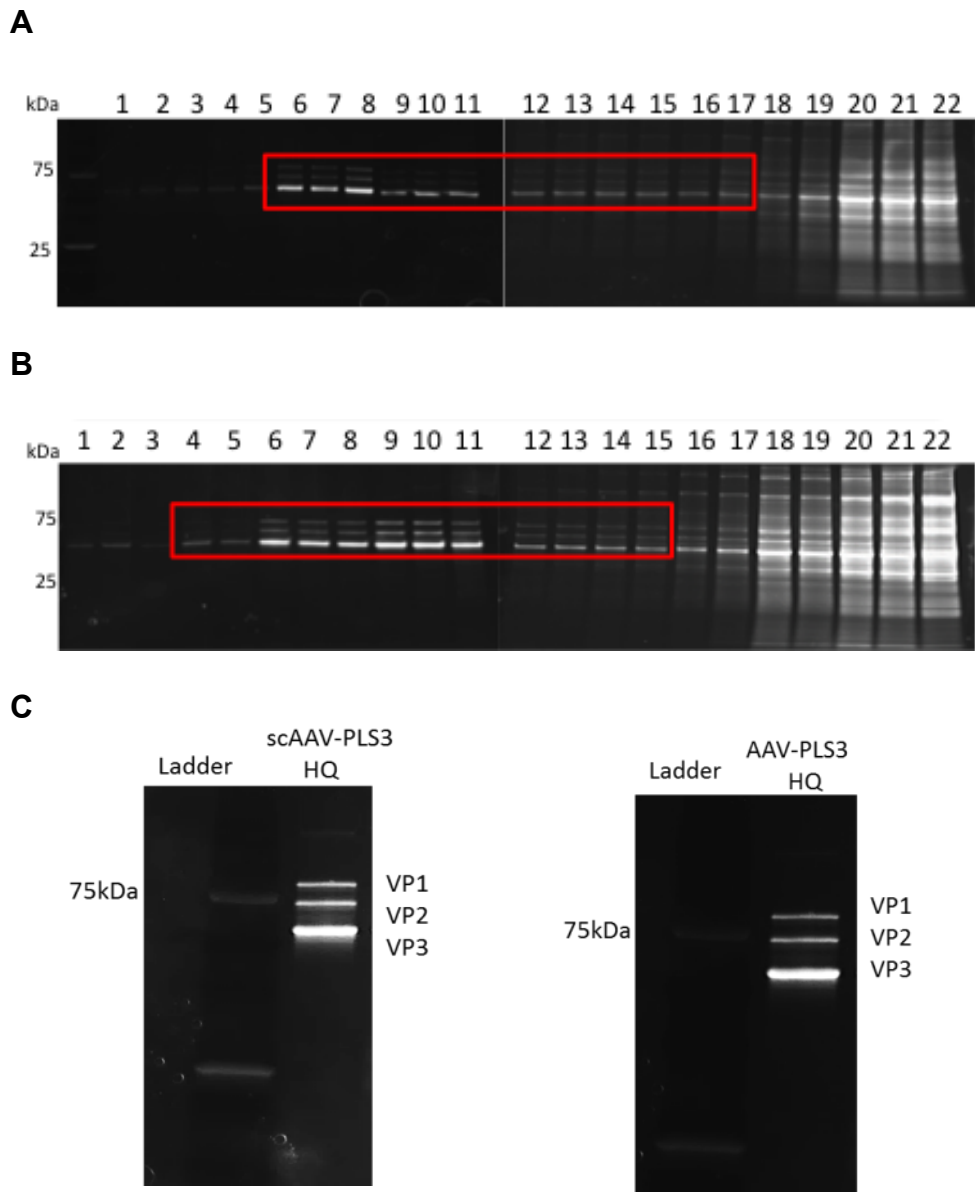


Figure 5.5. Production of high quality AAV9 viruses

SDS-PAGE gel stained with SYPRO-Ruby showing the purity of the different viral fractions. Fractions within the red box were pooled, concentrated and used as high quality virus. (A) scAAV9 fractions 6-17 showing three capsid bands are the high quality (HQ) preparations. (B) ssAAV9 fractions 4-15 showing three capsid bands are the high quality (HQ) preparations. (C) SDS-PAGE gel showing high quality preparations stained with SYPRO-Ruby. The three viral capsid proteins bands are present for the HQ preparation; VP1 at 87 kDa, VP2 at 72 kDa and VP3 at 62 kDa reflecting the purity of the viral preparations.

Fractions containing pure virus (red boxes in Figure 5.5) were pooled together and considered as high quality virus prep (Figure. 5.5A, Figure. 5.5B). Both viruses had clean fractions for pure virus, and the pooled high quality virus showed all 3 viral capsid proteins (Figure 5.5C). The viral titre was determined by qPCR (Table 5-1). Primers for determining titres were designed to detect the transgene, therefore empty viral vectors were not detected and did not interfere with the viral titre measurements obtained.

Table 5-1 Viral titres of high quality fractions (viral genomes per ml)

scAAV-PLS3	ssAAV-PLS3
7.9x10 ¹³ vg/ml	3.9x10 ¹³ vg/ml

Both viruses were validated *in vitro* for overexpression of PLS3 by transduction in HEK293T cells. Two different doses of virus (Table 5-2) were used for transduction in order to check for toxicity with a high dose of virus before it was tested *in vivo*.

Table 5-2 Viral concentrations used for transduction of HEK293T cells

Virus	Low dose	High dose
scAAV-PLS3	3.65E+10	4.9E+11
AAV-PLS3	3.95E+10	7.9E+11

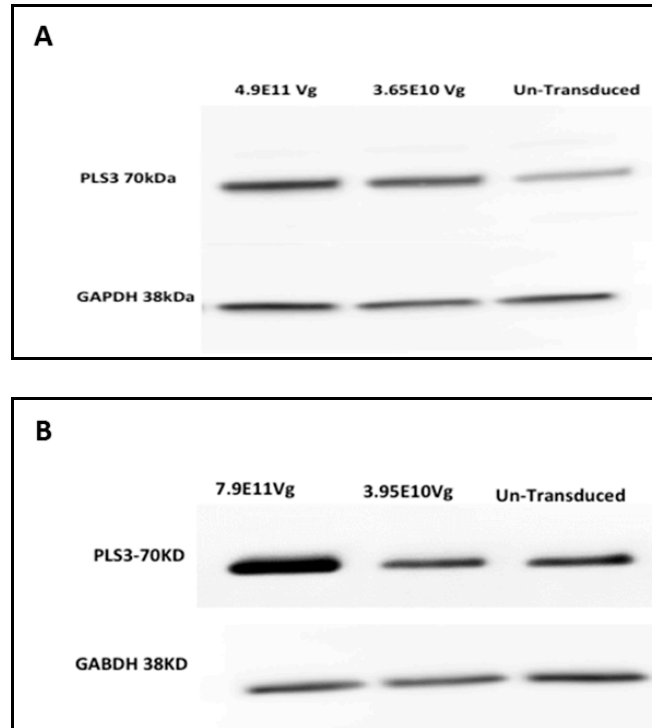


Figure 5.6. Validation of scAAV9-PLS3 and ssAAV9-PLS3 viruses

Western blot showing HEK293T cells transduced with two different concentrations of high quality virus. The membrane was probed with the primary anti-PLS3 antibody, GAPDH was used as a loading control. Un-transduced cells were considered as negative control for this experiment. (A) scAAV-PLS3 (B) ssAAV-PLS3

Both scAAV-PLS3 and ssAAV-PLS3 viruses were able to overexpress PLS3 in a human cell line (Figure. 5.6A, Figure. 5.6B). In both cases, the high doses showed stronger PLS3 protein levels when compared to low doses, suggesting dose-dependent overexpression (Figure. 5.6).

5.3.3 scAAV-PLS3 gene transfer *in vivo*

Self-complimentary AAV vectors are preferred to ssAAV due to faster gene expression. Following scAAV9-PLS3 production and validation *in vitro*, this vector was chosen to perform a pilot study to test whether the virus can overexpress PLS3 *in vivo*. The scAAV9-PLS3 virus, or scAAV-GFP control virus, were administered by facial vein injection into WT mice at P1 (25 μ l of 1×10^{10} vg/ml). Three mice were injected with each virus, (Figure 5.7) represent extracts from each animal.

No adverse effects were seen in the mice injected intravenously, revealing that the virus is not toxic and it is safe to be used for any further *in vivo* studies. After 21 days, mice were culled and protein extracts from spinal cord, brain and muscle were assessed for PLS3 expression.

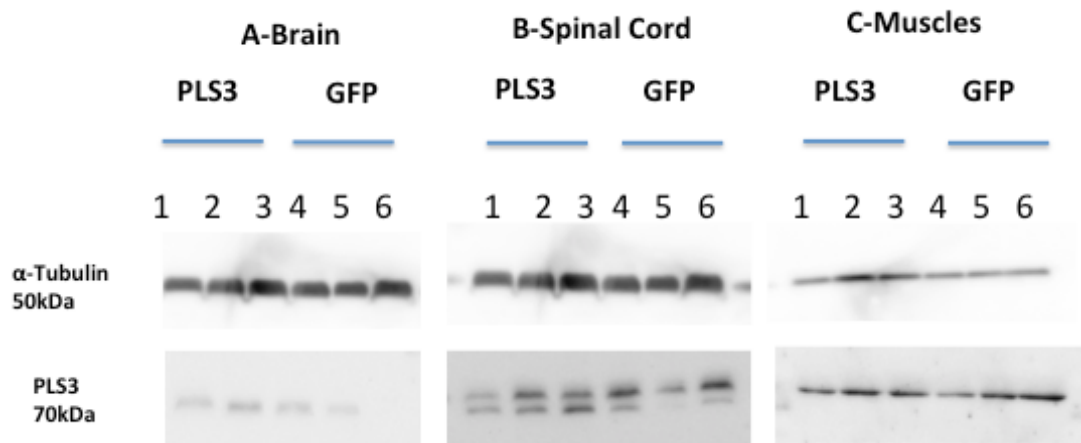


Figure 5.7. Postnatal day 21 PLS3 protein levels following scAAV9-PLS3 IV delivery in P1 mice

PLS3 protein levels at P21 in WT. Western blot showing PLS3 expression in (A) brain, (B) spinal cord and (C) muscle tissues. The membrane was probed with the primary anti-PLS3 antibody, α -tubulin is the house keeping control (n=3). Lanes 1-3 mice injected with scAAV9-PLS3, Lanes 4-6 mice injected with scAAV9-GFP

Tissues analysed by western blot at postnatal day 21 revealed no apparent difference between the two groups for PLS3 protein levels in the CNS (Figure. 5.7A, Figure. 5.7B) or muscles (Figure 5.7C). This suggests that there was no overexpression of PLS3 at P21 in these tissues. The reason for weak scAAV9-PLS3 expression could be due to the size of the insert at the limit of packaging capacity of scAAV backbone. Based upon the lack of expression of PLS3 seen with scAAV9-PLS3, it was decided not to proceed to *in vivo* proof-of-concept using this virus.

5.3.4 Gene transfer efficiency of ssAAV9-delivered via cisterna magna

Based on the outcome of the pilot study with scAAV9-PLS3 (see above) we decided to adopt a new strategy. ssAAV9-PLS3 showed promise in term of PLS3 expression when validated in HEK293T cells. The advantage of conventional ssAAV is the large cloning capacity (4.4 kb) compared to scAAV. The only issue for conventional ssAAV9 is the low ability of crossing BBB when delivered IV, therefore cisterna magna was adopted as delivery route for ssAAV9-PLS3.

At 29 days, the carrier littermate (HET) pups injected with ssAAV9-GFP or ssAAV9-PLS3 respectively were culled and spinal cord was collected for Western blot assessment. The spinal cord was separated into the three different regions; cervical, thoracic and lumbar; and human PLS3 protein was measured to determine the efficacy of ssAAV9-PLS3 in mediating PLS3 overexpression.

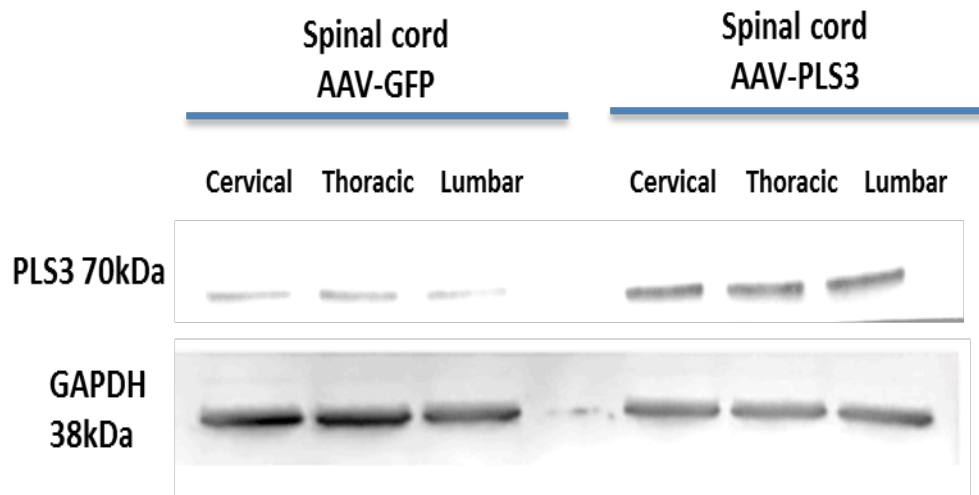


Figure 5.8. WB analysis of the spinal cord following cisterna magna delivery of ssAAV9-PLS3

The figure showing three parts of the spinal cord; cervical, thoracic and lumbar of HET SMN Δ 7 pups injected with ssAAV9-GFP or ssAAV9-PLS3 respectively. The membrane was incubated with anti-hPLS3 antibody.

The analysis summarised in Figure 5.8 demonstrates clear PLS3 overexpression in ssAAV9-PLS3 treated spinal cord compared to controls. A very weak band was seen in the control group injected with ssAAV9-GFP indicating cross-species reactivity between the human anti PLS3 antibody and the endogenous mouse PLS3; however, this was used as the baseline of PLS3 when measuring overexpression.

5.3.5 Efficacy study

In vivo pilot study using ssAAV9-PLS3 yielded good levels of PLS3 overexpression in the spinal cord. Therefore it was decided to proceed with cisterna magna as route of delivery to test the efficacy of ssAAV9-PLS3 in SMN Δ 7 mice.

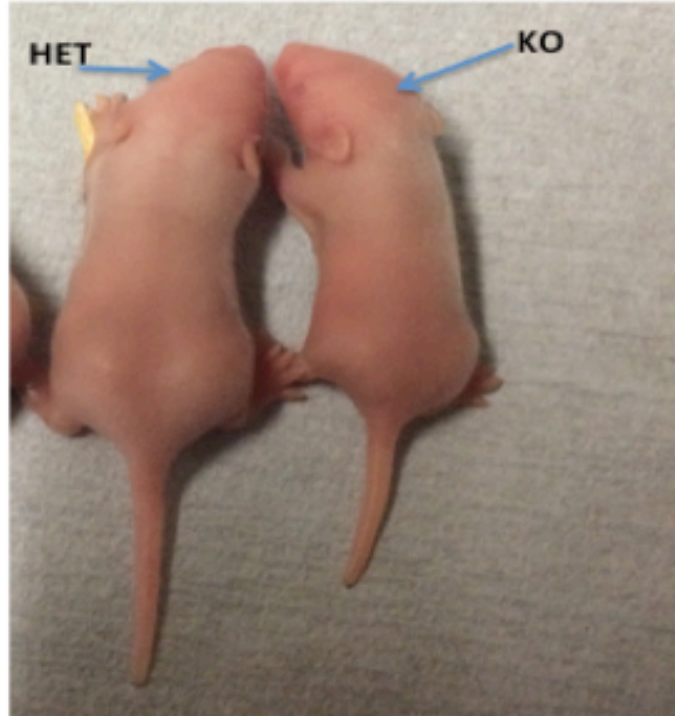
P1 SMN Δ 7 pups were injected with 1 μ l of ssAAV9-PLS3 containing 2×10^{13} vg (n=7) into the cisterna magna. As a control, SMN Δ 7 mice were injected with ssAAV9-GFP (1×10^{10} vg) (n=7) and a third group injected with PBS as a non-treated group (n=7). The carrier littermates (SMN2 $+/+$, SMN Δ 7 $+/+$, *smn* $+/-$) (N=3) were also injected with AAV-PLS3, AAV-GFP or PBS as further controls. Daily assessment of the mice was performed throughout their life to determine whether there was any effect on SMN Δ 7 phenotype. All the statistical analysis depending on the number of variables was performed by either one-way or two-way ANOVA.

5.3.6 Body Weight

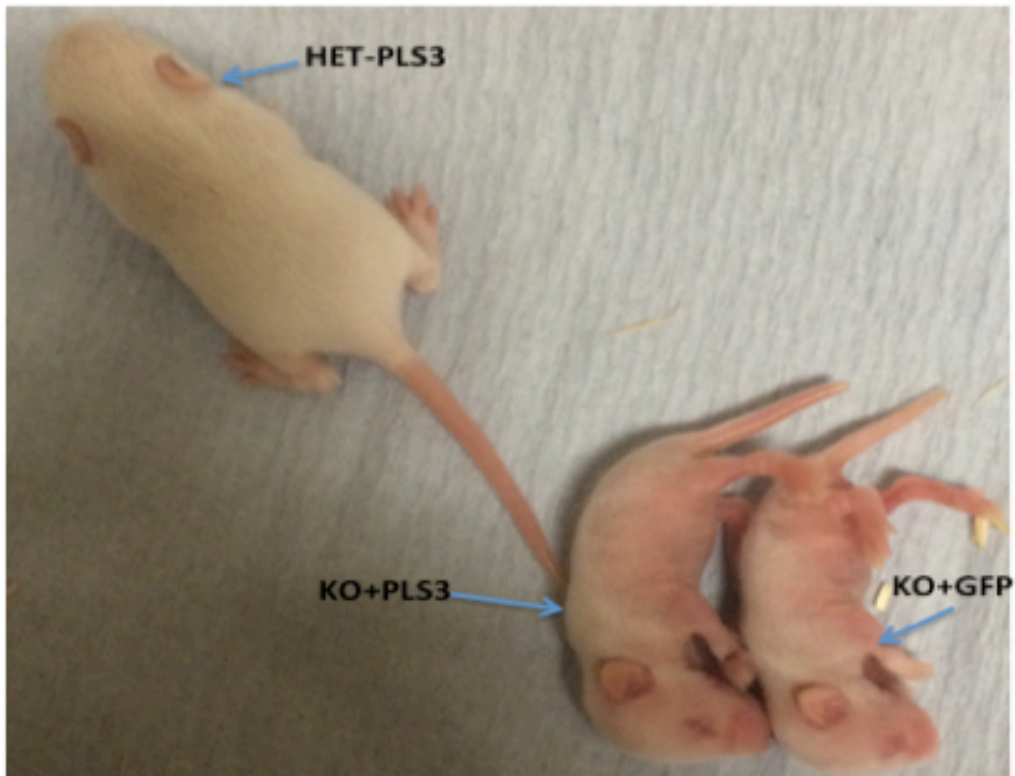
Slow growth and loss of body weight from postnatal day 8 is considered to be major feature of SMN Δ 7 mice phenotype El-Khodori et al, (2008), therefore the weight of all mice was monitored daily and changes of body weight were recorded throughout the study (El-Khodori et al., 2008).

A

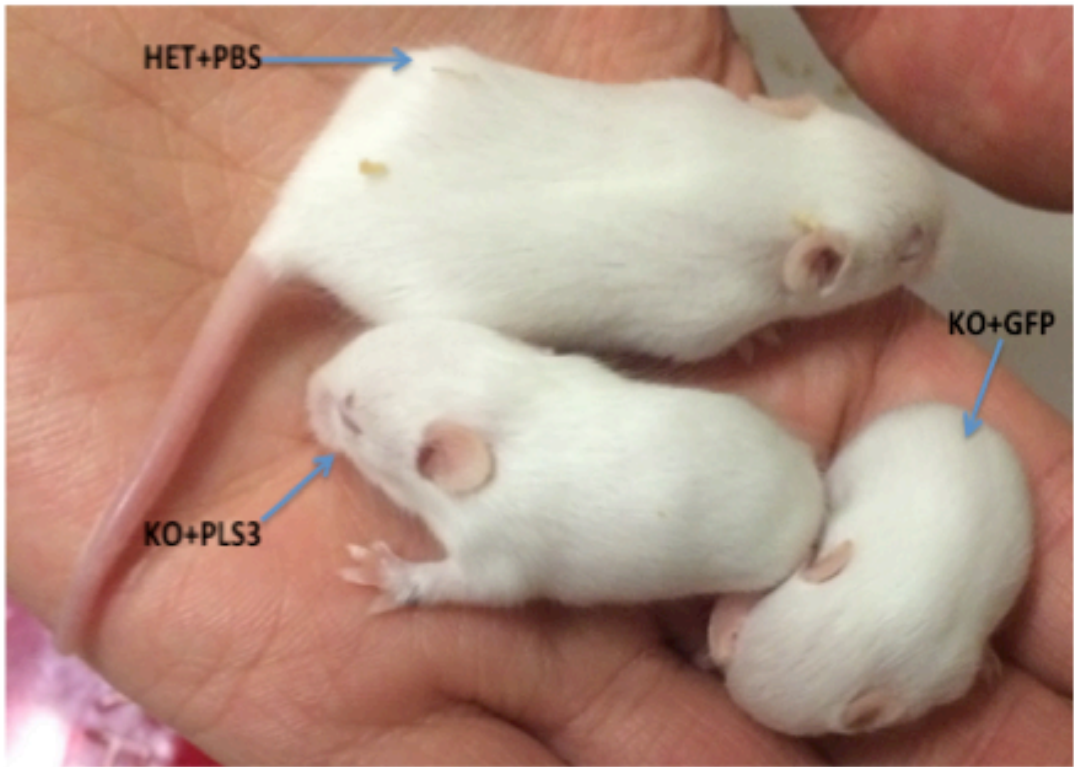
Day 2



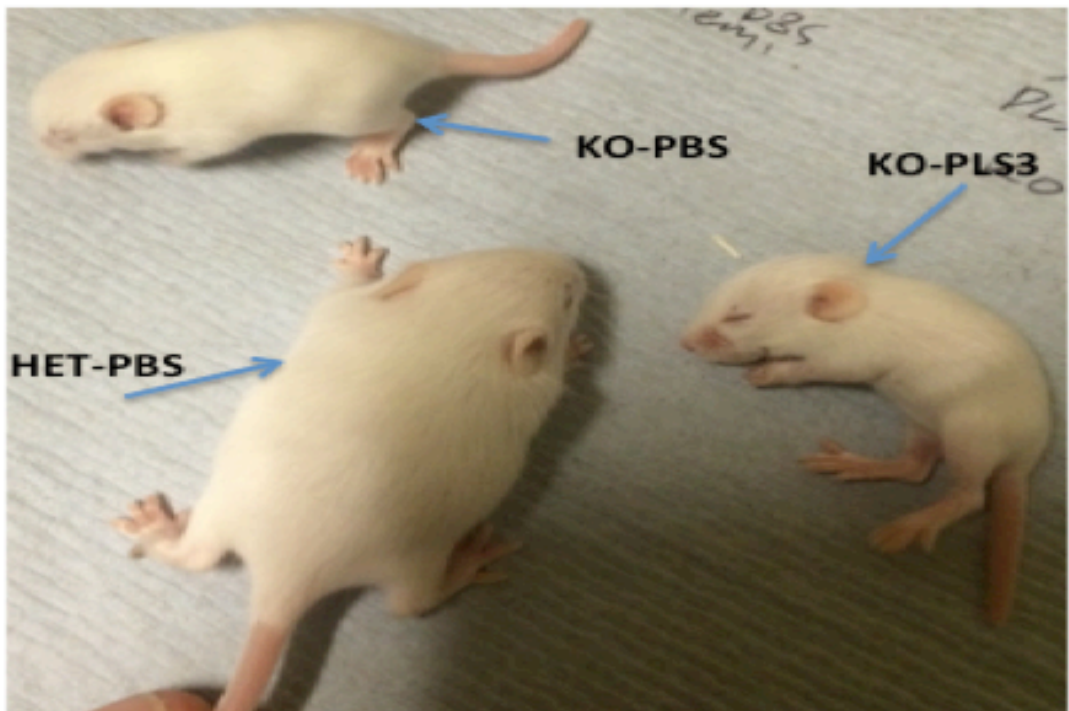
Day 8



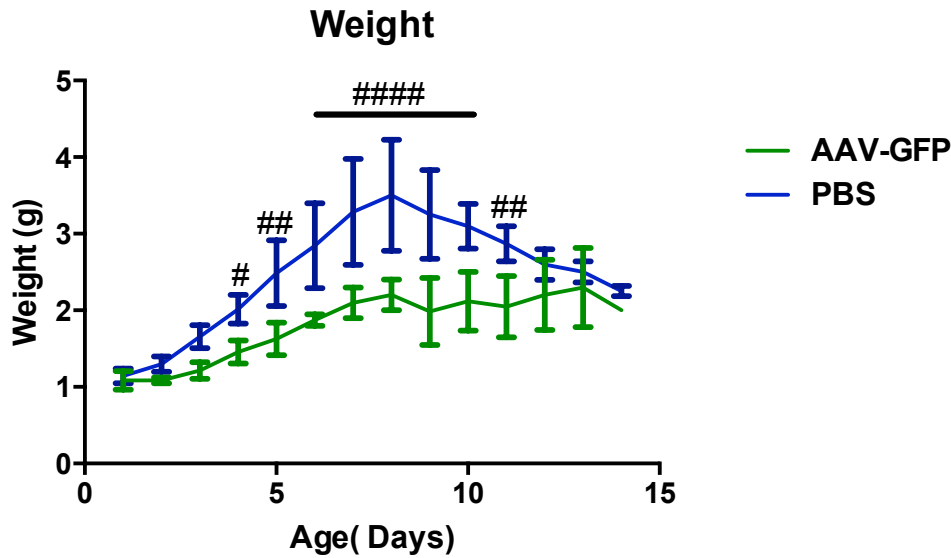
Day 11



Day 17



B



C

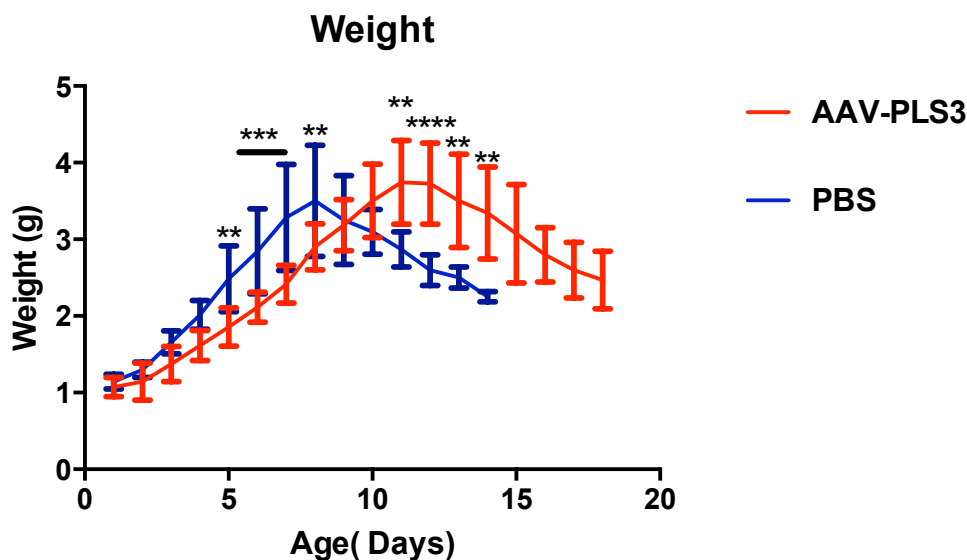


Figure 5.9 Body weight assessment of SMN Δ 7 mice

A: Images showing the same SMN Δ 7 pups at different ages, as indicated. A gender-matched carrier littermate is included in each picture for reference. The pups were injected at postnatal day 1 with either ssAAV9- PLS3 or ssAAV9-GFP or PBS. B: Body weight growth in SMN Δ 7 injected with PBS (n=7) or ssAAV9-GFP (n=7). C: Body weight growth in SMN Δ 7 injected with ssAAV9-PLS3 (n=7) or PBS (n=7). Untreated (injected with PBS) were included as controls. *p<0.05, ** p<0.01, *** p<0.001, **** p<0.0001 for AAV-PLS3 vs. PBS, #p<0.05, ## p<0.01, #### p<0.001, ##### p<0.0001 for AAV-GFP vs. two-way ANOVA with Dunnett's multiple comparisons test'. ssAAV9 – single stranded adeno-associated virus serotype 9; GFP – Green fluorescent protein; PLS3-Plastin3; PBS Phosphate-buffered saline.

There was a significant difference in body weight between ssAAV9-PLS3 treated, ssAAV9-GFP controls and PBS injected controls (two-way ANOVA, with Dunnett's multiple comparisons test, $p < 0.001$). Initially, as expected, a weight gain was shown with the untreated SMN Δ 7 mice, which was then followed by gradual weight loss from day 8 to death (Figure. 5.9). SMN Δ 7 mice treated with ssAAV9-PLS3 virus displayed a similar slow weight gain initially, however the body weight decline was noticed only after postnatal day 12. Interestingly, the body weight at death was similar in all control groups, irrespective of lifespan (Figure. 5.9), suggesting that the ssAAV9-PLS3 gene transfer cannot fully compensate for loss of SMN.

The ssAAV-PLS3-treated mice showed lower body weights than PBS untreated mice at 5-8 days of age ($p < 0.05$ at each time point), while at 11-14 days of age, PLS3 treated mice had higher body weight compared to PBS ($p < 0.001$). Notably there was a delayed peak of ssAAV9-PLS3 treated group in body weight compared to PBS by approximately 4 days.

Unexpectedly, there was a significant difference between the two control groups (PBS and AAV9-GFP treated) at days 5-11 of age ($p < 0.001$). The ssAAV9-GFP group showed a much slower gain in body weight. It has been shown that GFP is toxic and causes stress in neurons (Comley et al., 2011). The extra stress from producing GFP is putting a strain on already sick mice, slowing down weight gain further from the untreated control mice.

5.3.7 Effect of ssAAV9-PLS3 on mouse life span

The expected average lifespan of SMN Δ 7 mice is 12 days, therefore survival was monitored to assess whether PLS3 gene transfer could extend mouse survival. Heterozygous carriers have a normal life expectancy so survival was only monitored

for SMN Δ 7 mice.

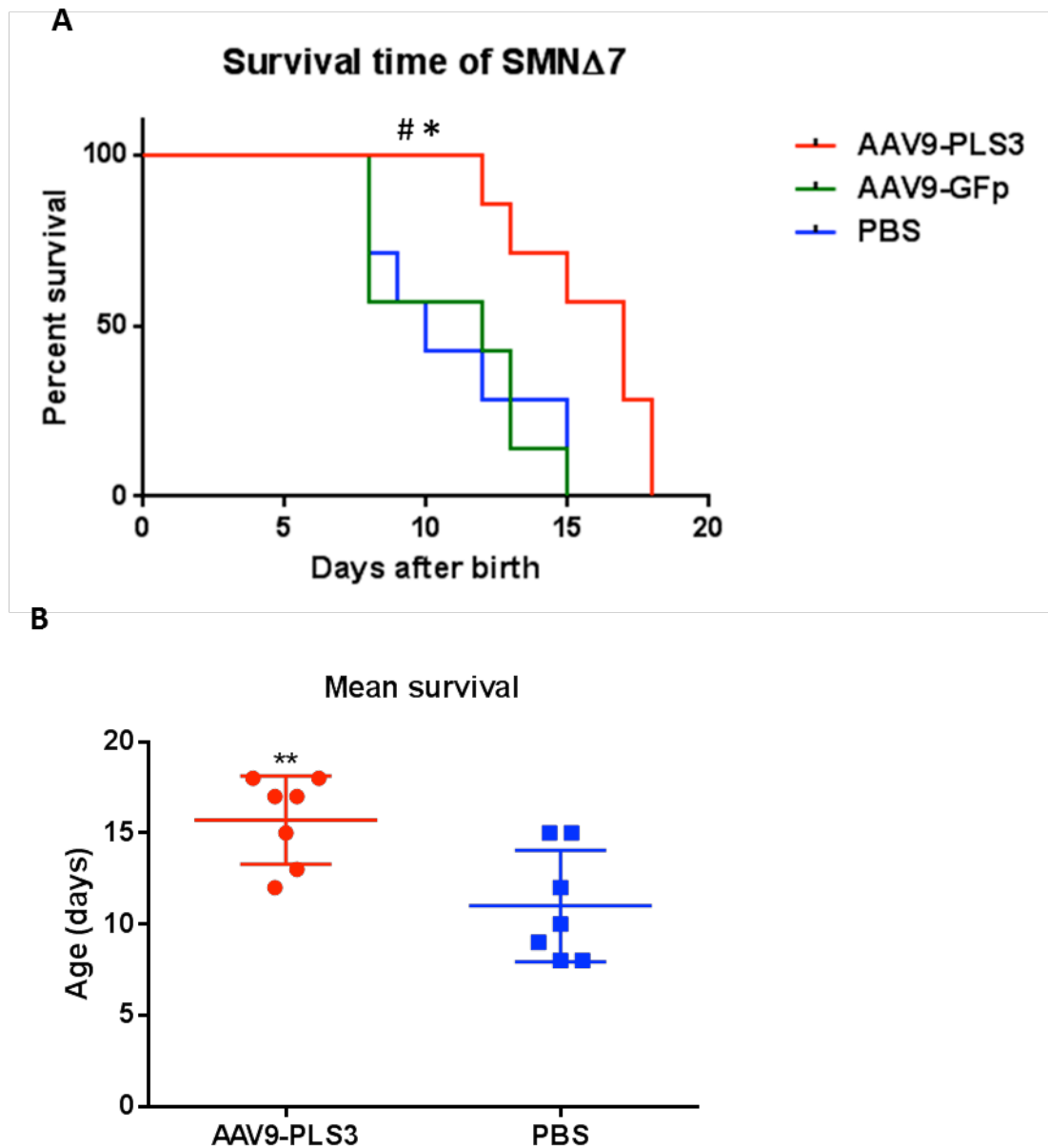


Figure 5.10 Survival curve and disease duration of SMN Δ 7 mice

(A) Kaplan-Meier plot to compare lifespan between all experimental groups of mice (N = 7 per group; overall Log-rank test $p < 0.05$ between all three groups; pairwise comparisons with Bonferroni correction $*p < 0.05$ between PLS3 and PBS and $\#p < 0.05$ between PLS3 and GFP). AAV9 – Adeno-associated virus serotype 9; GFP – Green fluorescent protein; PLS3 - Plastin3; PBS Phosphate-buffered saline. (B) Comparison of mean survival across the 2 groups ($p < 0.01$, t-test, between AAV-PLS3-treated and PBS mice).

The mean survival age for ssAAV9-PLS3 treated SMN Δ 7 mice was 17 days (\pm 1.54 days). The mean survival age of the PBS-treated group was 11 days (\pm 2.56 days) (Figure. 5.10B), and the mean survival age of the control group injected with ssAAV9-GFP was 12 days (\pm 1.52 days). Kaplan-Meier analysis was performed and showed that PLS3 treated mice had a longer survival time compared to both untreated and GFP treated groups (Log-rank test, $p < 0.05$ for PLS3 vs PBS and GFP vs PBS, pairwise comparison with Bonferroni corrections). Furthermore, the oldest mouse lived for 18 days after treatment with AAV9-PLS3 whereas the longest surviving mouse after treatment with AAV9-GFP lived for 15 days (Figure. 5.10). Overall, this study revealed an increase in survival of PLS3 treated mice compared to controls however, the effect on life span was small or marginal. We hypothesis that an increase in the dose of ssAAV9-PLS3 could yield a better impact on survival but this still needs testing in future studies.

5.3.8 The power calculation

Power calculations were carried out post-hoc. The G*Power version 3.03 software was used to calculate the statistical power using a T test between PBS and PLS3 groups. The minimum detectable difference was 1.63 x standard deviation of the control group, therefore 4.89. The control groups have an average survival of 11 days, therefore a survival of 15.89 days needed to be seen in the treated group to get a significant effect 80% of the time. This was confirmed through these experiments.

5.1.1.1 Disease onset and phenotype

Throughout the study as a measure of overall health, different parameters were monitored daily such as percentage weight loss from peak body weight, provoked behaviour, weakness of the hind limbs and general appearance (Figure 5.9).

ssAAV9-PLS3 treated SMN Δ 7 mice showed no difference in severity or onset of disease phenotype by the above observations. There was no difference between untreated or GFP treated controls.

5.1.1.1 Transduction efficiency

Due to the absence of phenotype improvement and lack of change in disease onset, transduction efficiency was checked to ensure that this was not due to inefficient viral vector delivery to the CNS, in particular to MNs. Immunofluorescence was performed on ssAAV-GFP-treated mice to assess the transduction yield of MNs.

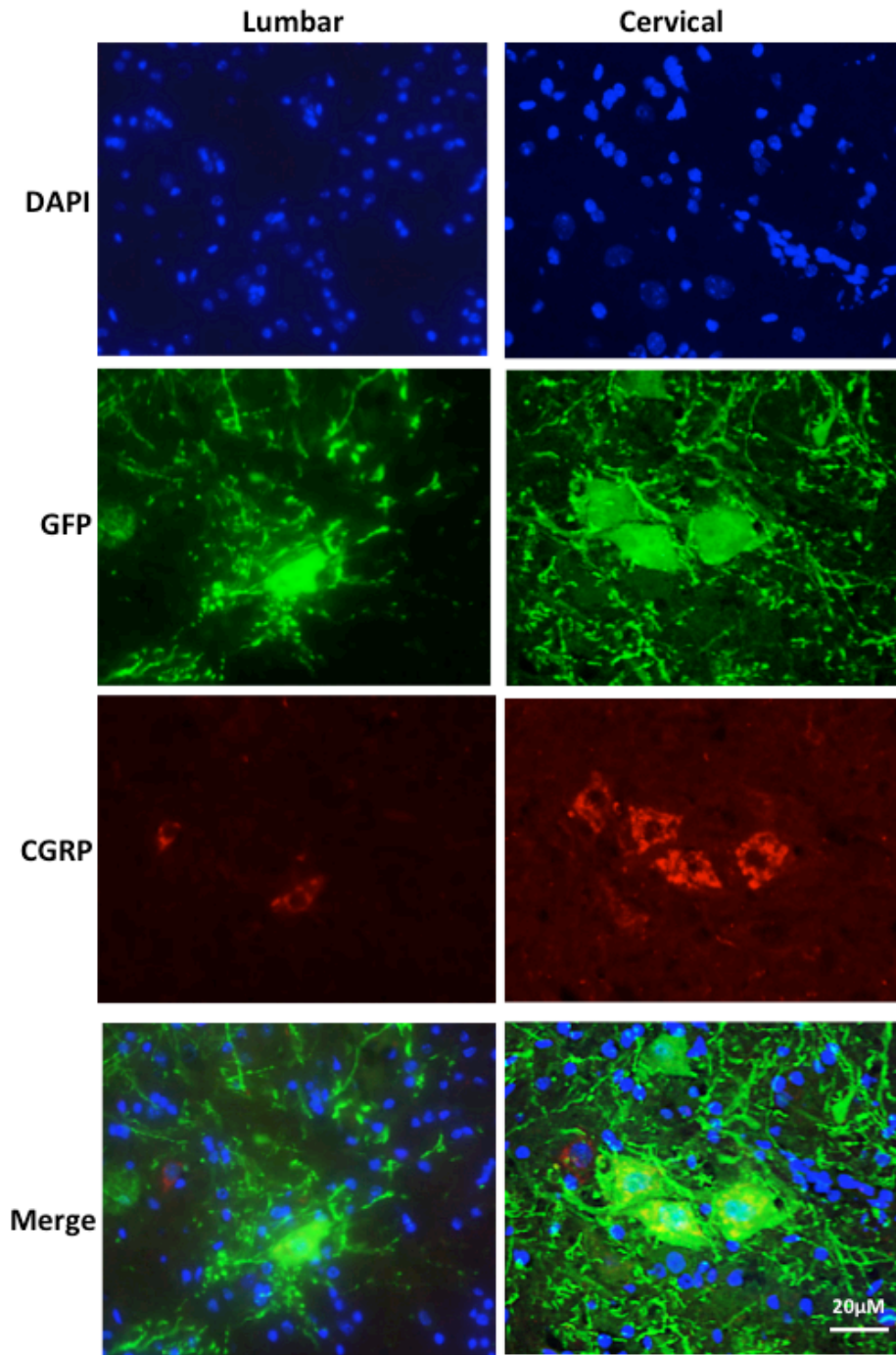


Figure 5.11 Transduction of spinal motor neurons in SMN Δ 7 mice

Heterozygous (carrier) mice were injected at postnatal day 1 with ssAAV9-GFP, spinal cords were extracted at 4 weeks post-injection. The cervical and Lumbar spinal cord sections were fixed and double labelled with anti-CGRP as a motor neuronal marker and anti-PLS3 antibodies. DAPI was used for visualization of nuclei. Transduced MNs pictures were taken using x63 magnification. AAV9 – Adeno-associated virus serotype 9; CGRP- Calcitonin Gene-Related Peptide; GFP – Green fluorescent protein and DAPI- Diamidino-2-phenylindole (blue)

The total number of motor neurons and the number of GFP positive motor neurons (Figure 5.11) were counted to calculate the percentage of transduced neurons. The transduction efficiency for GFP was around 24 % of total MNs (Table 5.3).

Table 5-3 Transduction efficiency of lumbar spinal motor neurons (GFP)

Mouse	Total motor neurons CGRP+	GFP Transduced motor neurons	Transduction efficiency
1	100	24	24%
2	100	20	20%
3	100	28	28%
Average			24%

5.1.1.2 ssAAV-mediated PLS3 expression in the spinal cord

Western blot analysis confirmed ssAAV9-PLS3 mediated PLS3 protein overexpression in whole tissue but did not identify the cell types producing the transgene from the virus, therefore immunohistochemistry was performed to identify whether the MNs have been targeted efficiently as this does not exclude targeting of other cell types. Cervical and lumbar spinal cord sections were double-labelled for PLS3 (green) and CGRP (red), and the sections analysed under a confocal microscope (Figure. 5.12).

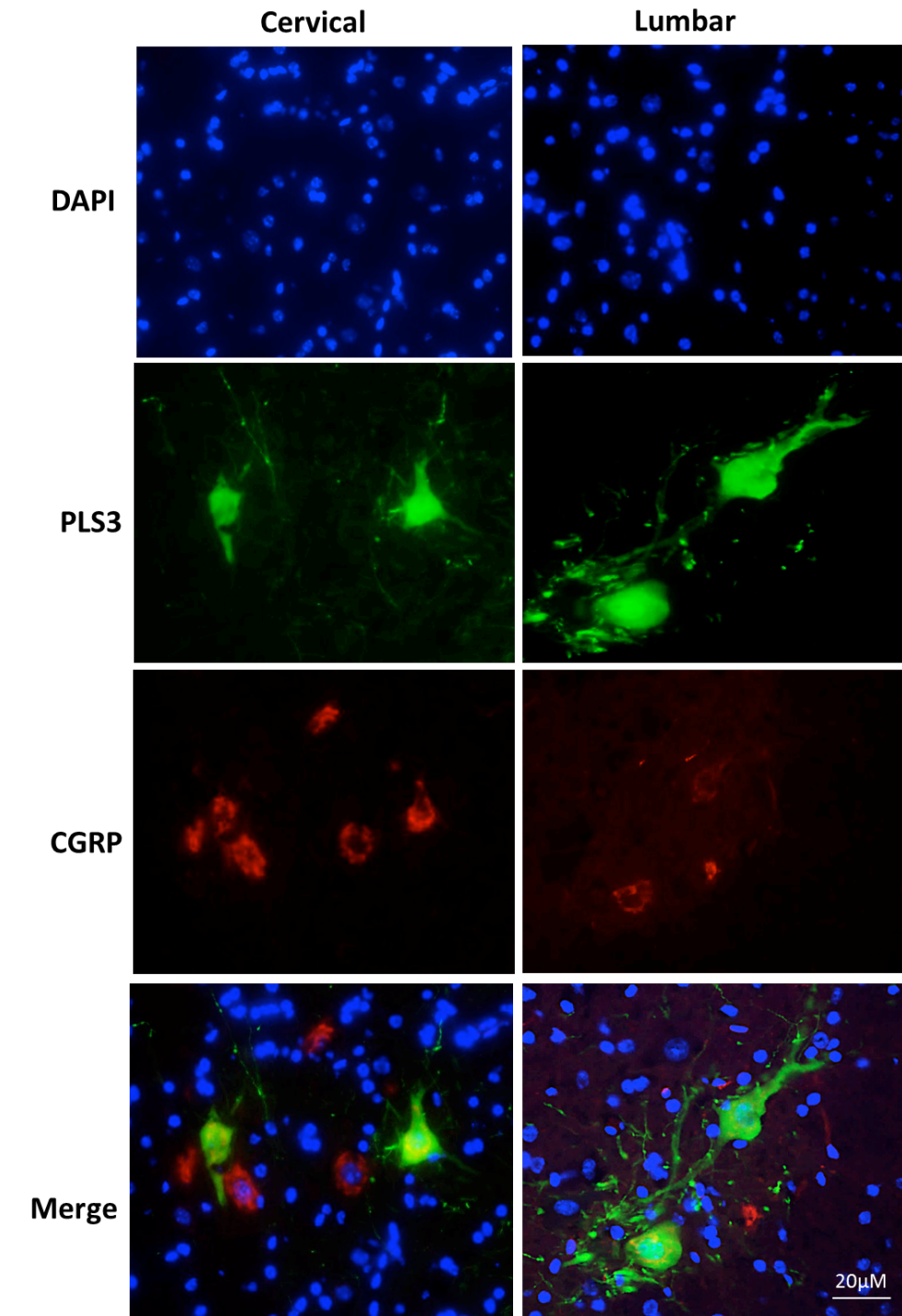


Figure 5.12 Transduction efficiency of spinal motor neurons in SMN Δ 7 mice in ssAAV9-PLS3 treated mice

Heterozygous pups were injected at postnatal day 1 with ssAAV9-PLS3, spinal cords were extracted at 4 weeks post-injection. The cervical and lumbar spinal cord sections were fixed and labelled with CGRP antibody as a motor neuronal marker (red), PLS3 antibody as an indicator of transduction (green), and DAPI for visualization of nuclei. Transduced MN pictures were taken using x63 magnification (scale bar 20 μ m). AAV9 – Adeno-associated virus serotype 9; CGRP- Calcitonin Gene-Related Peptide; PLS3- Plastin3 and DAPI- Diamidino-2-phenylindole (blue).

PLS3 was detected in motor neurons and some neuronal axons, showing that the virus is targeting motor neurons in the spinal cord (Figure. 5.12). Other cell morphologies were identified as PLS3-positive, however without further staining these aren't confirmed. This indicates that the virus has a higher affinity for, but not exclusively targeting MNs (Figure 5.12). The PLS3-positive MNs were counted and transduction efficiency calculated as the percentage of total CGRP-positive MNs (Table 5.4). (Table 5.4). Not all CGRP+ motor neurons expressed PLS3, instead quantification revealed around 29% of motor neurons were PLS3 positive.

Table 5-4 Transduction efficiency of lumbar spinal motor neurons (PLS3)

Mouse	Total motor neurons CGRP+	PLS3 Transduced motor neurons	Transduction efficiency
1	100	29	29%
2	100	32	32%
3	100	27	27%
Average			29.33%

5.4 Discussion

5.4.1 ssAAV9-mediated gene transfer to the CNS

Histological analysis of CNS showed that cisterna magna administered ssAAV9-GFP or ssAAV9-PLS3 could mediate significant transduction efficiency (Figure. 5.12) correlating with an overexpression of PLS3 or GFP in spinal cord MNs. A single injection of AAV9 expressing PLS3 or GFP was sufficient to mediate wide spread gene transfer in both cervical and lumbar spinal cord MNs. This shows that cisterna magna injection can disseminate virus effectively around the CNS, reaching cells in the lumbar spinal cord. This finding is in agreement with a previous study reporting that AAV9 can transduce both neurons and astrocytes following direct injection of this vector system to the CNS (Foust et al., 2010). This is an important consideration when designing therapies for neurodegenerative diseases. In neonates, AAV9 may target motor neurons efficiently, suggesting that the AAV vector was a suitable vector for PLS3 gene delivery.

Quantification of transduced MNs showed 29% transduction efficiency. In comparison, a previous study showed 68% and 51% of spinal motor neurons transduced by scAAV, which showed a significant improvement in disease in SMN Δ 7 mice (Foust et al., 2010, Valori et al., 2010). However, this does not necessarily indicate that a higher transduction rate with AAV-PLS3 would improve disease, as different serotypes and gene targets were used in these previous studies. Improvement of transduction efficiency may be addressed by increasing the dose of the virus, which may increase transgene expression levels. The issue of the dose has been a limitation because the Home Office licencing and regulation insists on a

maximum volume for cisterna magna delivery is around 1 μ l/g of body weight. Note that the body weight of a P1 mouse pup is around 1g.

PLS3 expression appears to be predominantly neuronal in the spinal cord when injected at P1, as glial cells were very rarely transduced. The importance of non-neuronal cells in disease is not fully understood. There is increasing evidence from different SMA mouse models and human patients that alongside MN dysfunction, defects in various other tissue types strongly contribute to the lethal phenotype indicating that other cell types also play a role in disease pathogenesis (Rindt et al., 2015). Expression may need to be restored in other cell types such as astrocyte and or even in different organs as well as MNs to improve the phenotype and survival.

5.4.2 ssAAV9-PLS3 mediate marginal increased in the life span of SMN Δ 7

AAV9-PLS3 treatment showed a small or marginal but significant effect on survival of SMN Δ 7 mice. Kaplan-Meier survival analysis showed mean survival of 17 ± 1.54 days, 12 ± 1.52 days and 11 ± 2.56 days for AAV9-PLS3, AAV9-GFP and PBS treated mice respectively. This shows an increase of a maximum lifespan of 57.14 %, with a median increase in lifespan of 154%. The finding is in agreement with previous reports by Ackermann et al. (2012) when PLS3 was over-expressed in a milder model of SMA. This study reported moderate increase in survival, but significant improvement of motor ability and improved NMJ function. This is in contrast to a similar study by the same group which did not detect any survival or phenotypic improvements in severely affected SMA_{PLS3} mice (a conditional PLS3-over-expressing mouse and bred into an SMA background) (Ackermann et al., 2012).

In the current study, there was mouse-to-mouse variability seen in lifespan of PLS3 treated mice. This may be due to inefficient gene transfer as previously reported (Valori et al., 2010) or technical failure during cisterna magna injection of the vector; the small size of mice at P1 can be challenging for efficient viral delivery. Thus, it is necessary to determine biodistribution of the virus to assess whether each mouse has a good delivery of virus to all tissues.

The small/marginal extension of lifespan in ssAAV9-PLS3 treated SMN Δ 7 mice could be explained further by: i) the dose used (2×10^{10} vg) is low to transduce a significant number of MNs and other cells in the CNS. The choice of the dose was based on the maximum volume allowed for cisterna magna delivery under the Home Office licencing and regulations; ii) conventional ssAAV9 needs to form double stranded DNA upon transduction of cells delaying the start of transgene expression. Early start of transgene expression is crucial for SMN Δ 7 mice rescue because of fast and severe phenotype of this animal model.

5.4.3 PLS3 does not rescue disease phenotype

Although this study has shown successful overexpression of PLS3 and a small increase in lifespan, there was no delay in onset of disease or improvement of disease phenotype. This suggests that PLS3 is an important modulator of disease but is not the only factor affected by the loss of SMN. It is not known whether there was any rescue of neuromuscular junctions but it can be predicted from the phenotype of the mice that there is still neuronal death and dysfunction despite PLS3 overexpression. However, it is important to bear in mind that this study has not tested different doses or optimised gene delivery and expression. The number of MNs (29%) targeted by the delivered dose of ssAAV9-PLS3 may simply not be high

enough to fully rescue disease phenotype. In addition this study used AAV9, which primarily targets neuronal cells over other cell types in the CNS of neonates, such as glial cells, which may also have an important role in the disease process.

Analysis of body weight showed significant difference between groups (Figure. 5.8). The weight gain pattern is the same for PLS3 treated and PBS treated mice but the decline in weight is delayed by 4 days in PLS3 treated mice. PLS3 treated mice body weight increased above the controls after 8 days, before weight loss began. This suggests that the overexpression of PLS3 achieved in this study was sufficient to rescue weight loss, but only for a short period of time, suggesting that PLS3 can overcome disease phenotype to a certain extent but is not enough to exert long-term effects. Interestingly, all groups reached the same body weight at death, irrespective of peak weight, however, is not known whether this is a significant finding or just a coincidence.

5.4.4 Expression of PLS3 in different vectors

Two different viral vectors were tested *in vivo*, a conventional ssAAV and scAAV. ssAAV-PLS3 virus showed good but not optimal overexpression of PLS3 *in vivo*. However, although the viral titre was high for scAAV9-PLS3, there was no overexpression of PLS3 three weeks post-IV injection. scAAV9 is the favoured vector for gene therapy due to its stability and faster gene transcription. It has been reported that scAAV9 achieves maximal expression levels within 48–72 h post-transduction (Gray et al., 2011). Moreover, the transduction efficiency of scAAV9 in some instances is 10- to 100-fold higher than conventional ssAAV (McCarty et al., 2003, Gray et al., 2011). An alternative study demonstrated the benefits of using scAAV compared with ssAAV (McCarty et al., 2001). ICV injection of ssAAV8

expressing human full-length SMN into SMN Δ 7 mouse model, has shown extended life up to ~50 days (Passini et al., 2010). The same study using scAAV8 through the same route of delivery showed a better survival up to 157 days (Passini et al., 2010). There are a number of possible reasons for why scAAV did not overexpress PLS3. Improper packaging of the insert is a problem for transgenes close to or over the packaging limit (Chen et al., 2010); the PLS3 gene is very close this packaging capacity limit. Large genomes may result in partial genomes packaged into virions, so even if the virus gets to its destination the genome is not complete. Long genomes might get packaged intact, but their large size can distort the capsid and make the overall virion less stable/efficient. Unstable virus could lead to low or no expression of PLS3.

5.4.5 Summary

In conclusion, these studies provide the first *in vivo* gene therapy proof-of-concept of PLS3-mediated protection against SMA in SMN Δ 7 mouse model, emphasizing the impact of PLS3 as a potential therapeutic target in SMA therapy. Both *in vitro* and *in vivo* data are promising however because of the marginal effect observed in SMN Δ 7mice, *in vivo* set up would need further optimisation to assess in more detail the impact of PLS3 in SMA.

Chapter 6: General Discussion

SMA is a debilitating fatal childhood neuromuscular disease, characterized by the degeneration of the anterior horn cells of the spinal cord due to reduced expression of the SMN protein (Stratigopoulos et al., 2010). Finding a treatment for SMA has been challenging, and despite enormous research on SMA there is no effective treatment available. Gene therapy is considered to be an attractive approach for SMN replacement in this disease (Lefebvre et al., 1995, Foust et al., 2010, Passini et al., 2010, Valori et al., 2010, Dominguez et al., 2011, Benkhelifa-Ziyyat et al., 2013, Little et al., 2014).

Previous studies have reported other disease-modifying genes, which could also be targeted for gene therapy-mediated treatment for SMA, including PLS3, PTEN and hnRNP-R (Rossoll et al., 2003, Oprea et al., 2008, Ning et al., 2010, Little et al., 2014). Stratified analysis of blood samples from SMA type I, II and III patients demonstrated that post-pubertal females show an inverse correlation between circulating PLS3 and SMA severity (Stratigopoulos et al., 2010). Investigation into the function of PLS3 has begun to shed light on its interaction with SMN and its role in neuroprotection against SMA. This project aimed to test whether overexpression of PLS3 by viral-mediated gene therapy could rescue neuronal loss and increase survival of an SMA mouse model and whether it could ultimately be developed into a potential clinical therapy.

6.1 PLS3 levels in the SMN Δ 7 SMA mouse model

In WT mice Pls3 is expressed in neuronal cells in the brain stem and in MNs in the spinal cord. Its distribution was as expected in the spinal cord, being expressed in cell bodies of MNs and the white matter where the axons of the neurons are located. This aligns with previous observations that Pls3 co-localizes with Smn in granules

throughout motor neuron axons (Oprea et al. 2008). If both proteins are co-localised they may have the ability to interact. They could influence each other stability, which has also been suggested by other groups (Dimitriadi et al., 2010).

The data in chapter 3 of this thesis confirmed differential Pls3 expression between Smn knockout mice from the SMN Δ 7 line and their wild type littermates. At birth there was no difference in Pls3 expression between the genotypes, however by end stage of the disease the KO animals showed significantly reduced or absent Pls3 expression in both CNS and muscles, relative to wild types. Heterozygote SMN Δ 7 mice also showed lower Pls3 levels in the spinal cord, although not in brain or muscles, suggesting that Smn protein is influencing Pls3 levels in some tissues. This supports previous reports of Pls3 down regulation in the brain and spinal cord of other animal models and in human patients (Hao et al., 2011). This report provides evidence that the SMN Δ 7 mouse is a good model for testing whether modulation of PLS3 can be used as a gene therapy for SMA.

The molecular mechanisms for PLS3's involvement in SMA are unclear; there are no structural or sequence similarities between SMN and PLS3 that may suggest they are functionally related, but several theories have been proposed. PLS3 overexpression has been demonstrated to increase levels of F-actin, and it has been suggested that its role in stabilising actin filaments is crucial to axon development and therefore rescue of SMA pathology. However, the effects of expressing a set of partial Pls3 molecules in zebrafish support a mechanism for PLS3 in SMA beyond that of actin binding (Lyon, 2013).

The crucial role of Ca²⁺ ions for both SMN and PLS3 proteins were demonstrated in two different studies for SMA disease, which may explain the role in neuro-

maintenance and protection (Jablonka et al., 2007). Interestingly, it was reported that calcium dysregulation has been associated with the pathogenesis of SMA (Jablonka et al., 2007, McGivern et al., 2013). A novel role for Ca^{2+} regulation in PLS3 function in MN development was defined recently (Lyon et al., 2013). The Ca^{2+} binding to the EF hand motifs is essential for PLS3 function in MN development. Also of interest was that the mutation of the residues that interact with Ca^{2+} ions within the EF hands resulted in a complete loss of PLS3 rescue (Lyon et al., 2013). Moreover, defective Ca^{2+} channel clustering in axon terminals disturbs excitability in MNs in SMA (Jablonka et al., 2007). On the other hand, *Smn*-deficient MNs exhibit defects in spontaneous excitability. These defects correlate with reduced integration of voltage-gated Ca^{2+} channels (VGCCs) in growth cones, which is responsible for reduced axon elongation (Lyon et al., 2013). Moreover, these defects could lead to disturbances of the presynaptic active zones, causing reduced transmitter release at the motor endplate which may contribute to MN malfunction and degeneration in SMA (Jablonka et al., 2007). This suggests that enhancing motor neuron survival could be achieved through restoration of growth cone excitability and function (Lyon et al., 2013).

6.2 Overexpression of PLS3 by viral vectors

This study has demonstrated that successful cloning of *PLS3* gene into LV or ssAAV viral vectors was able to significantly overexpress PLS3 protein by at least five fold, *in vitro* (Chapter 4) and *in vivo* (Chapter 5). This suggests that overexpression of PLS3 by a viral vector is feasible. *In vitro*, PLS3 doesn't appear to be toxic to cells; cells overexpressing PLS3 did not die and wild type cells treated with PLS3 showed no difference in cell death but slightly longer axons than untreated cells. On the

contrary, overexpression of PLS3 in cells lacking Smn rescued the axonal length deficit. The same is mirrored in vivo; there was no obvious toxicity associated with viral injection or PLS3 expression and it was demonstrated that ssAAV9-mediated overexpression of PLS3 improved the survival of SMN Δ 7 mice when injected into the cisterna magna at P1.

Administration of ssAAV9-PLS3 to the CNS (via cisterna magna) in postnatal day 1 SMA Δ 7 mice led to significant spinal MN transduction efficiency. Although PLS3 overexpression induced small but significant extension in SMA Δ 7 mouse survival this gene transfer strategy did not ameliorate the SMA phenotype nor delay disease onset. It is worth highlighting that ssAAV9 showed neuronal tropism and this study revealed that other cell type such as glial. Previous studies have shown that astrocytes from SMA-induced pluripotent stem cells and in SMN Δ 7 mouse spinal cord exhibit cellular and morphological changes as an indicator of activation before obvious MN loss (Yamanaka et al., 2008, McGivern et al., 2013). The late report indicates that early disruption of astrocytes may contribute to SMA disease pathology, which suggests that targeting of both MNs and glial cells may be needed for an effective therapy in SMA.

The function of spinal MNs is dramatically affected by motor neuron diseases or injuries. Glial cells support and interact with neurons, including MNs. Astrocytes are a particular subset of glial cells that produce neuronal survival factors that modulate the way neurons talk to each other. Recently it was reported that the mutations in genetic disorders affecting the spinal cord, such as SMA, also disable astrocytes. Astrocytes actively contribute to the progression of SMA disease, and could therefore be therapeutic targets themselves (Yamanaka et al., 2008).

The key feature of SMA is the loss of SMN, which is not addressed by overexpression of PLS3. PLS3 may be able to rescue some SMN functions but not all, such as calcium dysregulation, snRNP assembly and neuronal development which has been observed to be affected in SMA (McGivern et al., 2013). This along with the previous observation in humans, where PLS3 provides full protection against SMA only in SMN1-deleted individuals carrying three to four SMN2 copies, but not in those with only two SMN2 copies or less, suggests that a certain amount of SMN is required in order to benefit from PLS3 overexpression in individuals lacking SMN1.

6.3 Considerations for clinical studies

Although PLS3 can be successfully overexpressed *in vivo* and is a potential gene therapy for SMA, there are several considerations that will need to be addressed before this can be taken to clinical trials in humans, such as early delivery of the treatment to the SMA patient immediately after birth.

Recent preclinical trial data suggests that due to the developmental nature of the disease it's crucial for rescuing mechanisms to act right after birth in order to have any efficacy in preventing neuronal loss, especially in severe SMA. The therapeutic vectors must be introduced during this developmental stage in order to achieve the maximal therapeutic benefits. The data in the current thesis has demonstrated an increase in survival after P1 administration but did not look at any other time points for treatment. A study using scAAV9 expressing SMN protein strongly supports the view that only early administration between P0–P3 of recombinant viruses is able to rescue the SMA phenotype in mice (Foust et al., 2009, Gray et al., 2011). Systemic injection at postnatal day 2 of scAAV9-SMN leads to ~250 days of survival,

however, after P5 injection only ~15 days increase in survival and no increase after P10 injection was observed (Foust et al., 2010). In a severe SMA mouse model, weak effects or no effects have been observed with postsymptomatic administration (after P6) (Foust et al., 2010). Interestingly, P2 injection resulted in high-level MN transduction, while P10 injection led mostly to glial transduction. However, whether the lack of rescue in P10-injected mice is due to this pattern of transduction remains to be elucidated. The previous studies concluded that transduction could be altered in the CNS depending on the time of injection (Foust et al., 2010). This poses a problem as SMA children are often asymptomatic at birth and diagnosis is usually made months later, potentially missing the window of opportunity for treatment. This highlights the need for pre-natal or newborn screening if treatment is to be successful. Screening tests are being developed to detect SMA in newborns, supporting the possibility of delivering therapeutics including gene therapy based interventions to the affected children immediately after birth (Pyatt et al., 2007).

Another consideration is the treatment route. This study carried out injections into the cisterna magna, which would involve major surgery under general anaesthesia for newborns. This study also used IV injection, although the level of transduction in the CNS was not evaluated due to the lack of PLS3 expression. scAAV serotype 9 has previously been demonstrated to cross the BBB and show preferential transduction of neurons (Foust et al., 2009). In addition, IV injection of AAV9 has previously shown good transgene expression and viral spread around the CNS and other organs following facial vein injection in neonates, and tail vein injection in older animals (Benkhelifa-Ziyyat et al., 2013).

The delivery route makes a difference to where the virus ends up. Injecting into the CNS reduces the amount of virus found in the peripheral tissues but increases the

amount of MNs targeted (Shababi et al., 2015). However, some evidence suggests that in severe cases of disease the rescue of peripheral organs in addition to MNs is necessary for the complete rescue of SMA phenotype (Hua et al., 2011, Schreml et al., 2013, Shababi et al., 2015). Therefore, transduction of the peripheral organs after systemic injection may benefit SMA gene therapy.

Based on the recent findings in SMA mouse models of heart defects (Bevan et al., 2010, Shababi et al., 2010a, Valori et al., 2010), it was suggested that intravenous (IV) injection leads to better survival compared to ICV injection, which is possibly due to its direct cardiac transduction that protects the heart (Passini and Cheng, 2011). However, direct comparison of the two injection methods in the previous study is not advisable, since it requires all parameters to be identical, and in this case, the titre and the AAV serotypes were different.

Identifying the most efficient delivery route for SMA clinical trials will eliminate the requirement for introducing an enormous amount of the viral vector to achieve a great level of rescue. This needs more optimization by testing different routes in different SMA models in nonhuman primates.

6.4 Future work

There are various points that need to be addressed to further build upon the data from these experiments. This thesis explored PLS3 overexpression *in vivo* and generated promising preliminary data but did not assess the optimal dose or route of delivery with AAV-PLS3. Further studies should be carried out with different doses of virus to assess whether higher expression of PLS3 would improve phenotype or increase transduction levels. It is apparent that in the CNS the transduction efficiency achieved in this project was not high, while it was shown by others that at least more

than 50% of MNs needs to be transduced to show significant therapeutic effect (Little et al., 2014).

We provide evidence that PLS3 can improve MN axonal length *in vitro*, as has been shown previously (Oprea et al., 2008), (Oprea et al., 2008), however the lack of improvement of disease phenotype suggests that the expression of PLS3 was not enough to improve the disease phenotype. Another key element in SMA therapy development using viral vectors is the early start of gene transfer. This was not the case when using ssAAV9. Future efforts could look at reducing the size of PLS3 to fit the packaging capacity of scAAV.

Furthermore as mentioned above it would be useful to use AAV9 to assess the effect of overexpressing of other genes such as hnRNP R on SMN Δ 7 mice. The *in vitro* data shown from our group suggests that hnRNP R can modify the SMA phenotype. Therefore with the level of transduction generated by AAV9 it would be possible to assess how well hnRNP R overexpression can compensate for SMN deficiency *in vivo*. It would be interesting to see whether hnRNP would complement PLS3 treatment and provide a synergistic therapy to the MNs.

Since SMA is a multi-system disorder it would be interesting to see whether other cell types or even organs are important as a therapeutic target. Targeting more than just motor neurons in order to successfully provide therapy for SMA would be possible with AAV9 as it is able to enter the spinal cord through retrograde transport but also transduces multiple organs in peripheral tissues. It would therefore be interesting to study the efficiency of motor neuron transduction following intramuscular injection of AAV9.

Gene therapy approaches are highly promising, using AAV9-SMN vectors have entered a Phase I clinical trial. However, analysis of SMA patients and animal models has revealed some limitations that need to be taken into consideration, including: i) neonatal screening of SMA due to limited time-window for successful therapy delivery; ii) multi-organ damage, requiring systemic therapeutic delivery; iii) Combined therapies that both target pathways that rescue motor neuron function and increase SMN levels. Instead of only ameliorating symptoms of SMA, meeting these challenges will likely be essential to cure SMA, particularly in its most severe cases.

6.5 Final conclusions

In summary, evidence has been provided supporting the role of PLS3 downregulation in the pathology of spinal muscular atrophy, and that restoration of PLS3 expression using a lentiviral vector can rescue the axonal phenotype in spinal motor neurons cultured from a clinically relevant mouse model of SMA. It has been shown that ssAAV9-mediated PLS3 overexpression can improve the survival of SMN Δ 7 mouse model of SMA. The use of PLS3 overexpression to extend their lifespan demonstrates that PLS3 is a disease modifier of SMA and a good potential therapeutic target for SMA. PLS3 is a good therapeutic target and can be used in a gene therapy approach but may be required to be delivered in combination with other disease modulators to give meaningful rescue to motor neurons and alleviate the disease phenotype sufficiently.

BIBLIOGRAPHY

- Ackermann B (2011) Analysis of the modifying influence of Plastin 3 (PLS3) on Spinal Muscular Atrophy (SMA) by generation of transgenic mouse models. Universität zu Köln.
- Ackermann B, Kröber S, Torres-Benito L, Borgmann A, Peters M, Barkooie SMH, Tejero R, Jakubik M, Schreml J, Milbradt J (2012) Plastin 3 ameliorates spinal muscular atrophy via delayed axon pruning and improves neuromuscular junction functionality. *Human molecular genetics* dds540.
- Acsadi G, Lee I, Li X, Khaidakov M, Pecinova A, Parker GC, Hüttemann M (2009) Mitochondrial dysfunction in a neural cell model of spinal muscular atrophy. *Journal of neuroscience research* 87:2748-2756.
- Akten B, Kye MJ, Hao LT, Wertz MH, Singh S, Nie D, Huang J, Merianda TT, Twiss JL, Beattie CE (2011) Interaction of survival of motor neuron (SMN) and HuD proteins with mRNA cpg15 rescues motor neuron axonal deficits. *Proceedings of the National Academy of Sciences* 108:10337-10342.
- Alías L, Bernal S, Fuentes-Prior P, Barceló MJ, Also E, Martínez-Hernández R, Rodríguez-Alvarez FJ, Martín Y, Aller E, Grau E (2009) Mutation update of spinal muscular atrophy in Spain: molecular characterization of 745 unrelated patients and identification of four novel mutations in the SMN1 gene. *Human genetics* 125:29-39.
- Arnold WD, Burghes AH (2013) Spinal muscular atrophy: development and implementation of potential treatments. *Annals of neurology* 74:348-362.
- Arpin M, Friederich E, Algrain M, Vernel F, Louvard D (1994) Functional differences between L-and T-plastin isoforms. *The Journal of cell biology* 127:1995-2008.
- Aschauer DF, Kreuz S, Rumpel S (2013) Analysis of transduction efficiency, tropism and axonal transport of AAV serotypes 1, 2, 5, 6, 8 and 9 in the mouse brain. *PLoS One* 8:e76310.
- Avila AM, Burnett BG, Taye AA, Gabanella F, Knight MA, Hartenstein P, Cizman Z, Di Prospero NA, Pellizzoni L, Fischbeck KH (2007) Trichostatin A increases SMN expression and survival in a mouse model of spinal muscular atrophy. *Journal of Clinical Investigation* 117:659.
- Azzouz M, Kingsman SM, Mazarakis ND (2004a) Lentiviral vectors for treating and modeling human CNS disorders. *The journal of gene medicine* 6:951-962.
- Azzouz M, Le T, Ralph GS, Walmsley L, Monani UR, Lee DC, Wilkes F, Mitrophanous KA, Kingsman SM, Burghes AH (2004b) Lentivector-mediated SMN replacement in a mouse model of spinal muscular atrophy. *Journal of Clinical Investigation* 114:1726-1731.
- Azzouz M, Martin-Rendon E, Barber RD, Mitrophanous KA, Carter EE, Rohll JB, Kingsman SM, Kingsman AJ, Mazarakis ND (2002) Multicistronic lentiviral vector-mediated striatal gene transfer of aromatic L-amino acid decarboxylase, tyrosine hydroxylase, and GTP cyclohydrolase I induces sustained transgene expression, dopamine production, and functional improvement in a rat model of Parkinson's disease. *The Journal of neuroscience* 22:10302-10312.
- Bäumer D, Ansorge O, Almeida M, Talbot K (2010) The role of RNA processing in the pathogenesis of motor neuron degeneration. *Expert reviews in molecular medicine* 12:e21.
- Bäumer D, Lee S, Nicholson G, Davies JL, Parkinson NJ, Murray LM, Gillingwater TH, Ansorge O, Davies KE, Talbot K (2009) Alternative splicing events are

- a late feature of pathology in a mouse model of spinal muscular atrophy. *PLoS genetics* 5:e1000773.
- Benkhelifa-Ziyyat S, Besse A, Roda M, Duque S, Astord S, Carcenac R, Marais T, Barkats M (2013) Intramuscular scAAV9-SMN injection mediates widespread gene delivery to the spinal cord and decreases disease severity in SMA mice. *Molecular Therapy* 21:282-290.
- Bernal S, Also-Rallo E, Martínez-Hernández R, Alías L, Rodríguez-Alvarez FJ, Millán JM, Hernández-Chico C, Baiget M, Tizzano EF (2011) Plastin 3 expression in discordant spinal muscular atrophy (SMA) siblings. *Neuromuscular Disorders* 21:413-419.
- Bevan AK, Hutchinson KR, Foust KD, Braun L, McGovern VL, Schmelzer L, Ward JG, Petruska JC, Lucchesi PA, Burghes AH (2010) Early heart failure in the SMN Δ 7 model of spinal muscular atrophy and correction by postnatal scAAV9-SMN delivery. *Human molecular genetics* 19:3895-3905.
- Bienemann AS, Martin-Rendon E, Cosgrave AS, Glover C, Wong L-F, Kingsman SM, Mitrophanous KA, Mazarakis ND, Uney JB (2003) Long-term replacement of a mutated nonfunctional CNS gene: reversal of hypothalamic diabetes insipidus using an EIAV-based lentiviral vector expressing arginine vasopressin. *Molecular therapy: the journal of the American Society of Gene Therapy* 7:588-596.
- Boon K-L, Xiao S, McWhorter ML, Donn T, Wolf-Saxon E, Bohnsack MT, Moens CB, Beattie CE (2009) Zebrafish survival motor neuron mutants exhibit presynaptic neuromuscular junction defects. *Human molecular genetics* 18:3615-3625.
- Borg R, Cauchi RJ (2014) GEMINs: potential therapeutic targets for spinal muscular atrophy? *Frontiers in neuroscience* 8.
- Bowerman M, Anderson CL, Beauvais A, Boyl PP, Witke W, Kothary R (2009) SMN, profilin IIa and plastin 3: a link between the deregulation of actin dynamics and SMA pathogenesis. *Molecular and Cellular Neuroscience* 42:66-74.
- Bowerman M, Swoboda KJ, Michalski JP, Wang GS, Reeks C, Beauvais A, Murphy K, Woulfe J, Sreaton RA, Scott FW (2012) Glucose metabolism and pancreatic defects in spinal muscular atrophy. *Annals of neurology* 72:256-268.
- Bretscher A, Weber K (1980) Fimbrin, a new microfilament-associated protein present in microvilli and other cell surface structures. *The Journal of cell biology* 86:335-340.
- Brichta L, Hofmann Y, Hahnen E, Siebzehnrubl F, Raschke H, Blumcke I, Eyupoglu I, Wirth B (2003) Valproic acid increases the SMN2 protein level: a well-known drug as a potential therapy for spinal muscular atrophy. *Human molecular genetics* 12:2481-2489.
- Burghes AH, Beattie CE (2009) Spinal muscular atrophy: why do low levels of survival motor neuron protein make motor neurons sick? *Nature Reviews Neuroscience* 10:597-609.
- Butchbach ME, Singh J, Þorsteinsdóttir M, Saieva L, Slominski E, Thurmond J, Andrésón T, Zhang J, Edwards JD, Simard LR (2010) Effects of 2, 4-diaminoquinazoline derivatives on SMN expression and phenotype in a mouse model for spinal muscular atrophy. *Human molecular genetics* 19:454-467.

- Cartegni L, Krainer AR (2002) Disruption of an SF2/ASF-dependent exonic splicing enhancer in SMN2 causes spinal muscular atrophy in the absence of SMN1. *Nature genetics* 30:377-384.
- Cashman NR, Durham HD, Blusztajn JK, Oda K, Tabira T, Shaw IT, Dahrouge S, Antel JP (1992) Neuroblastoma \times spinal cord (NSC) hybrid cell lines resemble developing motor neurons. *Developmental dynamics* 194:209-221.
- Castresana J, Saraste M (1995) Does Vav bind to F-actin through a CH domain? *FEBS letters* 374:149-151.
- Castro D, Iannaccone ST (2014) Spinal Muscular Atrophy: Therapeutic Strategies. *Current treatment options in neurology* 16:1-11.
- Cearley CN, Wolfe JH (2006) Transduction characteristics of adeno-associated virus vectors expressing cap serotypes 7, 8, 9, and Rh10 in the mouse brain. *Molecular Therapy* 13:528-537.
- Chan YB, Miguel-Aliaga I, Franks C, Thomas N, Trülzsch B, Sattelle DB, Davies KE, van den Heuvel M (2003) Neuromuscular defects in a Drosophila survival motor neuron gene mutant. *Human molecular genetics* 12:1367-1376.
- Chang J-G, Hsieh-Li H-M, Jong Y-J, Wang NM, Tsai C-H, Li H (2001) Treatment of spinal muscular atrophy by sodium butyrate. *Proceedings of the National Academy of Sciences* 98:9808-9813.
- Chen M, Manley JL (2009) Mechanisms of alternative splicing regulation: insights from molecular and genomics approaches. *Nature reviews Molecular cell biology* 10:741-754.
- Chen T-H, Chang J-G, Yang Y-H, Mai H-H, Liang W-C, Wu Y-C, Wang H-Y, Huang Y-B, Wu S-M, Chen Y-C (2010) Randomized, double-blind, placebo-controlled trial of hydroxyurea in spinal muscular atrophy. *Neurology* 75:2190-2197.
- Cherry JJ, Androphy EJ (2012) Therapeutic strategies for the treatment of spinal muscular atrophy. *Future medicinal chemistry* 4:1733-1750.
- Cho S, Dreyfuss G (2010) A degron created by SMN2 exon 7 skipping is a principal contributor to spinal muscular atrophy severity. *Genes & development* 24:438-442.
- Cifuentes-Diaz C, Frugier T, Tiziano FD, Lacène E, Roblot N, Joshi V, Moreau MH, Melki J (2001) Deletion of murine SMN exon 7 directed to skeletal muscle leads to severe muscular dystrophy. *The Journal of cell biology* 152:1107-1114.
- Coady TH, Lorson CL (2010) Trans-splicing-mediated improvement in a severe mouse model of spinal muscular atrophy. *The Journal of neuroscience* 30:126-130.
- Comley LH, Wishart TM, Baxter B, Murray LM, Nimmo A, Thomson D, Parson SH, Gillingwater TH (2011) Induction of cell stress in neurons from transgenic mice expressing yellow fluorescent protein: implications for neurodegeneration research.
- Coovert DD, Le TT, McAndrew PE, Strasswimmer J, Crawford TO, Mendell JR, Coulson SE, Androphy EJ, Prior TW, Burghes AH (1997) The survival motor neuron protein in spinal muscular atrophy. *Human molecular genetics* 6:1205-1214.
- Dale JM, Shen H, Barry DM, Garcia VB, Rose Jr FF, Lorson CL, Garcia ML (2011) The spinal muscular atrophy mouse model, SMA Δ 7, displays altered axonal

- transport without global neurofilament alterations. *Acta neuropathologica* 122:331-341.
- Davidson BL, Breakefield XO (2003) Viral vectors for gene delivery to the nervous system. *Nature Reviews Neuroscience* 4:353-364.
- De Arruda MV, Watson S, Lin C-S, Leavitt J, Matsudaira P (1990) Fimbrin is a homologue of the cytoplasmic phosphoprotein plastin and has domains homologous with calmodulin and actin gelation proteins. *The Journal of cell biology* 111:1069-1079.
- Deglon N, Tseng JL, Bensadoun J-C, Zurn AD, Arsenijevic Y, Almeida LPD, Zufferey R, Trono D, Aebischer P (2000) Self-inactivating lentiviral vectors with enhanced transgene expression as potential gene transfer system in Parkinson's disease. *Human gene therapy* 11:179-190.
- Delanote V, Van Impe K, De Corte V, Bruyneel E, Vetter G, Boucherie C, Mareel M, Vandekerckhove J, Friederich E, Gettemans J (2005) Molecular Basis for Dissimilar Nuclear Trafficking of the Actin-Bundling Protein Isoforms T-and L-Plastin. *Traffic* 6:335-345.
- Di Penta A, Mercaldo V, Florenzano F, Munck S, Ciotti MT, Zalfa F, Mercanti D, Molinari M, Bagni C, Achsel T (2009) Dendritic LSm1/CBP80-mRNPs mark the early steps of transport commitment and translational control. *The Journal of cell biology* 184:423-435.
- DiMatteo D, Callahan S, Kmiec EB (2008) Genetic conversion of an *SMN2* gene to *SMN1*: A novel approach to the treatment of spinal muscular atrophy. *Experimental cell research* 314:878-886.
- Dimitriadi M, Sleight JN, Walker A, Chang HC, Sen A, Kalloo G, Harris J, Barsby T, Walsh MB, Satterlee JS (2010) Conserved genes act as modifiers of invertebrate SMN loss of function defects. *PLoS genetics* 6:e1001172.
- Doll R, Crandall J, Dyer C, Aucoin J, Smith F (1996) Comparison of promoter strengths on gene delivery into mammalian brain cells using AAV vectors. *Gene therapy* 3:437-447.
- Dombert B, Sivadasan R, Simon CM, Jablonka S, Sendtner M (2014) Presynaptic Localization of Smn and hnRNP R in Axon Terminals of Embryonic and Postnatal Mouse Motoneurons.
- Dominguez E, Marais T, Chatauret N, Benkhelifa-Ziyyat S, Duque S, Ravassard P, Carcenac R, Astord S, de Moura AP, Voit T (2011) Intravenous scAAV9 delivery of a codon-optimized SMN1 sequence rescues SMA mice. *Human molecular genetics* 20:681-693.
- Dubowitz V (1999) Very severe spinal muscular atrophy (SMA type 0): an expanding clinical phenotype. *European Journal of Paediatric Neurology* 3:49-51.
- Duque S, Joussemet B, Riviere C, Marais T, Dubreil L, Douar A-M, Fyfe J, Moullier P, Colle M-A, Barkats M (2009) Intravenous administration of self-complementary AAV9 enables transgene delivery to adult motor neurons. *Molecular Therapy* 17:1187-1196.
- Eaton SL, Roche SL, Llaverro Hurtado M, Oldknow KJ, Farquharson C, Gillingwater TH, Wishart TM (2013) Total protein analysis as a reliable loading control for quantitative fluorescent Western blotting. *PLoS One* 8:e72457.
- Echaniz-Laguna A, Miniou P, Bartholdi D, Melki J (1999) The promoters of the survival motor neuron gene (SMN) and its copy (SMNc) share common regulatory elements. *The American Journal of Human Genetics* 64:1365-1370.

- El-Khodor BF, Edgar N, Chen A, Winberg ML, Joyce C, Brunner D, Suárez-Fariñas M, Heyes MP (2008) Identification of a battery of tests for drug candidate evaluation in the SMN Δ 7 neonate model of spinal muscular atrophy. *Experimental neurology* 212:29-43.
- Fallini C, Bassell GJ, Rossoll W (2012) Spinal muscular atrophy: the role of SMN in axonal mRNA regulation. *Brain research* 1462:81-92.
- Fallini C, Zhang H, Su Y, Silani V, Singer RH, Rossoll W, Bassell GJ (2011) The survival of motor neuron (SMN) protein interacts with the mRNA-binding protein HuD and regulates localization of poly (A) mRNA in primary motor neuron axons. *The Journal of Neuroscience* 31:3914-3925.
- Farag E (2010) Dexmedetomidine in the neurointensive care unit. *Discovery medicine* 9:42-45.
- Fischer U, Liu Q, Dreyfuss G (1997) The SMN-SIP1 complex has an essential role in spliceosomal snRNP biogenesis. *Cell* 90:1023-1029.
- Foust KD, Nurre E, Montgomery CL, Hernandez A, Chan CM, Kaspar BK (2009) Intravascular AAV9 preferentially targets neonatal neurons and adult astrocytes. *Nature biotechnology* 27:59-65.
- Foust KD, Wang X, McGovern VL, Braun L, Bevan AK, Haidet AM, Le TT, Morales PR, Rich MM, Burghes AH (2010) Rescue of the spinal muscular atrophy phenotype in a mouse model by early postnatal delivery of SMN. *Nature biotechnology* 28:271-274.
- Frugier T, Tiziano FD, Cifuentes-Diaz C, Miniou P, Roblot N, Dierich A, Le Meur M, Melki J (2000) Nuclear targeting defect of SMN lacking the C-terminus in a mouse model of spinal muscular atrophy. *Human molecular genetics* 9:849-858.
- Giavazzi A, Setola V, Simonati A, Battaglia G (2006) Neuronal-specific roles of the survival motor neuron protein: evidence from survival motor neuron expression patterns in the developing human central nervous system. *Journal of Neuropathology & Experimental Neurology* 65:267-277.
- Giesemann T, Rathke-Hartlieb S, Rothkegel M, Bartsch JW, Buchmeier S, Jockusch BM, Jockusch H (1999) A Role for Polyproline Motifs in the Spinal Muscular Atrophy Protein SMN PROFILINS BIND TO AND COLOCALIZE WITH SMN IN NUCLEAR GEMS. *Journal of Biological Chemistry* 274:37908-37914.
- Giganti A, Plastino J, Janji B, Van Troys M, Lentz D, Ampe C, Sykes C, Friederich E (2005) Actin-filament cross-linking protein T-plastin increases Arp2/3-mediated actin-based movement. *Journal of cell science* 118:1255-1265.
- Gogliotti RG, Quinlan KA, Barlow CB, Heier CR, Heckman C, DiDonato CJ (2012) Motor neuron rescue in spinal muscular atrophy mice demonstrates that sensory-motor defects are a consequence, not a cause, of motor neuron dysfunction. *The Journal of Neuroscience* 32:3818-3829.
- Gray SJ, Matagne V, Bachaboina L, Yadav S, Ojeda SR, Samulski RJ (2011) Preclinical differences of intravascular AAV9 delivery to neurons and glia: a comparative study of adult mice and nonhuman primates. *Molecular Therapy* 19:1058-1069.
- Grzeschik SM, Ganta M, Prior TW, Heavlin WD, Wang CH (2005) Hydroxyurea enhances SMN2 gene expression in spinal muscular atrophy cells. *Annals of neurology* 58:194-202.

- Hao LT, Burghes AH, Beattie CE (2011) Generation and Characterization of a genetic zebrafish model of SMA carrying the human SMN2 gene. *Molecular neurodegeneration* 6:24.
- Hao LT, Wolman M, Granato M, Beattie CE (2012) Survival motor neuron affects plastin 3 protein levels leading to motor defects. *The Journal of Neuroscience* 32:5074-5084.
- Hayhurst M, Wagner AK, Cerletti M, Wagers AJ, Rubin LL (2012) A cell-autonomous defect in skeletal muscle satellite cells expressing low levels of survival of motor neuron protein. *Developmental biology* 368:323-334.
- Helmken C, Hofmann Y, Schoenen F, Oprea G, Raschke H, Rudnik-Schöneborn S, Zerres K, Wirth B (2003) Evidence for a modifying pathway in SMA discordant families: reduced SMN level decreases the amount of its interacting partners and Htra2-beta1. *Human genetics* 114:11-21.
- Hermonat PL, Quirk JG, Bishop BM, Han L (1997) The packaging capacity of adeno-associated virus (AAV) and the potential for wild-type-plus AAV gene therapy vectors. *FEBS letters* 407:78-84.
- Holehonnur R, Luong JA, Chaturvedi D, Ho A, Lella SK, Hosek MP, Ploski JE (2014) Adeno-associated viral serotypes produce differing titers and differentially transduce neurons within the rat basolateral amygdala. *BMC neuroscience* 15:28.
- Hsieh-Li HM, Chang J-G, Jong Y-J, Wu M-H, Wang NM, Tsai CH, Li H (2000) A mouse model for spinal muscular atrophy. *Nature genetics* 24:66-70.
- Hua Y, Sahashi K, Rigo F, Hung G, Horev G, Bennett CF, Krainer AR (2011) Peripheral SMN restoration is essential for long-term rescue of a severe spinal muscular atrophy mouse model. *Nature* 478:123-126.
- Jablonka S, Beck M, Lechner BD, Mayer C, Sendtner M (2007) Defective Ca²⁺ channel clustering in axon terminals disturbs excitability in motoneurons in spinal muscular atrophy. *The Journal of cell biology* 179:139-149.
- Jablonka S, Wiese S, Sendtner M (2004) Axonal defects in mouse models of motoneuron disease. *Journal of neurobiology* 58:272-286.
- James P, Sumner CJ (2011) Progress and promise: the current status of spinal muscular atrophy therapeutics. *Discovery medicine* 12:291-305.
- Jao L-E, Appel B, Wentz SR (2012) A zebrafish model of lethal congenital contracture syndrome 1 reveals Gle1 function in spinal neural precursor survival and motor axon arborization. *Development* 139:1316-1326.
- Jarecki J, Chen X, Bernardino A, Covert DD, Whitney M, Burghes A, Stack J, Pollok BA (2005) Diverse small-molecule modulators of SMN expression found by high-throughput compound screening: early leads towards a therapeutic for spinal muscular atrophy. *Human molecular genetics* 14:2003-2018.
- Kariya S, Park G-H, Maeno-Hikichi Y, Leykekhman O, Lutz C, Arkovitz MS, Landmesser LT, Monani UR (2008) Reduced SMN protein impairs maturation of the neuromuscular junctions in mouse models of spinal muscular atrophy. *Human molecular genetics* 17:2552-2569.
- Kashima T, Manley JL (2003) A negative element in SMN2 exon 7 inhibits splicing in spinal muscular atrophy. *Nature genetics* 34:460-463.
- Kaspar BK, Lladó J, Sherkat N, Rothstein JD, Gage FH (2003) Retrograde viral delivery of IGF-1 prolongs survival in a mouse ALS model. *Science* 301:839-842.

- Kinali M, Banks L, Mercuri E, Manzur A, Muntoni F (2004) Bone mineral density in a paediatric spinal muscular atrophy population. *Neuropediatrics* 35:325-328.
- Kinali M, Mercuri E, Main M, De Biasia F, Karatza A, Higgins R, Banks L, Manzur A, Muntoni F (2002) Pilot trial of albuterol in spinal muscular atrophy. *Neurology* 59:609-610.
- Kong L, Wang X, Choe DW, Polley M, Burnett BG, Bosch-Marcé M, Griffin JW, Rich MM, Sumner CJ (2009) Impaired synaptic vesicle release and immaturity of neuromuscular junctions in spinal muscular atrophy mice. *The Journal of Neuroscience* 29:842-851.
- Le TT, Pham LT, Butchbach ME, Zhang HL, Monani UR, Coovert DD, Gavrilina TO, Xing L, Bassell GJ, Burghes AH (2005) SMN Δ 7, the major product of the centromeric survival motor neuron (SMN2) gene, extends survival in mice with spinal muscular atrophy and associates with full-length SMN. *Human molecular genetics* 14:845-857.
- Lefebvre S, Bürglen L, Reboullet S, Clermont O, Burlet P, Viollet L, Benichou B, Cruaud C, Millasseau P, Zeviani M (1995) Identification and characterization of a spinal muscular atrophy-determining gene. *Cell* 80:155-165.
- Li DK, Tisdale S, Lotti F, Pellizzoni L (2014) SMN control of RNP assembly: from post-transcriptional gene regulation to motor neuron disease. In: *Seminars in cell & developmental biology*, vol. 32, pp 22-29: Elsevier.
- Lin C-S, Park T, Chen ZP, Leavitt J (1993) Human plastin genes. Comparative gene structure, chromosome location, and differential expression in normal and neoplastic cells. *Journal of Biological Chemistry* 268:2781-2792.
- Ling KK, Gibbs RM, Feng Z, Ko C-P (2011) Severe neuromuscular denervation of clinically relevant muscles in a mouse model of spinal muscular atrophy. *Human molecular genetics* ddr453.
- Little D, Valori C, Mutsaers C, Bennett E, Wyles M, Sharrack B, Shaw P, Gillingwater T, Azzouz M, Ning K (2014) PTEN Depletion Decreases Disease Severity and Modestly Prolongs Survival in a Mouse Model of Spinal Muscular Atrophy. *Molecular therapy: the journal of the American Society of Gene Therapy*.
- Locatelli D, Terao M, Kurosaki M, Zanellati MC, Pletto DR, Finardi A, Colciaghi F, Garattini E, Battaglia GS (2015) Different Stability and Proteasome-Mediated Degradation Rate of SMN Protein Isoforms. *PloS one* 10:e0134163.
- Long M, Song F, Qu Y, Meng Y, Wang H, Jin Y, Huang S (2008) [Quantitative analysis of SMN1 and SMN2 genes based on DHPLC: a reliable method for detection of non-homozygous patients with spinal muscular atrophy]. *Zhonghua yi xue za zhi* 88:1259-1263.
- Lorson CL, Androphy EJ (2000) An exonic enhancer is required for inclusion of an essential exon in the SMA-determining gene SMN. *Human molecular genetics* 9:259-265.
- Lorson CL, Hahnen E, Androphy EJ, Wirth B (1999) A single nucleotide in the SMN gene regulates splicing and is responsible for spinal muscular atrophy. *Proceedings of the National Academy of Sciences* 96:6307-6311.
- Lyon AN, Pineda RH, Kudryashova E, Kudryashov DS, Beattie CE (2013) Calcium binding is essential for plastin 3 function in Smn-deficient motoneurons. *Human molecular genetics* ddt595.

- Madabusi NK (2012) Characterization of three SMN missense mutations using mouse models of Spinal Muscular Atrophy. The Ohio State University.
- Martin-Rendon E, Azzouz M, Mazarakis N (2001) Lentiviral vectors for the treatment of neurodegenerative diseases. *Current opinion in molecular therapeutics* 3:476-481.
- Martínez-Hernández R, Bernal S, Also-Rallo E, Alías L, Barceló M, Hereu M, Esquerda JE, Tizzano EF (2013) Synaptic defects in type I spinal muscular atrophy in human development. *The Journal of pathology* 229:49-61.
- Martinez TL, Kong L, Wang X, Osborne MA, Crowder ME, Van Meerbeke JP, Xu X, Davis C, Wooley J, Goldhamer DJ (2012) Survival motor neuron protein in motor neurons determines synaptic integrity in spinal muscular atrophy. *The Journal of Neuroscience* 32:8703-8715.
- Matsudaira PT, Burgess DR (1979) Identification and organization of the components in the isolated microvillus cytoskeleton. *The Journal of cell biology* 83:667-673.
- Mattar C, Waddington S, Biswas A, Johana N, Ng X, Fisk A, Fisk N, Tan L, Rahim A, Buckley S (2012) Systemic delivery of scAAV9 in fetal macaques facilitates neuronal transduction of the central and peripheral nervous systems. *Gene therapy* 20:69-83.
- Matus A, Huber G, Bernhardt R (1983) Neuronal microdifferentiation. In: *Cold Spring Harbor symposia on quantitative biology*, vol. 48, pp 775-782: Cold Spring Harbor Laboratory Press.
- McAndrew P, Parsons D, Simard L, Rochette C, Ray P, Mendell J, Prior T, Burghes A (1997) Identification of Proximal Spinal Muscular Atrophy Carriers and Patients by Analysis of SMN^T and SMN^C Gene Copy Number. *The American Journal of Human Genetics* 60:1411-1422.
- McCarty D, Fu H, Monahan P, Toulson C, Naik P, Samulski R (2003) Adeno-associated virus terminal repeat (TR) mutant generates self-complementary vectors to overcome the rate-limiting step to transduction in vivo. *Gene therapy* 10:2112-2118.
- McCarty D, Monahan P, Samulski R (2001) Self-complementary recombinant adeno-associated virus (scAAV) vectors promote efficient transduction independently of DNA synthesis. *Gene therapy* 8:1248-1254.
- McGivern JV, Patitucci TN, Nord JA, Barabas MEA, Stucky CL, Ebert AD (2013) Spinal muscular atrophy astrocytes exhibit abnormal calcium regulation and reduced growth factor production. *Glia* 61:1418-1428.
- McGovern VL, Gavrilina TO, Beattie CE, Burghes AH (2008) Embryonic motor axon development in the severe SMA mouse. *Human molecular genetics* 17:2900-2909.
- McWhorter ML, Monani UR, Burghes AH, Beattie CE (2003) Knockdown of the survival motor neuron (Smn) protein in zebrafish causes defects in motor axon outgrowth and pathfinding. *The Journal of cell biology* 162:919-932.
- Melki J, Sheth P, Abdelhak S, Burlet P, Bachelot M, Frézal J, Munnich A, Lathrop M (1990) Mapping of acute (type I) spinal muscular atrophy to chromosome 5q12-q14. *The Lancet* 336:271-273.
- Merlini L, Solari A, Vita G, Bertini E, Minetti C, Mongini T, Mazzone E, Angelini C, Morandi L (2003) Role of Gabapentin in Spinal Muscular Atrophy Results of a Multicenter, Randomized Italian Study. *Journal of child neurology* 18:537-541.

- Mikesh M, Smith I, Rimer M, Thompson W (2011) Muscles in a mouse model of spinal muscular atrophy show profound defects in neuromuscular development even in the absence of failure in neuromuscular transmission or loss of motor neurons. *Developmental biology* 356:432-444.
- Miller R, Moore D, Dronsky V, Bradley W, Barohn R, Bryan W, Prior T, Gelinas D, Iannaccone S, Kissel J (2001) A placebo-controlled trial of gabapentin in spinal muscular atrophy. *Journal of the neurological sciences* 191:127-131.
- Miyake N, Miyake K, Yamamoto M, Hirai Y, Shimada T (2011) Global gene transfer into the CNS across the BBB after neonatal systemic delivery of single-stranded AAV vectors. *Brain research* 1389:19-26.
- Monani UR, Sendtner M, Coovert DD, Parsons DW, Andreassi C, Le TT, Jablonka S, Schrank B, Rossol W, Prior TW (2000) The human centromeric survival motor neuron gene (SMN2) rescues embryonic lethality in *Smn*^{-/-} mice and results in a mouse with spinal muscular atrophy. *Human molecular genetics* 9:333-339.
- Mulcahy PJ, Iremonger K, Karyka E, Herranz-Martín S, Shum K-T, Tam JKV, Azzouz M (2014) Gene Therapy: A Promising Approach to Treating Spinal Muscular Atrophy. *Human gene therapy* 25:575-586.
- Murray LM, Lee S, Bäumer D, Parson SH, Talbot K, Gillingwater TH (2009) Pre-symptomatic development of lower motor neuron connectivity in a mouse model of severe spinal muscular atrophy. *Human molecular genetics* ddp506.
- Mutsaers CA, Wishart TM, Lamont DJ, Riessland M, Schreml J, Comley LH, Murray LM, Parson SH, Lochmüller H, Wirth B (2011) Reversible molecular pathology of skeletal muscle in spinal muscular atrophy. *Human molecular genetics* ddr360.
- Namba Y, Ito M, Zu Y, Shigesada K, Maruyama K (1992) Human T cell L-plastin bundles actin filaments in a calcium dependent manner. *Journal of biochemistry* 112:503-507.
- Nanou A, Azzouz M (2009) Gene therapy for neurodegenerative diseases based on lentiviral vectors. *Progress in brain research* 175:187-200.
- Ning K, Drepper C, Valori CF, Ahsan M, Wyles M, Higginbottom A, Herrmann T, Shaw P, Azzouz M, Sendtner M (2010) PTEN depletion rescues axonal growth defect and improve survival in SMN-deficient motor neurons. *Human molecular genetics* ddq226.
- Oprea GE, Kröber S, McWhorter ML, Rossoll W, Müller S, Krawczak M, Bassell GJ, Beattie CE, Wirth B (2008) Plastin 3 is a protective modifier of autosomal recessive spinal muscular atrophy. *Science* 320:524-527.
- Otto JJ (1994) Actin-bundling proteins. *Current opinion in cell biology* 6:105-109.
- Pagliardini S, Giavazzi A, Setola V, Lizier C, Di Luca M, DeBiasi S, Battaglia G (2000) Subcellular localization and axonal transport of the survival motor neuron (SMN) protein in the developing rat spinal cord. *Human molecular genetics* 9:47-56.
- Palfi S, Gurruchaga JM, Ralph GS, Lepetit H, Lavisse S, Buttery PC, Watts C, Miskin J, Kelleher M, Deeley S (2014) Long-term safety and tolerability of ProSavin, a lentiviral vector-based gene therapy for Parkinson's disease: a dose escalation, open-label, phase 1/2 trial. *The Lancet* 383:1138-1146.
- Passini MA, Bu J, Roskelley EM, Richards AM, Sardi SP, O'Riordan CR, Klinger KW, Shihabuddin LS, Cheng SH (2010) CNS-targeted gene therapy improves survival and motor function in a mouse model of spinal muscular atrophy. *The Journal of clinical investigation* 120:1253.

- Passini MA, Cheng SH (2011) Prospects for the gene therapy of spinal muscular atrophy. *Trends in molecular medicine* 17:259-265.
- Pellizzoni L (2007) Chaperoning ribonucleoprotein biogenesis in health and disease. *EMBO reports* 8:340-345.
- Pellizzoni L, Charroux B, Dreyfuss G (1999) SMN mutants of spinal muscular atrophy patients are defective in binding to snRNP proteins. *Proceedings of the National Academy of Sciences* 96:11167-11172.
- Porensky PN, Mitropant C, McGovern VL, Bevan AK, Foust KD, Kaspar BK, Wilton SD, Burghes AH (2012) A single administration of morpholino antisense oligomer rescues spinal muscular atrophy in mouse. *Human molecular genetics* 21:1625-1638.
- Prior TW, Krainer AR, Hua Y, Swoboda KJ, Snyder PC, Bridgeman SJ, Burghes AH, Kissel JT (2009) A Positive Modifier of Spinal Muscular Atrophy in the *SMN2* Gene. *The American Journal of Human Genetics* 85:408-413.
- Pyatt RE, Mihal DC, Prior TW (2007) Assessment of liquid microbead arrays for the screening of newborns for spinal muscular atrophy. *Clinical chemistry* 53:1879-1885.
- Riessland M, Ackermann B, Förster A, Jakubik M, Hauke J, Garbes L, Fritzsche I, Mende Y, Blumcke I, Hahnen E (2010) SAHA ameliorates the SMA phenotype in two mouse models for spinal muscular atrophy. *Human molecular genetics* 19:1492-1506.
- Rindt H, Feng Z, Mazzasette C, Glascock JJ, Valdivia D, Pyles N, Crawford TO, Swoboda KJ, Patitucci TN, Ebert AD (2015) Astrocytes influence the severity of spinal muscular atrophy. *Human molecular genetics* ddv148.
- Rossoll W, Jablonka S, Andreassi C, Kröning A-K, Karle K, Monani UR, Sendtner M (2003) Smn, the spinal muscular atrophy-determining gene product, modulates axon growth and localization of β -actin mRNA in growth cones of motoneurons. *The Journal of cell biology* 163:801-812.
- Rossoll W, Kröning A-K, Ohndorf U-M, Steegborn C, Jablonka S, Sendtner M (2002) Specific interaction of Smn, the spinal muscular atrophy determining gene product, with hnRNP-R and gry-rbp/hnRNP-Q: a role for Smn in RNA processing in motor axons? *Human molecular genetics* 11:93-105.
- Ruiz R, Tabares L (2014) Neurotransmitter release in motor nerve terminals of a mouse model of mild spinal muscular atrophy. *Journal of anatomy* 224:74-84.
- Russman B, Buncher C, White M, Samaha F, Iannaccone S (1996) Function changes in spinal muscular atrophy II and III. *Neurology* 47:973-976.
- Sahashi K, Sobue G (2014) [The role of RNA splicing in the pathogenesis of spinal muscular atrophy and development of its therapeutics]. *Brain and nerve= Shinkei kenkyu no shinpo* 66:1471-1480.
- Sato-Yoshitake R, Shiomura Y, Miyasaka H, Hirokawa N (1989) Microtubule-associated protein 1B: molecular structure, localization, and phosphorylation-dependent expression in developing neurons. *Neuron* 3:229-238.
- Saunders NR, Ek CJ, Dziegielewska KM (2009) The neonatal blood-brain barrier is functionally effective, and immaturity does not explain differential targeting of AAV9. *Nature biotechnology* 27:804-805.
- Schmid A, DiDonato CJ (2007) Animal models of spinal muscular atrophy. *Journal of child neurology* 22:1004-1012.

- Schrank B, Götz R, Gunnensen JM, Ure JM, Toyka KV, Smith AG, Sendtner M (1997) Inactivation of the survival motor neuron gene, a candidate gene for human spinal muscular atrophy, leads to massive cell death in early mouse embryos. *Proceedings of the National Academy of Sciences* 94:9920-9925.
- Schreml J, Riessland M, Paterno M, Garbes L, Roßbach K, Ackermann B, Krämer J, Somers E, Parson SH, Heller R (2013) Severe SMA mice show organ impairment that cannot be rescued by therapy with the HDACi JNJ-26481585. *European Journal of Human Genetics* 21:643-652.
- See K, Yadav P, Giegerich M, Cheong PS, Graf M, Vyas H, Lee SG, Mathavan S, Fischer U, Sendtner M (2014) SMN deficiency alters Nrnx2 expression and splicing in zebrafish and mouse models of spinal muscular atrophy. *Human molecular genetics* 23:1754-1770.
- Sendtner M (2010) Therapy development in spinal muscular atrophy. *Nature neuroscience* 13:795-799.
- Shababi M, Glascock J, Lorson CL (2010a) Combination of SMN trans-splicing and a neurotrophic factor increases the life span and body mass in a severe model of spinal muscular atrophy. *Human gene therapy* 22:135-144.
- Shababi M, Habibi J, Yang HT, Vale SM, Sewell WA, Lorson CL (2010b) Cardiac defects contribute to the pathology of spinal muscular atrophy models. *Human molecular genetics* ddq329.
- Shababi M, Lorson CL, Rudnik-Schöneborn SS (2014) Spinal muscular atrophy: a motor neuron disorder or a multi-organ disease? *Journal of anatomy* 224:15-28.
- Shababi M, Osman EY, Lorson CL (2015) Gene Therapy in Spinal Muscular Atrophy (SMA) Models Using Intracerebroventricular Injection into Neonatal Mice. *Gene Delivery and Therapy for Neurological Disorders* 297-320.
- Shanmugarajan S, Tsuruga E, Swoboda KJ, Maria BL, Ries WL, Reddy SV (2009) Bone loss in survival motor neuron (Smn^{-/-} SMN2) genetic mouse model of spinal muscular atrophy. *The Journal of pathology* 219:52-60.
- Sharma A, Lambrechts A, Le TT, Sewry CA, Ampe C, Burghes AH, Morris GE (2005) A role for complexes of survival of motor neurons (SMN) protein with gemins and profilin in neurite-like cytoplasmic extensions of cultured nerve cells. *Experimental cell research* 309:185-197.
- Simic G, Mladinov M, Simic DS, Milosevic NJ, Islam A, Pajtak A, Barisic N, Sertic J, Lucassen PJ, Hof PR (2008) Abnormal motoneuron migration, differentiation, and axon outgrowth in spinal muscular atrophy. *Acta neuropathologica* 115:313-326.
- Singh NN, Lee BM, Singh RN (2015) Splicing regulation in spinal muscular atrophy by an RNA structure formed by long-distance interactions. *Annals of the New York Academy of Sciences* 1341:176-187.
- Sinn P, Sauter S, McCray P (2005) Gene therapy progress and prospects: development of improved lentiviral and retroviral vectors—design, biosafety, and production. *Gene therapy* 12:1089-1098.
- Sleigh JN, Gillingwater TH, Talbot K (2011) The contribution of mouse models to understanding the pathogenesis of spinal muscular atrophy. *Disease models & mechanisms* 4:457-467.
- Sreedharan J, Blair IP, Tripathi VB, Hu X, Vance C, Rogelj B, Ackerley S, Durnall JC, Williams KL, Buratti E (2008) TDP-43 mutations in familial and sporadic amyotrophic lateral sclerosis. *Science* 319:1668-1672.

- Stratigopoulos G, Lanzano P, Deng L, Guo J, Kaufmann P, Darras B, Finkel R, Tawil R, McDermott MP, Martens W (2010) Association of plastin 3 expression with disease severity in spinal muscular atrophy only in postpubertal females. *Archives of neurology* 67:1252-1256.
- Strong MJ, Volkening K, Hammond R, Yang W, Strong W, Leystra-Lantz C, Shoemith C (2007) TDP43 is a human low molecular weight neurofilament (hNFL) mRNA-binding protein. *Molecular and Cellular Neuroscience* 35:320-327.
- Sumner CJ, Huynh TN, Markowitz JA, Perhac JS, Hill B, Coovert DD, Schussler K, Chen X, Jarecki J, Burghes AH (2003) Valproic acid increases SMN levels in spinal muscular atrophy patient cells. *Annals of neurology* 54:647-654.
- Swoboda KJ, Prior TW, Scott CB, McNaught TP, Wride MC, Reyna SP, Bromberg MB (2005) Natural history of denervation in SMA: relation to age, SMN2 copy number, and function. *Annals of neurology* 57:704-712.
- Tam JKV, Karyka E, Azzouz M (2014) Current and investigational treatments for spinal muscular atrophy. *Expert Opinion on Orphan Drugs* 2:465-476.
- Tarn W-Y, Steitz JA (1997) Pre-mRNA splicing: the discovery of a new spliceosome doubles the challenge. *Trends in biochemical sciences* 22:132-137.
- Ting C-H, Wen H-L, Liu H-C, Hsieh-Li H-M, Li H, Lin-Chao S (2012) The spinal muscular atrophy disease protein SMN is linked to the Golgi network.
- Tisdale S, Lotti F, Saieva L, Van Meerbeke JP, Crawford TO, Sumner CJ, Mentis GZ, Pellizzoni L (2013) SMN is essential for the biogenesis of U7 small nuclear ribonucleoprotein and 3'-end formation of histone mRNAs. *Cell reports* 5:1187-1195.
- Todd AG, Morse R, Shaw DJ, McGinley S, Stebbings H, Young PJ (2010) SMN, Gemin2 and Gemin3 Associate with β -Actin mRNA in the Cytoplasm of Neuronal Cells *In Vitro*. *Journal of molecular biology* 401:681-689.
- Valori CF, Ning K, Wyles M, Mead RJ, Grierson AJ, Shaw PJ, Azzouz M (2010) Systemic delivery of scAAV9 expressing SMN prolongs survival in a model of spinal muscular atrophy. *Science translational medicine* 2:35ra42-35ra42.
- Vance C, Rogelj B, Hortobágyi T, De Vos KJ, Nishimura AL, Sreedharan J, Hu X, Smith B, Ruddy D, Wright P (2009) Mutations in FUS, an RNA processing protein, cause familial amyotrophic lateral sclerosis type 6. *Science* 323:1208-1211.
- Vitte JM, Davoult B, Roblot N, Mayer M, Joshi V, Courageot S, Tronche F, Vadrot J, Moreau MH, Kemeny F (2004) Deletion of murine Smn exon 7 directed to liver leads to severe defect of liver development associated with iron overload. *The American journal of pathology* 165:1731-1741.
- Voigt T, Meyer K, Baum O, Schümperli D (2010) Ultrastructural changes in diaphragm neuromuscular junctions in a severe mouse model for Spinal Muscular Atrophy and their prevention by bifunctional U7 snRNA correcting SMN2 splicing. *Neuromuscular Disorders* 20:744-752.
- Volkman N, DeRosier D, Matsudaira P, Hanein D (2001) An atomic model of actin filaments cross-linked by fimbrin and its implications for bundle assembly and function. *The Journal of cell biology* 153:947-956.
- Wadman RI, Bosboom WM, van der Pol WL, van den Berg LH, Wokke JH, Iannaccone ST, Vrancken AF (2012a) Drug treatment for spinal muscular atrophy type I. *The Cochrane Library*.

- Wadman RI, Vrancken AF, van den Berg LH, van der Pol WL (2012b) Dysfunction of the neuromuscular junction in spinal muscular atrophy types 2 and 3. *Neurology* 79:2050-2055.
- Wang Z, Ma H-I, Li J, Sun L, Zhang J, Xiao X (2003) Rapid and highly efficient transduction by double-stranded adeno-associated virus vectors in vitro and in vivo. *Gene therapy* 10:2105-2111.
- Wertz MH, Sahin M (2015) Developing therapies for spinal muscular atrophy. *Annals of the New York Academy of Sciences*.
- Winkler C, Eggert C, Gradl D, Meister G, Giegerich M, Wedlich D, Laggerbauer B, Fischer U (2005) Reduced U snRNP assembly causes motor axon degeneration in an animal model for spinal muscular atrophy. *Genes & development* 19:2320-2330.
- Wirth B, Barkats M, Martinat C, Sendtner M, Gillingwater TH (2015) Moving towards treatments for spinal muscular atrophy: hopes and limits. *Expert opinion on emerging drugs* 1-4.
- Workman E, Saieva L, Carrel TL, Crawford TO, Liu D, Lutz C, Beattie CE, Pellizzoni L, Burghes AH (2009) A SMN missense mutation complements SMN2 restoring snRNPs and rescuing SMA mice. *Human molecular genetics* 18:2215-2229.
- Yamanaka K, Chun SJ, Boillee S, Fujimori-Tonou N, Yamashita H, Gutmann DH, Takahashi R, Misawa H, Cleveland DW (2008) Astrocytes as determinants of disease progression in inherited amyotrophic lateral sclerosis. *Nature neuroscience* 11:251-253.
- Yanyan C, Yujin Q, Jinli B, Yuwei J, Hong W, Fang S (2013) Correlation of PLS3 expression with disease severity in children with spinal muscular atrophy. *Journal of human genetics* 59:24-27.
- Yokobori T, Iinuma H, Shimamura T, Imoto S, Sugimachi K, Ishii H, Iwatsuki M, Ota D, Ohkuma M, Iwaya T (2013) Plastin3 is a novel marker for circulating tumor cells undergoing the epithelial–mesenchymal transition and is associated with colorectal cancer prognosis. *Cancer research* 73:2059-2069.
- Young P, Le T, Dunckley M, thi Man N, Burghes A, Morris G (2001) Nuclear gems and Cajal (coiled) bodies in fetal tissues: nucleolar distribution of the spinal muscular atrophy protein, SMN. *Experimental cell research* 265:252-261.
- Young PJ, Le TT, thi Man N, Burghes AH, Morris GE (2000) The relationship between SMN, the spinal muscular atrophy protein, and nuclear coiled bodies in differentiated tissues and cultured cells. *Experimental cell research* 256:365-374.
- Zhang H, Xing L, Rossoll W, Wichterle H, Singer RH, Bassell GJ (2006) Multiprotein complexes of the survival of motor neuron protein SMN with Gemins traffic to neuronal processes and growth cones of motor neurons. *The Journal of neuroscience* 26:8622-8632.
- Zhang Z, Lotti F, Dittmar K, Younis I, Wan L, Kasim M, Dreyfuss G (2008) SMN deficiency causes tissue-specific perturbations in the repertoire of snRNAs and widespread defects in splicing. *Cell* 133:585-600.
- Zheleznyakova GY, Kiselev AV, Vakharlovsky VG, Rask-Andersen M, Chavan R, Egorova AA, Schiöth HB, Baranov VS (2011) Genetic and expression studies of SMN2 gene in Russian patients with spinal muscular atrophy type II and III. *BMC medical genetics* 12:96.

Zincarelli C, Soltys S, Rengo G, Rabinowitz JE (2008) Analysis of AAV serotypes 1–9 mediated gene expression and tropism in mice after systemic injection. *Molecular Therapy* 16:1073-1080.

APPENDIX

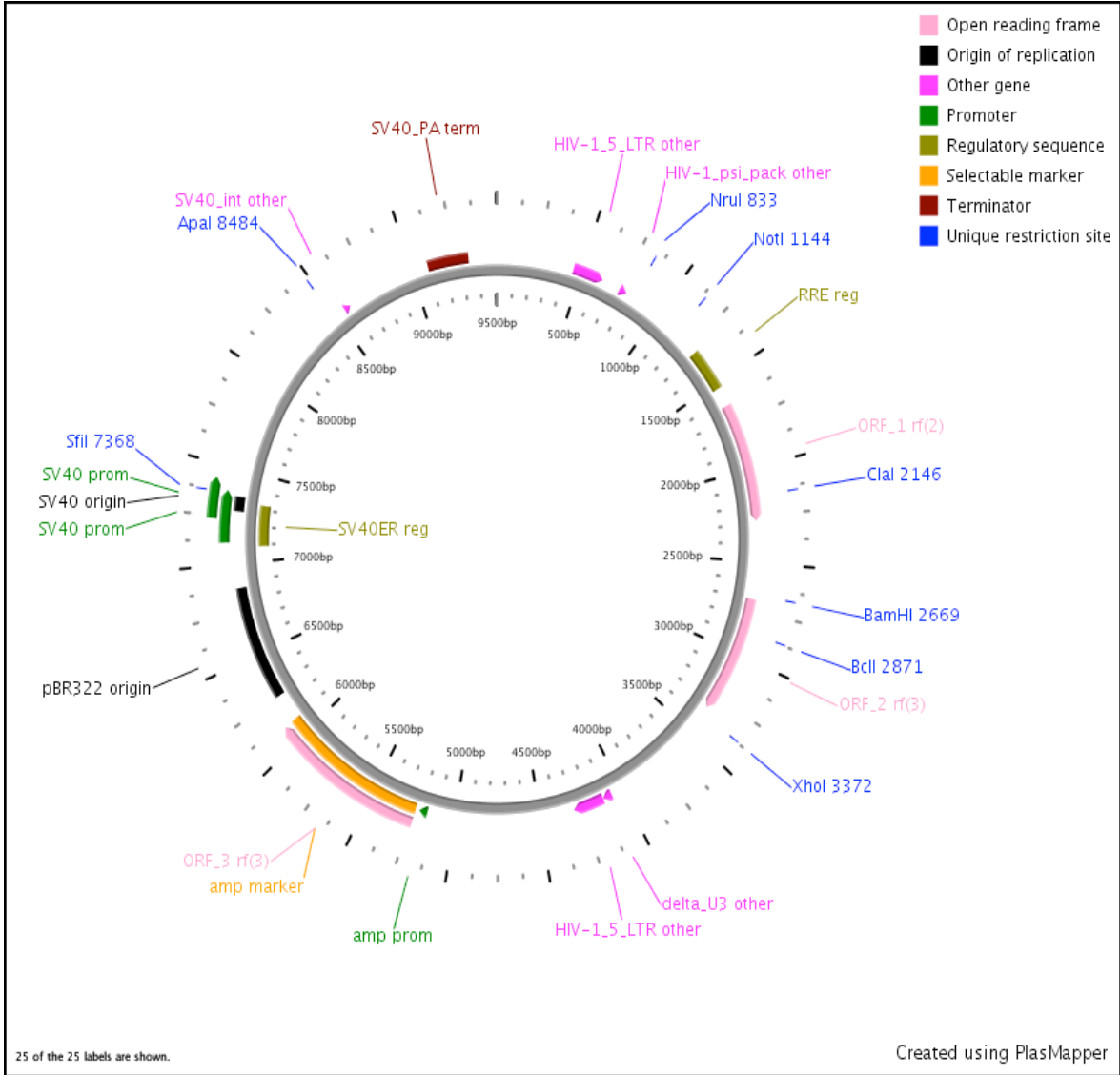
Appendix 1: Lab equipment

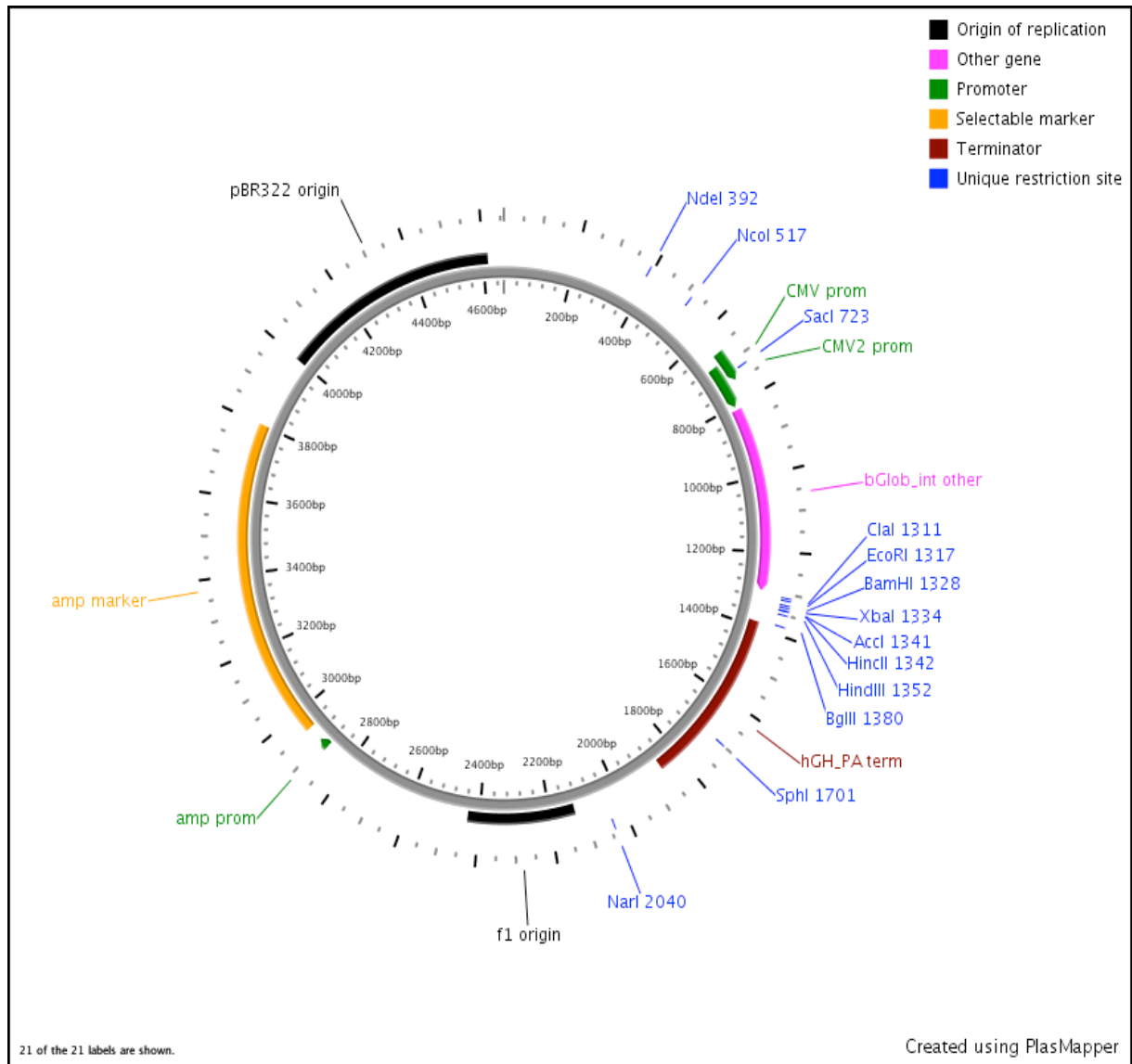
Equipment	Manufacture
G: Box gel imaging system	Syngene
NanoDrop 1000	Labtech
Optima L-100K Ultracentrifuge	Beckman Coulter
GENi imaging machine	Syngene
FLUOstar Omega plate reader	BMG Labtech
MX3000-P Real-time PCR system	BIO-RAD
Confocal microscope	Leica SP5 microscope system
Nikon microscope	Nikon
CFX96 Touch Real-time PCR detection system	BIO-RAD
Ultracentrifuge	Beckman Coulter

Appendix 2: Vector maps.

Maps of the LV and AAV Plasmids

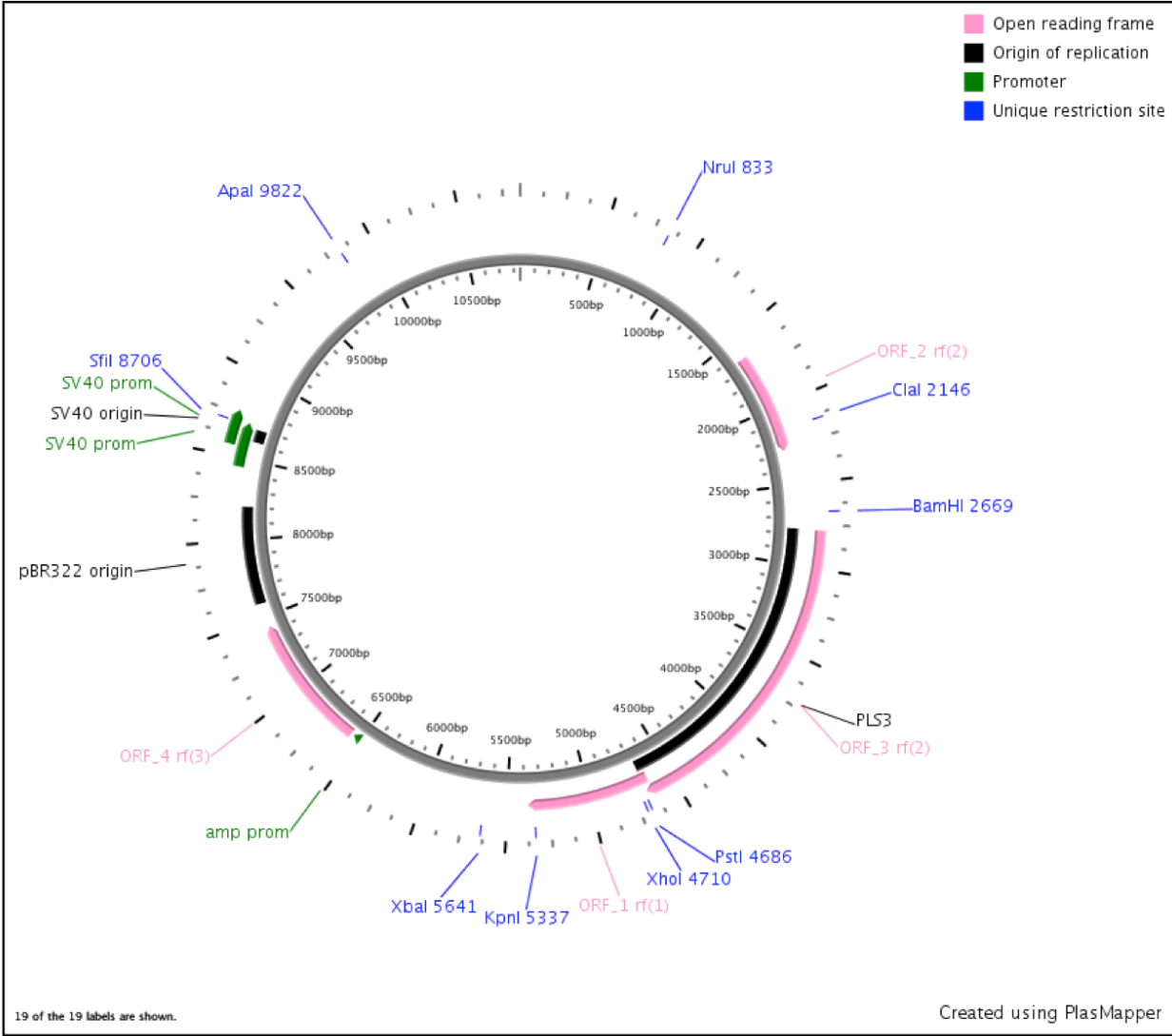
(A) Map of SIN-PGK-cPPT-GDNF-WHV



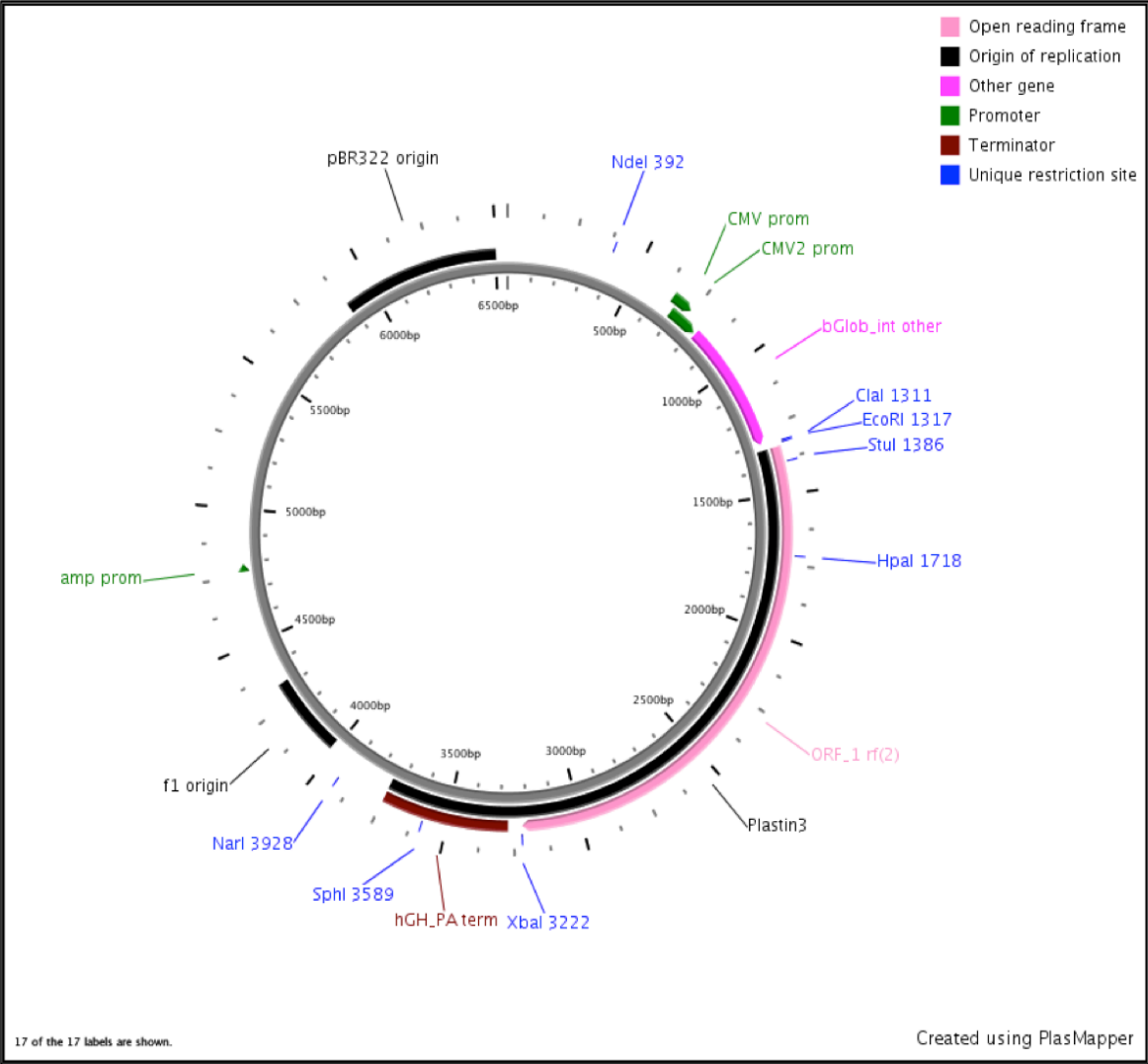
(B) Map of PAAV CMV MCS (conventional AAV)**Figure 8.1: Expression AAV viral plasmids used in this project**

The lentiviral vector (A.) SIN-PGK-cPPT-GDNF-WHV was used for all tissue culture experimental work, whereas the AAV vector (B.) was used for all the in vivo experimental work. Abbreviations: AAV – adeno-associated virus, amp – ampicillin, CMV – cytomegalovirus, cPPT – central polypurine tract, eGFP – enhanced green fluorescent protein, GDNF – glial cell linederived neurotrophic factor, LTR – long terminal repeat, LV – lentivirus, PGK – 3- phosphoglycerate kinase, poly-A – polyadenylation signal, RRE – Rev responsive element, SIN – self-inactivating, TR – terminal repeat, WHV – Woodchuck hepatitis virus, WT – wild type. The maps were Produced by PlasMapper version 2.0

Map of the LV-PLS3



Map of the AAV-PLS3



Appendix 3: Sequence.**PLS3 INSERT**

GCCACCATGGATGAGATGGCTACCACTCAGATTTCCAAAGATGAGCTTGATGAACTCAAAGAGGCCTT
 TGCAAAAGTTGATCTCAACAGCAACGGATTCATTTGTGACTATGAACTTCATGAGCTCTTCAAGGAAG
 CTAATATGCCATTACCAGGATATAAAGTGAGAGAAATTTATTCAGAAACTCATGCTGGATGGTGACAGG
 AATAAAGATGGGAAAATAAGTTTTGACGAATTTGTTTATATTTTTCAAGAGGTAAAAAGTAGTGATAT
 TGCCAAGACCTTCCGCAAAGCAATCAACAGGAAAGAAGGTATTTGTGCTCTGGGTGGAACCTCAGAGT
 TGTCCAGCGAAGGAACACAGCATTCTTACTCAGAGGAAGAAAAATATGCTTTTTGTTAACTGGATAAAC
 AAAGCTTTGGAAAATGATCCTGATTGTAGACATGTTATACCAATGAACCTAACACCGATGACCTGTT
 CAAAGCTGTTGGTGATGGAATTGTGCTTTGTAATAATGATTAACCTTTCAGTTCCTGATACCATTGATG
 AAAGAGCAATCAACAAGAAGAAACTTACACCTTCATCATTGAGAAAACCTTGAACCTGGCAGTGAAC
 TCTGCTTCTGCCATTGGGTGTGATGTTGTGAACATTGGTGCAGAAGATTTGAGGGCTGGGAAACCTCA
 TCTGGTTTTGGGACTGCTTTGGCAGATCATTAAAGATCGGTTTTGTTGCTGACATTTGAATTAAGCAGGA
 ATGAAGCCTTGGCTGCTTTACTCCGAGATGGTGAGACTTTGGAGGAACTTATGAAATTTGCTCCAGAA
 GAGCTTCTGCTTAGATGGGCAAACCTTTCATTTGGAAAACCTCGGGCTGGCAAAAAATTAACAACCTTAG
 TGCTGACATCAAGGATTCCAAAGCCTATTTCCATCTTCTCAATCAAAATCGCACCAAAAGGACAAAAGG
 AAGGTGAACCACGGATAGATATTAACATGTCAGGTTTCAATGAAACAGATGATTTGAAGAGAGCTGAG
 AGTATGCTTCAACAAGCAGATAAATTAGGTTGCAGACAGTTTGTACCCCTGCTGATGTTGTCAGTGG
 AAACCCCAAACCTCAACTTAGCTTTCTGCTGCTAACCTGTTTAAATAAATACCCAGCACTAACTAAGCCAG
 AGAACCCAGGATATTGACTGGACTCTATTAGAGGAGAAACTCGTGAAGAAAGAACCTTCCGTAACCTGG
 ATGAACTCTCTGGTGTCAATCCTCACGTAAACCATCTCTATGCTGACCTGCAAGATGCCCTGGTAAT
 CTTACAGTTATATGAACGAATTAAGTTTCTGTTGACTGGAGTAAGGTTAATAAACTCCATACCCGA
 AACTGGGAGCCAACATGAAAAAGCTAGAAAACCTGCAACTATGCTGTTGAATTAGGGAAGCATCCTGCT
 AAATTCTCCCTGGTTGGCATTGGAGGGCAAGACCTGAATGATGGGAACCAACCTGACTTTAGCTTT
 AGTCTGGCAGCTGATGAGAAGATATACCCTCAATGTCTGGAAGATCTTGGAGATGGTCAGAAAGCCA
 ATGACGACATCATTGTGAACCTGGGTGAACAGAACGTTGAGTGAAGCTGGAAAATCAACTTCCATTGAG
 AGTTTTAAGGACAAGACGATCAGCTCCAGTTTGGCAGTTGTGGATTTAATTGATGCCATCCAGCCAGG
 CTGTATAAACTATGACCTTGTGAAGAGTGGCAATCTAACAGAAGATGACAAGCACAATAATGCCAAGT
 ATGCAAGTGTCAATGGCTAGAAGAATCGGAGCCAGAGTGTATGCTCTCCCTGAGACCTTGTGGAAGTA
 AAGCCCAAGATGGTCATGACTGTGTTTTGCATGTTTTGATGGGCAGGGGAATGAAGAGAGTGTAA

SIN-PGK-cPPT-GDNF-WHV

TGGAAGGGCTAATTCACCTCCCAAAGAAGACAAGATATCCTTGATCTGTGGATCTACCACACACAAGGC
 TACTTCCCTGATTAGCAGAACTACACACCAGGGCCAGGGGTGAGATATCCACTGACCTTTGGATGGTG
 CTACAAGCTAGTACCAGTTGAGCCAGATAAGGTAGAAGAGGGCCAATAAAGGAGAGAACCACAGCTTGT
 TACACCCTGTGAGCCTGCATGGGATGGATGACCCGGAGAGAGAAGTGTAGAGTGGAGGTTTTGACAGC
 CGCCTAGCATTTTCATCACGTGGCCCGAGAGCTGCATCCGGAGTACTTCAAGAACTGCTGATATCGAGC
 TTGCTACAAGGGACTTTCCGCTGGGGACTTTCCAGGGAGCGGTGGCCTGGGCGGGACTGGGGAGTGGC
 GAGCCCTCAGATCCTGCATATAAGCAGCTGCTTTTTGCTTACTGGGTCTCTCTGTTAGACCAGAT
 CTGAGCCTGGGAGCTCTCTGGCTAACTAGGGAACCCACTGCTTAAGCCTCAATAAAGCTTGCCTTGAG
 TGCTTCAAGTAGTGTGTGCCCGTCTGTTGTGTGACTCTGGTAACTAGAGATCCCTCAGACCCTTTTAG
 TCAGTGTGGAATACTCTAGCAGTGGCGCCGAACAGGGACCTGAAAAGCGAAAAGGAAACCAGAGCTC
 TCTCGACGCAGGACTCGGCTTGTGTAAGCGCGCACGGCAAGAGGCGAGGGGCGGCGACTGGTGAGT
 ACGCCAAAATTTTACTAGCGGAGGCTAGAAGGAGAGAGATGGGTGCGAGAGCGTCAGTATTAAGCG
 GGGGAGAATTAGATCGCGATGGGAAAAAATTCGGTTAAGGCCAGGGGAAAAGAAAAATATAAATTA
 AACATATAGTATGGGCAAGCAGGGAGCTAGAACGATTCGCAGTTAATCCTGGCCTGTTAGAAAACATCA
 GAAGGCTGTAGACAAATACTGGGACAGCTACAACCATCCCTTCAGACAGGATCAGAAGAATTTAGATC
 ATTATATAATACAGTAGCAACCTCTATTGTGTGCATCAAAGGATAGAGATAAAGACACCAAGGAAG
 CTTTAGACAAGATAGAGGAAGAGCAAAAACAAAAGTAAGACCACCGCACAGCAAGCGGCCGCTGATCTT
 CAGACCTGGAGGAGGAGATATGAGGGACAATTTGGAGAAGTGAATTTATATAAATATAAAGTAGTAAAA
 TTGAACCATTAGGAGTAGCACCCACCAAGGCAAAAGAGAAGAGTGGTGCAGAGAGAAAAAGAGCAGTG
 GGAATAGGAGCTTTGTTCCCTTGGGTTCTTGGGAGCAGCAGGAAGCACTATGGGCGCAGCCTCAATGAC
 GCTGACGGTACAGGCCAGACAATTATTGTCTGGTATAGTGCAGCAGCAGAACAATTTGCTGAGGGCTA
 TTGAGGCGCAACAGCATCTGTTGCAACTCACAGTCTGGGGCATCAAGCAGCTCCAGGCAAGAATCCTG
 CTGTGGAAGATAACCTAAAGGATCAACAGCTCCTGGGGATTTGGGGTGTCTTGAAAACTCATTTG

CACCACTGCTGTGCCTTGGAAATGCTAGTTGGAGTAATAAATCTCTGGAACAGATTGGAATCACACGAC
CTGGATGGAGTGGGACAGAGAAATTAACAATTACACAAGCTTAATACTCCTTAATTGAAGAATCGC
AAAACCAGCAAGAAAAGAATGAACAAGAATTATTGGAATTAGATAAATGGGCAAGTTTGTGGAATTGG
TTTAACATAACAAATTGGCTGTGGTATATAAAATTATTCATAATGATAGTAGGAGGCTTGGTAGGTTT
AAGAATAGTTTTTGTCTACTTTCTATAGTGAATAGAGTTAGGCAGGGATATTCACCATTATCGTTTT
AGACCCACCTCCCAACCCCGAGGGGACCCGACAGGCCCGAAGGAATAGAAGAAGAAGGTGGAGAGAGA
GACAGAGACAGATCCATTTCGATTAGTGAACGGATCTCGACGGTATCGGTTAACTTTTAAAAAGAAAAG
GGGGATTGGGGGTACAGTGCAGGGGAAAGAATAGTAGACATAATAGCAACAGACATACAAACATAAAG
AATTACAAAAACAAATTACAAAAATTCAAAATTTTATCGATGGTCGAGTACCGGGTAGGGGAGGCGCT
TTTTCCCAAGGCAGTCTGGAGCATGCGCTTTAGCAGCCCGCTGGGCACCTGGCGCTACACAAGTGGCC
TCTGGCCCTCGCACACATTCCACATCCACCGGTAGGCGCCCAACCGGCTCCGTTCTTTGGTGGCCCTTC
GCGCCACCTTCTACTCCTCCCCTAGTCAGGAAGTTCCCCCCCCGCCCCGAGCTCGCGTCTGTCAGGAC
GTGACAAATGGAAGTAGCACGTCTCACTAGTCTCGTGCAGATGGACAGCACCGCTGAGCAATGGAAGC
GGGTAGGCCTTTGGGGCAGCGCCAATAGCAGCTTTGCTCCTTCGCTTTCTGGGCTCAGAGGCTGGGA
AGGGGTGGGTCCGGGGGCGGGCTCAGGGGCGGGCTCAGGGGCGGGGCGGGCGCCGAAGGTCCCTCCGG
AGGCCCCGGCATTCTGCACGCTTCAAAGCGCACGTCTGCCGCGCTGTTCTCCTCTTCTCATCTCCGG
GCCTTTCGACCTCTAGGATCCCGTCGAGAATTAGCTTCGCCACCATGAAGTTATGGGATGTCGTGGCT
GTCTGCCTGGTGTCTCCACACCGGCTCCGCTTCCCGCTGCCGCGGTAAGAGGCTCCCGAGGC
GCCCCCGGAAGACCGCTCCCTCGGCCGCGCCGCGCGCCCTTCGCGCTGAGCAGTACTCAAATATGC
CAGAGGATTATCCTGATCAGTTTCGATGATGTCATGGATTTTATTCAGCCACCATTAAAAGACTGAAA
AGGTACCAGATAAAACAAATGGCAGTGCTTCCTAGAAGAGAGCGGAATCGGCAGGCTGCAGCTGCCAA
CCCAGAGAATTCAGAGGAAAAGGTTCGGAGAGGCCAGAGGGGCAAAAACCGGGGTGTGTCTTAACTG
CAATACATTTAAATGTCACTGACTTGGGTCTGGGCTATGAAACCAAGGAGGAACTGATTTTTAGGTAC
TGCAGCGGCTCTTGCGATGCAGCTGAGACAACGTACGACAAAATATTGAAAACTTATCCAGAAATAG
AAGGCTGGTGTAGTGACAAAGTAGGGCAGGCATGTTGCAGACCCATCGCTTTGATGATGACCTGTCTGT
TTTTAGATGATAACCTGGTTTACCATATTCTAAGAAAGCATTCGCTAAAAGGTGTGGATGTATCTGA
GGTCAATTCACCGTGGTACCTCTAGAGTCGACCCCGCTGAGGGAAATCCGATAATCAACCTCTGG
ATTACAAAATTTGTGAAAGATTGACTGGTATTCTTAACTATGTTGCTCCTTTACGCTATGTGGATAC
GCTGCTTTAATGCCTTTGTATCATGCTATTGCTTCCCGTATGGCTTTCATTTTCTCCTTCTGTATAA
ATCCTGGTTGCTGTCTCTTTATGAGGAGTTGTGGCCCGTTGTCAGGCAACGTGGCGTGGTGTGCACTG
TGTTTTGCTGACGCAACCCCCACTGGTTGGGGCATTGCCACCACCTGTCAGCTCCTTTCCGGGACTTTC
GCTTTCCCCCTCCCTATTGCCACGGCGGAACCTCATCGCCGCTGCCTTGCCCGCTGCTGGACAGGGG
TCGGCTGTTGGGCACTGACAATTCCGTGGTGTGTCGGGGAAGCTGACGTCCCTTCCATGGCTGCTCG
CCTGTGTTGCCACCTGGATTCTGCGCGGGACGTCTTCTGCTACGTCCCTTCGGCCCTCAATCCAGCG
GACCTTCCCTTCCCGCGGCTGCTGCCGCTCTGCGGCTCTTCCGCGTCTTCGCTTCGCCCTCAGAC
GAGTCGGATCTCCCTTTGGGCCGCTCCCCGCATCGGGAATTCGAGCTCGGTACCTTTAAAACCAATG
ACTTACAAGGCAGCTGTAAATCTTAGCCACTTTTTAAAAGAAAAGGGGGGACTGGAAGGGCTAATTCA
CTCCCAACGAAAACAAAATCTGCTTTTTGCTTGTACTGGGTCTCTCTGGTTAGACCAAATCTGAGCCT
GGGAGCTCTCTGGCTAACTAGGGAACCCACTGCTTAAAGCCTCAATAAAAGCTTGCCCTTGAGTGCTTCAA
GTAGTGTGTGCCGCTCTGTTGTGTGACTCTGGTAACTAGAGATCCCTCAAACCTTTTAGTCAGTGTG
GAAAATCTCTAGCAGCATCTAGAATTAATTCCGTGTATTCTATAGTGTACCTAAATCGTATGTGTAT
GATACATAAGGTTATGTATTAATTGTAGCCGCTTCTAACGACAATATGTACAAGCCTAATTGTGTAG
CATCTGGCTTACTGAAGCAGACCCTATCATCTCTCTCGTAAACTGCCGTCAGAGTCGGTTTGGTTGGA
CGAACCTTTCGAGTTTCTGGTAACGCCGCTCCCGCAGCCGGAATGGTCAGCGAACCAATCAGCAGGGT
CATCGTACTGAGATCCTCTACGCCGGACGATCGTGGCCGGCATCACCGGCGCCACAGGTGCGGTTG
CTGGCGCCTATATCGCCGACATCACCGATGGGGAAGATCGGGCTCGCCACTTCGGGCTCATGAGCGCT
TGTTTTCGGCGTGGGTATGGTGGCAGGCCCCGTGGCCGGGGGACTGTTGGGCGCCATCCTCTGTCATGC
ACCATTCCCTTGCGGCGGCGGTGCTCAACGGCCTCAACCTACTACTGGGCTGCTTCCCTAATGCAGGAGT
CGCATAAGGGAGAGCGTCGATATGGTGCACCTCTCAGTACAATCTGCTCTGATGCCGCATAGTTAAGCC
AGCCCCGACACCCGCCAACACCCGCTGACGCGCCCTGACGGGCTTGTCTGCTCCCGGCATCCGCTTAC
AGACAAGCTGTGACCGTCTCCGGGAGCTGCATGTGTGAGAGGTTTTACCGTCATCACCGAAACGCGC
GAGACGAAAGGGCCTCGTGATACGCTATTTTTATAGGTTAATGTCATGATAATAATGGTTTTCTTAGA
CGTCAGGTGGCACTTTTTCGGGGAATGTGCGCGGAACCCCTATTTGTTTATTTTTCTAAATACATTCA
AATATGTATCCGCTCATGAGACAATAACCCTGATAAATGCTTCAATAATATTGAAAAAGGAAGATAT
GAGTATTC AACATTTCCGTGTCGCCCTTATTCCCTTTTTTTCGGCATTTTGGCTTCCGTTTTTGTCTC
ACCCAGAAACGCTGGTGAAAGTAAAAGATGCTGAAGATCAGTTGGGTGCACGAGTGGGTTACATCGAA
CTGGATCTCAACAGCGGTAAGATCCTTGAGAGTTTTTCGCCCCGAAGAAGCTTTTCCAATGATGAGCAC
TTTTAAAGTTCTGCTATGTGGCGGGTATTATCCCGTATTGACGCCGGGCAAGAGCAACTCGGTCCGC
GCATACACTATTCTCAGAATGACTTGGTTGAGTACTACCAGTACAGAAAAGCATCTTACGGATGGC
ATGACAGTAAGAGAATTATGCAGTGTGCCATAACCATGAGTGATAACACTGCGGCCAACTTACTTCT
GACAACGATCGGAGGACCGAAGGAGCTAACCGCTTTTTTGCACAACATGGGGGATCATGTAACTCGCC

TTGATCGTTGGGAACCGGAGCTGAATGAAGCCATACCAAACGACGAGCGTGACACCACGATGCCTGTA
 GCAATGGCAACAACGTTGCGCAAACCTATTAAGTGGCGAACTACTTACTCTAGCTTCCCAGCAACAATT
 AATAGACTGGATGGAGGCGGATAAAAGTTGCAGGACCCTTCTGCGCTCGGCCCTCCGGCTGGCTGGT
 TTATTGCTGATAAATCTGGAGCCGGTGAGCGTGGGTCTCGCGGTATCATTGCAGCACTGGGGCCAGAT
 GGTAAGCCCTCCCGTATCGTAGTTATCTACACGACGGGGAGTCAGGCAACTATGGATGAACGAAATAG
 ACAGATCGCTGAGATAGGTGCCTCACTGATTAAGCATTGGTAAGTGTGACACCAAGTTTACTCATATA
 TACTTTAGATTGATTTAAACTTCATTTTTAATTTAAAAGGATCTAGGTGAAGATCCTTTTTGATAAT
 CTCATGACCAAAATCCCTTAACGTGAGTTTTCTGTTCCACTGAGCGTCAGACCCCGTAGAAAAGATCAA
 AGGATCTTCTTGAGATCCTTTTTTCTGCGCGTAATCTGCTGCTTGCAAACAAAAAACACCAGCTAC
 CAGCGGTGGTTTTGTTGCGGATCAAGAGCTACCAACTCTTTTTCCGAAAGTAACTGGCTTCAGCAGA
 GCGCAGATACCAAACTACTGTCCTTCTAGTGTAGCCCTAGTTAGGCCACCCTCAAGAATCTGTAGC
 ACCGCCTACATACCTCGCTCTGCTAATCCTGTTACCAGTGGCTGCTGCCAGTGGCGATAAGTCGTGTC
 TTACCGGGTTGGACTCAAGACGATAGTTACCAGGATAAGGCGCAGCGGTCCGGCTGAACGGGGGGTTTCG
 TGCACACAGCCAGCTTGGAGCGAACGACCTACACCGAACTGAGATACCTACAGCGTGAGCTATGAGA
 AAGCGCCACGCTTCCCGAAGGGAGAAAGGCGGACAGGTATCCGGTAAGCGGCAGGGTCCGGAACAGGAG
 AGCGCACGAGGGAGCTTCCAGGGGAAACGCCTGGTATCTTTATAGTCTGTCGGGTTTTCGCCACCTC
 TGACTTGAGCGTCGATTTTTGTGATGCTCGTCAGGGGGCGGAGCCTATGGAAAAACGCCAGCAACGC
 GGCCTTTTTACGGTTCCTGGCCTTTTTGCTGGCCTTTTTGCTCACATGTTCTTTCCTGCGTTATCCCCTG
 ATTCTGTGGATAACCGTATTACCAGCTTTGAGTGTGCTGATACCGCTCGCCGAGCCGAACGACCGAG
 CGCAGCGAGTCAGTGTGAGCGAGGAAGCGGAAGAGCGCCCAATACGCAAACCGCTCTCCCCGCGCGTTG
 GCCGATTCATTAATGCAGCTGTGGAATGTGTGTGAGTTAGGGTGTGGAAAGTCCCCAGGCTCCCCAGC
 AGGCAGAAGTATGCAAAGCATGCATCTCAATTAGTCAGCAACCAGGTGTGGAAAGTCCCCAGGCTCCC
 CAGCAGGCAGAAGTATGCAAAGCATGCATCTCAATTAGTCAGCAACCATAGTCCCCCCCCTAACCTCCG
 CCCATCCCCCCCCTAACCTCCGCCAGTTCCGCCCATTTCTCCGCCCATGGCTGACTAATTTTTTTTTAT
 TTATGCAGAGGCCGAGGCCGCTCGGCCTCTGAGCTATTCAGAAAGTAGTGAGGAGGCTTTTTTGGAG
 GCCTAGGCTTTTTGCAAAAAGCTTGGACACAAGACAGGCTTGGGAGATATGTTTGAATAACCACTTA
 TCCCGCGCTCAGGGAGAGGCAGTGCCTAAAAGACGCGGACTCATGTGAAACTGTTTTTAGTGCGC
 CAGATCTCTATAAATCTCGCGCAACCTATTTTCCCCCTCGAACACTTTTTAAGCCGTAGATAAACGCGCT
 GGGACACTTCACATGAGCGAAAAATACATCGTCACCTGGGACATGTTGCAGATCCATGCACGTAAACT
 CGCAAGCCGACTGATGCCTTCTGAACAATGGAAAGGCATTATTGCCGTAAGCCGTGGCGGTCTGTACC
 GGGTGCCTTACTGGCGGTGAACTGGGTATTCGTGATGTCGATACCGTTTGTATTTCCAGCTACGATC
 ACGACAACCAGCGGAGCTTAAAGTGTGAAACGCGCAGAAAGGCGATGGCGAAGGCTTCATCGTTATT
 GATGACCTGGTGGATAACCGTGGTACTGCGGTGCGATTCGTGAAATGTATCCAAAAGCGCACTTTGT
 CACCATCTTCGCAAAACCGGCTGGTCCGCTGGTTGATGACTATGTTGTTGATATCCCGCAAGATA
 CCTGGATTGAACAGCCGTGGGATATGGGCGTCTGATTCGTCCCGCAATCTCCGTCGCTAATCTTTT
 CAACGCCTGGCACTGCCGGCGTTGTTCTTTTTAACTTCAGGCGGTTACAATAGTTTCCAGTAAGTA
 TTCTGGAGGCTGCATCCATGACACAGGCAAACCTGAGCGAAACCTGTTCAAACCCGCTTTAAACAT
 CCTGAAACCTCGACGCTAGTCCGCCGCTTTAATCACGGCGCACAAACCGCTGTGCAGTCGGCCCTTGA
 TGGTAAAACCATCCCTCACTGGTATCGCATGATTAACCGTCTGATGTGGATCTGGCGCGGCATTGACC
 CACGCGAAATCCTCGACGTCCAGGCACGTATTGTGATGAGCGATGCCGAACGTACCGACGATGATTTA
 TACGATACGGTGATTGGCTACCGTGGCGGCAACTGGATTTATGAGTGGGCCCGGATCTTTGTGAAGG
 AACCTTACTTCTGTGGTGTGACATAATTGGACAAACTACCTACAGAGATTTAAAGCTCTAAGGTAAT
 ATAAAATTTTTAAGTGTATAATGTGTTAACTACTGATTCATATGTTTGTGATTTTTAGATTCCAAC
 CTATGGAAGTGTGAATGGGAGCAGTGGTGAATGCCTTTAATGAGGAAAACCTGTTTTGCTCAGAAG
 AAATGCCATCTAGTGATGATGAGGCTACTGCTGACTCTCAACATTTACTCTCCAAAAAAGAAGAGA
 AAGGTAGAAGACCCCAAGGACTTTCCTTCAGAATTGCTAAGTTTTTTGAGTCATGCTGTGTTTAGTAA
 TAGAACTCTTGCTTGCTTTGCTATTTACACCACAAAGGAAAAAGCTGCACTGCTATACAAGAAAAATTA
 TGGAAAAATATTCTGTAACCTTTATAAGTAGGCATAACAGTTTATAATCATAACATACTGTTTTTTCTT
 ACTCCACACAGGCATAGAGTGTCTGCTATTAATAACTATGCTCAAAAAATTTGTGTAACCTTTAGCTTTTT
 AATTTGTAAAGGGTTAATAAGGAATATTTGATGTATAGTGCTTACTAGAGATCATAATCAGCCAT
 ACCACATTTGTAGAGCTTTTACTTGTCTTTAAAAAACCTCCACACCTCCCCCTGAACCTGAAACATAA
 AATGAATGCAATTGTTGTTGTTAACTTGTATTGTCAGCTTATAATGGTTACAAAATAAGCAATAGCA
 TCACAAATTTACAAATAAAGCATTTTTTTTCACTGCATTCCTAGTTGTGGTTTTGTCCAACTCATCAAT
 GTATCTTATCATGTGTGGATCAACTGGATAACTCAAGCTAACCAAAATCATCCAACTTCCCACCCC
 ATACCCTATTACCCTGCCAAATTAACCTGTGGTTTTCAATTTACTCTAAACCTGTGATTCTCTGAATTA
 TTTTCATTTTTAAAGAAATTGTATTTGTTAAATATGTACTACAACTTAGTAGT

SIN-PGK-Cppt-PLS3-WHV

TGGAAGGGCTAATTCACCTCCCAAAGAAGACAAGATATCCTTGATCTGTGGATCTACCACACACAAGGC
TACTTCCCTGATTAGCAGAACTACACACCAGGGCCAGGGGTGAGATATCCACTGACCTTTGGATGGTG
CTACAAGCTAGTACCAGTTGAGCCAGATAAGGTAGAAGAGGGCCAATAAAGGAGAGAACACCAGCTTGT
TACACCCTGTGAGCCTGCATGGGATGGATGACCCGGAGAGAGAAGTGTAGAGTGGAGTTTACAGC
CGCCTAGCATTTTCATCACGTGGCCCCGAGAGCTGCATCCGGAGTACTTCAAGAAGTGTGATATCGAGC
TTGCTACAAGGGACTTTCCGCTGGGGACTTTCCAGGGAGGCGTGGCTGGGCGGGACTGGGGAGTGGC
GAGCCCTCAGATCCTGCATATAAGCAGCTGCTTTTTGCTGTACTGGGTCTCTCTGGTTAGACCAGAT
CTGAGCCTGGGAGCTCTCTGGCTAACTAGGGAACCCACTGCTTAAGCCTCAATAAAGCTTGCCCTGAG
TGCTTCAAGTAGTGTGTGCCCGTCTGTTGTGTGACTCTGGTAAGTACAGATCCCTCAGACCCTTTTAG
TCAGTGTGGAAAATCTCTAGCAGTGGCGCCCCGAACAGGGACCTGAAAAGCGAAAAGGGAAACCAGAGCTC
TCTCGACGCAGGACTCGGCTTGTGAAAGCGCGCACGGCAAGAGGCGAGGGGGCGGCGACTGGTGAGT
ACGCCAAAAATTTGACTAGCGGAGGCTAGAAGGAGAGAGATGGGTGCGAGAGCGTCAGTATTAAGCG
GGGGAGAATTAGATCGCGATGGGAAAAAATTCGGTTAAGGCCAGGGGGAAAAGAAAAAATAAAATTA
AACATATAGTATGGGCAAGCAGGGAGCTAGAACGATTCGCAGTTAATCCTGGCCTGTTAGAAAACATCA
GAAGGCTGTAGACAAATACTGGGACAGCTACAACCATCCCTCAGACAGGATCAGAAGAAGCTTAGATC
ATTATATAATACAGTAGCAACCCCTCTATTGTGTGCATCAAAGGATAGAGATAAAGACACCAAGGAAG
CTTTAGACAAGATAGAGGAAGAGCAAAAACAAAAGTAAGACCACCGCACAGCAAGCGCCGCTGATCTT
CAGACCTGGAGGAGGAGATATGAGGGACAATTGGAGAAGTGAATTATATAAAATATAAAGTAGTAAAA
TTGAACCATTAGGAGTAGCACCCACCAAGGCAAAAGAGAAGAGTGGTGCAGAGAGAAAAAAGAGCAGTG
GGAATAGGAGCTTTGTTCCCTTGGGTTCTTGGGAGCAGCAGGAAGCACTATGGGCGCAGCCTCAATGAC
GCTGACGGTACAGGCCAGACAATTATTGTCTGGTATAGTGCAGCAGCAGAACAATTTGCTGAGGGCTA
TTGAGGCGCAACAGCATCTGTTGCAACTCACAGTCTGGGGCATCAAGCAGCTCCAGGCAAGAATCCTG
GCTGTGGAAAGATAACCTAAAGGATCAACAGCTCCTGGGGATTTGGGGTTGCTCTGAAAACTCATTTG
CACCCTGCTGTGCCCTTGGAAATGCTAGTTGGAGTAATAAATCTCTGGAACAGATTGGAATCACACGAC
CTGGATGGAGTGGGACAGAGAAATTAACAATTACACAAGCTTAATACACTCCTTAATTGAAGAATCGC
AAAACCAGCAAGAAAAGAATGAACAAGAATTATTGGAATTAGATAAATGGGCAAGTTTGTGGAATTGG
TTTTAACATAACAAATTTGGCTGTGGTATATAAAATTTATTCATAATGATAGTAGGAGGCTTGGTAGGTTT
AGAATAGTTTTTGTCTACTTTCTATAGTGAATAGAGTTAGGCAGGGATATTCACCATTATCGTTTTC
AGACCCACCTCCCAACCCCGAGGGGACCCGACAGGCCCGAAGGAATAGAAGAAGAAGGTGGAGAGAGA
GACAGAGACAGATCCATTTCGATTAGTGAACGGATCTCGACGGTATCGGTTAATTTTAAAAGAAAAGG
GGGATTTGGGGGTACAGTGCAGGGGAAAAGAATAGTAGACATAATAGCAACAGACATACAACTAAAG
AATTACAAAACAAATTACAAAATTTCAAATTTTATCGATGGTGCAGTACCGGGTAGGGGAGGCGCT
TTTTCCAAAGCAGTCTGGAGCATGCGCTTTAGCAGCCCGCTGGGCACTTGGCGCTACACAAGTGGCC
TCTGGCCTCGCACACATTTCCACATCCACCGTAGGCTAGGCGCCAAACCGGCTCCGTTCTTTGGTGGCCCTTC
GCGCCACCTTCTACTCCTCCCCTAGTCAGGAAGTTCCCCCGCCCCGACGCTCGCGTCTGTCAGGAC
GTGACAAATGGAAGTAGCACGTCTCACTAGTCTCGTGCAGATGGACAGCACCGCTGAGCAATGGAAGC
GGGTAGGCCTTTGGGGCAGCGCCAATAGCAGCTTTGCTCCTTCGCTTTCTGGGCTCAGAGGCTGGGA
AGGGGTGGGTCCGGGGGCGGGCTCAGGGGCGGGCTCAGGGGCGGGGCGGGCGCCGAAGGTCCCTCCGG
AGGCCCGGCAATTCTGCACGCTTCAAAGCGCACGTCTGCCGCGCTGTTCTCCTCTTCTCATCTCCGG
GCCTTTTCGACCTCTAGGATCCACTAGTCCAGTGTGGTGAATTTGCCCTTGAGGTGCAGAAGTTGTCTG
AGTGCCTTGGTTCGGCGGCAGTCCGGCCAGACCCAGGACTCTGCGACTTTACATCTTTAAATGGATGAG
ATGGCTACCACTCAGATTTCCAAAGATGAGCTTGTGAACTCAAAGAGGCTTTGCAAAAAGTTGATCT
CAACAGCAACGGATTCATTTGTGACTATGAACTTCATGAGCTCTTCAAGGAAGCTAATATGCCATTAC
CAGGATATAAAGTGAGAGAAATTTATTCAGAACTCATGCTGGATGGTGACAGGAATAAAGATGGGAAA
ATAAGTTTTGACGAATTTGTTTATATTTTTCAAGAGGTAAGAAAGTAGTGATATTGCCAAGACCTTCCG
CAAAGCAATCAACAGGAAAGAAGGTATTTGTGCTCTGGGTGGAACCTCAGAGTTGTCCAGCGAAGGAA
CACAGCATTCTTACTCAGAGGAAGAAAAATATGCTTTTGTAACTGGATAAAACAAAGCTTTGGAAAAT
GATCCTGATTGTAGACATGTTATAACCAATGAACCTAACACCGATGACCTGTTCAAAGCTGTTGGTGA
TGGAATTGTGCTTTGTAAAATGATTAACCTTTCACTTCTGATACCATTTGATGAAAGAGCAATCAACA
AGAAGAACTTACACCCCTTCACTATTACAGGAAACTTGAACCTTGGCACTGAACTCTGCTTCTGCCATT
GGGTGTCATGTTGTGAACATTGGTGCAGAAGATTTGAGGGCTGGGAAACCTCATCTGTTTGGGACT
GCTTTGGCAGATCATTAAGATCGGTTTTGTTGCTGACATTGAATTAAGCAGGAATGAAGCCTTGGCTG
CTTTACTCCGAGATGGTGAGACTTTGGAGGAACTTATGAAAATGTCTCCAGAAGAGCTTCTGCTTAGA
TGGGCAAACTTTTCAATTTGGAAAACCTCGGGCTGGCAAAAAATTAACAACCTTTAGTGCTGACATCAAGGA
TTCCAAAGCCTATTTCCATCTTCTCAATCAAATCGCACAAAAGGACAAAAGGAAGGTGAACCACGGA
TAGATATTAACATGTGAGGTTTCAATGAAACAGATGATTTGAAGAGAGCTGAGAGTATGCTTCAACAA
GCAGATAAATTAGGTTGCAGACAGTTTGTACCCTGCTGATGTTGTGCTGAGTGAACCCCAAACTCAA
CTTAGCTTTTCGTGGCTAACCTGTTTAATAAATACCCAGCACTAACTAAGCCAGAGAACCAGGATATTG
ACTGGACTCTATTAGAAGGAGAACTCGTGAAGAAAGAACCTTCCGTAAGTGGATGAACTCTCTTGGT

GTCAATCCTCACGTAAACCATCTCTATGCTGACCTGCAAGATGCCCTGGTAATCTTACAGTTATATGA
ACGAATTAAGTTCCTGTTGACTGGAGTAAGGTTAATAAACCTCCATACCCGAACTGGGAGCCAACA
TGAAAAAGCTAGAAAAGTCAACTATGCTGTTGAATTAGGGAAGCATCCTGCTAAATTTCTCCCTGGTT
GGCATTGGAGGGCAAGACCTGAATGATGGGAACCAACCTGACTTTAGCTTTAGTCTGGCAGCTGAT
GAGAAGATATACCCTCAATGTCTGGAAGATCTTGGAGATGGTCAGAAAAGCCAATGACGACATCATTG
TGAAGTGGGTGAACAGAAGCTTGGAGTGAAGCTGGAAAAATCAACTTCCATTCAGAGTTTTAAGGACAAG
ACGATCAGCTCCAGTTTGGCAGTTGTGGATTTAATTGATGCCATCCAGCCAGGCTGTATAAACATATGA
CCTTGTGAAGAGTGGCAATCTAACAGAAGATGACAAGCACAATAATGCCAAGTATGCAGTGTCAATGG
CTAGAAGAATCGGAGCCAGAGTGTATGCTCTCCCTGAAGACCTTGTGGAAGTAAAGCCCAAGATGGTC
ATGACTGTGTTTGCATGTTTGGATGGGCAGGGGAATGAAGAGAGTGTAAAGGGCAATTTCTGCAGATAATCC
AGCACAGTGGCGGGCCGCTCGAGGGAAATCCGATAATCAACCTCTGGATTACAAAATTTGTGAAAAGATT
GACTGGTATTCTTAAGTATGTTGCTCCTTTTACGCTATGTGGATACGCTGCTTTAATGCCCTTTGTATC
ATGCTATTGCTTCCCGTATGGCTTTTCAATTTTCTCCTCCTTGTATAAAATCCTGGTTGCTGTCTTTTAT
GAGGAGTTGTGGCCCGTTGTGACGCAACGTGGCGTGGTGTGCACTGTGTTTGTGACGCAACCCCCAC
TGGTTGGGGCATTGCCACCACCTGTGAGCTCCTTTCCGGGACTTTGCTTTCCCCCTCCCTATTGCCA
CGGCGGAACCTCATCGCCGCTGCCTTGCCGCTGCTGGACAGGGGCTCGGCTGTTGGGCACGTACAAT
TCCGTGGTGTGTCGGGGAAGCTGACGTCCTTTCCATGGCTGCTCGCCTGTGTTGCCACCTGGATTCT
GCGCGGGACGTCCTTCTGCTACGTCCTTCCGGCCCTCAATCCAGCGGACCTTCTTCCCGCGCCTGC
TGCCGGCTCTGCGGCCTCTTCCGCGTCTTCCGCTTCCGCTCAGACGAGTCGGATCTCCCTTTGGGCC
GCCTCCCCGCATCGGGAATTCGAGCTCGGTACCTTTAAAACCAATGACTTACAAGGCAGCTGTAAATC
TTAGCCACTTTTTTAAAAGAAAAGGGGGGACTGGAAGGGCTAATTCACTCCCAACGAAAACAAAATCTG
CTTTTTGCTTGTACTGGGTCTCTCTGGTTAGACCAAAATCTGAGCCTGGGAGCTCTCTGGCTAACTAGG
GAACCCACTGCTTAAAGCCTCAATAAAGCTTGCCCTTGGAGTGTCAAGTAGTGTGTGCCCGTCTGTTGT
GTGACTCTGGTAACTAGAGATCCCTCAAACCTTTTAGTCAGTGTGGAATAATCTTAGCAGCATCTAG
AATTAATTCGGTGTATTCTATAGTGTACCTAAATCGTATGTGTATGATACATAAGGTTATGTATTA
TTGTAGCCGCGTTCTAACGACAATATGTACAAGCCTAATTTGTGTAGCATCTGGCTTACTGAAGCAGAC
CCTATCATCTCTCTGTAACCTGCGCTCAGAGTCGGTTCGGTTTGGTTGGACGAACCTTCTGAGTTTCTGGTA
ACCCCGTCCCGCACCCGGAATGGTCAGCGAACCAATCAGCAGGGTTCATCGTAGCCAGTCCCTCTAC
GCCGGACGCATCGTGGCCGGCATCACCGGCGCCACAGGTGCGGTTGCTGGGCGCTATATCGCCGACAT
CACCGATGGGGAAGATCGGGCTCGCCACTTCCGGCTCATGAGCGCTTGTTCGGCGTGGGTATGGTGG
CAGGCCCCGTGGCCGGGGGACTGTTGGGCGCCATCTCCTTGCATGCACCATTCCCTTGGCGCGGGTG
CTCAACGGCCTCAACCTACTACTGGGCTGCTTCCCTAATGCAGGAGTCGCATAAGGGAGAGCGTCGATA
TGGTGCACCTCTCAGTACAATCTGCTCTGATGCCGCATAGTTAAGCCAGCCCCGACACCCGCCAACACC
CGCTGACGCGCCCTGACGGGCTTGTCTGCTCCCGCATCCGCTTACAGACAAGCTGTGACCGTCTCCG
GGAGCTGCATGTGTGACAGGTTTTACCGTGCATCACCGAAACGCGGAGACGAAAGGGCCTCGTGATA
CGCCTATTTTTATAGGTTAATGTGCATGATAATAATGGTTTCTTAGACGTCAGGTGGCACTTTTCCGGG
AAATGTGCGCGGAACCCCTATTTGTTTTATTTTTCTAAATACATTCAAATATGTATCCGCTCATGAGAC
AATAACCCCTGATAAATGCTTCAATAATATTGAAAAAGGAAGAGTATGAGTATTCACATTTCCGTGTC
GCCCTTATTTCCCTTTTTTTCGGCATTTTTGCTTCCCTGTTTTTGTCTCACCCAGAAACGCTGGTGAAGT
AAAAGATGCTGAAGATCAGTTGGGTGCACGAGTGGGTTACATCGAACTGGATCTCAACAGCGGTAAGA
TCCTTGAGAGTTTTTCGCCCCGAAGAAGCTTTTCCAATGATGAGCACTTTTAAAGTTCTGCTATGTGGC
GCGGTATTATCCCGTATTGACGCCGGGCAAGAGCAACTCGGTGCGCCGATACACTATTCTCAGAATGA
CTTGGTTGAGTACTACCCAGTACAGAAAAGCATCTTACGGATGGCATGACAGTAAGAGAATTTATGCA
GTGCTGCCATAACCATGAGTGAACACTGCGGCCAACTTACTTCTGACAACGATCGGAGGACCGAAG
GAGCTAAACCGCTTTTTTGCACAACATGGGGGATCATGTAACCTGCCTTGATCGTTGGGAACCGGAGCT
GAATGAAGCCATAACCAACGACGAGCGTGACACCACGATGCCGTGAGCAATGGCAACAACGTTGGCCA
AACTATTAAGTGGCGAACTACTTACTCTAGCTTCCCGGCAACAATTAATAGACTGGATGGAGCGGAT
AAAGTTGACAGGACCACTTCTGCGCTCGGCCCTTCCGGCTGGCTGGTTTATTGCTGATAAAATCTGGAGC
CGGTGAGCGTGGGTCTCGCGGTATCATTGCAGCACTGGGGCCAGATGGTAAGCCCTCCCGTATCGTAG
TTATCTACACGACGGGAGTCAAGCAACTATGGATGAACGAAATAGACAGATCGCTGAGATAGGTGCC
TCACTGATTAAGCATTGGTAACTGTGACACCAAGTTTACTCATATATACTTTAGATTGATTTAAACT
TCATTTTTTAATTTAAAAGGATCTAGGTGAAGATCCTTTTTGATAATCTCATGACCAAAATCCCTTAA
GTGAGTTTTTCGTTCCACTGAGCGTCAAGCCCGTAGAAAAGATCAAAGGATCTTCTTGAGATCCTTTT
TTTCTGCGCGTAATCTGCTGCTTGCACCAAAAAAACCACCGCTACCAGCGGTGGTTTTGTTTGGCGGA
TCAAGAGCTACCAACTCTTTTTCCGAAGGTAAGTGGCTTACAGCAGAGCGAGATACCAAAATCTGTCC
TTCTAGTGTAGCCGTAGTTAGGCCACCACTTCAAGAACTCTGTAGCACCCGCTACATACCTCGCTCTG
CTAATCCTGTTACCAGTGGCTGCTGCCAGTGGCGATAAGTCGTGTCTTACCGGGTTGGACTCAAGACG
ATAGTTACCGGATAAGGGCGCAGCGGTGGGCTGAACGGGGGGTTCGTGCACACAGCCAGCTTGGAGC
GAACGACCTACACCGAACTGAGATACCTACAGCGTGAAGTATGAGAAAAGCGCCACGCTTCCCGAAGGG
AGAAAGGCGGACAGGTATCCGGTAAGCGGCAGGGTCCGAACAGGAGAGCGCACGAGGGAGCTTCCAGG
GGGAAACGCCTGGTATCTTTATAGTCTGTGGGTTTCGCCACCTCTGACTTGGAGTGCATTTTTTGT

GATGCTCGTCAGGGGGGCGGAGCCTATGGAAAAACGCCAGCAACGCGGCCTTTTTACGGTTCCTGGCC
TTTTGCTGGCCCTTTTGTCTACATGTTCTTTCTGCGTTATCCCCTGATTCTGTGGATAACCGTATTAC
CGCCTTTGAGTGAGCTGATACCGCTCGCCGCAGCCGAACGACCGAGCGCAGCGAGTCAAGTGCAGCGAGG
AAGCGGAAGAGCGCCCAATACGCAAACCGCCTCTCCCCGCGCGTTGGCCGATTCAATTAATGCAGCTGT
GGAATGTGTGTAGTTAGGGTGTGGAAAGTCCCCAGGCTCCCCAGCAGGCAGAAAGTATGCAAAGCATG
CATCTCAATTAGTCAGCAACCAGGTGTGGAAAGTCCCCAGGCTCCCCAGCAGGCAGAAAGTATGCAAAG
CATGCATCTCAATTAGTCAGCAACCATAGTCCCGCCCTAACTCCGCCCATCCCGCCCCTAACCCGC
CCAGTTCGCCCATTTCTCCGCCCATGGCTGACTAATTTTTTTTATTTATGCAGAGGCCGAGGCCGCC
TCGGCCTCTGAGCTATTCCAGAAGTAGTGAGGAGGCTTTTTTGGAGGCCTAGGCTTTTGCAAAAAGCT
TGGACACAAGACAGGCTTGCAGATATGTTTGAGAATACCACCTTATCCCGCTCAGGGAGAGGCAGT
CGGTAAAAAGACGCGGACTCATGTGAAATACTGGTTTTTTAGTGCGCCAGATCTCTATAATCTCGCGCA
ACCTATTTTCCCCTCGAACACTTTTTAAGCCGTAGATAAACAGGCTGGGACACTTCACATGAGCGAAA
AATACATCGTCACCTGGGACATGTTGCAGATCCATGCACGTAAACTCGCAAGCCGACTGATGCCTTCT
GAACAATGGAAAGGCATTATTGCCGTAAGCCGTGGCGGTCTGTACCGGGTGC GTTACTGGCGCGTGAA
CTGGGTATTGTCATGTGATACCGTTTGTATTTCCAGCTACGATCACGACAACCAGCGCGAGCTTAA
AGTGCTGAAACGCGCAGAAGGCGATGGCGAAGGCTTCATCGTTATTGATGACCTGGTGGATAACCGGTG
GTACTGCGGTTGCGATTGCGTAAATGTATCCAAAAGCGCACTTTGTCACCATCTTCGCAAAAACCGGCT
GGTCGTCCGCTGGTTGATGACTATGTTGTTGATATCCCGCAAGATACCTGGATTGAACAGCCGTGGGA
TATGGGCGCTCGTATTGTCGCCCAATCTCCGGTCGCTAATCTTTTCAACGCTGGCACTGCCGGGCG
TTGTTCTTTTTAACTTCAGGCGGGTTACAATAGTTTCCAGTAAGTATTCTGGAGGCTGCATCCATGAC
ACAGGCAAACCTGAGCGAAACCTGTTCAAACCCCGCTTTAAACATCCTGAAACCTCGACGCTAGTCC
GCCGCTTTAATCACGGCGCACAACCCGCTGTGCAGTCGGCCCTTGATGGTAAAACCATCCCTCACTGG
TATCGCATGATTAACCGTCTGATGTGGATCTGGCGCGGCATTGACCCACGCGAAAATCCTCGACGTCCA
GGCACGTATTGTGATGAGCGATGCCGAACGTACCGACGATGATTTATACGATACGGTGATTGGCTACC
GTGGCGGCAACTGGATTTATGAGTGGGCCCCGGATCTTTGTGAAGGAACCTTACTTCTGTGGTGTGAC
ATAATTGGACAAAACCTACCTACAGAGATTTAAAGCTCTAAGGTAAATATAAAATTTTTAAGTGTATAAT
GTGTTAAACTACTGATTCTAATTGTTTGTGATTTAGATTCCAACCTATGGAAGTATGAAATGGGAG
CAGTGGTGAATGCCTTTAATGAGGAAAACCTGTTTTGCTCAGAAGAAAATGCCATCTAGTGTATGATGA
GGCTACTGCTGACTCTCAACATTCTACTCCTCCAAAAAAGAAGAGAAAAGGTAGAAGACCCCAAGGACT
TTCTTTCAGAATTGCTAAGTTTTTTGAGTCATGCTGTGTTTTAGTAATAGAACTCTTGCTTGCTTTGCT
ATTTACACCACAAAAGGAAAAAGCTGCACTGCTATACAAGAAAAATATGGAAAAATATCTGTAAACCTT
TATAAGTAGGCATAACAGTTATAATCATAACATACTGTTTTTCTTACTCCACACAGGCATAGAGTGT
CTGCTATTAATAACTATGCTCAAAAATTGTGTACCTTTAGCTTTTTAATTTGTAAAGGGGTTAATAAG
GAATATTTGATGTATAGTGCCTTGACTAGAGATCATAATCAGCCATAACCACATTTGTAGAGCTTTTAC
TTGCTTTAAAAAACCTCCCACACCTCCCCCTGAACCTGAAACATAAAAATGAATGCAATTTGTTGTTGTT
AACTTGTTTATTGCGCTTATAATGGTTACAAAATAAAGCAATAGCATCACAAAATTCACAAAATAAAGC
ATTTTTTTTCACTGCATTCTAGTTGTGGTTTTGTCCAAACTCATCAATGTATCTTATCATGTGTGGATCA
ACTGGATAACTCAAGCTAACCAAAAATCATCCCAAACCTTCCCACCCCATACCTATTACCCTGCCAAA
TTACCTGTGGTTTTCAATTTACTCTAAACCTGTGATTCTCTGAATTTATTTTCATTTTAAAGAAATTGTA
TTTGTAAATATGTACTACAACTTAGTAGT

scAAV-CMV-PLS3 (FULL)

AAAGCTTCCCGGGGGATCTGGGCCACTCCCTCTCTGCGGCTCGCTCGCTCACTGAGGCCGGGCGAC
CAAAGGTCGCCCCGACGCCCGGCTTTGCCCGGGCGCCTCAGTGAGCGAGCGAGCGCGCAGAGAGGGA
GTGGCCAACCTCCATCACTAGGGGTTCTGGAGGGGTGGAGTCGTGACCCCTAAAAATGGGCAAACATTG
CGCTAGCGCGGCGCGGTACCTACCGATGTACGGGCCAGATATACGCGTTAGTTATTAATAGTAATCA
ATTACGGGGTCATTAGTTCATAGCCCATATATGGAGTTCCGCGTTACATAAATACGGTAAATGGCCC
GCCTGGCTGACCGCCCAACGACCCCCGCCATTGACGTCAATAATGACGTATGTTCCCATAGTAACGC
CAATAGGGACTTTCCATTGACGTCAATGGGTGGACTATTTACGGTAAACTGCCCACTTGGCAGTACAT
CAAGTGTATCATATGCCAAGTACGCCCCCTATTGACGTCAATGACGGTAAATGGCCCCCTGGCATT
TGCCCAGTACATGACCTTATGGGACTTTCTACTTGGCAGTACATCTACGTATTAGTCAATCGCTATTA
CCATGGGAATTCTGCAGTCGACGGTACCGCGGGCCGGGATCCACCGGTCGCCACCATGGTGGAGCAAG
GGCGAGGAGCTGTTACCGGGGTGGTGCCATCCTGGTCGAGCTGGACGGCGACGTAAACGGCCACAA
GTTACAGCTGTCCGGCGAGGGCGAGGGCATGCCACTACGGCAAGCTGACCTGAAGTTCATCTGCA
CCACCCGCAAGCTGCCCGTCCCTGGCCACCTCGTACCCACCTGACCCCGTGCAGTTCGAGTCTTC
AGCCGCTACCCCGACCACATGAAGCAGCACGACTTCTTCAAGTCCGCCATGCCGAAGGCTACGTTCCA
GGAGCGCACCATCTTCTTCAAGGACGACGGCAACTACAAGACCCGCGCCGAGGTGAAGTTCGAGGGCG
ACACCCTGGTGAACCGCATCGAGCTGAAGGGCATCGACTTCAAGGAGGACGGCAACATCCTGGGGCAC
AAGCTGGAGTACAACATAACAGCCACAACGTCTATATCATGGCCGACAAGCAGAAGAACGGCATCAA

GGTGAACCTTCAAGATCCGCCACAACATCGAGGACGGCAGCGTGCAGCTCGCCGACCACTACCAGCAGA
ACACCCCCATCGGGCGACGGCCCCGTGCTGCTGCCCCGACAACCACTACCTGAGCACCAGTCCGCCCTG
AGCAAAGACCCCAACGAGAAGCGCGATCACATGGTCTGCTGGAGTTCGTGACCGCCGCGGGATCAC
TCTCGGCATGGACGAGCTGTACAAGTAAAGCGGCCGCGACTCTAGAGTCGACCTGCAGGGAAGACCAA
GCTGACCTGACTCGATGCTTTATTTGTGAAATTTGTGATGCTATTGCTTTATTTGTAACCAATTATAAG
CTGCAATAAAACAAGTTAACAACAACAATTGCATTCATTTTATGTTTCAGGTTTCAGGGGGAGGTGTGGG
AGGTTTTTTAAACTAGTCCACTCCCTCTCTGCGCGCTCGCTCGCTCACTGAGGCCGGGGACCAAAGG
TCGCCCCGACGCCCGGGCTTTGCCCGGGCGGCCTCAGTGAGCGAGCGAGCGCGCAGAGAGGGACAGATC
CGGGCCCCGCATGCGTCGACAATTCACTGGCCGTCGTTTTACAACGTCGTGACTGGGAAAACCCCTGGCG
TTACCCCAACTTAATCGCCTTGACGACATCCCCCTTTCGCCAGCTGGCGTAATAGCGAAGAGGCCCGC
ACCGATCGCCCTTCCCAACAGTTGCGCAGCCTGAATGGCGAATGGCGCCTGATGCGGTATTTTCTCCT
TACGCATCTGTGCGGTATTTACACCCGCATATGGTGCACCTCTCAGTACAATCTGCTCTGATGCCGCAT
AGTTAAGCCAGCCCCGACACCCGCCAACACCCGCTGACGCGCCCTGACGGGCTTGCTGCTCCCGGCA
TCCGCTTACAGACAAGCTGTGACCGTCTCCGGGAGCTGCATGTGTGACAGGTTTTCCACCGTCATCACC
GAAACGCGCGAGACGAAAGGGCCTCGTGATACGCTATTTTTATAGGTTAATGTCATGATAATAATGG
TTTTCTTAGACGTCAGGTGGCACTTTTCGGGAAATGTGCGCGGAACCCCTATTTGTTTTATTTTTCTAA
ATACATTCAAATATGTATCCGCTCATGAGACAATAACCCGTATAAATGCTTCAATAATATTGAAAAAG
GAAGAGTATGAGTATTCAACATTTCCGTGTGCGCCTTATTCCCTTTTTTGCGGCATTTCCTTCCTG
TTTTTGTCTACCCAGAAACGCTGGTGAAGTAAAAGATGCTGAAGATCAGTTGGGTGCACGAGTGGGT
TACATCGAAGTGGATCTCAACAGCGGTAAGATCCTTGAGAGTTTTCGCCCCGAAGAACGTTTTCCAAT
GATGAGCACTTTTTAAAGTTCTGCTATGTGGCGCGGTATTATCCCGTATTGACGCCGGGCAAGAGCAAC
TCGGTTCGCCGCATACACTATTCTCAGAATGACTTGGTTGAGTACTCACCAGTCACAGAAAAGCATCTT
ACGGATGGCATGACAGTAAGAGAATTATGCAGTGTGCCATAACCATGAGTGATAACACTGCGGCCAA
CTTACTTCTGACAACGATCGGAGGACCGAAGGAGCTAACCCTTTTTTGACAACATGGGGGATCATG
TAACTCGCCTTGATCGTTGGGAACCGGAGCTGAATGAAGCCATAACAAACGACGAGCGTGACACCACG
ATGCCTGTAGCAATGGCAACAACGTTGCGCAAATTAACCTGCGGAACTACTTACTCTAGCTTCCCG
GCAACAATTAAGACTGGATGGAGCGGATAAGTTGACAGGACCACTTCTGCGCTCGGCCCTTCCCG
CTGCTGGTTTTATTGCTGATAAATCTGGAGCCGGTGAGCGTGGGTCTCGCGTATCATTCAGCAGCATG
GGGCCAGATGGTAAGCCCTCCCGTATCGTAGTTATCTACACGACGGGGAGTCAGGCAACTATGGATGA
ACGAAATAGACAGATCGCTGAGATAGGTGCCTCACTGATTAAGCATTGGTAACGTGACAGCCAAGTTT
ACTCATATATACTTTAGATTGATTTAAAACCTTCATTTTTTAATTTAAAAGGATCTAGGTGAAGATCCTT
TTTGATAATCTCATGACAAAATCCCTTAACGTGAGTTTTTCGTTCCACTGAGCGTCAGACCCCGTAGA
AAAGATCAAAGGATCTTCTTGAGATCCTTTTTTCTGCGGTAATCTGCTGCTTGCAAAACAAAAAAC
CACCGCTACCAGCGGTGGTTTTGTTTCCCGGATCAAGAGCTACCAACTCTTTTTCCGAAGGTAACGGC
TTCAGCAGAGCGCAGATAACAAATACTGTTCTTCTAGTGTAGCCGTAGTTAGGCCACCCTTCAAGAA
CTCTGTAGCACCGCTACATACTCGCTCTGCTAATCCTGTTACCAGTGGCTGCTGCCAGTGGCGATA
AGTCGTGTCTTACCGGGTTGGACTCAAGACGATAGTTACCGGATAAGGCGCAGCGGTGGGCTGAACG
GGGGTTTCGTGCACACAGCCCAGCTTGGAGCGAACGACCTACACCGAACTGAGATACCTACAGCGTGA
GCTATGAGAAAGCGCCACGCTTCCCGAAGGGAGAAAAGGCGGACAGGTATCCGGTAAGCGGCAGGGTCCG
GAACAGGAGAGCGCACGAGGGAGCTTCCAGGGGGAAACGCTGGTATCTTTATAGTCTGTCGGGTTTT
CGCCACCTCTGACTTGAGCGTCGATTTTTGTGATGCTCGTCAGGGGGGCGGAGCCTATGGAAAAACGC
CAGCAACGCGGCCTTTTTACGGTTCCCTGGCCTTTTGTGTCGCTTTTGTGCTCATATGTTCTTTCTGCGT
TATCCCCTGATTCTGTGGATAACCGTATTACCGCCTTTGAGTGAGCTGATACCGCTCGCCGACGCCGA
ACGACCGAGCGCAGCGAGTCAGTGAGCGAGGAAGCGGAAGAGCGCCCAATACGCAAACCGCCTCTCCC
CGCCGTTGGCCGATTCAATTAATGCAGCTGGCACGACAGGTTTTCCCGACTGGAAAGCGGGCAGTGAGC
GCAACGCAATTAATGTGAGTTAGTCACTCATTAGGCACCCAGGCTTACACTTTATGCTTCCGGCT
CGTATGTTGTGGAATTGTGAGCGGATAACAATTTACACAGGAAACAGCTATGACCATGATTACGC
CAAGCTCTCGAGATCTAG

scAAV-CMV-PLS3

AAAGCTTCCCGGGGGATCTGGGCCACTCCCTCTCTGCGCGCTCGCTCGCTCACTGAGGCCGGGCGAC
 CAAAGGTCGCCCCGACGCCCGGGCTTTGCCCGGGCGGCCTCAGTGAGCGAGCGAGCGCGCAGAGAGGGA
 GTGGCCAACCTCCATCACTAGGGGTTCTGGAGGGGTGGAGTCGTGACCCCTAAAAATGGGCAAACATTG
 CGCTAGCGCGGGCCGCGGTACCTACCGATGTACGGGCCAGATATACGCGTTGACATTGATTATTGACTA
 GTTATTAATAGTAATCAATTACGGGGTCATTAGTTCATAGCCCATATATGGAGTTCGCGTTACATAA
 CTTACGGTAAATGGCCCCGCTGGCTGACCGCCCAACGACCCCCGCCATTGACGTCAATAATGACGTA
 TGTTCCCATAGTAACGCCAATAGGGACTTTCCATTGACGTCAATGGGTGGACTATTTACGGTAAACTG
 CCCACTTGGCAGTACATCAAGTGTATCATATGCCAAGTACGCCCCCTATTGACGTCAATGACGGTAAA
 TGGCCCGCTGGCATTATGCCAGTACATGACCTTATGGGACTTTCTACTTGGCAGTACATCTACGT
 ATTAGTCATCGCTATTACCATGGTGATGCGGTTTTGGCAGTACATCAATGGGCGTGGATAGCGGTTTTG
 ACTCACGGGGATTTCCAAGTCTCCACCCCATTTGACGTCAATGGGAGTTTTGTTTTGGCACCAAAATCAA
 CGGGACTTTCCAAAATGTGCTAACAACTCCGCCCCATTGACGCAAAATGGGCGGTAGGCGTGTACGGTG
 GGAGGTCTATATAAGCAGAGCTCTCTGGCTAACTAGAGAACCCTGCTTACTGGCTTATCGAAATTA
 ATACGACTCACTATAGGGAGACCCAAGCTGGCTAGCGTTTAAACTTAAGCTTGGTACCGAGCTCGGAT
 CCACTAGTCCAGTGTGGTGAATTGCCCTTGGAGTGCAGAAGTTGTCTGAGTGCCTTGGTCCGCGGCA
 TCGGGCCAGACCCAGGACTCTGCGACTTTACATCTTTAAATGGATGAGATGGTACCACACTCAGATTT
 CCAAAGATGAGCTTGATGAACTCAAAGAGGCCCTTTGCAAAAAGTTGATCTCAACAGCAACGGATTCATT
 TGTGACTATGAACTTCATGAGCTCTTCAAGGAAGCTAATATGCCATTACCAGGATATAAAGTGAGAGA
 AATTATTTCAGAACTCATGCTGGATGGTGACAGGAATAAAGATGGGAAAAATAAGTTTTGACGAATTTG
 TTTATATTTTTCAAGAGGTAAAAAGTAGTGATATTGCCAAGACCTTCCGCAAAAGCAATCAACAGGAAA
 GAAGGTATTTGTGCTCTGGGTGGAACCTCAGAGTTGTCCAGCGAAGGAACACAGCATTCTTACTCAGA
 GGAAGAAAAATATGCTTTTTGTTAACTGGATAAAACAAAGCTTTGGAAAAATGATCCTGATTGTAGACATG
 TTATACCAATGAACCCTAACACCGATGACCTGTTCAAAGCTGTTGGTGTGGAATTTGTCTTTGTAAA
 ATGATTAACCTTTTCAGTTCCCTGATACCATTGATGAAAGAGCAATCAACAAGAAGAACTTACACCCTT
 CATCATTCAGGAAAACCTTGAACCTGGCACTGAACTCTGCTTCTGCCATTGGGTGTATGTTGTGAACA
 TTGGTGCAGAAGATTTGAGGGCTGGGAAACCTCATCTGGTTTTGGGACTGCTTTGGCAGATCATTAAG
 ATCGGTTTTGTTGCTGACATTGAATTAAGCAGGAATGAAGCCTTGGCTGCTTTACTCCGAGATGGTGA
 GACTTTGGAGGAACCTTATGAAATTTGCTCCAGAAGAGCTTCTGCTTAGATGGGCAAACTTTCAATTTGG
 AAAACTCGGGCTGGCAAAAAATTAACAACCTTTAGTGCTGACATCAAGGATTCCAAAGCCTATTTCCAT
 CTTCTCAATCAAATCGCACCAAAAAGGACAAAAGGAAGGTGAACCACGGATAGATATTAACATGTCAGG
 TTTCAATGAAACAGATGATTTGAAGAGAGCTGAGAGTATGCTTCAACAAGCAGATAAAATAGGTTGCA
 GACAGTTTTGTTACCCCTGCTGATGTTGTCACTGAGGAAACCCCAACTCAACTTAGCTTTCGTGGCTAAC
 CTGTTTTAATAAATACCCAGCATAACTAAGCCAGAGAACCAGGATATTGACTGGACTCTATTAGAAGG
 AGAAACTCGTGAAGAAAGAACCTTCCGTAACCTGGATGAACTCTCTTGGTGTCAATCTCAGCTAAACC
 ATCTCTATGCTGACCTGCAAGATGCCCTGGTAATCTTACAGTTATATGAACGAATTAAGTTCCCTGTT
 GACTGGAGTAAGGTTAATAAACCTCCATACCCGAAACTGGGAGCCAACATGAAAAAGCTAGAAAACCTG
 CAACTATGCTGTTGAATTAGGGAAGCATCCTGCTAAAATTTCTCCCTGGTTGGCATTGGAGGGCAAGACC
 TGAATGATGGGAACCAACCCCTGACTTTAGCTTTAGTCTGGCAGCTGATGAGAAGATATACCCCAAT
 GTCCTGGAAGATCTTGGAGATGGTCAGAAAGCCAATGACGACATCATTTGTAACCTGGGTGAACAGAAC
 GTTGAGTGAAGCTGGAAAATCAACTTCCATTTCAGAGTTTTAAGGACAAGACGATCAGCTCCAGTTTTGG
 CAGTTGTGGATTTAATTGATGCCATCCAGCCAGGCTGTATAAACTATGACCTTGTGAAGAGTGGCAAT
 CTAACAGAAGATGACAAGCACAATAATGCCAAGTATGCAGTGTCAATGGCTAGAAGAATCGGAGCCAG
 AGTGTATGCTCTCCCTGAAGACCTTGTGGAAGTAAAGCCCAAGATGGTCATGACTGTGTTTGCATGTT
 TGATGGGCAGGGGAATGAAGAGAGTGTAAAAGGGCAATTTCTGCAGATTAAGCTGCAATAAACAAGTTA
 ACAACAACAATTCATTTATGTTTTAGGTTTCAAGGTTCAAGGGGAGGTGTGGGAGGTTTTTTAAACTAGT
 CCACTCCCTCTCTGCGCGCTCGCTCGCTCACTGAGGCCGGGCGACCAAAAGTTCGCCCCGACGCCCGGGC
 TTTGCCCGGGCGGCCTCAGTGAGCGAGCGAGCGCGCAGAGAGGGACAGATCCGGGCCCGCATGCGTCCG
 ACAATTCACCTGGCCGTCGTTTTACAACGTCGTGACTGGGAAAACCTGGCGTTACCAACTTAATCCG
 CTTGCAGCACATCCCCCTTTCCGCCAGCTGGCGTAATAGCGAAGAGGCCCGCACCGATCGCCCTTCCCA
 ACAGTTTGCAGCAGCTGAATGGCGAATGGCGCTGATCGGATTTTTCTCCTTACGCATCTGTGCGGTA
 TTTTACACCCGCATATGGTGCACCTCAGTACAATCTGCTCTGATGCCGCATAGTTAAGCCAGCCCCGA
 CACCCGCCAACACCCGCTGACGCGCCCTGACGGGCTTGTCTGCTCCCGCATCCGCTTACAGACAAGC
 TGTGACCGTCTCCGGGAGCTGCATGTGTGAGAGTTTTTACCCTCATCACCGAAACGCGCGAGACGAA
 AGGGCCTCGTGATACGCCTATTTTTATAGGTTAATGTCATGATAATAATGGTTTTCTTAGACGTCAGGT
 GGCATTTTTCGGGGAAATGTGCGCGGAACCCCTATTTGTTTTATTTTTCTAAATACATTCAAATATGTA
 TCCGCTCATGAGACAATAACCCTGATAAATGCTTCAATAATATGAAAAAGGAAGATATGAGTATTC
 AACATTTCCGTGTGCGCCCTTATTCCTTTTTTGGCGCATTTTGCCTTCTGTTTTTGCTCACCCAGAA
 ACGCTGGTGAAGTAAAAGATGCTGAAGATCAGTTGGGTGCACGAGTGGGTTACATCGAACTGGATCT
 CAACAGCGGTAAGATCCTTGAGAGTTTTTCGCCCGAAGAACGTTTTCCAATGATGAGCACTTTTAAAG

TTCTGCTATGTGGCGCGGTATTATCCCCTATTGACGCCGGGCAAGAGCAACTCGGTGCGCCGATACAC
 TATTCTCAGAATGACTTGGTTGAGTACTCACCAGTCACAGAAAAGCATCTTACGGATGGCATGACAGT
 AAGAGAATTATGCAGTGCTGCCATAACCATGAGTGATAACACTGCGGCCAACTTACTTCTGACAACGA
 TCGGAGGACCGAAGGAGCTAACCGCTTTTTTGCACAACATGGGGGATCATGTAACCTCGCCTTGATCGT
 TGGGAACCGGAGCTGAATGAAGCCATACCAAACGACGAGCGTGACACCACGATGCCTGTAGCAATGGC
 AACAACGTTGCGCAAACCTATTAACCTGGCGAACTACTTACTCTAGCTTCCCGGCAACAATTAATAGACT
 GGATGGAGGCGGATAAAGTTGCAGGACCACTTCTGCGCTCGGCCCTTCCGGCTGGCTGGTTTATTGCT
 GATAAATCTGGAGCCGGTGAGCGTGGGTCTCGCGGTATCATTCGAGCACTGGGGCCAGATGGTAAGCC
 CTCCCCTATCGTAGTTATCTACACGACGGGGAGTCAGGCAACTATGGATGAACGAAAATAGACAGATCG
 CTGAGATAGGTGCCCTCACTGATTAAGCATTGGTAACCTGTGACACCAAGTTTACTCATATATACTTTAG
 ATTGATTTAAAACCTTCACTTTTAAATTTAAAAGGATCTAGGTGAAGATCCTTTTTGATAATCTCATGAC
 CAAAATCCCTTAACGTGAGTTTTCTGTTCCACTGAGCGTCAGACCCCGTAGAAAAGATCAAAGGATCTT
 CTTGAGATCCTTTTTTTCTGCGCGTAATCTGCTGCTTGCAAACAAAAAAACCACCGCTACCAGCGGTG
 GTTTTGTTTGGCGGATCAAGAGCTACCAACTCTTTTTCCGAAAGGTAACGGCTTCAGCAGAGCGCAGAT
 ACCAAATACTGTTCTTCTAGTGTAGCCGTAGTTAGGCCACCACTTCAAGAACTCTGTAGCACCGCCA
 CATACTCGCTCTGCTAATCCTGTTACCAGTGGCTGCTGCCAGTGGCGATAAGTCGTGTCTTACCGGG
 TTGGACTCAAGACGATAGTTACCGGATAAGGCGCAGCGGTGCGGCTGAACGGGGGGTTCGTGCACACA
 GCCCAGCTTGGAGCGAACGACCTACACCGAACTGAGATACCTACAGCGTGAGCTATGAGAAAAGCGCCA
 CGCTTCCCGAAGGGGAGAAAAGGCGGACAGGTATCCGGTAAGCGGCAGGGTCCGGAACAGGAGAGCGCAG
 AGGGAGCTTCCAGGGGGAAACGCCTGGTATCTTTATAGTCTGTCGGGTTTCGCCACCTCTGACTTGA
 GCGTCGATTTTTGTGATGCTCGTCAGGGGGGGCGGAGCCTATGGAAAAACGCCAGCAACGCGGCCTTTT
 TACGGTTCCTGGCCTTTTTGCTGGCCTTTTTGCTCACATGTTCTTTCTGCGTTATCCCCTGATTCTGTG
 GATAACCGTATTACCGCCTTTGAGTGAGCTGATACCGCTCGCCGACGCCGAACGACCGAGCGCAGCGA
 GTCAGTGAGCGAGGAAGCGGAAGAGCGCCCAATACGCAAACCGCCTCTCCCCGCGGTTGGCCGATTC
 ATTAATGCAGCTGGCAGCAGAGTTTCCCGACTGGAAAGCGGGCAGTGAGCGCAACGCAATTAATGTG
 AGTTAGCTCACTCATTAGGCACCCCAGGCTTTACACTTATGCTTCCGGCTCGTATGTTGTGTGGAAT
 TGTGAGCGGATAACAATTTACACAGGAAACAGCTATGACCATGATTACGCCAAGCTCTCGAGATCTA
 G

PAAV CMV MCS (conventional AAV)

CCTGCAGGCAGCTGCGCGCTCGCTCGCTCACTGAGGCCGCCGGGCAAAGCCCGGGCGTGGGGCGACC
 TTTGGTGCCCCGCCCTCAGTGAGCGAGCGAGCGCGCAGAGAGGGAGTGGCCAACTCCATCACTAGGGG
 TTCTGCGGCCGCACGCGTGGAGCTAGTTATTAATAGTAATCAATTACGGGGTCAATAGTTCATAGCC
 CATATATGGAGTTCCGCGTTACATAACTTACGGTAAATGGCCCCGCTGGCTGACCGCCCAACGACCCC
 CGCCCATGACGTCAATAATGACGTATGTTCCCATAGTAACGTCAATAGGGACTTTCCATTGACGTCA
 ATGGGTGGAGTATTTACGGTAAACTGCCCACTTGGCAGTACATCAAGTGATCATATGCCAAGTACGC
 CCCCTATTGACGTCAATGACGGTAAATGGCCCCGCTGGCATTATGCCAGTACATGACCTTATGGGAC
 TTTCTACTTGGCAGTACATCTACGTATTAGTCATCGCTATTACCATGGTGATGCGGTTTTGGCAGTA
 CATCAATGGGCGTGGATAGCGGTTTACTCACGGGAAATTTCCAAGTCTCCACCCCATGACGTCAATG
 GGAGTTGTTTTGCACCAAATCAACGGGACTTTCCAAAATGTCGTAACAACCTCCGCCCATTTGACGC
 AAATGGGCGGTAGGCGTGTACGGTGGGAGGCTATATAAAGCAGAGCTCGTTTGTGAACCGTCAATC
 GCCTGGAGACGCCATCCACGCTGTTTTGACCTCCATAGAAGACACCGGGACCGATCCAGCCTCCGCGG
 ATTCGAATCCCGGCCGGGAACGGTGCATTGGAACGCGGATTCCCCGTGCCAAGAGTGACGTAAGTACC
 GCCTATAGAGTCTATAGGCCACAAAAATGCTTTCTTCTTTAATATACTTTTTTGTTTATCTTATT
 TCTAATACTTTCCCTAATCTCTTTCTTTTCAAGGGCAATAATGATACAATGTATCATGCCTCTTTGCACC
 ATTCTAAAGAATAACAGTGATAATTTCTGGGTAAAGGCAATAGCAATATTTCTGCATATAAATATTTT
 TGCATATAAATTTGTAACCTGATGTAAGAGGTTTCAATTTGCTAATAGCAGCTACAATCCAGCTACCATT
 CTGCTTTTATTTTATGGTTGGGATAAGGCTGGATTATTCTGAGTCCAAGCTAGGCCCTTTTGTAAATC
 ATGTTTCATACCTCTTATCTTCCCTCCACAGCTCCTGGGCAACGTGCTGGTCTGTGTGCTGGCCCATCA
 CTTTGGCAAAGAATTGGGATTGGAACATCGATTGAATCCCCGGGGATCCTCTAGAGTCGACCTGCAG
 AAGCTTGCCCTCGAGCAGCGCTGCTCGAGAGATCTACGGGTGGCATCCCTGTGACCCCTCCCCAGTGCC
 TCTCCTGGCCCTGGAAGTTGCCACTCCAGTGCCACCAGCCTTGTCCATAATAAAATTAAGTTGCATCA
 TTTTGTCTGACTAGGTGTCCTTCTATAATATTATGGGGTGGAGGGGGTGGTATGGAGCAAGGGGCAA
 GTTGGGAAGACAACCTGTAGGGCCTGCGGGGTCTATTGGGAACCAAGCTGGAGTGCAGTGGCACAATC
 TTGGCTCACTGCAATCTCCGCCTCCTGGGTTCAAGCGATTCTCCTGCCTCAGCCTCCCGAGTTGTTGG
 GATTCCAGGCATGCATGACCAGGCTCAGCTAATTTTTGTTTTTTTGGTAGAGACGGGGTTTTACCATA
 TTGGCCAGGCTGGTCTCCAACCTCCTAATCTCAGGTGATCTACCCACCTTGGCCTCCCAAATGCTGGG
 ATTACAGGCGTGAACCACTGCTCCCTTCCCTGTCTTCTGATTTTGTAGGTAACCACGTGCGGACCGA

GCGGCCGAGGAACCCCTAGTGATGGAGTTGGCCACTCCCTCTCTGCGCGCTCGCTCGCTCACTGAGG
 CCGGGCGACCAAAGGTCGCCCCGACGCCCGGGCTTTGCCCGGGCGGCTCAGTGAGCGAGCGAGCGCGC
 AGCTGCCTGCAGGGGGCGCTGATGCGGTATTTTCTCCTTACGCATCTGTGCGGTATTTTACACCCGCAT
 ACGTCAAAGCAACCATAGTACGCGCCCTGTAGCGGGCGCATTAAAGCGCGGGGTGTGGTGGTTACGCG
 CAGCGTGACCGCTACACTTGGCAGCGCCCTAGCGCCCCGCTCCTTTTCGCTTTCTTCCCTTCCCTTCTCG
 CCACGTTTCGCGGGCTTTCCCGTCAAGCTCTAAATCGGGGGCTCCCTTTAGGGTCCGATTTAGTGTCT
 TTACGGCACCTCGACCCCAAAAACTTGATTTGGGTGATGGTTCACGTAGTGGGCCATCGCCCTGATA
 GACGGTTTTTCGCCCTTTGACGTTGGAGTCCACGTTCTTTAATAGTGGACTCTTGTTCAAACTGGAA
 CAACACTCAACCCTATCTCGGGCTATTCTTTTATTATAAGGGATTTTGGCGATTTTCGGCCTATTGG
 TTAATAAATGAGCTGATTTAACAATAAATTAACGCGAATTTTAAACAAAATATTAACGTTTACAATTTT
 ATGGTGCACCTCTCAGTACAATCTGCTCTGATGCCGCATAGTTAAGCCAGCCCCGACCCGCGCAACAC
 CCGCTGACGCGCCCTGACGGGCTTGTCTGCTCCCGCATCCGCTTACAGACAAGCTGTGACCGTCTCC
 GGGAGCTGCATGTGTGAGAGGTTTTTACCCTCATCACCGAAACGCGCGAGACGAAAGGGCCTCGTGAT
 ACGCCTATTTTTATAGGTTAATGTCATGATAATAATGGTTTTCTTAGACGTCAGGTGGCACTTTTTCGGG
 GAAATGTGCGCGGAACCCCTATTTGTTTATTTTTCTAAATACATTCAAAATATGTATCCGCTCATGAGA
 CAATAACCCTGATAAATGCTTCAATAATATTGAAAAAGGAAGAGTATGAGTATCAACATTTCCGTGT
 CGCCCTTATTCCCTTTTTTTCGGCATTTTTGCCTTCTGTTTTTGTCTACCCAGAAACGCTGGTGAAG
 TAAAGATGCTGAAGATCAGTTGGGTGCACGAGTGGGTACATCGAACTGGATCTCAACAGCGGTAAG
 ATCCTTGAGAGTTTTTCGCCCCGAAGAACGTTTTTCCAATGATGAGCACTTTTAAAGTCTGTATGTGG
 CGCGGTATTATCCCGTATTGACGCCGGGAAGAGCAACTCGGTCGCCGCATACACTATTCTCAGAATG
 ACTTGGTTGAGTACTACCAGTACAGAAAAGCATCTTACGGATGGCATGACAGTAAGAGAATTTATGC
 AGTGCTGCCATAACCATGAGTGATAAAGTGCAGGCAACTTACTTCTGACAACGATCGGAGGACCGAA
 GGAGCTAACCGCTTTTTTGCACAACATGGGGGATCATGTAACCTCGCCTTGATCGTTGGGAACCGGAGC
 TGAATGAAGCCATACAAACGACGAGCGTGACACCACGATGCCTGTAGCAATGGCAACAACGTTGCGC
 AAATATTAAGTGGCAACTACTTACTCTAGCTTCCCGGCAACAATTAATAGACTGGATGGAGGCGGA
 TAAAGTTGCAGGACCACTTCTGCGCTCGGCCCTTCCGGCTGGCTGGTTTTATTGCTGATAAATCTGGAG
 GTTATCTACACGACGGGGAGTCAGGCAACTATGGATGAACGAAATAGACAGATCGCTGAGATAGGTGC
 CTCACTGATTAAGCATTGGTAACTGTCAGACCAAGTTTACTCATATATACTTTAGATTGATTTAAAAC
 TTCATTTTTAATTTAAAAGGATCTAGGTGAAGATCCTTTTTTGATAATCTCATGACCAAAATCCCTTAA
 CGTGAGTTTTTTCGTTCCACTGAGCGTCAGACCCCGTAGAAAAGATCAAAGGATCTTCTTGAGATCCTTT
 TTTTCTGCGCGTAATCTGCTGCTTGCAACAAAAAAACCACCGCTACCAGCGGTGGTTTTGTTTGC
 ATCAAGAGCTACCAACTCTTTTTCCGAAGGTAACCTGGCTTACAGCAGAGCGCAGATACCAAAATCTGTC
 CTTCTAGTGTAGCCGTAGTTAGGCCACCCTTCAAGAACTCTGTAGCACCAGCTACATACTCGCTCT
 GCTAATCCTGTTACCAGTGGCTGCTGCCAGTGGCGATAAGTGTGCTTACCAGGTTGGACTCAAGAC
 GATAGTTACCGGATAAGGCGCAGCGGTCCGGCTGAACGGGGGTTGCTGCACACAGCCAGCTTGGAG
 CGAACGACCTACACCGAACTGAGATACCTACAGCGTGAGCTATGAGAAAAGCGCCAGCTTCCCGAAGG
 GAGAAAGGCGGACAGGTATCCGGTAAGCGGCAGGGTCGGAACAGGAGAGCGCACGAGGGAGCTTCCAG
 GGGGAAACGCTGGTATCTTTATAGTCTGTGCGGGTTTTGCCCACCTCTGACTTGAGCGTTCGATTTTTG
 TGATGCTCGTCAGGGGGGCGGAGCCTATGGAAAAACGCCAGCAACGCGGCTTTTTACGGTTCTTGGC
 CTTTTGCTGGCCTTTTGGCTCACATGT

AAV-PLS3

CCTGCAGGCAGCTGCGCGCTCGCTCGCTCACTGAGGCCGCCCGGGCAAAGCCCGGGCGTGGGGCGAC
 TTTGGTGCCTCGGCTCAGTGAGCGAGCGAGCGCGCAGAGAGGGAGTGGCCAACTCCATACTAGGGGT
 TCCTGCGGCCGACGCGTGGAGCTAGTTATTAATAGTAATCAATTACGGGGTCATTAGTTTCATAGCCC
 ATATATGGAGTTCCGCGTTACATAAATTACGGTAAATGGCCCGCTGGCTACCGCCAACGACCCCCG
 CCCATTGACGTCAATAATGACGTATGTTCCCATAGTAACGTCAATAGGGACTTTCCATTGACGTCAAT
 GGTGGAGTATTTACGGTAAACTGCCACTTGGCAGTACATAAGTGTATCATATGCCAAGTACGCCCC
 CTATTGACGTCAATGACGGTAAATGGCCCCGCTGGCATATGCCCAGTACATGACCTTATGGGACTTT
 CCTACTTGGCAGTACATCTACGTATTAGTCTGCTATTACCATGGTGATGCGGTTTTGGCAGTACATC
 AATGGGCGTGGATAGCGGTTTTGACTCACGGGGATTTCCAAGTCTCCACCCCATGACGTCAATGGGAG
 TTTGTTTTGCACCAAAATCAACGGACTTTCCAATAATGTCGTAACAACCTCCGCCCATGACGCAAATG
 GGCGGTAGGCGTGTACGGTGGGAGGTCTATATAAGCAGAGCTCGTTTTAGTGAACCGTTCAGATCGCCTG
 GAGACGCCATCCACCTGTTTTGACCTCCATAGAAGACACCGGGACCGATCCAGCTCCGCGGATTCGA
 ATCCCGGCCGGGAACGGTGCATTGGAACGCGGATTTCCCGTGCAGAGTACGTAAGTACCGCCTAT
 AGAGTTATAGGCCACAAAAAATGCTTTCTTCTTTAATATACTTTTTTGTATTATTTCTAATA
 CTTTCCCTAATCTCTTTCTTTTTCAGGGCAATAATGATACAATGTATCATGCCTCTTTGCACCATTTAA
 GAATAACAGTGATAATTTCTGGGTTAAGGCAATAGCAATATTTCTGCATATAAATATTTCTGCATATA

AATTGTAAGTATGTAAGAGGTTTCATATTGCTAATAGCAGCTACAATCCAGCTACATTCTGCTTTTA
TTTTATGGTTGGGATAAGGCTGGATTATTCTGAGTCCAAGCTAGGCCCTTTTGCTAATCATGTTCCATA
CCTCTTATCTTCCCTCCCACAGCTCCTGGGCAACGTGCTGGTCTGTGGCTGGCCCATCATTGGGCAA
GAATTGGGATTTCGAACATCGATTGaatcGCCACCATGGATGAGATGGCTACCACTCAGATTTCCAAA
GATGAGCTTGATGAACTCAAAGAGGCTTTGCAAAAAGTTGATCTCAACAGCAACGGATTTCATTTGTGA
CTATGAACTTCATGAGCTCTTCAAGGAAGCTAATATGCCATTACCAGGATATAAAAGTGAGAGAAATTA
TTCAGAACTCATGCTGGATGGTGACAGGAATAAAGATGGGAAAAATAAGTTTTGACGAATTTGTTTTAT
ATTTTTCAAGAGGTAAAAAGTAGTGATATTGCCAAGACCTTCCGCAAAGCAATCAACAGGAAAGAAGG
TATTTGTGCTCTGGGTGGAACCTTCAAGGTTGTCCAGCGAAGGAACACAGCATTTCTACTCAGAGGAAG
AAAAATATGCTTTTGTAACTGGATAAACAAAAGCTTTGGAAAAATGATCCTGATTGTAGACATGTTATA
CCAATGAACCCTAACACCGATGACCTGTTCAAAGCTGTTGGTGATGGAATTTGTGCTTTGTAAAAATGAT
TAACCTTTTCAGTTCTGATACCATTGATGAAAGAGCAATCAACAAGAAGAACTTACACCCCTTCATCA
TTCAGGAAAACCTTGAACCTTGGCACTGAACTCTGCTTCTGCCATTGGGTGTCATGTTGTGAACATTGGT
GCAGAAGATTTGAGGGCTGGGAAACCTCATCTGGTTTTGGGACTGCTTTGGCAGATCATTAAAGATCGG
TTTGTTCGCTGACATTGAATTAAGCAGGAATGAAGCCTTGGCTGCTTTACTCCGAGATGGTGAGACTT
TGGAGGAACTTATGAAATTTGTCTCCAGAAGAGCTTCTGCTTAGATGGGCAAACCTTCATTTGGAAAAC
TCGGGCTGGCAAAAATTAACAACCTTAGTGCTGACATCAAGGATTCAAAAGCCTATTTCCATCTTCT
CAATCAAATCGCACAAAAGGACAAAAGGAAGGTGAACCACGGATAGATATTAACATGTCAGTTTTCA
ATGAAACAGATGATTTGAAGAGAGCTGAGAGTATGCTTCAACAAGCAGATAAATTAGGTTGCAGACAG
TTTGTACCCTGCTGATGTTGTGTCAGTGGAAACCCCAAACCTCAACTTAGCTTTCGTGGCTAACCTGTT
TAATAAATACCCAGCACTAACTAAGCCAGAGAACCAGGATATTGACTGGACTCTATTAGAAGGAGAAA
CTCGTGAAGAAAGAACCTTCCGTAACCTGGATGAACTCTCTTGGTGTCAATCCTCACGTAAACCATCTC
TATGCTGACCTGCAAGATGCCCTGGTAATCTTACAGTTATATGAACGAATTAAGTTCCCTGTTGACTG
GAGTAAGGTTAATAAACCTCCATACCCGAAACTGGGAGCCAACATGAAAAAGCTAGAAAAC TGCAACT
ATGCTGTTGAATTAGGGAAGCATCCTGCTAAATTTCTCCCTGGTTGGCATTGGAGGGCAAGACCTGAAT
GATGGGAACCAACCCCTGACTTTAGCTTTAGTCTGGCAGCTGATGAGAAGATATACCCTCAATGTCCCT
GGAAGATCTGGAGATGGTCAGAAAGCCAATGACGACATCATTGTGAACTGGGTGAACAGAAAGTTGA
GTGAAGCTGGAAAATCAACTTCCATTCAGAGTTTTAAAGGACAAGACGATCAGTCCAGTTTGGCAGTT
GTGGATTTAATTGATGCCATCCAGCCAGGCTGTATAAACTATGACCTTGTGAAGAGTGGCAATCTAAC
AGAAGATGACAAGCACAATAATGCCAAGTATGCAGTGTCAATGGCTAGAAGAATCGGAGCCAGAGTGT
ATGCTCTCCCTGAAGACCTTGTGGAAGTAAAGCCCAAGATGGTTCATGACTGTGTTTGCATGTTTGATG
GGCAGGGGAATGAAGAGAGTGTAAtCTAGAGTGCACCTGCAGAAGCTTGCCTCGAGCAGCGCTGCTCG
AGAGATCTACGGGTGGCCTCCTGTGACCCCTCCCAGTGCCTCTCCTGGCCCTGGAAAGTTGCCACTCC
AGTGCCCAACAGCCTTGTCTAATAAAAATTAAGTTGCATCATTTTGTCTGACTAGGTGTCTTCTATA
ATATTATGGGGTGAGGGGGTGGTATGGAGCAAGGGGCAAGTTGGGAAGACAACCTGTAGGGCCTGCG
GGGTCTATTGGGAACCAAGCTGGAGTGCAGTGGCACAATCTTGGCTCACTGCAATCTCCGCTCCTGG
GTTAAGCGATTCTCCTGCCTCAGCCTCCCAGATTGTTGGGATTCCAGGCATGCATGACCAGGCTCAGC
TAATTTTTGTTTTTTTGGTAGAGACGGGGTTTACCATATTGGCCAGGCTGGTCTCCAACCTCAATCT
CAGGTGATCTACCCACCTTGGCCTCCCAAATGCTGGGATTACAGGCGTGAACCACTGCTCCCTTCCC
TGTCTTCTGATTTTGTAGGTAACCACGTGCGGACCGAGCGGCCGAGGAACCTTAGTGATGGAGTTG
GCCACTCCCTCTCTGCGCGCTCGCTCGCTCACTGAGGCCGGGCGACCAAAAGGTCGCCCGACGCCCCGG
CTTTGCCCGGGCGGCCTCAGTGAGCGAGCGAGCGCGCAGCTGCCGAGGGGCGCCTGATGCGGTATTT
TCTCCTTACGCATCTGTGCGGTATTTACACCCGATACGTCAAAGCAACCATAGTACGCGCCCTGTAG
CGCCGCATTAAGCGCGGCGGGTGTGGTGGTTACGCCAGCGTGACCGCTACACTTGCAGCGCCCTAGC
GCCCCTCCTTTTCGCTTTCTCCCTTCTTCTCGCCACGTTTCGCCGCTTTCCCGTCAAGCTTAA
ATCGGGGGCTCCCTTTAGGGTTCCGATTAGTGCTTTACGGCACCTCGACCCCAAAAAACTTGATTTGG
GTGATGGTTACGTAGTGGGCCATCGCCCTGATAGACGGTTTTTTCGCCCTTTGACGTTGGAGTCCACG
TTCTTTAATAGTGACTCTTGTTCAAAAGTGAACAACAACCTCAACCTATCTCGGGCTATTCTTTTGA
TTTATAAGGGATTTTGGCGATTTGGCTATTGGTTAAAAAATGAGCTGATTTAACAAAAATTTAACGC
GAATTTTAAACAAAATATTAACGTTTACAATTTTATGGTGCACCTCTCAGTACAATCTGCTCTGATGCCG
CATAGTTAAGCCAGCCCGACACCCGCCAACACCCGCTGACGCGCCCTGACGGGCTTGTCTGCTCCCGG
CATCCGCTTACAGACAAGCTGTGACCGTCTCCGGGAGCTGCATGTGTGAGAGTTTTTACCCTCATCA
CCGAACGCGCGAGACGAAAGGGCCTCGTGATACGCTATTTTTATAGGTTAATGTATGATAATAATG
GTTTTCTTAGACGTGAGGTGGCACTTTTTCGGGAAATGTGCGCGGAACCCCTATTTGTTTTATTTCTAA
ATACATTCAAAATATGTATCCGCTCATGAGACAATAACCTGATAAATGCTTCAATAAATTTGAAAAAG
GAAGAGTATGAGTATTCAACATTTCCGTGTGCCCCATTATCCCTTTTTTTCGGCATTGCTTCCCTGT
TTTTGCTCACCCAGAAACGCTGGTGAAGTAAAAAGATGCTGAAAGATCAGTTGGGTGCACGAGTGGGT
ACATCGAACTGGATCTCAACAGCGGTAAGATCCTTGAGAGTTTTTCGCCCGAAGAACGTTTTTCCAATGA
TGAGCACTTTTAAAGTTCTGCTATGTGGCGCGGTATTATCCCGTATTGACGCCGGCAAGAGCAACTC
GGTCGCCGCATACACTATTCTCAGAATGACTTGGTTGGTACTCACCAGTCACAGAAAAGCATCTTACG
GATGGCATGACAGTAAGAGAATTATGCAGTGTGCCATAACCATGAGTGATAAACAATGCGGCCAACTT

ACTTCTGACAACGATCGGAGGACCGAAGAGCTAACCGCTTTTTTGCACAACATGGGGGATCATGTAAC
TCGCCTTGATCGTTGGGAACCGGAGCTGAATGAAGCCATACCAAACGACGAGCGTGACACCACGATGC
CTGTAGCAATGGCAACAACCTTGCGCAAACCTATTAAGTGGCGAACTACTTACTCTAGCTTCCCGGCAAC
AATTAATAGACTGGATGGAGGCGGATAAAAGTTGCAGGACCCTTCTGCGCTCGGCCCTCCGGCTGGC
TGGTTTATTGTGATAAATCTGGAGCCGGTGAGCGTGGGTCTCGCGGTATCATTGCAGCACTGGGGCCA
GATGGTAAGCCCTCCCGTATCGTAGTTATCTACACGACGGGGAGTCAGGCAACTATGGATGAACGAAA
TGACAGATCGCTGAGATAGGTGCCTCACTGATTAAGCATTGGTAAGACAGATCGCTGAGATAGGTGCC
TCACTGATTAAGCATTGGTAACTGTCAGACCAAGTTTACTCATATATACTTTAGATTGATTTAAACT
TCATTTTTAATTTAAAAGGATCTAGGTGAAGATCCTTTTGATAATCTCATGACCAAAATCCCTTAACG
TGAGTTTTTCGTTCCACTGAGCGTCAGACCCCGTAGAAAAGATCAAAGGATCTTCTTGAGATCCTTTTT
TTCTGCGCGTAATCTGCTGCTTGCAAAAAAAAAAACCCCGCTACCAGCGGTGGTTTGGTTTGCCGGATC
AAGAGCTACCAACTCTTTTTCCGAAGGTAAGTGGCTTCAGCAGAGCGCAGATACCAAATACTGTCCTT
CTAGTGTAGCCGTAGTTAGCCACCCTTCAAGAACTCTGTAGCACCGCCCTACATACCTCGCTCTGCTA
ATCCTGTTACCAGTGGCTGCTGCCAGTGGCGATAAGTCGTGTCTTACCGGGTTGGACTCAAGACGATA
GTTACCGGAAAGGCGCAGCGGTCCGGCTGAACGGGGGGTTTCGTGCACACAGCCCAGCTTGGAGCGAAC
GACCTACACCGAACTGAGATACCTACAGCGTGAGCTATGAGAAAAGCGCCACGCTTCCCGAAGGGAGAA
GGCGGACAGGTATCCGGTAAGCGGCAGGGTCGGAACAGGAGAGCGCACGAGGGAGCTTCCAGGGGGAA
ACGCCTGGTATCTTTATAGTCTGTGCGGGTTTCGCCACCTCTGACTTGAGCGTCGATTTTGTGATGCT
CGTCAGGGGGGGCGGAGCCTATGGAAAAACGCCAGCAACGCGGCCCTTTTACGGTTCCTGGCCTTTTGC
TGGCCTTTTGTCTCACATGT